Universidade de Aveiro Departamento de Química
2019

Diana Cléssia Vieira Belchior

Aplicação de sistemas aquosos bifásicos na separação de aminoácidos e proteínas

Application of aqueous biphasic systems for the separation of amino acids and proteins

Universidade de Aveiro Departamento de Química
2019

Diana Cléssia Vieira Belchior

Aplicação de sistemas aquosos bifásicos na separação de aminoácidos e proteínas

Application of aqueous biphasic systems for the separation of amino acids and proteins

Tese apresentada à Universidade de Aveiro para cumprimento dos requisitos necessários à obtenção do grau de Doutor em Engenharia Química, realizada sob a orientação científica da Doutora Mara Guadalupe Freire Martins, Investigadora Coordenadora do Departamento de Química, CICECO, da Universidade de Aveiro, e coorientação da Doutora Iola Duarte, Investigadora Principal, do Departamento de Química, CICECO, da Universidade de Aveiro.

Apoio financeiro do POCTI no âmbito do III Quadro Comunitário de Apoio.

O doutoramento agradece o apoio financeiro do Conselho Nacional de Desenvolvimento Científico e Tecnológico – CNPq, Brasil (202337/2015-4).
Parte da investigação que conduziu aos resultados aqui apresentados foi financiada pelo Conselho Europeu de Investigação ao abrigo do Sétimo Programa Quadro da União Europeia (FP7/2007-2013)/ERC no. 337753

o júri

presidente

Professor Doutor Aníbal Guimarães da Costa
Professor Catedrático do Departamento de Engenharia Civil da Universidade de Aveiro

Professor Doutor José António Couto Teixeira
Professor Catedrático do Centro de Engenharia Biológica da Universidade do Minho

Professora Doutora Cândida Ascensão Teixeira Cruz
Professora Associada do Departamento de Química da Universidade da Beira Interior

Doutora Ana Belén Pereiro Estévez
Investigadora Auxiliar do Departamento de Química da Universidade Nova de Lisboa

Doutora Ana Paula Mora Tavares
Investigadora Auxiliar do Departamento de Quimica, CICECO – Instituto de Materiais de Aveiro, da Universidade de Aveiro

Doutora Mara Guadalupe Freire Martins
Investigadora Coordenadora do Departamento de Quimica, CICECO – Instituto de Materiais de Aveiro, da Universidade de Aveiro

Agradecimentos

Agradeço primeiramente a DEUS, pelo dom da vida e proteção.
Aos meus amados pais, Maria Divina e André Luiz, pelo amor e incentivo. Vocês sempre serão o meu exemplo de vida.
Aos meus irmãos, Anderson Peixoto e Amanda Peixoto, pelo amor, carinho e união. Vocês fazem parte desta conquista.
Ao meu eterno namorado e esposo, Althiéris Saraiva, pelo valioso e incansável apoio e compreensão em todos os momentos desta jornada. Você é o melhor de mim.
Aos meus familiares: tios, tias, primos, primas, avó e avô ("In Memorian"). Família sempre acima de tudo.
À Tânia Sintra, Maria João e Carlos Mendonça pelo carinho, disponibilidade, opiniões/críticas e pelas palavras de incentivo. Serei eternamente grata.
Aos amigos (Nazaré Ribeiro, Tânia Sintra, Maria João, Ana Maria, Ana Mafalda, Carlos Mendonça, João Santos e Catarina Neves) pelo suporte, apoio e ombro amigo. Amizade só faz sentido se trás o céu para mais perto.
Às minhas orientadoras Doutoras Mara Freire e Iola Duarte e Professor Doutor João Coutinho pela oportunidade de aprendizagem, a qual contribuiu também para o meu desenvolvimento pessoal.
Ao investigador Pedro Carvalho pelo empenho e dedicação em transmitir o saber.
A todos os integrantes do grupo Path/CICECO (Universidade de Aveiro, Portugal).
Ao CNPq pela concessão da bolsa, a qual possibilitou a realização deste trabalho.

Palavras-chave: Sistema aquoso bifásico, líquido iónico, polímero, extração, separação, aminoácidos, proteínas.

resumo Este trabalho teve como objectivo a aplicação de sistemas aquosos bifásicos (SAB) constituídos por líquidos iónicos (LIs) da família dos tetraalquilamónios no desenvolvimento de processos de separação mais eficientes para aminoácidos e proteínas.

É primeiramente demonstrado o efeito do comprimento da cadeia alquílica do anião do LI na formação de SAB e no desempenho destes sistemas na extração de aminoácidos, tendo-se identificado efeitos par-ímpar. Os LIs constituídos por aniões com cadeias alquílicas pares exibem uma capacidade ligeiramente superior para formar SAB, enquanto que os sistemas formado por LIs com aniões compreendendo cadeias alquílicas ímpares conduzem a coeficientes de partição de aminoácidos ligeiramente superiores. Depois de avaliar o desempenho de SAB com LIs para extrair aminoácidos, foi demonstrada a influência da estrutura química dos LIs e do efeito do pH na extração e no rendimento de recuperação de ovalbumina e lisozima, duas proteínas existentes na clara de ovo. A pH 7, obtiveram-se extrações e recuperações completas de lisozima para a fase enriquecida em LI; no entanto, foram obtidos rendimentos de recuperação de ovalbumina inferiores utilizando SAB compreendendo LIs com cadeias laterais alquílicas mais longas. Estudos por molecular docking reveleram que os LIs que estabelecem preferencialmente interações hidrofóbicas com essas proteínas levam à sua agregação e a menores rendimentos de recuperação. A recuperação das proteínas (até 99%) da fase rica em LI por precipitação com etanol também foi demonstrada. Por fim, foram estudos SAB utilizando LIs como adjuvantes (a 5 m/m%) na formação destes sistemas e para manipular a seletividade das fases visando a separação simultânea da ovalbumina e lisozima. Foram realizados estudos com proteínas comerciais e com clara de ovo. Com os sistemas em que não foi adicionado LI, observou-se a partição preferencial da ovalbumina para a fase enriquecida em polímero que contém o LI, enquanto a lisozima tende a precipitar na interface. Foi observada uma tendência semelhante quando se aplicaram os mesmos sitemas para separar ambas as proteínas da clara de ovo. No entanto, quando se adiciona LI, a ovalbumina e a lisozima particional preferencialmente para as fases enriquecidas em sal e polímero, respectivamente, evitando também a precipitação da última proteína. Entretanto, não se observou a mesma tendência quando se aplicaram os mesmos sistemas à clara de ovo, revelando que existe um fenómeno mais complexo que se deve à presença de outras proteínas da clara de ovo. Embora ainda sejam necessários estudos adicionais sobre a viabilidade de alguns dos LIs e sistemas estudados, os resultados obtidos neste trabalho revelam a relevância de SAB compreendendo LIs no desenvolvimento de processos de separação para aminoácidos e proteínas.

Keywords Aqueous biphasic system, ionic liquid, polymer, extraction, separation, amino acids, proteins.

abstract This work was focused on the application of aqueous biphasic systems (ABS) composed of tetraalkylammonium-based ionic liquids (ILs) aiming at developing more effective separation processes for amino acids and proteins.

It is first demonstrated the impact of the alkyl chain length of the IL anion on the ABS formation and on these systems performance to extract amino acids, where odd-even effects have been identified. ILs composed of anions with even alkyl chains exhibit a slightly higher capacity to form ABS, whereas systems formed by ILs with anions comprising odd alkyl chains lead to slightly higher amino acid partition coefficients. After addressing the IL-based ABS performance to extract amino acids, it is then demonstrated the influence of the IL chemical structure and the effect of pH on the extraction and recovery yield of ovalbumin and lysozyme, two proteins present in egg white. At pH 7, the complete extraction and recovery of lysozyme to the IL-rich phase was achieved with all systems; however, low ovalbumin recovery yields were obtained with ABS formed by ILs with longer alkyl side chains. Molecular docking studies revealed that ILs that preferentially establish hydrophobic interactions with these proteins lead to their aggregation and lower recovery yields. The recovery of the proteins (up to 99%) from the IL-rich phase by precipitation with ice-cold ethanol was also demonstrated. Finally, polymer-salt ABS comprising ILs as adjuvants (at 5 wt%) were investigated to tailor the phases polarities and these systems selectivity to simultaneously separate ovalbumin and lysozyme. Studies with commercial proteins and directly from egg white were carried out. With the systems in which no IL was added it was observed a preferential partition of ovalbumin to the polymer-rich phase, which contains the IL, whereas lysozyme tends to precipitate at the interphase. A similar trend was observed when applying the same systems to separate both proteins from egg white. However, when ILs are added, the ovalbumin and lysozyme preferentially partition to the salt-rich and PEG-rich phases, respectively, while avoiding the precipitation of the latter protein. Nevertheless, when the same systems are applied to egg white, the same behavior was not observed, indicating that a more complex phenomenon occurs due to the presence of other proteins in egg white.

Although further research on the viability of some of the studied ILs and systems is still required, the results presented in this work disclose the relevance of ABS comprising ILs in the development of efficient separation processes for amino acids and proteins.

Contents

List of tables

List of figures

List of symbols

k_s	Setschenow salting-out coefficient
K_i	Partition coefficient of component *i*
wt%	Weight fraction percentage
EE_i%	Extraction efficiency percentage of component *i*
Y_i%	Recovery yield of component *i*
E_{int}	Cation-anion total interaction energies of component *i*
K_{ow}	Octanol-water partition coefficient

List of acronyms

Ionic liquid cations

$[Ch]^+$	cholinium	$[N_{222(C7H7)}]^+$	Benzyltriethylammonium
$[N_{2222}]^+$	tetraethylammonium	$[N_{444(C7H7)}]^+$	Benzyltributylammonium
$[N_{4444}]^+$	tetrabutylammonium	$[N_{1118}]^+$	n-octytrimethylammonium
$[N_{111(C7H7)}]^+$	benzyltrimethylammonium	$[C_nC_1im]^+$	1-alkyl-3-methylimidazolium
$[C_3C_1pip]^+$	1-propyl-3-methylpiperidinium	$[C_4(C_1C_1C_1Si)im]^+$	1-butyl-3-trimethylsilylimidazolium
$[C_4C_1pyrr]^+$	1-butyl-3-methylpyrrolidinium	$[OHC_2mim]^+$	1-hydroxyethyl-3-methylimidazolium
$[P_{4444}]^+$	tetrabutylphosphonium	$[P_{4441}]^+$	tributyl(methyl)phosphonium
$[P_{i(444)4}]^+$	triisobutyl(methyl)phosphonium	$[N_{111(2OH)}]_3^{3+}$	tri-cholinium
$[N_{111(2OH)}]_2^{2+}$	di-cholinium	$[(CH_2CONHC_4H_9)C_2im]^+$	3-(2-(butylamino)-2-oxoethyl)-1-ethylimidazolium

Ionic liquid anions

$[C_1CO_2]^-$, $[Ac]^-$ or $[CH_3CO_2]^-$	acetate	Cl^-	chloride
$[C_2CO_2]^-$	propanoate	Br^-	bromide
$[C_3CO_2]^-$	butanoate	$[cit]^-$	citrate
$[C_4CO_2]^-$	pentanoate	$[Ox]^-$	oxalate
$[C_5CO_2]^-$	hexanoate	$[TOS]^-$	tosylate
$[C_6CO_2]^-$	heptanoate	$[BE]^-$	benzoate
$[C_7CO_2]^-$	octanoate	$[Pro]^-$	prolinate
$[C_nSO_4]^-$	alkylsulfate	$[SCN]^-$	thiocyanate
$[HSO_4]^-$	hydrogensulfate	$[DHCit]^-$	dihydrogencitrate
$[MeSO_4]^-$	methylsulphate	$[DMP]^-$	dimethylphosphate
$[N(CN)_2]^-$	dicyanamide	$[CHES]^-$	2-(cyclohexylamino)ethanesulfonate
$[C_nCO_2]^-$	alkanoate	$[MES]^-$	2-(N-morpholino)ethanesulfonate
$[Lac]^-$	lactate	$[Tricine]^-$	N- tris(hydroxymethyl)methyl]glycine
$[Gly]^-$	glycine	$[Tf_2N]^-$	bis(trifluoromethylsulfonyl)imide
$[Bit]^-$	bitartarate	$[Tf\text{-}Leu]^-$	*N*-trifluoromethanesulfonylleucine
$[DHP]^-$	dihydrogenphosphate	$[CF_3SO_3]^-$	trifluoromethanesulfonate
$[PF_6]^-$	hexafluorophosphate	$[TES]^-$	2-[(2-hydroxy-1,1-bis(hydroxymethyl) ethyl)amino]ethanesulfonate
$[BF_4]^-$	tetrafluoroborate	$[HEPES]^-$	2-[4-(2-Hydroxyethyl)piperazin-1-yl]ethane sulfonate

List of abbreviations

AA	Amino acid	TLL	Tie-line length
ABS	Aqueous biphasic system	HPLC	High performance liquid chromatography
CMC	Critical micellar concentration	PBS	Phosphate buffered saline solution
IL	Ionic liquid	NMR	Nuclear magnetic resonance
LLE	Liquid−liquid extraction	PEG	Poly(ethylene)glycol
TL	Tie-line	PAA	Poly(acrylic acid)
pI	Isoelectric point	PPG	Polypropylene glycol
NAPA	Sodium poly(acrylate)		

1.Introduction

1.1 Scopes and Objectives

Separation methods explore the differences in the physicochemical properties of the target compounds and impurities present in the original medium. However, due to the complexity of the original medium in which amino acids and proteins are produced and/or are present, numerous steps are required to purify and recover these products. This multistep approach is the main reason behind the high cost of highly pure amino acids and proteins, thus reinforcing the need of developing cost-effective processes. In addition to the well-established chromatographic techniques, the separation of bio-based products with liquid-liquid systems is typically carried out using volatile organic solvents because of their immiscibility with aqueous media or with conventional polymer-based aqueous biphasic systems (ABS). However, most common organic solvents used present some disadvantages, such as high volatility and toxicity, and the possibility of denaturing proteins and enzymes. On the other hand, polymer-based ABS usually display a low selectivity and are of high viscosity. Aiming at replacing the use of volatile organic solvents and to improve the separation processes efficiency and selectivity, IL-based aqueous biphasic systems (ABS) have been largely investigated. In addition to other remarkable features of ILs such as their non-volatility and non-flammability, which are valuable in the development of sustainable liquid-liquid separation processes, ILs are designer solvents, allowing to tailor the ILs chemical structures to act as enhanced extraction solvents of a wide variety of bio-based compounds.

Based on the advantages of ILs and on the need of developing effective strategies to separate amino acids and proteins, this PhD thesis is focused on the investigation of novel ABS formed by ILs to separate amino acids and proteins. In particular, special emphasis was given to ABS constituted by more biocompatible tetraalkylammonium-based ILs over imidazolium-based compounds preferentially studied up to date. Overall, ABS composed of ILs were investigated to separate amino acids and proteins, and comparisons with analogous polymer-based ABS and ABS using ILs as adjuvants have been carried out. Most works were carried out with the goal of understanding the partitioning behavior of amino acids and proteins in IL-based ABS to design effective separation platforms. For a better understanding of the organization of this thesis and results obtained, an illustrative representation of its layout is displayed in Figure 1.1.

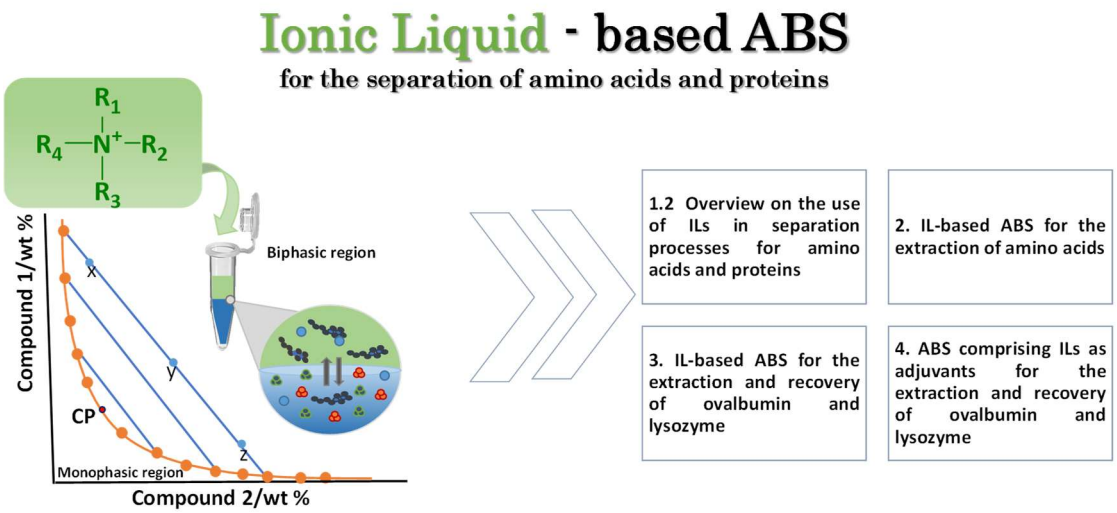

Figure 1.1. Layout of the current thesis.

Chapter 1.2 corresponds to a literature review on the use of hydrophobic ILs and IL-based ABS to separate amino acids and proteins. In this chapter it is shown the large interest given to imidazolium-based ILs, supporting the novelty of the ABS composed of tetraalkylammonium-based ILs studied in this PhD. **Chapter 2** presents results on the use of ABS composed of cholinium-based ILs and K_2HPO_4 to separate amino acids. Additionally to the ILs synthesis and characterization, the respective ABS phase diagrams were determined. These novel systems were evaluated regarding their ability to separate amino acids, allowing to comprehensively address the IL anion alkyl chain length effect, and where an odd-even effect in both these systems salting-out aptitude and extraction performance was identified. ABS composed of ammonium-based ILs and phosphate-based salts were then investigated to separate proteins, namely ovalbumin and lysozyme (proteins present in egg white), whose results and discussion are given in **Chapter 3**. The respective phase diagrams have been determined, and these ABS extraction performance for both proteins was evaluated according to the IL chemical structure and pH. Beyond the use of ILs as constituents of aqueous biphasic systems, ILs have been applied as adjuvants in polymer-based ABS to tailor the coexisting phase's polarities. This approach is advantageous since lower amounts of IL are required. Accordingly, **Chapter 4** is focused on the development of ABS composed of different poly(ethylene)glycols (PEGs) of different molecular weights and various ILs as adjuvants to separate ovalbumin and lysozyme. All the respective phase diagrams have been determined, and these systems extraction efficiencies and recoveries were first evaluated with model proteins, followed by their direct application to separate both proteins from egg white.

1.2. Ionic Liquids in Bioseparation Processes

Chapter based on the published book chapter:[1]

Belchior, D. C. V., Duarte, I. F., & Freire, M. G. Ionic Liquids in Bioseparation Processes. Chapter 1 in Advances in Biochemical Engineering/Biotechnology. Springer, Berlin, Heidelberg , 2018, 1-29. Doi:10.1007/10_2018_66

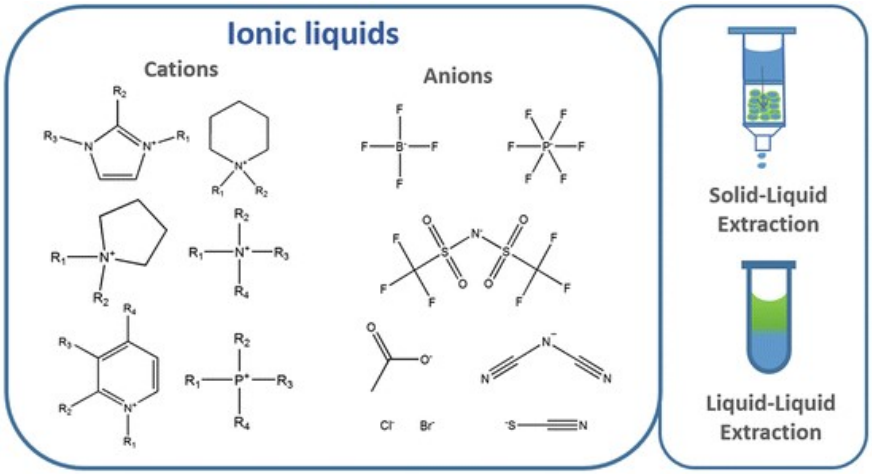

Abstract

Bioseparation processes are a relevant part of modern biotechnology, particularly regarding the development of efficient and biocompatible methods for the separation and purification of biologically active compounds. In this field, ionic liquids (ILs) have been proposed, either in liquid-liquid extractions, in which non-water miscible ILs or aqueous biphasic systems (ABS) formed by ILs can be used, or in solid-liquid extractions, in which they are covalently attached to create supported IL phases (SILPs). Aprotic ILs possess unique properties, such as non-volatility and designer ability, which are transferrable to their use in bioseparation processes. In this chapter, we summarize and discuss bioseparation processes based on ILs, comprising both liquid-liquid and solid-liquid extractions, applied to amino acids and proteins. The most recent and remarkable advances in this area are emphasized, and improvements brought by the use of ILs properly discussed. New insights and envisaged directions with IL-based bioseparation processes are suggested.

Keywords: Ionic Liquid • Liquid–liquid extraction • Solid–liquid extraction • Amino acids • Proteins

[1]Contributions: M.G.F. and I.F.D. conceived and directed this work. The manuscript was mainly written by D.C.V.B., with contributions from M.G.F. and I.F.D.

1.2.1. Introduction

In bioengineering and biotechnological processes the high cost associated to the downstream processing, aimed at the purification and recovery of target products, is one of the major issues limiting the widespread use of many bio-based products. Bioseparations are an important part of modern biotechnology, particularly regarding the development of new and biocompatible methods for the separation and purification of added-value amino acids, proteins and enzymes. Biocompatibility is however a crucial feature in the design of these separation platforms, mainly when dealing with biologically active products [1].

Separation methods explore the differences in physicochemical properties of target compounds and contaminants present in the original media [2]. Separation and purification stages in biotechnological processes usually require numerous steps, associated to high energy and chemicals consumption, while typically representing 20–60% of the final cost of the product; this value may even reach 90% in particular products [1]. In addition to the well-established chromatographic approaches, the separation of bio-based products with liquid-liquid systems is typically carried out using volatile organic solvents because of their immiscibility with aqueous media[3]. However, most common organic solvents used (e.g. toluene, ethyl acetate, hexane) [3] present some disadvantages, such as high volatility and toxicity, and the possibility of denaturing proteins and enzymes to be recovered[1]. Aiming at replacing the use of volatile organic solvents as extraction media, non-water soluble ionic liquids (ILs) and IL-based aqueous biphasic systems (ABS) have been investigated [4]. ILs belong to the molten salts group; they are composed of inorganic or organic anions, and relatively large and asymmetric organic cations, which do not easily form an ordered crystal and therefore may be liquid at or near room temperature [5]. In addition to their negligible vapor pressure, non-flammability and high chemical stability [5], ILs present excellent solvation qualities [5], and have thus shown to be effective in liquid-liquid separation methods [4]. In addition to these features, which are valuable in the development of sustainable liquid-liquid separation processes, ILs are considered as designer solvents due to the large number of cation-anion combinations [5]. Therefore, specific ILs can be designed to act as enhanced extraction solvents of a wide variety of bio-based compounds.

Within the field of liquid-liquid separation techniques, ABS have been reported as benign alternatives due to the possibility of combining two non-volatile components in water-rich media [6]. ABS consist of two aqueous-rich phases that coexist in equilibrium after the dissolution, at given concentrations, of pairs of appropriate solutes, such as two polymers or a polymer and a salt [6]. The aqueous two-phase extraction of biomolecules was first proposed by

Albertsson [6] in the 50's, and has been widely studied over the past decades. This technique has gained attention because it is able to combine several processing stages, such as clarification, concentration and primary purification, in one step [6]. ABS are considered a gentler and more biocompatible alternative than other extraction techniques since they are mainly composed of water. Moreover, ABS are amenable to be scaled-up, and allow continuous operation and process integration. Iqbal et al. [7] recently reviewed the potential and recent advances of ABS as separation platforms.

ABS have been investigated for the separation of a wide range of biologically active substances, such as amino acids, proteins, including enzymes and antibodies, and nucleic acids [8]. Most of the polymers used as phase-forming components of traditional ABS have a stabilizing effect over the proteins tertiary structure [9], thus further contributing to the enhanced performance of these systems. More traditional ABS are composed of two polymers or a polymer and a salt [6]. However, this type of systems is limited in terms of the range of polarities offered by the coexisting phases, thus turning selective and enhanced separations difficult to occur in a single-step [10]. To overcome this drawback, several approaches have been proposed, e.g. by the functionalization of polymers [11, 12] by the use of additives [13], by designing hybrid processes [14], among others. In 2003, ILs have been proposed as alternative phase-forming components of ABS, being able to replace conventional polymers and to form ABS combined with inorganic salts [15]. Their large plethora of chemical structures allows to design ILs for specific tasks or applications, which is extended to ABS. In addition to the possibility of forming ABS by combining ILs with salts, polymers, amino acids, and carbohydrates[16], it has been demonstrated that their separation performance can be tuned by the IL chemical structure [10]. The number of estimated ILs is *ca.* 1 million, suggesting that almost any desirable property may be obtained with a particular IL [5]. Even so, most reported IL-based ABS are formed by imidazolium-based fluids, most of the times combined with the non-water stable $[BF_4]^-$ anion [4]. This tendency has however started to be overwhelmed, and some recent works have been focused on the use of more attractive ILs to create ABS [4].

Still taking advantage of the ILs unique properties, supported ionic liquid phase (SILP) materials have been proposed as a more recent concept in separation processes, where ILs are immobilized (covalently attached) in a solid phase which could act as new chromatographic columns or in solid-phase extraction (SPE) approaches [17]. Materials such as silica, polymers, magnetic nanoparticles or carbon nanotubes have been successfully modified by ILs [17]. Overall, ILs have been reported as enhanced extraction solvents, both neat and in aqueous solutions, while being able to increase the stability of added-value biomolecules, such as proteins, enzymes and nucleic acids. In the same line, SILPs have been successfully used in the

separation of amino acids and proteins. Based on the high performance of ILs in bioseparation processes, we present and discuss herein recent advances achieved by the use of ILs in liquid-liquid extractions, employing hydrophobic ILs and ABS, and solid-liquid extractions based on the use of IL-modified materials, for the separation of amino acids and proteins, including enzymes and biopharmaceuticals (Figure 1.2).

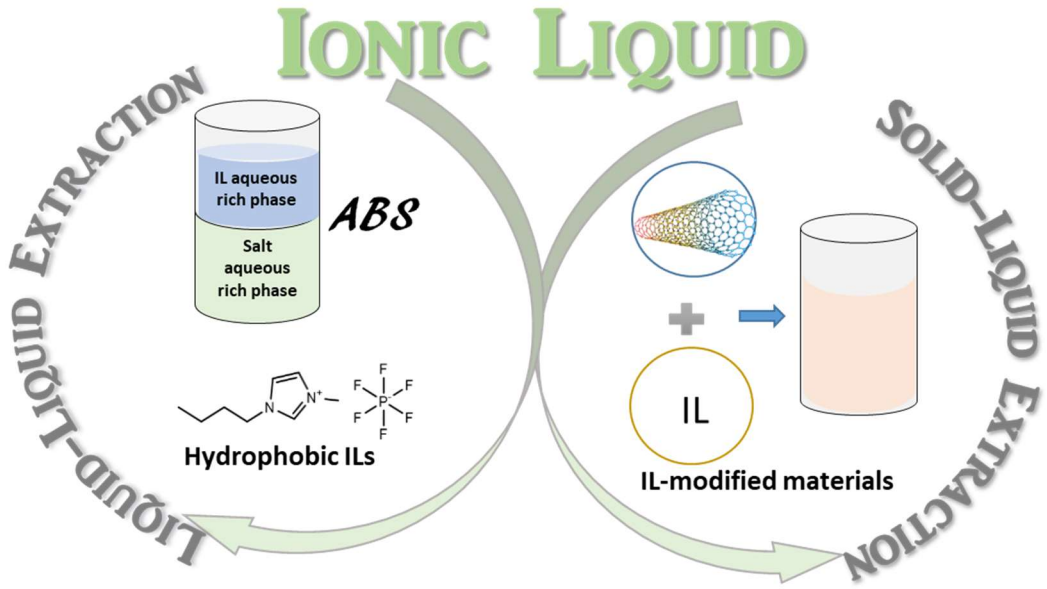

Figure 1.2. Overview of the use of ILs in liquid-liquid extractions, employing hydrophobic ILs and ABS, and solid-liquid extractions based on IL-modified materials.

1.2.2. ILs in liquid-liquid bioseparation processes

In the beginning of the 21st century, with the appearance of air and water-stable ILs, and more recently with the synthesis and characterization of bio-based ILs, the research on novel ILs and on their potential applications increased significantly. The major reasons behind this trend are the ILs unique properties, which can be tailored, including their ability to solvate a large array of compounds, coupled to the requisite of finding "greener" solvents to be applied in separation processes. The research carried out up to date in liquid–liquid extractions from aqueous media using water-immiscible ILs and water-soluble ILs by the creation of ABS for the separation of amino acids and proteins is reviewed and discussed below.

1.2.3. Water-immiscible ILs in liquid-liquid extractions

Table 1.1 lists the ILs that have been investigated and are discussed in this sub-chapter, including their description, abbreviations and chemical structures. IL-based liquid-liquid

approaches employing hydrophobic ILs to separate amino acids were pioneeringly proposed by Carda-Broch et al [18]. using a crown ether (dibenzo-18-crown-6)-modified IL, folowed by a report on a similar modified IL [19], namely dicyclohexano-18-crown-6-based, to extract the amino acids tryptophan, glycine, alanine, leucine, arginine, valine and lysine. Both groups of researchers showed that the partitioning behavior of amino acids is pH-dependent, and that ILs allow to obtain partition coefficients two orders of magnitude higher than those achieved without the respective crown ethers modifications [18, 19].

In addition to the functionalized ILs described above, more conventional imidazolium-based ILs ($[C_4C_1im][PF_6]$, $[C_6C_1im][PF_6]$, $[C_6C_1im][BF_4]$ and $[C_8C_1im][BF_4]$) were also tested for the recovery of tryptophan, phenylalanine, tyrosine, leucine, valine, lysine, alanine, and glutamic acid [20–22]. The authors [20] proposed hydrophobic interactions as the driving forces responsible for the enrichment of amino acids in the IL-phase, supported by a demonstrated correlation between the logarithm function of the partition coefficient and the hydrophobicity of the studied amino acids. Also in these works it was shown a pH-dependent partitioning behavior, where higher extraction efficiencies to the IL-rich phase are obtained at lower pH values [20, 21]. Therefore, these results support the existence of electrostatic interactions occurring between the cationic form of the amino acids and the IL anions in addition to the proposed dispersive-type interactions. Besides the well-studied imidazolium-based ILs, Tomé et al. [22] investigated the partition coefficients of L-tryptophan between water and different ILs, including pyrrolidinium-, piperidinium- and pyridinium-based. The authors demonstrated that pyrrolidinium-based ILs act as the better extraction phases amongst the ILs investigated [22]. These authors also demonstrated that the pH of the aqueous phase strongly influences the success of the amino acids separation [22].

Table 1.1. Description, abbreviation and chemical structure of non-water soluble ILs used in liquid-liquid extractions.

Description	**Abbreviation**	**Chemical Structure**
1-alkyl-3-methylimidazolium hexafluorophosphate	$[C_nC_1im][PF_6]$ (n = 4, 6, 8)	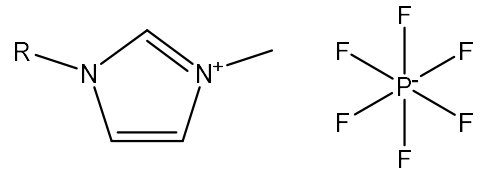
1-alkyl-3-methylimidazolium tetrafluoroborate	$[C_nC_1im][BF_4]$ (n = 6, 8)	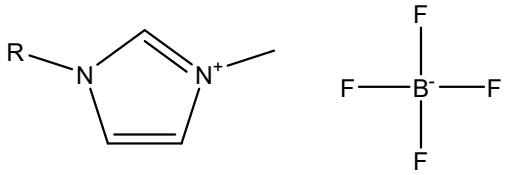
1-butyl-3-trimethylsilylimidazolium hexafluorophosphate	$[C_4(C_1C_1C_1Si)im][PF_6]$	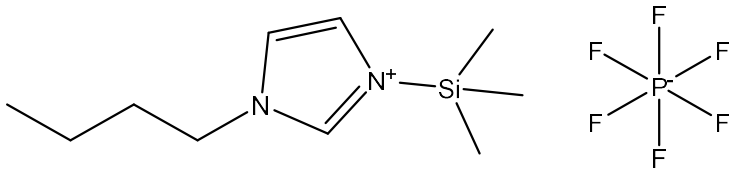
1-ethyl-3-methylimidazolium bis(trifluoromethylsulfonyl)imide	$[C_2C_1im][Tf_2N]$	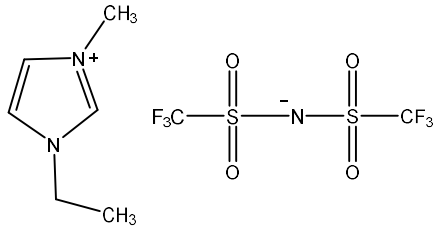

1-butyl-2,3-dimethylimidazolium bis(trifluoromethylsulfonyl)imide	$[C_4C_1C_1im][Tf_2N]$	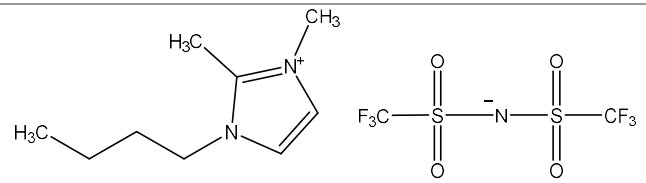
1,3-diethylimidazolium bis(trifluoromethylsulfonyl)imide	$[C_2C_2im][Tf_2N]$	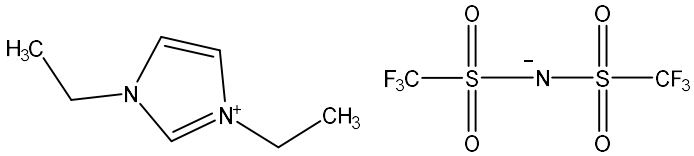
1-propyl-3-methylpiperidinium bis(trifluoromethylsulfonyl)imide	$[C_3C_1pip][Tf_2N]$	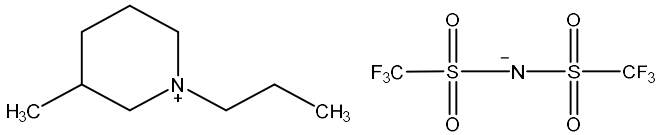
1-butyl-3-methylpyrrolidinium bis(trifluoromethylsulfonyl)imide	$[C_4C_1pyr][Tf_2N]$	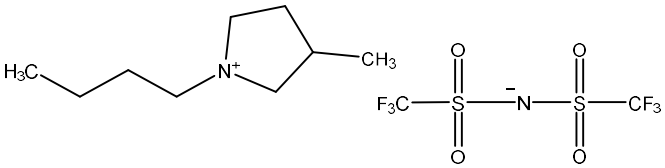
3-(2-(butylamino)-2-oxoethyl)-1-ethylimidazolium bis(trifluoromethylsulfonyl)imide	$[(CH_2CONHC_4H_9)C_2im][NTf_2]$	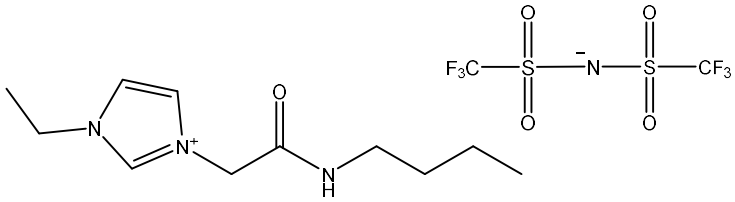

1-alkyl-3-methylimidazolium prolinate	[$C_nC_1$im][Pro] (*n* = 2, 6, 8)	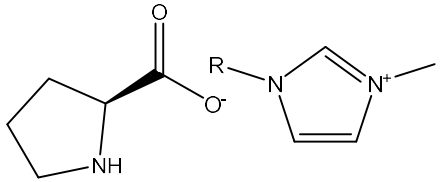
tetrabutylphosphonium *N*-trifluoromethanesulfonylleucine	[P_{4444}][Tf-Leu]	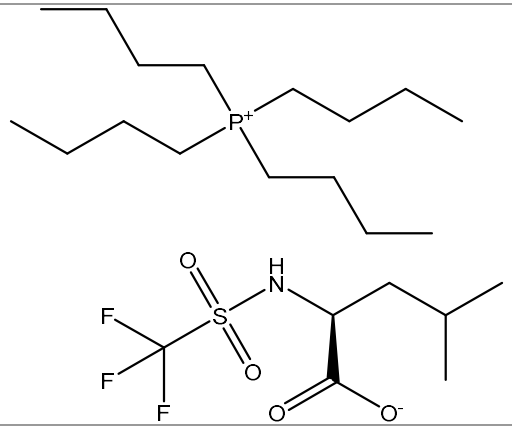

Huaxi et al. [23] synthesized a new hydrophobic amide-based functionalized IL, [($CH_2CONHC_4H_9$)C_2im][NTf_2], and evaluated its performance to extract amino acids. Again, the partition coefficients were shown to be dependent of the medium pH, while the new functionalized IL demonstrated to allow a higher partition coefficient and selectivity for L-tryptophan than more traditional ILs. Although contradicting in part the previous findings on the relevance of dispersive-type and electrostatic interactions [20–22], the IL enhanced performance was explained by the favourable hydrogen bonding interactions established between the acetyl group of the IL and the amino acid NH_2 group. All of the described works thus suggest that there is a wide plethora of interactions taking place, and that all are important for the separation of amino acids. Tang et al. [24] further employed functional hydrophobic amino-acid-based ILs as both solvents and selectors for the extraction of racemic mixtures of amino acids, being able to recover the L-enantiomer at the IL-rich phase. Most of the works described before addressed the pH effect on the amino acids partition coefficients, demonstrating that these biomolecules are better extracted to the IL-rich phase at acidic conditions. This pH dependence was additionally found to be useful to recover amino acids from the IL-rich phase [21, 23], which can be considered as a remarkable advantage in the recovery of target products from the non-volatile studied IL solvents.

In addition to amino acids, hydrophobic IL-water systems have been also investigated for the separation of proteins. It should be however highligthed that only a limited number of works on proteins extraction has been reported, which is probably due to the labile nature of proteins and the requeriment of a water-rich medium. Shimojo et al[25]. were the first to investigate the extraction of heme proteins using hydrophobic ILs from an aqueous phase through the addition of dicyclohexano-18-crown-6 (DCH18C6), demonstrating a high peroxidase activity of the cytocrome-c-DCH18C6 complex in the IL-phase. Tzeng et al. [26] used an imidazolium-based IL ([C_4C_1im]Cl) merged with a dye [silver salt Cibacron Blue 3GA (CB)] for the extraction of lysozyme, cytochrome-c, ovalbumin, and bovine serum albumin **(**BSA). As observed with amino acids, authors demonstrated that the proteins partitioning behaviour is pH-dependent, where an increase in pH leads to lower extraction efficiencies [26]. Accordingly, the authors discussed the relevance of electrostatic interactions between the solvent and the positive surface charge of lysozyme [26]. Finally, it was addressed the recyclability of the ILs used, showing that the IL phase could be reused for at least eight times without losses on the systems extraction performance [26].

Kohno et al. [27] functionalized an IL with leucine, [P_{4444}][Tf-Leu]. Although being hydrophobic, this IL still dissolves a high water content, and with 21 wt% of water cytochrome-

c was completly extracted into the IL-rich phase. Other proteins (lysozyme, myoglobin, chymotrypsin, laccase, hemoglobin, horseradish peroxidase and BSA) were also investigated, leading to the conclusion that this IL is not capable of extracting laccase and horseradish peroxidase. Ohno and co-workers[28] also investigated the cytochrome-c extraction using a phosphonium-type zwitterion, while attempting the control of the water content at the zwitterion phase. By combining different zwitterions, authors [28] were able to increase the water content from 0.4 to 62.7%, favorable to increase the dissolution and partition of the target protein. Finally, the authors demonstrated the back-extraction of the protein by the addition of an inorganic salt, without significant changes in the structure of the recovered protein [28]. Two works regarding the extraction of recombinant proteins using a triazacyclononane-IL phase were recently published [29, 30]. Authors demonstrated that the selective partitioning of hexahistidine-tagged (His-tagged) proteins between the IL and aqueous phases is governed by the proteins' affinity to the IL, the presence and nature of coordinated metal ions, and by the medium ionic strength.

In addition to the studies carried out with pure and model proteins discussed above, Cheng et al. [31] reported the direct extraction of hemoglobin from human whole blood using $[C_4(C_1C_1C_1Si)im][PF_6]$. The same non-water miscible IL was applied in the extraction of cytochrome-c from an aqueous solution [32]. In both works [31, 32], a pH-dependent back-extraction process to recover proteins and the IL was developed. In the same line, Hu et al. [33] addressed the separation of bacteriorhodopsin from *Halobacterium salinarium* using the IL $[C_6C_1im][PF_6]$, where it was shown that this IL displays a high capacity to remove the main contaminants (lipids, proteins and sugars). Imidazolium-based hydrophobic ILs ($[C_4C_1im][NTf_2]$ and $[C_4C_1im][PF_6]$) were also used to separate lactoferrin from bovine whey[34]. It was found that the IL extraction efficiency is enhanced at neutral pH, low ionic strength and low concentration. Even so, the maximum extraction efficiencies reported to the IL-rich were *ca*. 20%. Therefore, hydrophobic ILs seem more attractive to tailor the extractions selectivity than to obtain enhanced extraction efficiencies.

Overall, the aforementioned works show that under appropriate conditions and using adequate IL chemical structures, hydrophobic ILs are enhanced extraction media to recover amino acids and proteins from aqueous solutions. The range of hydrophobic ILs is however more limited than hydrophilic (water-soluble) ones typically used in the formation of IL-based ABS, discussed in the next section, which may impose some constraints in the design of effective separation processes. Furthermore, most studies described above were focused on ILs formed by imidazolium-based cations, mainly combined with fluorinated anions, raising thus concerns

in terms of the ILs biocompatibility. When dealing with proteins, water content seems to be a relevant issue, which may also justify the scarce number of works dealing with hydrophobic ILs to separate proteins.

1.2.4. Water-soluble ILs in liquid-liquid extractions

The limited number of hydrophobic ILs when compared to hydrophilic (water-soluble) ones and its impact in terms of chemical structure design, coupled to the low water content in the first set, are the main reasons behind the significantly larger number studies found with IL-based ABS for the separation of amino acids and proteins. In fact, a vaster number of water-miscible ILs can be considered for the formation of ABS, while their environmental and toxicity impact is also reduced [16]. The fundamentals and applications of IL-based ABS were recently reviewed [4]. In this section, we will only focus on their use for the separation of amino acids and proteins, while highlighting some recent and innovative works. The description, abbreviations and chemical structures of the ILs used and discussed in this section are given in Table 1.2.

Table 1.2. Description, abbreviation, and chemical structure of the ILs used in the formation of ABS for liquid-liquid extractions.

Description	Abbreviation	Chemical Structure
1-alkyl-3-methylimidazolium bromide	$[C_nC_1im]Br$ (n = 2,4, 6, 8)	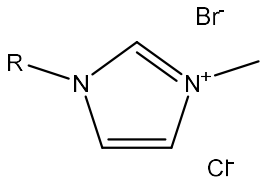
1-alkylimidazolium chloride	$[C_nim]Cl$ (n = 1,2)	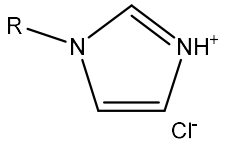
1-alkyl-3-methylimidazolium chloride	$[C_nC_1im]Cl$ (n = 2, 4, 6, 8)	
1-butyl-2,3-dimethylimidazolium chloride	$[C_4C_1C_1im]Cl$	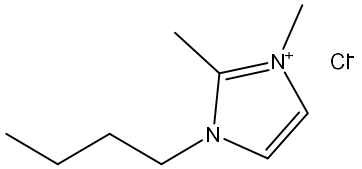
1-allyl-3-methylimidazolium chloride	[amim]Cl	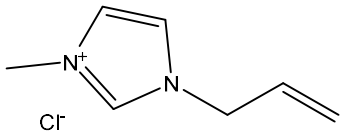
1-hydroxyethyl-3-methylimidazolium chloride	$[OHC_2mim]Cl$	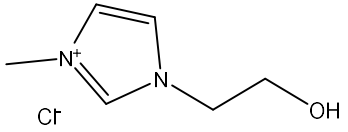

1-benzyl-3-methylimidazolium chloride	$[C_7H_7C_1im]Cl$	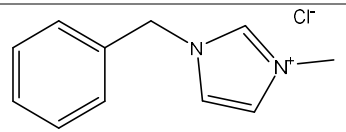
1-alkyl-3-methylimidazolium acetate	$[C_nC_1im][CH_3CO_2]$ (n = 2, 4, 6)	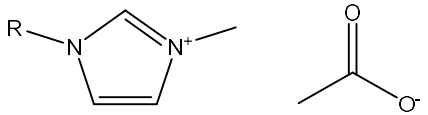
1-ethyl-3-methylimidazolium alkylsulfate	$[C_nC_1im][C_nSO_4]$ (n = 1, 2)	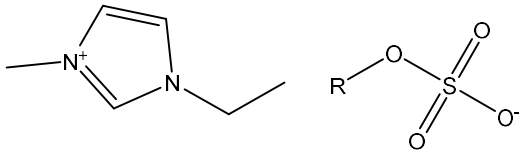
1-alkyl-3-methylimidazolium trifluoromethanesulfonate	$[C_nC_1im][CF_3SO_3]$ (n = 2, 4, 6)	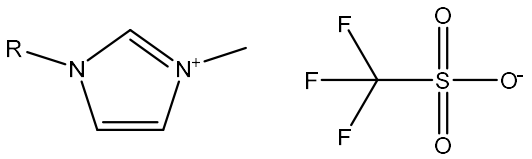
1-alkyl-3-methylimidazolium methanesulfonate	$[C_nC_1im][CH_3SO_3]$ (n = 2, 4)	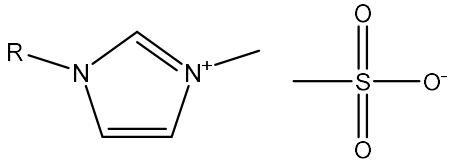
1-butyl-3-methylimidazolium hydrogensulfate	$[C_4C_1im][HSO_4]$	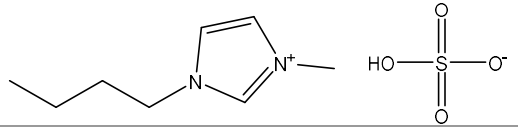

tetraalkylammonium chloride	[N*nnnn*]Cl (*n* = 2, 4)	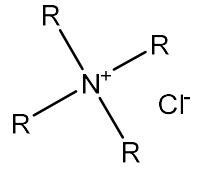
tetraalkylammonium bromide	[N*nnnn*]Br (*n* = 2, 4)	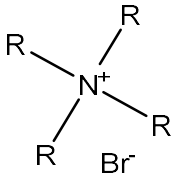
tetrabutylphosphonium chloride	[P_{4444}]Cl	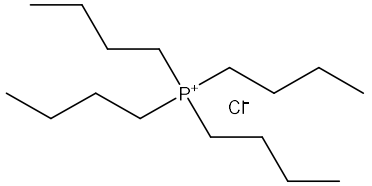
tetrabutylphosphonium bromide	[P_{4444}]Br	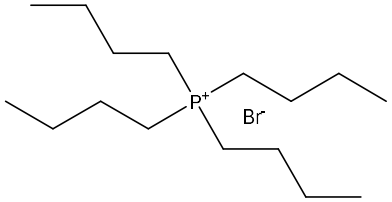
triisobutyl(methyl)phosphonium tosylate	[$P_i(_{444})_4$][Tos]	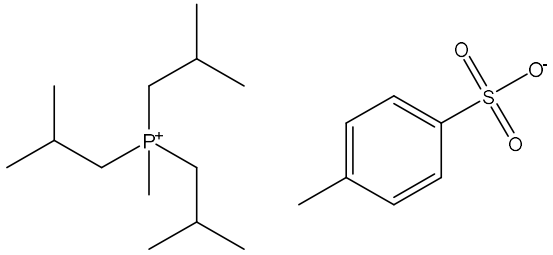

tributyl(methyl)phosphonium methylsulphate	$[P_{4441}][MeSO_4]$	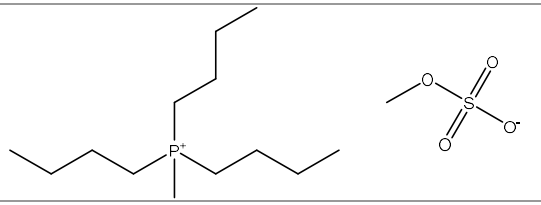
1-butyl-3-methylimidazolium tetrafluoroborate	$[C_4C_1im][BF_4]$	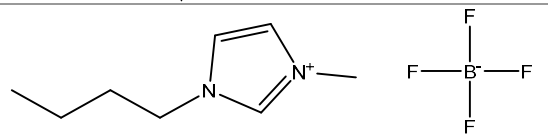
1-butyl-3-methylimidazolium thiocyanate	$[C_4C_1im][SCN]$	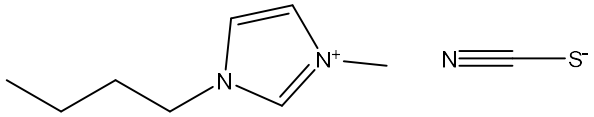
1-butyl-3- methylimidazolium dicyanamide	$[C_4C_1im][N(CN)_2]$	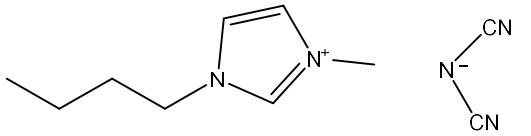
1-butyl-3-methylimidazolium tosylate	$[C_4C_1im][TOS]$	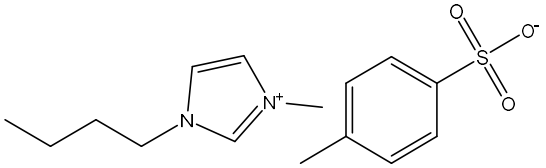
1-ethyl-1-methylpyrrolidinium trifluoromethanesulfonate	$[C_2C_1pyr][CF_3SO_3]$	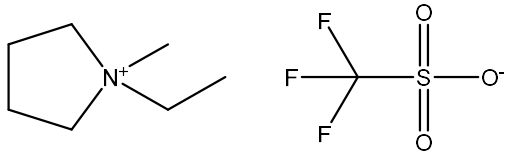

1-ethyl-3-methylimidazolium butylsulfate	$[C_2C_1im][C_4SO_4]$	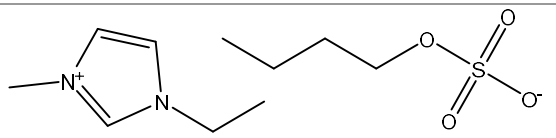
1-ethyl-3-methylimidazolium dimethylphosphate	$[C_2C_1im][DMP]$	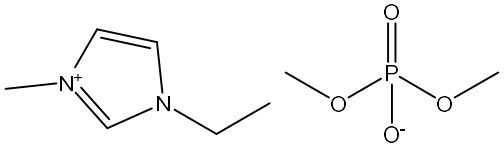
tri(butyl)methylphosphonium methylsulfate	$[P_{4441}][MeSO_4]$	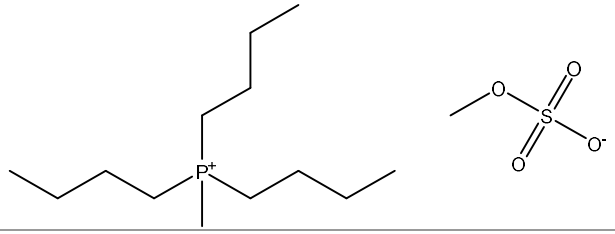
***N,N* – dimethylethanolamine alkanoate**	$[N_{011(2OH)}][C_nCO_2]$ (n = 3, 4, 5, 6)	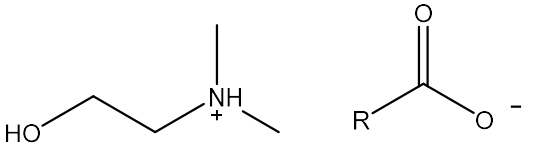
***N,N* – diethylethylenediamine alkanoate**	$[N_{022(2OH)}][C_nCO_2]$ (n = 3, 4, 5, 6)	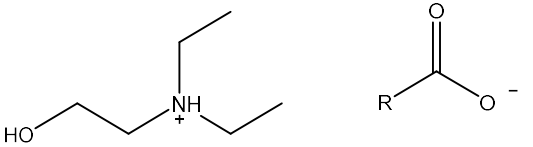
tetraalkylammonium glycine	$[N_{nnnn}][Gly]$ (n = 1, 2, 4, 5)	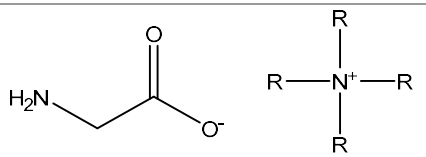

tetrabutylphosphonium glycine	$[P_{4444}][Gly]$	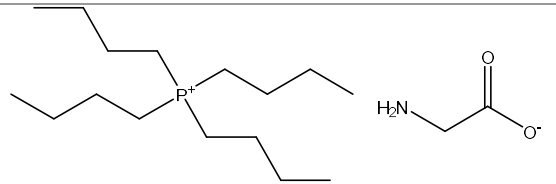
cholinium 2-[4-(2-hydroxyethyl)piperazin-1-yl]ethane sulfonate	$[N_{111(2OH)}][HEPES]$	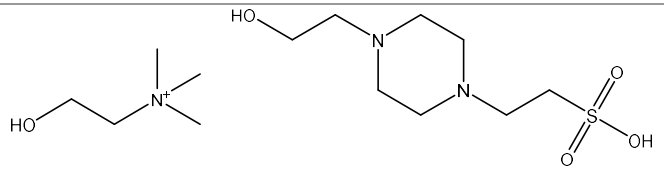
cholinium N-[tris(hydroxymethyl)methyl]glycine	$[N_{111(2OH)}][Tricine]$	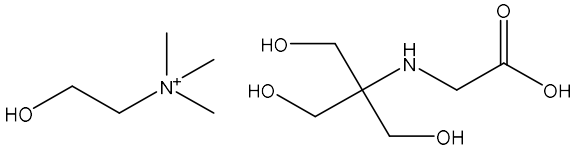
cholinium 2-(cyclohexylamino)ethanesulfonate	$[N_{111(2OH)}][CHES]$	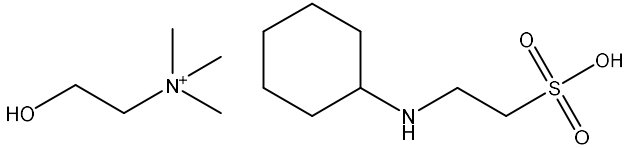
cholinium 2-(N-morpholino)ethanesulfonate	$[N_{111(2OH)}][MES]$	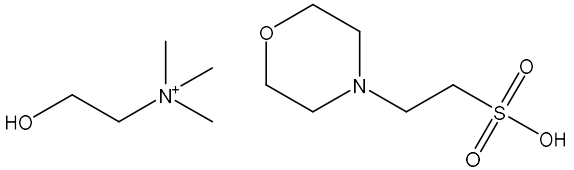
cholinium 2-[(2-hydroxy-1,1-bis(hydroxymethyl) ethyl)amino]ethanesulfonate	$[N_{111(2OH)}][TES]$	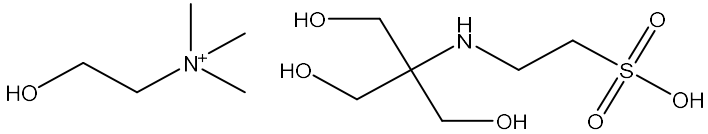

cholinium chloride	$[N_{111(2OH)}]Cl$	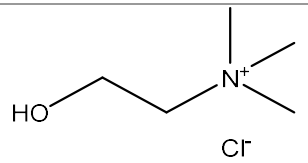
cholinium alkanoate	$[N_{111(2OH)}][C_nCO_2]$ (n = 2, 3, 4)	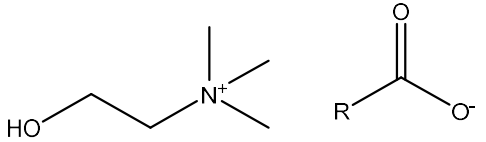
cholinium bitartarate	$[N_{111(2OH)}][Bit]$	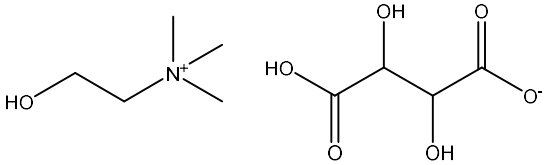
cholinium dihydrogencitrate	$[N_{111(2OH)}][DHCit]$	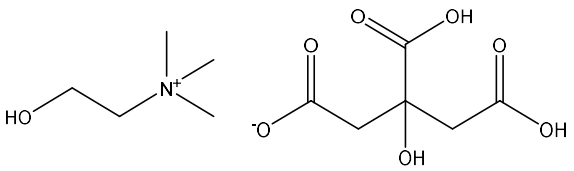
cholinium dihydrogenphosphate	$[N_{111(2OH)}][DHP]$	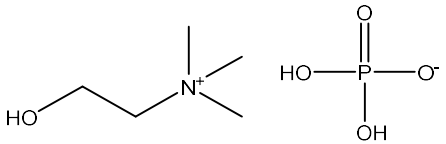
cholinium glycolate	$[N_{111(2OH)}][Gly]$	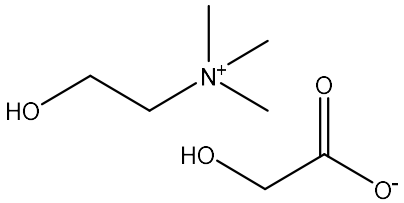

cholinium lactate	$[N_{111(2OH)}][Lac]$	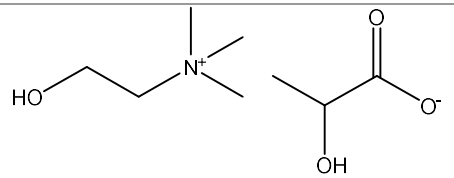
cholinium benzoate	$[N_{111(2OH)}][BE]$	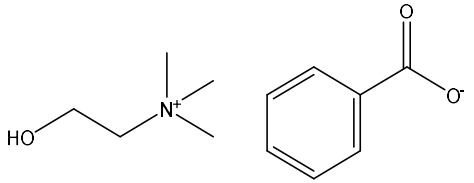
di-cholinium oxalate	$[N_{111(2OH)}]_2[Ox]$	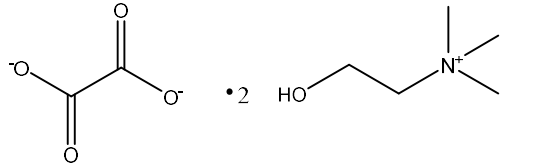
tri-cholinium citrate	$[N_{111(2OH)}]_3[cit]$	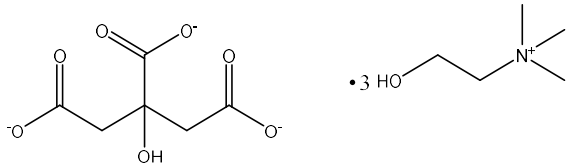

The extraction of a wide range of amino acids (Figure 1.3) has been investigated using IL-based ABS, while the pioneering work in this field was demonstrated in 2009 [35,36]. ABS formed by $[C_nC_1im][C_1CO_2]$ (n = 4, 6, 8) or $[C_nC_1im]Br$ (n =4, 6, 8) and inorganic salts (K_3PO_4, K_2HPO_4, and K_2CO_3) were further explored for the separation of tryptophan, glycine, alanine, 2-aminobutyric acid, valine, leucine, threonine, methinoine and tyrosine [37, 38]. In these works [37, 38] it was found that ILs with more hydrophobic cations lead to best extraction results, which is in contradiction with the results of Louros et al. [39] with ABS formed by phosphonium-based ILs in the extraction of common amino acids. Additional investigations on the separation of amino acids (L-tryptophan, L-phenylalanine, L-tyrosine, L-leucine, and L-valine) by IL-based based ABS were carried out by Zafarani-Moattar and Hamzehzadeh [40]. The authors concluded that hydrophobic interactions are the main forces responsible for the amino acids preferential migration to the IL-rich phase, although other parameters, such as amino acid size, accessible surface area and polarizability were described as also relevant. ABS formed by several types of ILs, namely imidazolium-, pyrrolidinium-, phosphonium- and ammonium-based ILs, for the separation of L-tryptophan, were latter investigated [41]. A high extraction performance was displayed by these systems, with extraction efficiencies ranging between 72% and 99% [41]. Contrarily to the trend observed with hydrophobic ILs, with IL-based ABS lower partition coefficients were observed at lower pH values. This trend is however predictable since in the studied ABS a citrate-based salt is used, which at lower pH values is protonated and thus acts as a weaker salting-out species. Furthermore, two imidazolium-based chiral ILs were synthesized to separate racemic amino acids [42]. The gathered results showed that D-enantiomer amino acids partition to the IL-rich phase, whereas L-enantiomer amino acids are transferred into the Na_2SO_4-rich phase. Overall, all these works combining ABS formed by ILs and salts lead to significantly higher extraction efficiencies than those observed with more conventional ABS formed by polymers and salts [43].

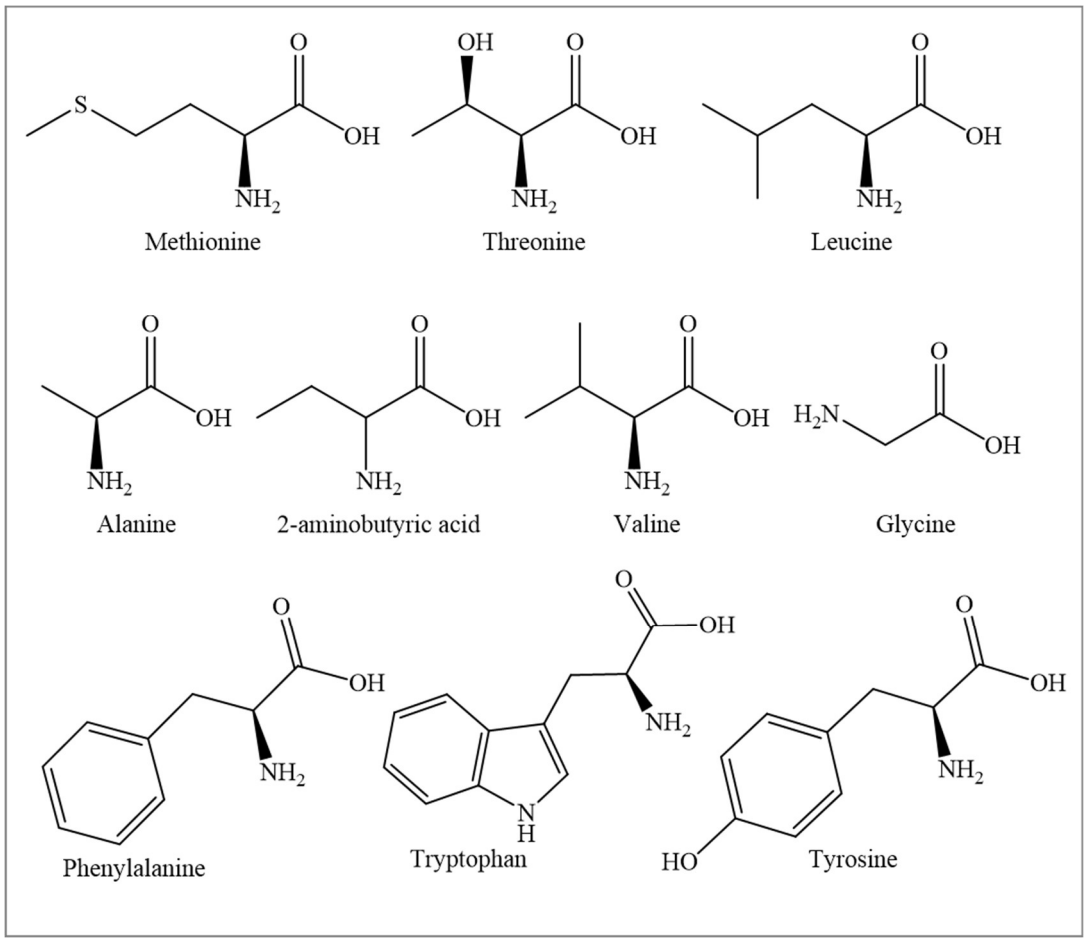

Figure 1.3. Chemical structures of amino acids separated with IL-based ABS.

Aiming the design of biocompatible ABS, Zafarani-Moattar and Hamzehzadeh [44] proposed ABS formed by polypropylene glycol (PPG) 400 (instead of salts) and hydrophilic ILs, [$C_nC_1$im]Br (n = 2, 4), for the extraction of L-tryptophan and L-tyrosine. In this type of polymer-IL-based ABS, and contrarily to the behavior observed in IL-salt ABS, L-tyrosine displays a preferential partition towards the polymer-rich phase, while L-tryptophan preferentially migrates to the IL-rich phase. This difference was explained according to the lack of one pyrrole ring in L-tyrosine when compared to L-tryptophan [44]. Nevertheless, it should be highlighted that in this type of systems the strong salting-out species, *i.e.* salts, were replaced by polymers, and thus there is a more tailored balance between the nature and properties of the phase-forming components and the target amino acids partition between the coexisting phases. Focused on the same goal, Xie et al. [45] investigated novel ABS formed by biocompatible ILs, composed of the cholinium cation and anions derived from long chain carboxylic acids. The authors [45] showed that ILs with long chain carboxylate anions are favorable to improve the systems extraction

performance. Freire et al. [46] also replaced the typically used inorganic/organic salts by mono- and disaccharides combined with $[C_4C_1im][CF_3SO_3]$ to form ABS, and evaluated the performance of these systems to extract amino acids. Despite the advantages of the biodegradable and nontoxic nature of carbohydrates, the extraction efficiencies obtained in this work were significantly lower (*ca.* 50%) than those previously discussed with ABS formed by ILs and salts. Organic biological buffers, namely Good's Buffers, were later used in combination with ILs to form ABS to recover L-tryptophan and L-phenylalanine from aqueous media [47]. In these systems, L-phenylalanine completely partitions to the GB-rich phase, while L-tryptophan shows a preferential migration to the opposite phase. These systems [47] and those reported by Zafarani-Moattar and Hamzehzadeh [44] can be thus employed in the fractionation of amino acids from complex mixtures, such as fermentation broths or hydrolysed peptide mixtures, and should be explored in such a direction. With this idea in mind, recently, Capela et al. [48] demonstrated the formation of IL-amino-acid-based systems, which allow the selective separation of mixtures of aliphatic and aromatic amino acids in one-step (Figure 1.4). These systems were designed based on the particular ability of aliphatic amino acids to form ABS with ILs. Finally, authors [48] used a solid-phase extraction approach, by means of a cation exchange column, to retain the ILs used in ABS formation and thus recover the target amino acids.

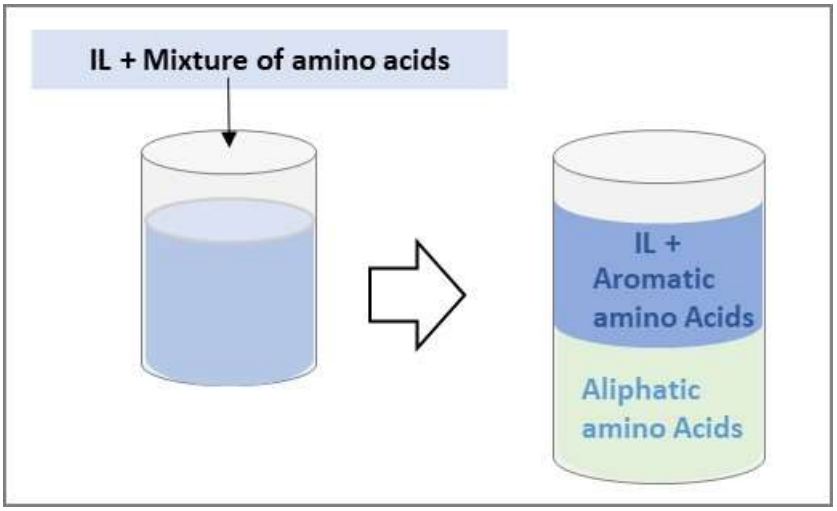

Figure 1.4. Schematic representation of the selective separation of aliphatic and aromatic amino acids mixtures (adapted from [48]).

In addition to IL-salt and IL-polymer ABS, the use of ILs as additives in polymer-salt systems have been explored to tailor the separation of amino acids. Pereira et al. [13] investigated several imidazolium-based ILs added at 5 wt% to an ABS formed by polyethylene glycol PEG 600 and $NaSO_4$. The authors [13] demonstrated that both an increase and decrease in the extraction efficiencies can be obtained, and that these depend on the chemical structure of the IL

employed. In the same line, [C_4C_1im]Br was also investigated as an adjuvant in PEG 400 + potassium citrate ABS to tailor the partition of amino acids towards the polymer-rich phase[49]. In summary, a large number of IL-based ABS and amino acids have been investigated in the past decade, whereas in most cases high extraction efficiencies to the IL-rich phase are obtained in a single-step. However, with ABS not employing salts, but instead polymers or biological buffers, there is a more amenable tailoring of the amino acids partitioning, which could be useful to separate mixtures of amino acid from real matrices. With systems not composed of strong salting-out species there is a more tailored balance between the nature and properties of the phase-forming components and the target amino acids partition between the coexisting phases. In terms of effectiveness and cost, the most adequate systems for extracting amino acids are those using ILs as adjuvants, mainly because they also allow high extraction efficiencies associated to reduced costs by the low amounts of ILs used. Although poorly investigated, Capela et al. [48] demonstrated the potential of ILs to be added directly to aqueous mixtures of amino acids allowing their direct fractionation. The same authors demonstrated the amino acid recovery from the IL-rich phase by applying a cation exchange column, allowing the IL reuse, which is a scarcely investigated strategy [48].

In addition to amino acids, IL-based ABS have been investigated as separation strategies for several proteins, namely BSA, hemoglobin, ovalbumin, lysozyme, myoglobin, immunoglobulin Y, immunoglobulin G, cytochrome c, trypsin, pepsin, and rubisco. Due to the labile nature of proteins, they are easily denatured by organic solvents or hydrophobic ILs, and therefore ABS are more appropriate media due to their high water content. Proteins are highly sensitive biomolecules and can lose their native structure by slight changes in the surrounding environment, such as changes in pH, temperature, and ABS phase-forming component compositions. Several works have been conducted in this direction, *i.e.* aiming at understanding the effect of several parameters and phase-forming components on the partition behavior of proteins in IL-based ABS. For instance, the influence of pH, IL concentration, temperature, protein size, conformation and surface structure were studied a large number of proteins. Studies at variable pH values showed that the extraction efficiency of cytochrome-c decreases as the pH increases [50], whereas the water content in the coexisting phases also demonstrated to play a role [51]. Pei et al. [52] explored IL-based ABS to recover proteins from wastewater, using BSA, lysozyme and hemoglobin as model proteins. In this work, hydrophobic interactions were identified as the driving forces in the proteins partitioning amongst the coexisting phases, since the complete extraction into the IL-rich phase was only achieved when the pH of the systems was close to the proteins pI [52]. Authors [52] further demonstrated that higher temperatures favor the protein extraction, contradicting previous results on the extraction of

BSA using [$C_{10}C_1$im]Cl-based ABS [53], meaning that both endothermic and exothermic processes may occur, and that these depend on the protein and phase-forming components used. Lin et al. [54] described the relevance of IL-protein complexes on the extraction performance of IL-based ABS, being in agreement with the findings of Pei and co-authors [55]. An additional study on the partitioning of model proteins (lysozyme, myoglobin, BSA) was performed in IL + salt ABS, however using a dye (Reactive Red-120) as ligand to afford affinity-induced partitions [56]. Authors demonstrated that the nature of the proteins, pH, temperature and ABS composition are parameters that influence the partition coefficients. In this work [56], the hydrophilic IL used was recovered by adding a hydrophobic one [C_4C_1im][PF_6] that acted as extractant.

In addition to the well-studied imidazolium-based ILs, the separation of BSA, ovalbumin and hemoglobin was also addressed using a series of protic ammonium-based ILs [57]. Under optimum conditions, N,N-dimethylethanolamine propionate [$N_{11(2OH)}$][C_2CO_2] allows extraction efficiencies up to 99.5% in a single-step [57]. Furthermore, it has been reported that the stability of lysozyme in ammonium-based ILs decreases with the IL concentration [58]. The separation of cytochrome-c was investigated by Santos et al. [59], using a quaternary system formed by PEG 8000, sodium poly(acrylate) (NaPA8000), water, and ILs as electrolytes. With these systems cytochrome-c is enriched in the NaPA8000-rich phase (extraction efficiency > 96%).

Foreseeing the development of biocompatible IL-based ABS, Wu et al. [60] employed amino-acid-based ILs combined with K_2HPO_4 to separate cytochrome-c, which preferentially partitions to the IL-rich phase. In the same line, [$N_{111(2OH)}$]Cl and related ILs were used in the design of ABS to extract and purify proteins (BSA, trypsin, papain and lysozyme) [61, 62]. With an ABS formed by [$N_{11(2OH)(3OH)}$]Cl and KH_2PO_4, BSA is mainly enriched in the IL-rich phase (extraction yield of 84.3%), thus representing better alternatives to ABS formed by imidazolium-based fluids (extraction yields ranging between 60 and 68%) [61]. ILs formed by the cholinium cation and anions derived from carboxylic acids, namely [$N_{111(2OH)}$][C_1CO_2], [$N_{111(2OH)}$][C_2CO_2], [$N_{111(2OH)}$][C_3CO_2], [$N_{111(2OH)}$][Glyc], [$N_{111(2OH)}$][Lac], [$N_{111(2OH)}]_2$[Oxa] and [$N_{111(2OH)}]_3$[Cit], were combined with PPG400 (a non-toxic, biodegradable and thermo-sensitive polymer) to form ABS, demonstrating to be enhanced systems to separate proteins [62]. Cholinium-based ILs and PPG400 were used in three other works to extract BSA[63–65]. The preferential partition of BSA to the IL-rich phase was always observed, with two of these works reporting the complete extraction of BSA into the IL phase in a single-step [63, 64]. In both works, the partition of BSA seems to be dictated by specific interactions occurring between the protein and the IL, such as hydrogen bonding and dispersive interactions. The remarkable extraction efficiencies obtained (between 92 % and 100 % for the IL-rich phase) were far superior to those observed with typical

polymer-based ABS, and without evidence of protein denaturation in concentrations at the aqueous media up to 10 $g.L^{-1}$ [64]. The authors further corroborated their results by extracting BSA from bovine serum, where the extraction efficiencies for the target protein were kept at 100% in a single-step. The BSA partition behavior in ABS formed by ILs composed of cholinium as cation and amino-acid-derived anions was then investigated by Song et al. [65]. In this work, the authors manipulated the interactions between the phase-forming components and the proteins by changing their surface charge through pH variations. When the pH of the system was higher than the pI of the proteins and the amino acid anions, proteins mainly partition to the IL phase, whereas the reverse occurs at lower pH values [65].

In most of the works described before, a buffered salt aqueous solution was used to maintain the medium pH. Recently, ILs with self-buffering characteristics, namely Good's buffer ILs (GB-ILs), were suggested, and their ability to form ABS and to extract BSA evaluated [66]. Remarkably, extraction efficiencies of 100% of BSA to the GB-IL rich phase were obtained in a single-step. Authors also found that GB-ILs display a higher stabilizing effect over the studied protein when compared to conventional ILs [66]. Recently, protic ILs were proposed to form thermoreversible ABS when combined with polymers [67]. Contrarily to imidazolium-based ILs, the phase diagrams of ABS formed by protic ILs display a large dependence on temperature, thus allowing monophasic-biphasic transitions by small changes in temperature. The complete extraction of cytochrome-c and azocasein was accomplished in a single-step using these systems and maintained along three cooling-heating cycles, with no stability losses [67].

Most studies discussed before were carried out with pure/model proteins, and only the extraction efficiency of IL-based ABS and their impact on the proteins stability and enzymes activity were addressed. Nevertheless, proteins with biological, clinical, pharmaceutical and industrial relevance are produced in complex media, therefore requiring downstream processes for their purification and recovery. Even so, few works are find on the application of IL-based ABS to separate proteins from real matrices. Among these, Taha et al. [68] prepared novel ABS formed by self-buffering cholinium-based ILs and PPG 400 for the separation of immunoglobulin Y (IgY) from chicken egg yolk. The combination of the investigated ILs with PPG 400 to form ABS allow the preferential partition of IgY to the IL-rich phase, with extraction efficiencies ranging between 79 and 94% in a single-step. Still, the greatest challenge was to purify IgY, since the total separation of IgY from the major contaminant proteins was not achieved [68]. In the same line, Ferreira et al. [69] investigated the separation of immunoglobulin G (IgG) from a rabbit serum source, using ABS composed of PEG of different molecular weights and potassium citrate, with 5 wt% of ILs as adjuvants. The tuning ability of ILs was confirmed since the complete extraction (100%) of the target antibody was obtained in a single-step, as well as higher recovery

yields and enhancements in the IgG purity, by applying ILs (as compared to the IL-free ABS). More recently, ABS formed by cholinium-based ILs + PPG 400 were investigated to separate IgG from rabbit serum [70, 71]. These systems allowed an efficient extraction performance and recovery yields > 80% , with a purity level up to 66% [71].

Still dealing with more complex matrices, Desai and co-workers [72] addressed the recovery of rubisco from plant extracts using ABS formed by ammonium-based ILs (Ammoeng 110) and phosphate salts. Rubisco migrates to the IL-rich phase with partition coefficients 3-4 times higher than those obtained with PEG-based systems. However, at high concentrations of ILs (>50%), the studied protein starts to aggregate, demonstrating that there is a limited range of appropriate ILs concentrations to be used in proteins extraction [72]. Pei and co-workers applied IL-based ABS to separate proteins from polyssacharides [55]. BSA was successively separated into the IL-rich phase, with saccharides preferentially enriched into the opposite phase. Similar studies were further published aiming the fractionation of sugars and proteins from plants extracts [57, 73, 74]. In order to decrease the environmental and economic impact of IL-based ABS as separation strategies for proteins, some studies attempted to recover the ABS phase-forming components after the extraction of proteins [73–75]. For instance, Freire and co-workers studied the recyclability and reusability of phosphonium- and ammonium-based ILs after the extraction of BSA into the IL-rich phase, by recovering the protein by dialysis [75]. Extraction efficiencies were kept at 100% in three-step sequential extractions comprising both the BSA recovery and the IL reusability. With the same purpose, Li et al. [62] used a thermosensitive polymer in the formulation of ABS allowing its recovery by temperature increase (Figure 1.5).

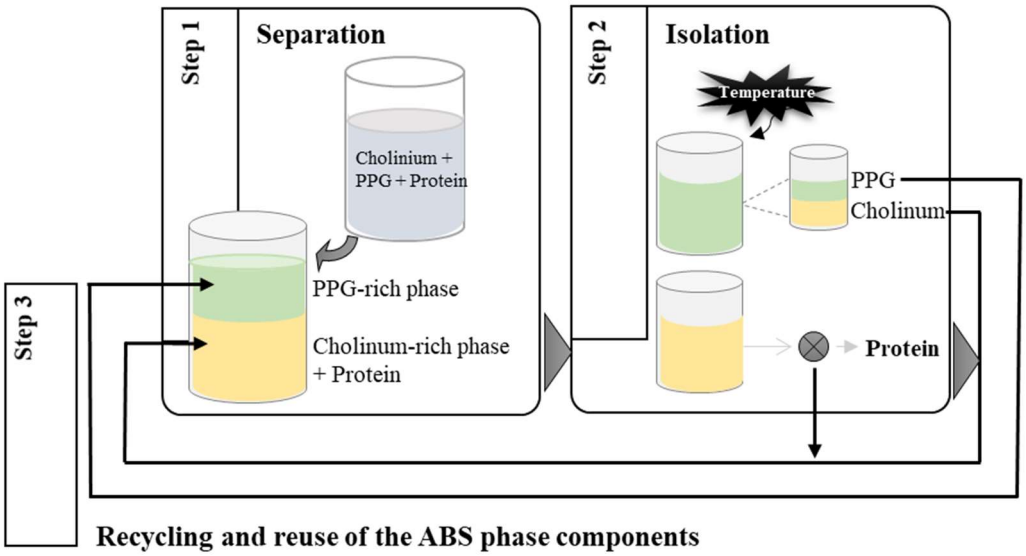

Figure 1.5. Schematic representation of the separation and recovery steps of the ABS phase-forming components and proteins by a temperature increase (adapted from [62]).

IL-based ABS were also investigated to separate lipases [76–82]. Deive et al. [76] explored the partition behavior of Thermomyces lanuginosus lipase (TLL), where under optimized conditions the authors recovered 99% of TLL from aqueous solutions, while preserving the enzyme biocatalytic activity [76]. The same research group employed ABS formed by ILs and inorganic salts to separate *Candida antarctica* lipase A (CaLA) [77]. The results obtained revealed that ABS formed by $[C_2C_1im][C_4SO_4]$ allow extraction efficiencies higher than 99%. Additional investigations on lipase (*C. antarctica* lipase B, CaLB) partitioning were carried out by Ventura et al. using a wide variety of IL-based ABS [78]. With IL + salt ABS, the enzyme recovery efficiencies are higher than 97%, with a maximum purification factor of 2.6. The same group of researchers then applied IL-ABS as downstream processes to purify an extracellular lipolytic enzyme produced by *Bacillus* sp. ITP-001 from its fermentation broth [79]. The best results were obtained with ABS formed by $[C_8C_1im]Cl$ (recovery = 92.2% and purification factor (PF) = 51). Finally, the authors applied ABS formed by polymers and salts, while using ILs as adjuvants[80]. With this type of systems, a significant increase in the PF was achieved (PF = 245, when compared with IL-based ABS (PF ≈ 51-137) [78, 81] and with polymer-based ABS (PF = 202) [79]. This last type of ABS also allows a decrease of the concentration of the IL employed, thus resulting in a more sustainable separation process. Recently, the same group of researchers [82] investigated the impact of different cations and anions of self-buffering ILs to form ABS when conjugated with salts or polymers aiming at recovering lipase produced via submerged fermentation by *Burkholderia cepacia* ST8. The authors showed that lipase preferentially partitions towards the IL-rich phase in both types of systems investigated, with a recovery yield of 94% [82].

In addition to lipases, other enzymes have been investigated with IL-based ABS. ABS formed by $[C_4C_1im]Cl$ or $[C_4C_1im]Br + K_2HPO_4$ have been investigated to separate papain [83]. The increase of $[C_4C_1im]Br$ and K_2HPO_4 concentrations allow a maximum extraction of 98% to the IL-rich phase [83]. A similar ABS has been applied to the extraction of horseradish peroxidase, with a recovery of 80% into the IL-rich phase and preservation of more than 90% of the enzyme activity [84]. Several ABS (polymer-polymer, polymer-salt, alcohol-salt, and IL-salt) were studied for the recovery of superoxide dismutases (SOD) by Simental-Martinez et al. [85]. The authors found that although IL-based ABS allow a better enzyme recovery, a polymer-salt ABS is more adequate in terms of SOD recovery, enzyme specific activity maintenance and purification. Recently, Santos et al. demonstrated an efficient integrated downstream process for the purification of L-asparaginase (ASNase) using IL-based ABS (Figure 1.6) [86]. In this work it was evaluated the use of polymer-salt ABS employing ILs as adjuvants, combined with the permeabilization of cell membrane using *n*-dodecane and glycine for the in situ purification of periplasmatic ASNase

from *Escherichia coli* cells. The results obtained show that ASNase partitions mostly to the PEG-rich phase, which was explained based on hydrophobic interactions established between the polymer and the enzyme. With the addition of 5 wt% of $[C_4C1im][CH_3SO_3]$, recoveries of the enzyme up to 88% have been reported.

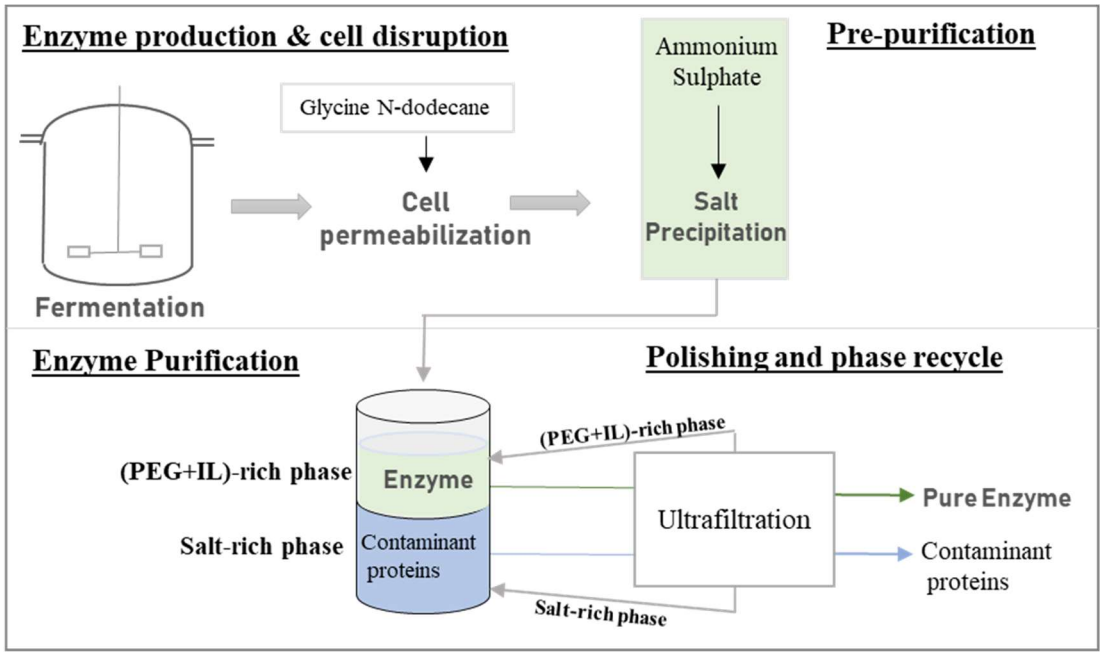

Figure 1.6. Schematic representation of the in situ purification of enzymes with the recycling of the ABS phase-forming components (adapted from [86]).

Jiang and co-authors [87] evaluated IL-based ABS for the extraction and purification of wheat esterase. It was demonstrated that the enzyme preferentially partitions into the IL-rich phase, and under optimized conditions an extraction yield of 88.93% and a purification factor of 4.23 were obtained [87]. Aiming the purification of proteins in continuous mode, Novak et al. [88] addressed the intensification of BSA purification by IL-based ABS applying microfluidic devices. By adjusting the fluid flow pattern, the BSA extraction within the microchannels was successfully carried out, yielding partition coefficients of 14.6, 20-fold higher than those achieved with conventional ABS composed of polymers and salts [88]. Amongst the several advantages of IL-based ABS over more conventional systems, the low viscosity of the coexisting phases was reported as the most significant within the microfluidics approach [88].

Within IL-based ABS for the separation of proteins, it is clear that the largest fraction of published works is devoted to studies on the partition of model proteins and enzymes, which give no indications on the behavior of contaminants and how these systems are useful to purify proteins from complex matrices. Some works started however to appear on the application of IL-based ABS to separate proteins from biological-based media, showing that IL-based ABS represent a promising alternative to deal with complex matrices. Nevertheless, the major

challenge still is to optimize the ILs chemical structures to separate target proteins, which differ for each protein and matrix.

1.2.5. ILs in solid-liquid bioseparation processes

Solid-phase extraction (SPE) is the most widely used sample-preparation technique for liquid samples, belonging to the group of sorptive-based extraction techniques [89]. The development of new materials as effective and selective adsorbents in sample preparation has been explored in the past few years [89, 90]. Taking advantage of the chemical versatility and designer ability that ILs can impart, in recent years, IL-modified materials (also known as supported IL phases – SILPs) have been focus of remarkable attention [17]. However, their use for the separation of amino acids and proteins is still limited.

IL-based SPE methods aimed at extracting and separating amino acids, although scarce, comprise ILs immobilized on silica and the use of ILs on the preparation of molecularly imprinted polymers (MIPs). Marwani et al. [91] immobilized a chiral IL [C_2(L-Phe)][NTf_2] on silica envisioning the enantioselective separation of D-phenylalanine from aqueous solutions. The determined adsorption isotherms revealed that the adsorption capacity of the solid support for D-phenylalanine was of 97.35% at pH 3.0, for an initial concentration of the amino acid at 0.1 gL^{-1}. The authors proved the enhanced performance of the prepared material by applying it to real water samples (ground water, lake water, seawater, waste water) with satisfactory results [91]**.** Yang et al. [92] applied the IL 1-butyl-3-methylimidazolium aminohydrocinnamic acid in acetonitrile to prepare surfaces of MIPs for the selective recovery of L-phenylalanine. Studies on the adsorption kinetics, SPE application, and on the chiral resolution of racemic phenylalanine mixtures were performed. The IL-based copolymerizing process carried out in acetonitrile, when compared with the traditional imprinting process with acetonitrile/H_2O, allows a higher adsorption of L-phenylalanine, further resulting in the selective separation of L-phenylalanine from other amino acids (L-tryptophan and L-histidine). Although these materials appear as promising to recover amino acids, with recovery values above 91% as reported [92], no further studies for amino acids are so far available.

In the field of proteins, Shu and co-workers [93] immobilized $[C_1im]^+$ moieties onto polyvinyl chloride (PVC), forming [C_1im]Cl–PVC materials. The authors demonstrated that the immobilization of the IL strongly depends on the [C_1im]/PVC molar ratio during the reaction step. A maximum immobilization ratio of 15.1% was obtained with a 4:1 molar ratio of [C_1im]:PVC, further showing that these materials adsorb lysozyme, cytochrome-c and hemoglobin with efficiencies of 97%, 98% and 94%, respectively. On the other hand, this material was found to be not promising for the removal of BSA, transferrin and IgG [93]. These results were justified

based on the pH and pI of the proteins and ionic strength of the solutions. The selective isolation of hemoglobin was also studied using imidazolium-modified polystyrene materials [94]. In this work, imidazolium cations were grafted onto the surface of a chloromethyl polystyrene, forming PS-CH_2-[C_1im]$^+Cl^-$, which is a crosslinked rigid polymer that can act directly as a support [94]. Adsorption efficiencies of this material to hemoglobin reached values up to 91% [94]. Two other polymer materials were synthesized and used for protein separation, in which 1-allyl-3-butylimidazolium chloride and 1-vinyl-3-octylimidazolium bromide were used as functional monomers, and acrylamide as a co-functional monomer [95]. The first ionic liquid polymeric material has a high binding capacity for hemoglobin, whilst the former possesses a high binding capacity for BSA. These results suggest that these materials can be tailored to adsorb specific proteins, and thus can be envisioned as promising strategies to separate target proteins from complex matrices. IL-modified magnetic nanoparticles (ILs-MNPs) were recently proposed to recover BSA (Figure 1.7), leading to extraction efficiencies of 86.9% [96]. The recovery of the protein from the material was also addressed; with NaCl at concentrations higher than 1.1 mol.L^{-1} the desorption ratio of BSA reaches 95.3%. Moreover, almost 95% of the prepared MNPs were recovered, with no significant losses on their extraction efficiency over four cycles [96]. Recently, Wen et al. [97] investigated the performance of an amino functional dicationic ionic liquid (AFDCIL) coated on the surface of magnetic graphene oxide (Fe@GO) as a magnetic adsorbent (Fe@GO@AFDCIL) for proteins. The authors reported that, compared with conventional Fe@GO@IL composites, the Fe@GO@AFDCIL composite exhibits the highest extraction capacity for bovine haemoglobin; it was also suggested that this magnetic adsorbent could be successfully employed in extraction of bovine haemoglobin from real samples [97].

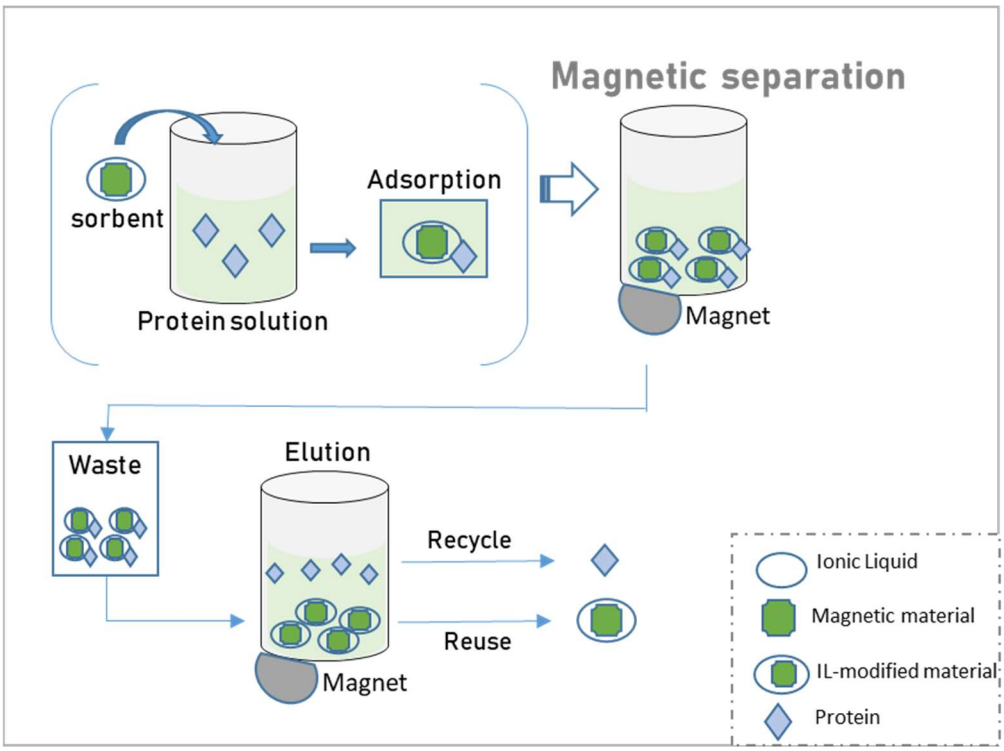

Figure 1.7. Schematic representation of magnetic solid phase extractions of proteins [96].

Altough all described works highlight the potential of SILPs to recover proteins, there are no indications regarding their selective nature or performance when applied to real and complex matrices, in which a large number of proteins or other metabolites may be present. The use of SILPs for the separation of proteins is giving its first steps. Based on the versatility of ILs that is transferred to SILPs, it is however predicted that further work in this arena will confirm the potential of these materials in proteins downstream processing.

1.2.6. Conclusions

In the past decade, an increased attention has been given to the use of ILs in bioseparation processes. This chapter provides an overview of the potential and suitability of IL-based liquid-liquid extractions, employing hydrophobic ILs and ABS, and solid-liquid extractions based on the use of IL-modified materials, for the separation of amino acids and proteins, including enzymes and biopharmaceuticals. Most of the discussed works show that IL-based strategies lead to improved extraction and separation performance when compared to more traditional approaches. This trend is a direct result of the ILs tailoring ability, which is transferrable to bioprocesses in which they are used, thus allowing the design of specific ILs and processes for target separations.

Most of the discussed works are based on imidazolium-based ILs, majorly combined with fluorinated anions. However, more recently, other classes of ILs start to be considered, such as

with cholinium- and amino-acid-based ILs, bringing additional biocompatible features to bioseparation processes. Furthermore, most works dealing with the separation of amino acids and proteins employing ILs are focused on ABS, which may be explained by the advantages of these liquid-liquid systems over the application of hydrophobic ILs. ABS are water-rich and usually lead to improved extraction efficiencies and recovery yields – a result that is also directly connected to the second phase-forming component of ABS that most of the times is a strong salting-out species. In addition to liquid-liquid extractions, SILPs seem to be a promising option. However, the number of works on SILPs are still scarce, with no reports on their use to purify amino acids and proteins from complex/real matrices found.

In summary, this chapter aimed providing an overview on the application of ILs in bioseparation processes. From the works discussed, it is clear that the use of appropriate ILs leads to high extraction efficiencies, recovery yields and purification factors. Still, a quite a number of requisites needs to be addressed before their application in scaled-up separation processes becomes a reality, namely to: (i) find efficient and low-cost ILs able to compete with common organic solvents; (ii) develop integrated processes, particularly focused on decreasing the number of steps involved and the process cost; (iii) develop strategies for biomolecules recovery and IL recycling; (iv) perform scale-up studies of the optimized processes; and (v) carry out economic and life cycle analysis of the developed processes. Although there is still a path to follow, IL-based separation processes display several advantages to become an industrial reality in the following decades.

1.2.7. References

1. Martínez-Aragón M, Burghoff S, Goetheer ELV, de Haan AB (2009) Guidelines for solvent selection for carrier mediated extraction of proteins. Sep Purif Technol 65:65–72.
2. Ahamed T, Ottens M, Nfor BK, Van Dedem GWK, Van Der Wielen L.AM (2006) A generalized approach to thermodynamic properties of biomolecules for use in bioseparation process design. Fluid Phase Equilib 241:268–282.
3. Bhawsar CM, Pandit B, Sawant B, Joshi B (1994) Enzyme mass transfer coefficient in a sieve plate extraction column. Chem Eng J 55:B1–B17.
4. Ventura SPM, Silva FA, Quental MV, Mondal D, Freire MG, Coutinho JAP (2017) Ionic-Liquid-Mediated Extraction and Separation Processes for Bioactive Compounds: Past, Present, and Future Trends. Chem Rev 117:6984–7052.
5. Plechkova NV, Seddon KR (2008) Applications of ionic liquids in the chemical industry. Chem Soc Rev 37:123–150.
6. Albertsson P (1986) Partition of Cell Particles and Macromolecules: Separation and Purification of Biomolecules, Cell Organelles, Membranes, and Cells in Aqueous Polymer Two-phase Systems and Their Use in Biochemical Analysis and Biotechnology. 3rd ed.; John Wiley and Sons: Chichester, New York.
7. Iqbal M, Tao Y, Xie S, Zhu Y, Chen D, Wang X, Huang L, Peng D, Sattar A, Shabbir MAB, Hussain HI, Ahmed S, Yuan Z, (2016) Aqueous two-phase system (ATPS): an overview and advances in its applications. Biol Proced Online 18:1–18.
8. Grilo AL, Aires-Barros MR, Azevedo AM (2014) Partitioning in Aqueous Two-Phase Systems: Fundamentals, Applications and Trends. Sep Purif Rev 45:68–80.

9. Azevedo AM, Fonseca LP, Prazeres DMF (1999) Stability and stabilization of penicillin acylase. J Chem Technol Biotechnol 74:1110–1116.
10. Pereira JFB, Rebelo LPN, Rogers RD, Coutinho JAP, Freire MG (2013) Combining ionic liquids and polyethylene glycols to boost the hydrophobic-hydrophilic range of aqueous biphasic systems. Phys Chem Chem Phys 15:19580–19583.
11. Li J, Kao WJ (2003) Synthesis of polyethylene glycol (PEG) derivatives and PEGylated - Peptide biopolymer conjugates. Biomacromolecules 4:1055–1067.
12. Rosa PAJ, Azevedo AM, Ferreira IF, Vries J, Korporaal R, Verhoef H J, Visser TJ, Aires-Barros MR (2007) Affinity partitioning of human antibodies in aqueous two-phase systems. J Chromatogr A 1162:103–113.
13. Pereira JFB, Lima ÁS, Freire MG, Coutinho JAP (2010) Ionic liquids as adjuvants for the tailored extraction of biomolecules in aqueous biphasic systems. Green Chem 12:1661-1669.
14. Dhadge VL, Rosa SASL, Azevedo AM, Aires-Barros R, Roque ACA (2014) Magnetic aqueous two-phase fishing: A hybrid process technology for antibody purification. J Chromatogr A 1339:59–64.
15. Gutowski KE, Broker GA, Willauer HD, Huddleston JG, Swatloski RP, Holbrey JD, Rogers RD (2003) Controlling the aqueous miscibility of ionic liquids: Aqueous biphasic systems of water-miscible ionic liquids and water-structuring salts for recycle, metathesis, and separations. J Am Chem Soc 125:6632–6633.
16. Freire MG, Cláudio AFM, Araújo JMM, Coutinho JA, Marrucho IM, Canongia Lopes JN, Rebelo LP (2012) Aqueous biphasic systems: a boost brought about by using ionic liquids. Chem Soc Rev 41:4966–4995.
17. Abd A, Ahmed A, Xiashi Z (2017) Developments / Application of Ionic Liquids/ Poly Ionic Liquids in Magnetic Solid-Phase Extraction and Solid Phase Microextraction. Colloid Surf Sci 2:162–170.
18. Carda-Broch S, Berthod A, Armstrong DW (2003) Solvent properties of the 1-butyl-3-methylimidazolium hexafluorophosphate ionic liquid. Anal Bioanal Chem 375:191–199.
19. Smirnova SV, Torocheshnikova II, Formanovsky AA, Pletnev IV (2004) Solvent extraction of amino acids into a room temperature ionic liquid with dicyclohexano-18-crown-6. Anal Bioanal Chem 378:1369–1375.
20. Wang J, Pei Y, Zhao Y, Hu Z (2005) Recovery of amino acids by imidazolium based ionic liquids from aqueous media. Green Chem 7:196–202.
21. Absalan G, Akhond M, Sheikhian L (2010) Partitioning of acidic, basic and neutral amino acids into imidazolium-based ionic liquids. Amino Acids 39:167–174.
22. Tomé LIN, Catambas VR, Teles ARR, et al (2010) Tryptophan extraction using hydrophobic ionic liquids. Sep Purif Technol 72:167–173.
23. Huaxi L, Zhuo L, Jingmei Y, Changping L, Yansheng C, Qingshan L, Xiuling Z, Urs WB (2012) Liquid–liquid extraction process of amino acids by a new amide-based functionalized ionic liquid. Green Chem 14:172-1727.
24. Tang F, Zhang Q, Ren D, Nie Z, Liu Q, Yao S (2010) Functional amino acid ionic liquids as solvent and selector in chiral extraction. J Chromatogr A 1217:4669–4674.
25. Shimojo K, Kamiya N, Tani F, Naganawa H, Naruta Y, Goto M (2006) Functional Conversion of Cytochrome c in Ionic Liquids via Crown Ether Complexation. Anal Chem 78:7735–7742.
26. Tzeng YP, Shen CW, Yu T (2008) Liquid-liquid extraction of lysozyme using a dye-modified ionic liquid. J Chromatogr A 1193:1–6.
27. Kohno Y, Saita S, Murata K, Nakamura N, Ohno H (2011) Extraction of proteins with temperature sensitive and reversible phase change of ionic liquid/water mixture. Polym Chem 2:862-867.
28. Ito Y, Kohno Y, Nakamura N, Ohno H (2013) Design of phosphonium-type zwitterion as an additive to improve saturated water content of phase-separated ionic liquid from aqueous phase toward reversible extraction of proteins. Int J Mol Sci 14:18350–18361.
29. Xu W, Cao H, Ren G, Xie H, Huang J, Li S (2014) An AIL/IL-based liquid/liquid extraction system for the purification of His-tagged proteins. Appl Microbiol Biotechnol 98:5665–5675.
30. Ren G, Gong X, Wang B, Chen Y, Huang J (2015) Affinity ionic liquids for the rapid liquid-liquid extraction purification of hexahistidine tagged proteins. Sep Purif Technol 146:114–120.
31. Cheng DH, Chen XW, Shu Y, Wang JH (2008) Selective extraction/isolation of hemoglobin with ionic liquid 1-butyl-3-trimethylsilylimidazolium hexafluorophosphate (BtmsimPF6). Talanta 75:1270–1278.
32. Cheng D-H, Chen X-W, Shu Y, Wang J-H (2008) Extraction of Cytochrome C by Ionic Liquid 1-Butyl-3-trimethylsilylimidazolium Hexafluorophosphate. Chinese J Anal Chem 36:1187–1190.
33. Huh YS, Jeong CM, Chang HN, Lee SY, Hong WH, Park TJ (2010) Rapid separation of bacteriorhodopsin using a laminar-flow extraction system in a microfluidic device. Biomicrofluidics 4:14103(1) -14103(10).
34. Alvarez-Guerra E, Irabien A (2012) Extraction of lactoferrin with hydrophobic ionic liquids. Sep Purif Technol 98:432–440.

35. Ventura PM, Neves CMSS, Freire MG, Marrucho IM, Oliveira J, Coutinho JAP (2009) Evaluation of Anion Influence on the Formation and Extraction Capability of Ionic-Liquid-Based Aqueous Biphasic Systems. J Phys Chem B 113:9304–9310.
36. Neves CMSS, Ventura SPM, Freire MG, Marrucho IM, Coutinho JAP (2009) Evaluation of cation influence on the formation and extraction capability of ionic-liquid-based aqueous biphasic systems. J Phys Chem B 113:5194–5199.
37. Li Z, Pei Y, Liu L, Wang J (2010) (Liquid+liquid) equilibria for (acetate-based ionic liquids+inorganic salts) aqueous two-phase systems. J Chem Thermodyn 42:932–937.
38. Pei Y, Li Z, Liu L, Wang J (2012) Partitioning behavior of amino acids in aqueous two-phase systems formed by imidazolium ionic liquid and dipotassium hydrogen phosphate. J Chromatogr A 1231:2–7.
39. Louros CLS, Claudio AFM, Neves CMSS, Freire MG, Marrucho IM, Pauly J, Coutinho JAP (2010) Extraction of biomolecules using phosphonium-based ionic liquids + K3PO4 aqueous biphasic systems. Int J Mol Sci 11:1777–1791.
40. Zafarani-Moattar MT, Hamzehzadeh S (2011) Partitioning of amino acids in the aqueous biphasic system containing the water-miscible ionic liquid 1-butyl-3-methylimidazolium bromide and the water-structuring salt potassium citrate. Biotechnol Prog 27:986–997.
41. Passos H, Ferreira AR, Cláudio AFM, Coutinho JAP, Freire MG (2012) Characterization of aqueous biphasic systems composed of ionic liquids and a citrate-based biodegradable salt. Biochem Eng J 67:68–76.
42. Wu D, Zhou Y, Cai P, Shen S, Pan Y (2015) Specific cooperative effect for the enantiomeric separation of amino acids using aqueous two-phase systems with task-specific ionic liquids. J Chromatogr A 1395:65–72.
43. Salabat A, Abnosi MH, Motahari A (2008) Investigation of Amino Acid Partitioning in Aqueous Two-Phase Systems Containing Polyethylene Glycol and Inorganic Salts. J Chem Eng Data 53:2018–2021.
44. Zafarani-Moattar MT, Hamzehzadeh S, Nasiri S (2011) A new aqueous biphasic system containing polypropylene glycol and a water-miscible ionic liquid. Biotechnol Prog 28:146–156.
45. Xie Y, Xing H, Yang Q, Bao Z,Su B, Ren Q (2015) Aqueous Biphasic System Containing Long Chain Anion-Functionalized Ionic Liquids for High-Performance Extraction. ACS Sustain Chem Eng 3:3365–3372.
46. Freire MG, Louros CLS, Rebelo LPN, Coutinho JAP (2011) Aqueous biphasic systems composed of a water-stable ionic liquid + carbohydrates and their applications. Green Chem 13**:**1536-1545.
47. Luis A, Dinis TBV, Passos H, et al (2015) Good's buffers as novel phase-forming components of ionic-liquid-based aqueous biphasic systems. Biochem Eng J 101:142–149.
48. Capela E V, Quental MV, Domingues P, Coutinho JAP, Freire MG (2017) Effective separation of aromatic and aliphatic amino acid mixtures using ionic-liquid-based aqueous biphasic systems. Green Chem 19:1850-1854.
49. Hamzehzadeh S, Vasiresh M (2014) Ionic liquid 1-butyl-3-methylimidazolium bromide as a promoter for the formation and extraction capability of poly(ethylene glycol)-potassium citrate aqueous biphasic system at T=298.15K. Fluid Phase Equilib 382:80–88.
50. Lu Y, Lu W, Wang W, Guo Q, Yang Y (2011) Thermodynamic studies of partitioning behavior of cytochrome c in ionic liquid-based aqueous two-phase system. Talanta 85:1621–1626.
51. Dreyer S, Salim P, Kragl U (2009) Driving forces of protein partitioning in an ionic liquid-based aqueous two-phase system. Biochem. Eng. J. 46:176–185.
52. Pei Y, Li L, Li Z, Wu C, Wang J (2012) Partitioning Behavior of Wastewater Proteins in Some Ionic Liquids-Based Aqueous Two-Phase Systems. Sep Sci Technol 47:277–283.
53. Yan H, Wu J, Dai G, Zhong A, Chen H, Yang J, Han D (2012) Interaction mechanisms of ionic liquids [Cnmim]Br (n=4, 6, 8, 10) with bovine serum albumin. J Lumin 132:622–628.
54. Lin X, Wang Y, Zeng Q, Ding X, Chen J (2013) Extraction and separation of proteins by ionic liquid aqueous two-phase system. Analyst 138:6445–6453.
55. Pei Y, Li Z, Liu L, Wang J, Wang H (2010) Selective separation of protein and saccharides by ionic liquids aqueous two-phase systems. Sci China Chem 53:1554–1560.
56. Sheikhian L, Akhond M, Absalan G, Goltz DM (2013) Dye-Affinity Partitioning of Acidic, Basic, and Neutral Proteins in Ionic Liquid-Based Aqueous Biphasic Systems. Sep Sci Technol 48:2372–2380.
57. Chen J, Wang Y, Zeng Q, Ding X, Huang Y (2014) Partition of proteins with extraction in aqueous two-phase system by hydroxyl ammonium-based ionic liquid. Anal Methods 6:4067–4076.
58. Bisht M, Kumar A, Venkatesu P (2015) Analysis of the driving force that rule the stability of lysozyme in alkylammonium-based ionic liquids. Int J Biol Macromol 81:1074–1081.

59. Santos JHPM, E Silva FA, Coutinho JAP, Ventura SPM, Junior AP (2015) Ionic liquids as a novel class of electrolytes in polymeric aqueous biphasic systems. Process Biochem 50:661–668.
60. Wu C, Wang J, Li Z, Jing J, Wang H (2013) Relative hydrophobicity between the phases and partition of cytochrome-c in glycine ionic liquids aqueous two-phase systems. J Chromatogr A 1305:1–6.
61. Huang S, Wang Y, Zhou Y, Li L, Zeng Q, Ding X (2013) Choline-like Ionic Liquid-based Aqueous Two-phase Extraction of Selected Proteins. Anal Methods 5:3395−3402.
62. Li Z, Liu X, Pei Y, Wang J, He M (2012) Design of environmentally friendly ionic liquid aqueous two-phase systems for the efficient and high activity extraction of proteins. Green Chem 14:2941.
63. Taha M, Quental MV, Correia I, Freire MG, Coutinho JAP (2015) Extraction and stability of bovine serum albumin (BSA) using cholinium-based Good's buffers ionic liquids. Process Biochem 50:1158–1166.
64. Quental M V, Caban M, Pereira MM, Stepnowski P, Coutinho JAP, Freire MG (2015) Enhanced extraction of proteins using cholinium-based ionic liquids as phase-forming components of aqueous biphasic systems. Biotechnol J 10:1457–66.
65. Song CP, Ramanan RN, Vijayaraghavan R, McFarlane DR, Chan ES, Ooi CW (2015) Aqueous Two-Phase Systems Based on Cholinium Aminoate Ionic Liquids with Tunable Hydrophobicity and Charge Density. ACS Sustain Chem Eng 3:3291−3298.
66. Taha M, e Silva FA, Quental MV, Ventura SPM, Freire MG, Coutinho JAP (2014) Good's buffers as a basis for developing self-buffering and biocompatible ionic liquids for biological research. Green Chem 16:3149–3159.
67. Passos H, Luís A, Coutinho JAP, Freire MG (2016) Thermoreversible (Ionic-Liquid- Based) Aqueous Biphasic Systems. Sci. Rep. 6:1–7.
68. Taha M, Almeida MR, Francisca A, Domingues P (2015) Novel biocompatible and self-buffering ionic liquids for biopharmaceutical applications. Chem Eur J 21:4781–4788.
69. Ferreira AM, Faustino VFM, Mondal D, Coutinho JAP, Freire MG (2016) Improving the extraction and purification of immunoglobulin G by the use of ionic liquids as adjuvants in aqueous biphasic systems. J Biotechnol 236:166–175.
70. Ramalho CC, Neves CMSS, Quental MV, Coutinho JAP, Freire MG (2018) Separation of immunoglobulin G using aqueous biphasic systems composed of cholinium-based ionic liquids and poly(propylene glycol). J Chem Technol Biotechnol 93:1931-1939
71. Mondal D, Sharma M, Quental MV, Tavares APM, Prasad K, Freire MG (2016) Suitability of bio-based ionic liquids for the extraction and purification of IgG antibodies. Green Chem 18:6071–6081.
72. Desai RK, Streefland M, Wijffels RH, H. M. Eppink M (2014) Extraction and stability of selected proteins in ionic liquid based aqueous two-phase systems. Green Chem 16:2670–2679.
73. Tan ZJ, Li FF, Xu XL, Xing JM (2012) Simultaneous extraction and purification of aloe polysaccharides and proteins using ionic liquid based aqueous two-phase system coupled with dialysis membrane. Desalination 286:389–393.
74. Yan JK, Ma H Le, Pei JJ, Wang ZB, Wu JY (2014) Facile and effective separation of polysaccharides and proteins from Cordyceps sinensis mycelia by ionic liquid aqueous two-phase system. Sep Purif Technol 135:278–284.
75. Pereira MM, Pedro SN, Quental MV, Lima AS, Coutinho JAP, Freire MG (2015) Enhanced extraction of bovine serum albumin with aqueous biphasic systems of phosphonium-and ammonium-based ionic liquids. J Biotechnol 206:17–25.
76. Deive FJ, Rodríguez A, Pereiro AB, Araujo JMM, Longo MA, Coelho MAZ, Lopes JNC, Esperança JMSS, Rebelo LPN, Marrucho IM (2011) Ionic liquid-based aqueous biphasic system for lipase extraction. Green Chem 13:390–396.
77. Deive FJ, Rodríguez A, Rebelo LPN, Marrucho IM (2012) Extraction of Candida antarctica lipase A from aqueous solutions using imidazolium-based ionic liquids. Sep Purif Technol 97:205–210.
78. Ventura SPM, Sousa SG, Freire MG, Serafim LS, Lima AS, Coutinho JAP (2011) Design of ionic liquids for lipase purification. J Chromatogr B Anal Technol Biomed Life Sci 879:2679–2687.
79. Ventura SPM, de Barros RLF, de Pinho Barbosa JM, Soares CMF, Lima AL, Coutinho JAP (2012) Production and purification of an extracellular lipolytic enzyme using ionic liquid-based aqueous two-phase systems. Green Chem 14:734-740.
80. Souza RL, Ventura SPM, Soares CMF, Coutinho JAP, Lima AS (2015) Lipase purification using ionic liquids as adjuvants in aqueous two-phase systems. Green Chem 17:3026–3034.
81. Souza RL, Lima RA, Coutinho JAP, Soares CMF, Lima AS (2015) Aqueous two-phase systems based on cholinium salts and tetrahydrofuran and their use for lipase purification. Sep Purif Technol 155:118–126.
82. Lee SY, Khoiroh I, Coutinho JAP, Show PL, Ventura SPM (2017) Lipase production and purification by self-buffering ionic liquid-based aqueous biphasic systems. Process Biochem 63:221–228.

83. Bai Z, Chao Y, Zhang M, Han C, Zhu W, Chang Y, Li H, Sun Y (2013) Partitioning behavior of papain in ionic liquids-based aqueous two-phase systems. J Chem 213:1–6.
84. Cao Q, Quan L, He C, Li N, Liu F (2008) Partition of horseradish peroxidase with maintained activity in aqueous biphasic system based on ionic liquid. Talanta 77:160–165.
85. Simental-Martínez J, Rito-Palomares M, Benavides J (2014) Potential application of aqueous two-phase systems and three-phase partitioning for the recovery of superoxide dismutase from a clarified homogenate of Kluyveromyces marxianus. Biotechnol Prog 30:1326–1334.
86. Santos JHPM, Santos JC, Meneguetti GP, Rangel-Yagui CO, Coutinho JAP, Vitolo M, Ventura SPM, Junior AP (2018) In situ purification of periplasmatic L-asparaginase by aqueous two phase systems with ionic liquids (ILs) as adjuvants. J Chem Technol Biotechnol 93: 1871-1880.
87. Jiang B, Feng Z, Liu C, Xu Y, Li D, Ji G (2015) Extraction and purification of wheat-esterase using aqueous two-phase systems of ionic liquid and salt. J Food Sci Technol 52:2878–2885.
88. Novak U, Pohar A, Plazl I, Žnidaršič-Plazl P (2012) Ionic liquid-based aqueous two-phase extraction within a microchannel system. Sep Purif Technol 97:172–178.
89. Vidal L, Riekkola ML, Canals A (2012) Ionic liquid-modified materials for solid-phase extraction and separation: A review. Anal Chim Acta 715:19–41.
90. Fumes BH, Silva MR, Andrade FN, Nazario CED, Lanças FM (2015) Recent advances and future trends in new materials for sample preparation. TrAC - Trends Anal Chem 71:9–25.
91. Marwani HM, Bakhsh EM, Al-Turaif HA, Asiri AM (2014) Enantioselective separation and detection of D-phenylalanine based on newly developed chiral ionic liquid immobilized silica gel surface. Int J Electrochem Sci 9:7948–7964
92. Yang L, Hu X, Guan P, Li J, Wu D, Gao B (2015) Molecularly imprinted polymers for the selective recognition of l -phenylalanine based on 1-buty-3-methylimidazolium ionic liquid. J Appl Polym Sci 132: 42485(1) – 42485(9).
93. Shu Y, Chen XW, Wang JH (2010) Ionic liquid-polyvinyl chloride ionomer for highly selective isolation of basic proteins. Talanta 81:637–642.
94. Zhao G, Chen S, Chen XW, He RH (2013) Selective isolation of hemoglobin by use of imidazolium-modified polystyrene as extractant. Anal Bioanal Chem 405:5353–5358.
95. Liu Y, Ma R, Deng Q, Zhang L, Liu C, Wang S (2014) Preparation of ionic liquid polymer materials and their recognition properties for proteins. RSC Adv 4:52147–52154.
96. Chen J, Wang Y, Ding X, Huang Y, Xu J (2014) Magnetic solid-phase extraction of proteins based on hydroxy functional ionic liquid-modified magnetic nanoparticles. Anal Methods 6:8358–8367.
97. Wen Q, Wang Y, Xu K, Li N, Zhang H, Yang Q, Zhou Y (2016) Magnetic solid-phase extraction of protein by ionic liquid-coated Fe@graphene oxide. Talanta 160:481–488.

2. Odd-even Effect in the Formation and Extraction Performance of Ionic-Liquid-based Aqueous Biphasic Systems

Odd-even Effect in the Formation and Extraction Performance of Ionic-Liquid-based Aqueous Biphasic Systems

Based on the published manuscript: [2]

D. C. V. Belchior, M. R. Almeida, T. E. Sintra, S. P.M. Ventura, I. F. Duarte and M.G. Freire. Industrial & Engineering Chemistry Research, 2019, 58, 8323-8331.

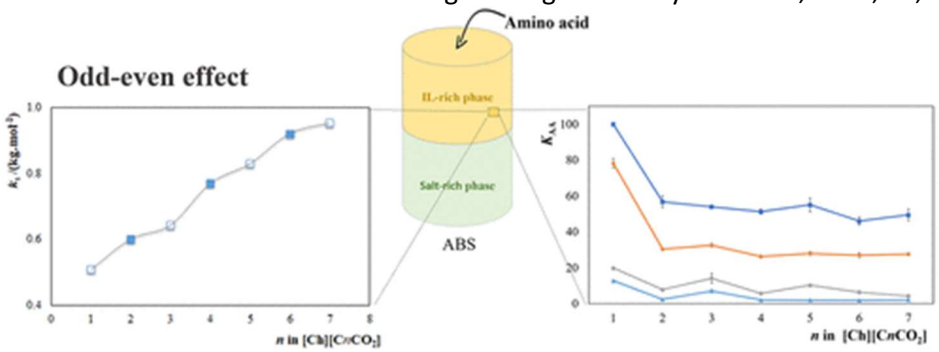

Abstract

Ionic-liquid-based aqueous biphasic systems (IL-based ABS) have been extensively investigated in the separation of high-value biomolecules. However, the understanding of the molecular-level mechanisms ruling phase separation and extraction performance of these systems is crucial to successfully design effective separation processes. In this work, IL-based ABS composed of K_2HPO_4 and cholinium carboxylate ILs ([Ch][C_nCO_2] with n = 1 to 7, comprising anions with odd and even alkyl chain length) were investigated. The respective ternary phase diagrams, including binodal curves, tie-lengths, tie-line lengths and critical points, as well as the Setschenow salting-out coefficients (k_s) that is a quantitative measure of the two-phase formation ability, were determined at 298 K. The extraction performance of these systems was then evaluated for four amino acids (L-tryptophan, L-phenylalanine, L-tyrosine, L-3,4-dihydroxyphenylalanine/L-dopa). It was found that ILs composed of anions with even alkyl chains display slightly higher ks values, meaning that these ILs are more easily salted-out or more easily phase separate to form ABS. On the other hand, ABS formed by ILs with anions comprising odd alkyl chains lead to slightly higher partition coefficients of amino acids. Beyond the neat ILs odd-even effect resulting from their nanostructuration, being this a well-known phenomenon occurring in a series of their thermophysical properties, it is here shown the existence of an odd-even effect displayed by the IL anion aliphatic moiety in aqueous solution, visible both in the two-phase formation ability and extraction performance of ABS. These findings contribute to elucidate the molecular-level mechanisms governing ABS formation and partitioning of biomolecules, ultimately allowing the design of effective separation platforms.

Keywords: Aqueous biphasic systems • cholinium carboxylate ionic liquids • salting-out coefficient • extraction, partition coefficient • odd-even effect.

[2]Contributions: M.G.F. conceived and directed this work. D.C.V.B., T.E.S. and M.R.A. acquired the experimental data. D.C.V.B., T.E.S., M.R.A., M.G.F., S.P.M.V. and I.F.D. interpreted the obtained experimental data. The manuscript was mainly written by D.C.V.B. and M.G.F. with contributions from the remaining authors.

2.1 Introduction

Separation and purification steps within biotechnological processes are still major challenges due to difficulties in purifying and recovering the target products from the original complex media in which they are produced [1]. Furthermore, these should be cost-effective and should be able to keep the products biological activity. Research on alternative separation techniques has been carried out with Aqueous Biphasic Systems (ABS), which correspond to liquid-liquid extraction systems formed by water and two solutes (e.g. two polymers, a polymer and a salt, two salts, etc.) that undergo phase separation above given concentrations [2-5]. In ABS, both phases are mostly composed of water, meaning that such media may be compatible with biologically active molecules [2].

In addition to more conventional ABS formed by polymers, in the last decade, a large interest has been placed in ionic-liquid-based ABS, initially demonstrated to be formed by mixing ionic liquids and inorganic salts in aqueous media [6]. Ionic liquids (ILs) are poorly coordinated organic salts, and therefore may be liquid at or close to room temperature. In addition to other relevant properties, the major advantage associated to IL-based ABS relies on these compounds designer ability, resulting in a virtually endless opportunity of tuning the ILs chemical structures for specific applications [7]. As a result, IL-based ABS have been successfully used in the separation of a wide number of biomolecules, such as amino acids, proteins, antioxidants, among others [8]. Still, most of the ILs studied up to date are imidazolium-based, most of the times combined with $[BF_4]^-$, which may raise some toxicity and biodegradability concerns [8]. The ample versatility of ILs should however permit the synthesis of new fluids with both an acceptable environmental footprint and enhanced biocompatibility to be used in the creation of novel ABS. Cholinium-based ILs are a promising family of ILs, which can be prepared from natural sources, and may present high biodegradability and, in some cases, marginal (eco)toxicity [9-11]. In particular, cholinium chloride is an essential nutrient with an important role in living processes, namely as precursor in the synthesis of vitamins (e.g., thiamine) and enzymes that participate in the carbohydrates metabolism [12-13]. Taking into account their advantageous features, several works have been published reporting the use of cholinium-based ILs to form ABS with salts. Xie et al. [14] investigated novel ABS composed of four cholinium-based ILs combined with carboxylate anions and K_3PO_4 to extract tryptophan, phenylalanine, and caffeine. The authors reported novel ABS liquid-liquid phase diagrams and showed their enhanced extraction performance, as well as the presence of liquid crystal structures in ABS formed by ILs with long alkyl chain anions. Shahriari et al. [15] determined the phase diagrams of novel ABS formed by a series of cholinium-based ILs with different anions and K_3PO_4, having evaluated their performance to extract antibiotics. This type of ABS has also been used to extract antibiotics from real fermentation broths [16], and it was latter demonstrated that they represent a more

economical alternative to recover tetracycline from the fermentation broth than more traditional ABS formed by polymers [17].

To design effective ABS for separation processes, it is relevant to determine and characterize their phase diagrams. The respective ternary phase diagrams provide valuable information on the phase-forming components compositions required to form two-phase systems, and on the composition of each phase for a given overall mixture. Accordingly, a significant number of works have focused on the determination of novel IL-based ABS ternary phase diagrams [8]. Furthermore, it is well known that ILs with long alkyl side chains tend to self-aggregate in aqueous media, a trend that was further demonstrated to occur in ABS [18] and that may lead to unfavorable extraction results [19]. In a previous work, the effect of the IL cation alkyl side chain length in the formation of ABS has been comprehensively investigated by employing the 1-alkyl-3-methylimidazolium chloride series, with both odd and even alkyl side chains [20]. An odd-even effect on the Setschenow salting-out coefficient (k_s), a quantitative measure of the two-phase formation ability, along the number of methylene groups of the longest IL cation alkyl side chain was identified [20]. ILs comprising cations with even alkyl side chains display higher molar volumes and are thus more easily salted-out and more prone to undergo phase separation in aqueous media. Although this trend was observed for the IL cation, the effect of the IL anion on ABS formation is scarcely studied. Some reports exist on the effect of the IL anion alkyl chain length on ABS formation [14,21-24], but most of these studies employed ILs with chemically different anions or only with even alkyl chains at the anion. In general, it is understood that ILs with longer aliphatic chains at the anion require less inorganic salt to undergo phase separation. However, no studies on the self-aggregation impact of long alkyl chain anion ILs and on the possibility of an odd-even effect have been performed. Furthermore, to the best of our knowledge, the impact of the odd-even effect in the partitioning of target molecules in ABS was never investigated. It should be remarked that although the odd-even effect is scarcely studied in aqueous solutions, the ILs odd-even effect is an already well-established phenomenon occurring in a series of neat ILs properties, such as molar volumes, viscosities and entropy and enthalpy of vaporization [25-28]. Santos and co-workers [26-28], by studying several series of imidazolium-based ILs with cations of different alkyl side chain length, demonstrated that the odd-even effect is a result of the ILs nanosegregation and orientation of the terminal methyl groups to the imidazolium ring cation, with a consequent effect in the ILs cohesive energy.

Aiming at better understanding the effect of the IL anion alkyl chain length on ABS formation, in this work, seven cholinium-based ILs with carboxylate anions, from acetate to octanoate and comprising both even and odd alkyl side chains ([Ch][C_nCO_2], n = 1 to 7), were synthesized and used in ABS formation with dipotassium hydrogen phosphate (K_2HPO_4). The respective ternary phase diagrams were determined at (298 ± 1) K, including tie-lines and critical points, and further evaluated in terms of their extraction potential for amino acids, namely L-tryptophan, L-

phenylalanine, L-tyrosine and L-3,4-dihydroxyphenylalanine/L-dopa. The Setschenow coefficient of each ABS was determined, and the odd-even effect was addressed in both ABS formation and amino acids partitioning between the coexisting phases.

2.2 Experimental Section

2.2.1. Materials

The ABS studied in this work were prepared using aqueous solutions of potassium phosphate, K_2HPO_4 (>98% of purity), purchased from Sigma–Aldrich, and aqueous solutions of each IL. The investigated cholinium-based ILs comprise anions derived from carboxylic acids, corresponding to cholinium acetate ([Ch][C_1CO_2], > 98 wt % pure) from Iolitec, and cholinium propanoate ([Ch][C_2CO_2]), cholinium butanoate ([Ch][C_3CO_2]), cholinium pentanoate ([Ch][C_4CO_2]), cholinium hexanoate ([Ch][C_5CO_2]), cholinium heptanoate ([Ch][C_6CO_2]), and cholinium octanoate ([Ch][C_7CO_2]) that were synthetized in our laboratory following protocols previously described [29]. All ILs synthesized showed high purity (>97 wt%), confirmed by ^1H and ^{13}C NMR (see the Appendix A for further details). The required precursors, namely cholinium hydroxide solution (46 wt%, Sigma-Aldrich), propanoic, butanoic, pentanoic, hexanoic and heptanoic acids (99 %, Acros Organics), and octanoic acid (98 %, Sigma-Aldrich), were commercially acquired. Briefly, the corresponding acids were added drop wise into an aqueous solution of [Ch][OH] (1.1 equivalents of acid) at 298 K, and the mixture was continuously stirred at room temperature and under inert atmosphere for at least 12 h to produce the cholinium-based ILs. The mixtures were then dried for 4 h under vacuum using a rotary evaporator. The remaining acid was removed by liquid-liquid extraction with ethyl acetate. The residual solvent was removed under reduced pressure. The obtained ILs were dried under high vacuum for at least 72 h.

The water used was double distilled, passed by a reverse osmosis system and further treated with a Milli-Q plus 185 water purification apparatus. For the partition studies, four amino acids were investigated, namely L-phenylalanine (99.0 wt% of purity) acquired from Alfa Aesar, L-tyrosine (99.0 wt% of purity) acquired from Fluka, and L-tryptophan (99.0 wt% of purity) and L-3,4-dihydroxyphenylalanine or L-dopa (98.0 wt% of purity) acquired from Sigma–Aldrich. The chemical structure of the amino acids investigated are depicted in Figure 2.1.

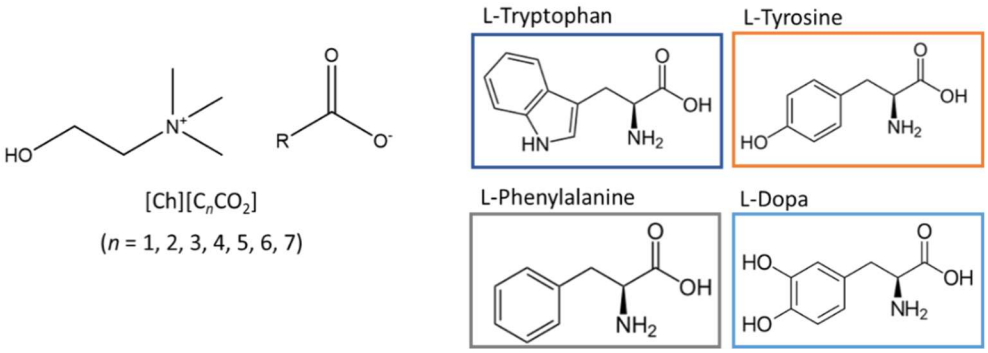

Figure 2.1. Chemical structures of the investigated ILs and amino acids.

2.2.2. Phase diagrams, tie-lines, critical points and Setschenow coefficients

The binodal data were determined through the cloud point titration method at (298 ± 1)K and atmospheric pressure. The experimental procedure adopted in this work follows the method previously described by us [21]. Briefly, the salt K_2HPO_4 at 40 wt% in aqueous solution, and aqueous solutions of the different ILs with concentrations ranging from 60 to 80 wt%, were prepared and used for the determination of binodal curves. All additions were carried out under constant stirring, and the ternary system compositions were determined by weight quantification ($\pm 10^{-4}$ g). The experimental solubility curves were correlated using the equation proposed by Merchuk et al. [30]:

$$[\mathrm{IL}] = A\exp[(B \times [\mathrm{Salt}]^{0.5}) - (C \times [\mathrm{Salt}]^{3})] \quad (1)$$

where [IL] and [Salt] represent the IL and salt weight fraction percentages, respectively, and *A*, *B*, and *C* are constants obtained by the regression of the experimental data.

The tie-lines (TLs) associated to each binodal curve, which give the composition of each phase for a given mixture composition, were determined by the gravimetric method proposed by Merchuk et al. [30]. Several ternary mixtures constituted by IL + K_2HPO_4 + water at the biphasic region were prepared by weight and vigorously agitated. Each mixture was then centrifuged for 30 min at 298 K aiming for the separation of the two phases. Both phases were carefully separated and individually weighed. Each TL was determined by the lever-arm rule [30] through the relationship between the top phase and the total system composition, according to the following system of four Eqs. (2-5):

$$[\mathrm{IL}]_{\mathrm{T}} = A\exp[(B \times [\mathrm{Salt}]_{\mathrm{T}}^{0.5}) - (C \times [\mathrm{Salt}]_{\mathrm{T}}^{3})] \quad (2)$$

$$[\mathrm{IL}]_{\mathrm{B}} = A\exp[(B \times [\mathrm{Salt}]_{\mathrm{B}}^{0.5}) - (C \times [\mathrm{Salt}]_{\mathrm{B}}^{3})] \quad (3)$$

$$[\mathrm{IL}]_{\mathrm{T}} = \frac{[\mathrm{IL}]_{\mathrm{M}}}{\alpha} - \frac{1-\alpha}{\alpha} \times [\mathrm{IL}]_{\mathrm{B}} \quad (4)$$

$$[\mathrm{Salt}]_{\mathrm{T}} = \frac{[\mathrm{Salt}]_{\mathrm{M}}}{\alpha} - \frac{1-\alpha}{\alpha} \times [\mathrm{Salt}]_{\mathrm{B}} \quad (5)$$

where the subscripts M, T and B designate, respectively, the initial mixture, the top and bottom phases. The value α is the ratio between the mass of the top phase and the total mass of the mixture experimentally determined. In all systems, the top phase corresponds to the IL-rich phase, whereas the salt is majorly enriched in the bottom phase.

Each tie-line length (TLL) was determined through the application of the following Eq.:

$$\mathrm{TLL} = \sqrt{([\mathrm{Salt}]_\mathrm{T} - [\mathrm{Salt}]_\mathrm{B})^2 + ([\mathrm{IL}]_\mathrm{T} - [\mathrm{IL}]_\mathrm{B})^2} \quad (6)$$

The critical point of each system (the mixture composition at which the composition of the two aqueous phases becomes identical) was estimated through the application of the Sherwood method using the TLs slopes [31], according to Eq. (7),

$$[IL] = f[salt] + g \quad (7)$$

where [IL] and [salt] are the weight fraction percentages of IL and Salt, and f and g are parameters obtained from the fitting.

Salting-out effects may be quantified by correlating the solubility data with the empirical equation of Setschenow [32]. In this work the modified version of the original Setschenow equation proposed by Hey et al. [33], previously used in the description of polymer-based ABS [34] and of IL-salt-based ABS [34-35], was applied:

$$ln\frac{[\mathrm{IL}]_\mathrm{T}}{[\mathrm{IL}]_\mathrm{B}} = k_{IL}([\mathrm{IL}]_\mathrm{B} - ([\mathrm{IL}]_\mathrm{T}) + k_s([\mathrm{Salt}]_\mathrm{B} - [\mathrm{Salt}]_\mathrm{T}) \quad (8)$$

where [IL] and [Salt] represent the molality of IL and salt, T and B designate the top (IL-rich) and bottom (salt-rich) phases, respectively, and k_{IL} and k_s are parameters relating the activity coefficient of the IL to its concentration and the salting-out coefficient, respectively.

2.2.3. Cation-anion interaction energies

The cation-anion total interaction energies of each IL, E_{Int}, were determined using the COSMO-RS thermodynamic model. This model combines quantum chemistry, based on the dielectric continuum model known as COSMO (COnductor-like Screening MOdel for Real Solvents), with statistical thermodynamic calculations. The process employed in this work to determine the interaction energies was previously described by Kurnia et al.[36] The quantum chemical COSMO calculations were performed with the TURBOMOLE 6.1 program package at the density functional theory (DFT) level, applying the BP functional B88-P86 with a triple-z valence polarized basis set (TZVP) and the resolution of identity standard (RI) approximation [37]. The

COSMOthermX program usin the parameter file BP_TZVP_C20_0111 (COSMOlogic GmbH & Co KG, Leverkusen, Germany) was used in all calculations [38].

2.2.4. Extraction of amino acids

ABS containing aqueous solutions of amino acids at a concentration of 5 $g.L^{-1}$ for L-tryptophan, 15 $g.L^{-1}$ for L-phenylalanine, 2.5 $g.L^{-1}$ for L-tyrosine and 1.5 $g.L^{-1}$ for L-dopa, defined according to the amino acids solubility in water, were prepared and used to study the amino acids partitioning between the ABS coexisting phases. The ternary mixtures compositions used in the partitioning experiments were chosen based on the phase diagrams and TLs determined in this work. To avoid discrepancies in the results, which could arise from the different phase compositions and, with the goal of addressing the odd-even effect in the amino acids partitioning, all extraction studies were performed at a constant TLL (*ca.* 58 ± 2). Each mixture was vigorously stirred to allow equilibration and then centrifuged for 30 min at 298 K to reach complete separation between the coexisting phases. A careful separation of the phases was performed and the amount of amino acid in each phase was quantified by UV-spectroscopy, using a BioTeck Synergy HT microplate reader, at a wavelength of 280 nm for L-tryptophan, L-tyrosine and L-dopa, and at 260 nm for L-phenylalanine, using calibration curves previously established. At least three independent ABS were prepared, and three samples of each phase quantified.

The ABS performance to extract different amino acids to the IL-rich phase was evaluated by their partition coefficient (K_{AA}), defined as the ratio of the concentration of each amino acid in the IL-rich phase to that in the salt-rich phase, as described by Eq. (9).

$$K_{\mathrm{AA}} = \frac{[AA]_{IL}}{[AA]_{Salt}} \qquad (9)$$

where $[AA]_{IL}$ and $[AA]_{Salt}$ are the concentration of each amino acid (AA) in the IL- and in the salt-rich aqueous phases, respectively.

The pH of the IL- and K_2HPO_4-rich aqueous phases containing the amino acids was measured at 298 K using a Mettler Toledo S47 SevenMulti™ dual meter pH/conductivity equipment (data shown in the Supporting Information). The calibration of the pH meter was carried out with two buffers (pH values of 4.00 and 7.00, acquired from Metrohm).

2.3. Results and Discussion

2.3.1. Phase diagrams, tie-lines and critical points

Novel ternary phase diagrams of ABS composed of water, K_2HPO_4 and cholinium-based ILs with carboxylate anions of variable alkyl chain length were determined in this work at (298 ± 1) K.

Their orthogonal representations, both in percentage weight fraction and in molality units, are shown in Figure 2.2. The detailed weight fraction data are provided in the Appendix A (Tables A1-A7). The experimental binodal data were fitted using the empirical relationship described by Equation (1), also shown in Figure 2.2. The regression parameters *A*, *B* and *C* were estimated by the least squares regression, and their values and corresponding standard deviations are provided in the Appendix A (Table A8). At least 4 TLs and respective length (TLL) were determined for each system by Equations (2) to (6), with the detailed results shown in the Appendix A (Table A9). In addition, the critical point of each system was determined, being provided in Figure 2.2. (Appendix A for detailed data- Table A10).

Since the cholinium cation is common to all ILs, the results depicted in Figure 2.2 reflect the effect of the IL anion on the formation of ABS with K_2HPO_4. The biphasic region is located above the solubility curve; the larger this region, the higher is the ability of the IL to be salted-out by K_2HPO_4 and to form ABS. It is well documented [39] that small IL anions derived from organic acids are excellent hydrogen bond acceptors and exhibit high capability to establish hydrogen bonds with water. Furthermore, the hydroxyl group at the end of the ethyl group of the cholinium cation is able to establish strong hydrogen bonds or dipole-dipole interactions with water molecules [40,41]. Therefore, cholinium carboxylate ILs display a high affinity for water and only moderate to strong salting-out salts able to create ABS. Accordingly, it was previously shown that these ILs form ABS with K_3PO_4 [14], and in this work we show that they form ABS with K_2HPO_4. However, the studied cholinium carboxylate ILs do not form ABS with weaker salting-out salts, such as KH_2PO_4 or K_2HPO_4/KH_2PO_4 at pH 7 (as experimentally attempted by us in this work - data not shown).

The ability of the investigated ILs to form ABS at ~ 22 wt% of K_2HPO_4 follows the order: $[Ch][C_1CO_2] \approx [Ch][C_7CO_2] < [Ch][C_6CO_2] < [Ch][C_2CO_2] < [Ch][C_5CO_2] < [Ch][C_3CO_2] \approx [Ch][C_4CO_2]$. When weight fraction is used [Figure 2.2(a)], a direct correlation of the ILs' aptitude to be salted-out cannot be straightforwardly assessed. When using molality units, the differences arising from different molecular weights of ILs are avoided, allowing for a more comprehensive analysis of the effect of individual solutes on promoting liquid−liquid demixing. The binodal curves represented in molality units, shown in Figure 2.2(b), illustrate that the ILs ability for ABS formation, e.g. at 2.0 mol·kg^{-1} of K_2HPO_4, follows the order: $[Ch][C_1CO_2] < [Ch][C_2CO_2] < [Ch][C_7CO_2] \approx [Ch][C_6CO_2] < [Ch][C_3CO_2] < [Ch][C_4CO_2] \approx [Ch][C_5CO_2]$. This order shows that the capability to form ABS (or of the IL to be salted-out) increases with the increase of the alkyl chain length of the IL anion, at least up to $[Ch][C_5CO_2]$, in which the ILs self-aggregation is not playing a role yet. When self-aggregation of ILs occurs, there is a decrease in their ability to create ABS, as observed for $[Ch][C_6CO_2]$ (cholinium heptanoate) and $[Ch][C_7CO_2]$ (cholinium octanoate). Both ILs have alkyl chains sufficiently long to self-aggregate in aqueous media at 298 K (Critical micellar concentration (CMC) values: (410 ± 13) mM for $[Ch][C_6CO_2]$ and 383.0 mM for

[Ch][C_7CO_2] [42]). Details on the CMC determination are given in the Supporting Information. This trend in ABS formation is in agreement with what has been previously observed for the IL cation effect [20] and seems to be independent of the salt used.

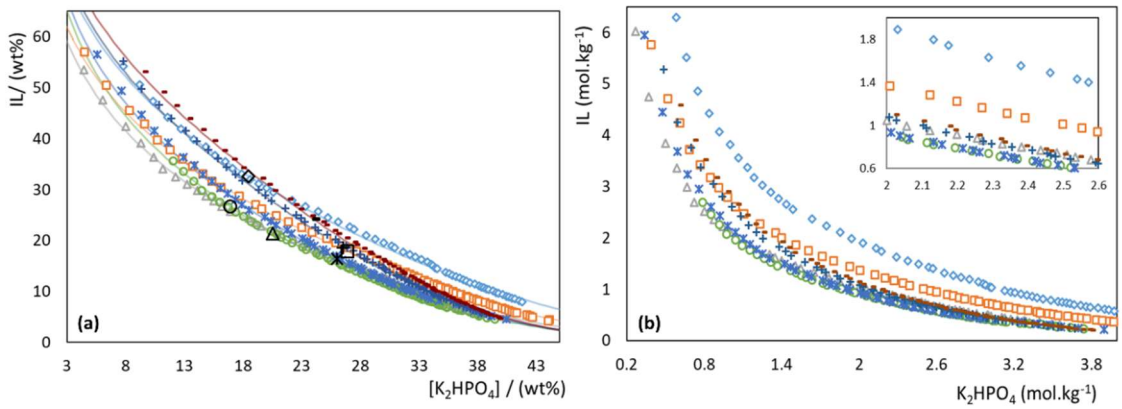

Figure 2.2. Phase diagrams in an orthogonal representation in **(a)** weight fraction and **(b)** molality units for the ABS formed by cholinium-based ILs + K_2HPO_4 + water at (298 ± 1) K and atmospheric pressure. ILs: [Ch][C_1CO_2] (◇), [Ch][C_2CO_2] (□), [Ch][C_3CO_2] (△), [Ch][C_4CO_2] (○), [Ch][C_5CO_2] (✳), [Ch][C_6CO_2] (+), [Ch][C_7CO_2] (-). The lines correspond to the fitting by Equation (1) and larger symbols correspond to the critical point of each system.

The phase separation in ABS is a result of the salting-out of the salt over the IL in aqueous media, which can be quantified by the Setschenow salting-out coefficient, k_s. The Setschenow constant of each IL-based ABS was determined by the simultaneous regression of at least four experimentally determined TLs, at initial mixture compositions falling within the biphasic region. The respective values are reported in the Appendix A (Table A11). Figure 2.3 depicts the behavior of the salting-out coefficient, k_s, as a function of the IL anion alkyl chain length. Although there is a continuous increase of the salting-out coefficient with the size of the IL anion aliphatic moiety, as expected due to IL anion hydrophobicity increase, a subtle odd-even effect is identified in these results. A slightly higher value of the salting-out coefficient is visible for ILs comprising anions with even alkyl chains, meaning that these are more easily salted-out by K_2HPO_4 or are more prone to undergo phase separation in aqueous media. The current results are in good agreement with our previous findings on the effect of the IL cation alkyl chain in ABS formation using the [$C_nC_1$im]Cl (n = 2-12) IL series and K_2CO_3 [20]. In this previous work [20], the odd-even effect in the k_s values was however more significant, and particularly in ILs up to n=6 where the nanostructuration/nanosegregation of ILs plays a less relevant role. This difference in intensity is thus connected to the cation vs. anion effect towards the ILs nanostructuration. The odd-even effect has been previously identified in several ILs properties, such as viscosities, molar volumes and entropy and enthalpy of vaporization [25-28]. It is here demonstrated that it also occurs in aqueous solution, indicating that the ILs organization and their nanostructuration in aqueous media contribute to the observed phenomenon. For the ILs pure properties, the odd-even effect has been explained based on the orientation of the terminal methyl groups and

further influence on the ILs cohesive energy [26-28], which is here shown to have a direct impact on their behaviour in aqueous solution and visible also as a result of the IL anion aliphatic moiety. Contrarily to the IL cation effect on the formation of ABS, which is mostly governed by steric and entropic contributions [21], the IL anion influence on the formation of biphasic systems is a main result of favorable (or non-favorable) interactions with water. Due to their more diffuse valence electronic configuration, anions are typically more polarizable than cations; thus, their hydration is usually stronger than that of the cations [43]. The anions tendency to form hydration complexes is directly connected to their cation-anion interaction strength. Accordingly, there is a close correlation between the salting-out coefficient and the total cation-anion energy of each IL, which in this work was determined by COSMO-RS, and as shown in Figure 2.3. The odd-even effect observed is a direct result of the k_s odd-even effect itself. It should be remarked that the cation-anion total interaction energies of each IL is a good indicator of the complexity of the interactions taking place in ABS, particularly van der Waals, electrostatic and hydrogen-bonding interactions, since the same type of interactions occur in the neat ILs contributing to their cohesive energy.

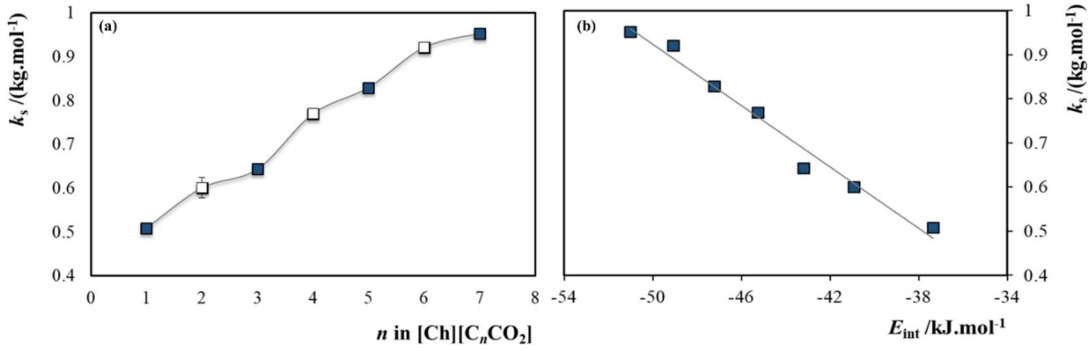

Figure 2.3. Salting-out coefficients (k_s) as a function of the IL anion alkyl chain length, *n*, in [Ch][C$_n$CO$_2$] ILs, and of the cation-anion total interaction energies of each IL (E_{int}).

2.3.2. Extraction of amino acids

The potential of ABS for extracting target compounds depends on the ability to manipulate the properties of the coexisting phases, which can be achieved by changing the IL used in ABS formulation. In this work, the potential of ABS composed of cholinium carboxylate ILs and K_2HPO_4 to act as separation platforms for hydrophobic amino acids, namely L-tryptophan, L-phenylalanine, L-tyrosine and L-dopa, was evaluated by their partition coefficients. These aromatic amino acids, and thus hydrophobic amino acids, were chosen to identify differences in partitioning that could mainly arise from dispersive interactions established with the IL anion aliphatic moieties. The results obtained are given in Figure 2.4. The extraction efficiencies of these systems are provided in the Appendix A, as well as the respective detailed results for both parameters. All partition studies were performed at a constant TLL (*ca.* 58 ± 2) to prevent the

effects that could result from the TLL effect or differences in the composition between the coexisting phases.

ABS formed by cholinium carboxylate ILs and K_2HPO_4 present a satisfactory extraction ability for amino acids. In all systems, amino acids preferentially partition to the most hydrophobic phase, *i.e.* the IL-rich phase, with extraction efficiencies ranging from 66.8% to 99.9% (Appendix A). The partition coefficients of amino acids (K_{AA}), depicted in Figure 2.4, range between 1.88 and complete extraction. In Figure 2.4, a K_{AA} of 100 is shown for the cases where complete extraction was achieved. These high values in both partition coefficients and extraction efficiencies result from the salting-out effect exerted by K_2HPO_4 and favorable interactions established between the IL-rich phase-forming components and the amino acids. Zafarani-Moattar and Hamzehzadeh [44] investigated the separation of several amino acids (L-tryptophan, L-phenylalanine, L-tyrosine, L-leucine, and L-valine) using IL-based ABS formed by $[C_4mim]Br$ and potassium citrate. The authors [44] concluded that the dispersive interactions are the main driving force for the amino acids partition. The results obtained for a given IL or ABS agree with the findings of Zafarani-Moattar and Hamzehzadeh [44] since the extraction efficiencies (Table A12 and Figure A3 in the Appendix A) and the partition coefficients (Table A13 in the Appendix A and Figure 2.4) follow the amino acids octanol-water partition coefficients ($\log(K_{ow})$: L-tryptophan = -1.06; L-phenylalanine = -1.38; L-tyrosine= -2.26; L-dopa = -2.74) [45]. In general, more hydrophobic amino acids are better extracted to the most hydrophobic IL-rich phase. However, ABS composed of ILs with shorter alkyl chains have a better performance at extracting amino acids to the IL-rich phase, meaning that hydrophobic interactions are not the only factor ruling the partition of a given amino acid along the $[Ch][C_nCO_2]$ series of ILs. This trend shows that the partitioning results are related with the affinity of each amino acid for each phase, which is ruled by multiple effects, including salting-out effects, hydrogen-bonding, dispersive and electrostatic interactions.

In addition to the two-phase formation ability, the occurrence of an even-odd effect is also observed in the partition coefficient results along the size of the anion aliphatic moiety – Figure 2.4. The odd-even effect occurs in the partition coefficients of all amino acids. In general, ABS formed by ILs with odd alkyl chains at the anion lead to slightly higher partition coefficients. These results suggest that the salting-out effect exerted by the salt is not the main factor ruling the amino acids partition since higher k_s values are observed for ABS composed of IL with even alkyl chains at the anion (Figure 2.3). Taking into account the previous discussion, there is thus a multitude of simultaneous effects governing the amino acids partitioning to the IL-rich phase, where salting-out effects and non-covalent interactions occurring between the amino acids and the ABS phase-forming components play a major role. As observed in several properties of pure ILs [26-28], the orientation of the terminal methyl groups of the carboxylate anion and their

influence on the ILs cohesive energy directly influences the ILs ability to interact with amino acids, which may thus be responsible for the observed odd-even effect.

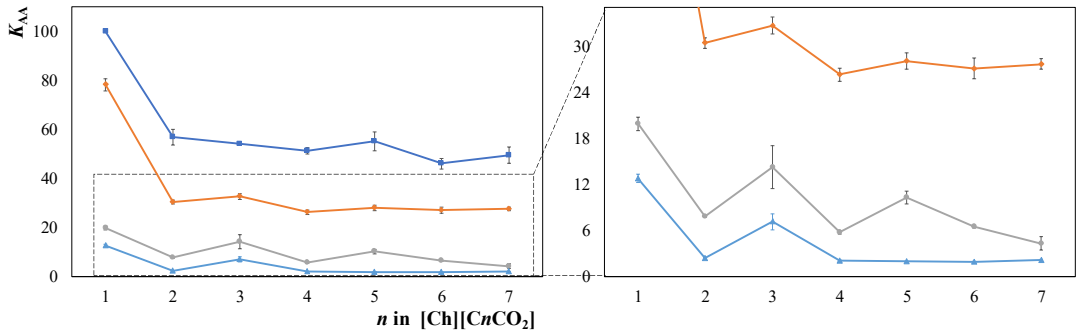

Figure 2.4. Partition coefficients (K_{AA}) of the studied ABS at 298 K for L-tryptophan (■), L-phenylalanine (◆), L-tyrosine (●), and L-dopa (▲).

In addition to previously reported odd-even effects in several thermophysical and thermodynamic properties of pure ILs [26-28], a similar phenomenon is here shown to occur in aqueous solutions of ILs, namely in ABS formed by ILs and salts, and that it is visible also as a result of the IL anion. The gathered data allow to confirm the existence of an odd-even effect derived from the IL anion alkyl chain length, with impact on both the two-phase or ABS formation ability and partitioning behavior of biomolecules.

2.4. Conclusions

IL-based ABS have been largely studied as separation strategies, demonstrating their outstanding performance on the extraction and purification of a variety of biomolecules. However, to achieve optimal extraction and separation performance, *a priori* characterization of the respective ABS ternary phase diagrams is required. In this work, we determined the phase diagrams of ABS formed by cholinium carboxylate ILs and K_2HPO_4 and evaluated their performance to extract hydrophobic amino acids. The [Ch][C_nCO_2] IL series, with n = 1 to 7, was chosen to appraise the existence of odd-even effects. It is here demonstrated that this phenomenon occurs in both the ABS formation ability and extraction performance. ILs comprising even alkyl chains display slightly higher k_s values, meaning that these ILs are more easily salted-out or more easily phase separated. The phase separation ability in ABS formed by ILs and salts is largely controlled by the IL anion capability to form hydration complexes, largely depending on the interactions established between the IL anion and water, as demonstrated by the correlation found between k_s and the total cation-anion IL interaction energy. On the other hand, ABS formed by ILs with odd alkyl chains at the anion lead to slightly higher partition coefficients, demonstrating that the salting-out effect does not play the major role on defining the partitioning trend. In addition to the previously reported odd-even effect in several properties of pure ILs, these results confirm an odd-even effect induced by the IL anion alkyl

chain length in aqueous media, valuable to a better understanding of the molecular-level mechanisms ruling the ABS formation ability and their extraction performance.

2.5. References

1. Marrucho IM, Freire MG (2016) Aqueous Biphasic Systems Based on Ionic Liquids for Extraction, Concentration and Purification Approaches. In Ionic Liquids for Better Separation Processes. Green Chemistry and Sustainable Technology. Springer, Berlin, Heidelberg. pp 91.119.
2. Albertsson P (1986) Partition of Cell Particles and Macromolecules: Separation and Purification of Biomolecules, Cell Organelles, Membranes, and Cells in Aqueous Polymer Two-phase Systems and Their Use in Biochemical Analysis and Biotechnology. 3rd ed.; John Wiley and Sons: Chichester, New York.
3. Zaslavsky BY (1995) Aqueous Two-Phase Partitioning: Physical Chemistry and Bioanalytical Applications. New York, M. Dekker.
4. Chen J, Spear SK, Huddleston JG, Holbrey JD, Swatloski RP, Rogers RD (2004) Application of Poly(ethylene glycol)-based Aqueous Biphasic Systems as Reaction and Reactive Extraction Media. Ind Eng Chem Res 43: 5358-5364.
5. Asenjo JA., Andrews BA (2011) Aqueous Two-Phase Systems for Protein Separation: A Perspective. J Chromatogr A 1218: 8826-8835.
6. Gutowski KE, Broker GA., Willauer HD, Huddleston JG, Swatloski RP, Holbrey JD, Rogers RD (2003) Controlling the Aqueous Miscibility of Ionic Liquids: Aqueous Biphasic Systems of Water-Miscible Ionic Liquids and Water-Structuring Salts for Recycle, Metathesis, and Separations. J Am Chem Soc 125: 6632-6633.
7. Garcia-Chavez L.Y, Garsia C.M, Schuur B, Haan AB (2012) Biobutanol Recovery Using Nonfluorinated Task-Specific Ionic Liquids. Ind Eng Chem Res 51: 8293-8301.
8. Freire MG, Cláudio AFM, Coutinho AP, Marrucho IM, Lopes JNC, Rebelo LPN (2012) Aqueous Biphasic Systems: A Boost Brought about by Using Ionic Liquids. Chem Soc Rev 41: 4966-4995.
9. Coleman D, Gathergood N (2010) Biodegradation Studies of Ionic Liquids. Chem Soc Rev 39: 600-637.
10. Stolte S, Steudte S, Areitioaurtena O, Pagano F, Thöming J, Stepnowski P, Igartua A (2012) Ionic Liquids as Lubricants or Lubrication Additives: An Ecotoxicity and Biodegradability Assessment. Chemosphere 89: 1135-1141.
11. Hou XD, Liu QP, Smith TJ, Li N, Zong MH (2013) Evaluation of Toxicity and Biodegradability of Cholinium Amino Acids Ionic Liquids. PLoS One 8: e59145.
12. Meck WH, Williams CL (1999) Choline Supplementation during Prenatal Development Reduces Proactive Interference in Spatial Memory. Brain Res Dev Brain Res 118: 51-59.
13. Zeisel, SH, Costa K.A (2009) Choline: An Essential Nutrient for Public Health Steven. Nutr Rev 67: 615-623.
14. Xie Y, Xing H, Yang Q, Bao Z, Su B, Ren Q (2015) Aqueous Biphasic System Containing Long Chain Anion-Functionalized Ionic Liquids for High-Performance Extraction. ACS Sustain Chem Eng 3: 3365-3372.
15. Shahriari S, Tomé L.C, Araújo JMM, Rebelo LPN, Coutinho JAP, Marrucho IM, Freire MG (2013) Aqueous Biphasic Systems: A Benign Route Using Cholinium-Based Ionic Liquids. RSC Adv 3: 1835-1843.
16. Pereira JFB, Vicente F, Santos-Ebinuma VC, Araújo JM, Pessoa A, Freire MG, Coutinho JAP (2013) Extraction of Tetracycline from Fermentation Broth Using Aqueous Two-Phase Systems Composed of Polyethylene Glycol and Cholinium-Based Salts. Process Biochem 48: 716-722.
17. Torres-Acosta MA, Pereira JFB, Freire MG, Aguilar-Yáñez JM, Coutinho JAP, Titchener-Hooker NJ, Rito-Palomares M (2018) Economic Evaluation of the Primary Recovery of Tetracycline with Traditional and Novel Aqueous Two-Phase Systems. Sep Purif Technol 203: 178-184.
18. Freire MG, Neves CMSS, Lopes JNC, Marrucho IM, Coutinho JAP, Rebelo LPN (2012) Impact of Self-Aggregation on the Formation of Ionic-Liquid-Based Aqueous Biphasic Systems. J Phys Chem B 116: 7660-7668.
19. Passos H, Trindade MP, Vaz TSM, Costa LP, Freire MG, Coutinho JAP (2013) The Impact of Self-Aggregation on the Extraction of Biomolecules in Ionic-Liquid-Based Aqueous Two-Phase Systems. Sep Purif Technol 108: 174-180.
20. Belchior DCV, Sintra TE, Carvalho PJ, Soromenho MRC, Esperança JMSS, Ventura SPM, Rogers RD, Coutinho JAP, Freire MG (2018) Odd-Even Effect on the Formation of Aqueous Biphasic Systems Formed by 1-Alkyl-3-Methylimidazolium Chloride Ionic Liquids and Salts. J Chem Phys 148: 193842.
21. Ventura SPM; Sousa SG, Serafim LS, Lima ÁS, Freire MG, Coutinho JAP (2012) Ionic Liquid Based Aqueous Biphasic Systems with Controlled pH: The Ionic Liquid Anion Effect. J Chem Eng Data 57: 507-512.

22. Najdanovic-Visak V, Canongia Lopes JN, Visak ZP, Trindade J, Rebelo L.PN (2007) Salting-out in Aqueous Solutions of Ionic Liquids and K_3PO_4: Aqueous Biphasic Systems and Salt Precipitation. Int J Mol Sci 8: 736-748.
23. Cláudio AFM, Ferreira AM, Shahriari S, Freire MG, Coutinho JAP (2011) Critical Assessment of the Formation of Ionic-Liquid-Based Aqueous Two-Phase Systems in Acidic Media. J Phys Chem B 115: 11145-11153.
24. Deive FJ, Rodríguez A, Marrucho IM, Rebelo L.PN (2011) Aqueous Biphasic Systems Involving Alkylsulfate-Based Ionic Liquids. J Chem Thermodyn 43: 1565-1572.
25. Adamová G, Gardas RL, Rebelo LPN, Robertson AJ, Seddon KR (2011) Alkyltrioctylphosphonium Chloride Ionic Liquids: Synthesis and Physicochemical Properties. Dalton Trans 40: 12750-12764.
26. Rocha MAA, Neves CMSS, Freire MG, Russina O, Triolo A, Coutinho JAP, Santos LMNBF (2013) Alkylimidazolium Based Ionic Liquids: Impact of Cation Symmetry on Their Nanoscale Structural Organization. J Phys Chem B 117: 10889-10897.
27. Rocha MAA, Coutinho JAP, Santos LMNBF (2012) Cation Symmetry effect on the Volatility of Ionic Liquids. J Phys Chem. B 116: 10922-10922.
28. Rocha MAA, Coutinho JAP, Santos LMNBF (2014) Vapor Pressures of 1,3-Dialkylimidazolium bis(trifluoromethylsulfonyl)imide Ionic Liquids with Long Alkyl Chains. J Chem Phys 141: 134502.
29. Quental MV, Caban M, Pereira MM, Stepnowski P, Coutinho JAP, Freire MG (2015) Enhanced Extraction of Proteins Using Cholinium-Based Ionic Liquids as Phase-Forming Components of Aqueous Biphasic Systems. Biotechnol J 10: 1457-1466.
30. Merchuk JC, Andrews BA, Asenjo JA (1998) Aqueous Two-Phase Systems for Protein Separation. Studies on phase inversion. J Chromatogr B Biomed Sci Appl 711: 285-293.
31. Seader JD, Henley EJ (2006) Separation Process Principles, 2nd Ed., John Wiley & Sons, Inc., Wiley.
32. Setschenow, JZ (1889) Über Die Konstitution Der Salzlösungen Auf Grund Ihres Verhaltens Zu Kohlensäure. J Phys Chem 4: 117-125.
33. Hey MJ, Jackson DP, Yan H (2005) The Salting-out Effect and Phase Separation in Aqueous Solutions of Electrolytes and Poly(Ethylene Glycol). Polymer 46: 2567-2572.
34. Zafarani-Moattar MT, Hamzehzadeh S (2009) Phase Diagrams for the Aqueous Two-Phase Ternary System Containing the Ionic Liquid 1-Butyl-3-Methylimidazolium Bromide and Tri-Potassium Citrate at T = (278.15, 298.15, and 318.15) K. J Chem Eng Data 54: 833-841.
35. Zafarani-Moattar MT, Hamzehzadeh S (2010) Salting-out Effect, Preferential Exclusion, and Phase Separation in Aqueous Solutions of Chaotropic Water-Miscible Ionic Liquids and Kosmotropic Salts: Effects of Temperature, Anions, and Cations. J Chem Eng Data 55: 1598-1610.
36. Kurnia KA, Lima F, Cláudio AFM, Coutinho JAP, Freire MG (2015) Hydrogen-Bond Acidity of Ionic Liquids: An Extended Scale. Phys Chem Chem Phys 17: 18980- 18990.
37. Univ. Karlsruhe Forschungszentrum Karlsruhe GmbH, TURBOMOLE V6.1. (2009) Univ. Karlsruhe Forschungszentrum Karlsruhe GmbH, TURBOMOLE V6.1 2009, 1989–2007, 25 GmbH, since 2007, available from http//www.turbomole.com, 1989.
38. Eckert F, Klamt A. (2006) COSMOtherm Version C2.1 Release 01.08, Cosmol. GmbH Co. KG, Leverkusen, Ger.
39. Araújo JMM, Ferreira R, Marrucho IM, Rebelo LPN (2011) Solvation of Nucleobases in 1,3-Dialkylimidazolium Acetate Ionic Liquids: NMR Spectroscopy Insights into the Dissolution Mechanism. J Phys Chem B 115: 10739-10749.
40. Costa AJL, Soromenho MRC, Shimizu K, Marrucho IM, Esperança JMSS, Lopes JNC, Rebelo LPN (2012) Liquid-Liquid Equilibrium of Cholinium-Derived Bistriflimide Ionic Liquids with Water and Octanol. J Phys Chem B 116: 9186-9195.
41. Mão de Ferro A, Reis PM, Soromenho MRC, Bernardes CES, Shimizu K, Freitas AA, Esperança JMSS, Lopes JNC, Rebelo LPN (2018) Designing the ammonium cation to achieve a higher hydrophilicity of bistriflimide-based ionic liquids. Phys. Chem. Chem. Phys., 20, 19307-19313.
42. Rengstl D, Kraus B, Van Vorst M, Elliott GD, & Kunz W (2014) Effect of choline carboxylate ionic liquids on biological membranes. Colloids and Surf B Biointerfaces 123: 575-581.
43. Freire MG, Carvalho PJ, Silva, AMS, Santos LMNBF, Rebelo LPN, Marrucho IM, Coutinho JAP (2009) Ion Specific Effects on the Mutual Solubilities of Water and Hydrophobic Ionic Liquids Ion Specific Effects on the Mutual Solubilities of Water and Hydrophobic Ionic Liquids. J Phys Chem B 113: 202-211.
44. Zafarani-Moattar, MT, Hamzehzadeh S (2011) Partitioning of Amino Acids in the Aqueous Biphasic System Containing the Water-Miscible Ionic Liquid 1-Butyl-3-Methylimidazolium Bromide and the Water-Structuring Salt Potassium Citrate. Biotechnol Prog 27: 986-997.
45. Chemspider, The free chemical database, http://www.chemspider.com.

3. Performance of Tretraalkylammonium-Based Ionic Liquids as Constituents of Aqueous Biphasic Systems in the Extraction of Ovalbumin and Lysozyme

Performance of Tetraalkylammonium-Based Ionic Liquids as Constituents of Aqueous Biphasic Systems in the Extraction of Ovalbumin and Lysozyme

Based on the submitted manuscript: [3]

D. C. V. Belchior, M. V. Quental, M. M. Pereira, C. M. N. Mendonça, I. F. Duarte and M. G. Freire. Separation and Purification Technology, 2019. Submitted.

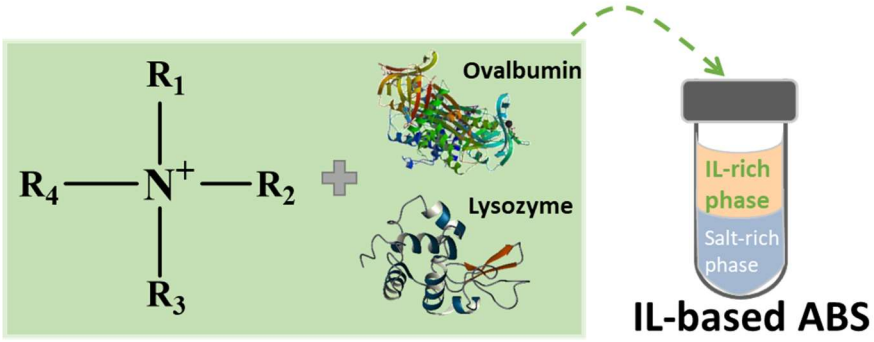

Abstract

Ionic-liquid-based aqueous biphasic systems (IL-ABS) have been highlighted as promising platforms for the extraction of proteins. However, imidazolium-based ILs have been the preferred choice, which may raise some biocompatibility and biodegradability concerns. In this work, novel ABS composed of tetraalkylammonium-based ILs and potassium phosphate solutions at different pH values (pH = 7, 8, 9 and 13, using K_2HPO_4/KH_2PO_4 or K_3PO_4) were investigated in the extraction and recovery yield of ovalbumin and lysozyme. These two proteins were selected due to their wide application in several sectors, being present in egg white. At pH 7, the complete extraction and recovery of lysozyme to the IL-rich phase is achieved in all systems; however, low recovery yields of ovalbumin are obtained with ABS formed by ILs with longer alkyl side chains. Furthermore, an increase in the pH above the proteins isoelectric point is deleterious for their recovery. In order to characterize the molecular-level mechanisms that could maximize the proteins recovery, molecular docking studies were carried out, showing that ILs that preferentially establish hydrophobic interactions with these proteins are those that lead to aggregation and lower recovery yields. Finally, it is shown the proteins recovery from the IL-rich phase by ice cold ethanol precipitation, where up to 99% of lysozyme can be recovered. These results support the viability of adequate IL-based ABS to extract ovalbumin and lysozyme and the possibility of recovering stable proteins from the IL-rich phase into an adequate buffered aqueous solution, thus contributing to the design of effective separation processes.

Keywords: Aqueous two-phase systems • ionic liquids • proteins • extraction • recovery • molecular docking.

[3]Contributions: M.G.F. and I.F.D. conceived and directed this work. D.C.V.B. acquired the experimental data. M.M.P performed the molecular docking. D.C.V.B., M.V.Q., M.M.P, M.C.M., M.G.F. and I.F.D. interpreted the obtained experimental data. The manuscript was mainly written by D.C.V.B. and M.G.F. with contributions from the remaining authors.

3.1. Introduction

Proteins play a crucial role in biological processes and are of fundamental value in biotechnological, therapeutic and diagnostic applications [1]. Their function and biological activity is related to their native structure, which is however delicate since their three-dimensional structure can be disturbed by changes in the medium composition, pH and/or temperature [2]. Therefore, current purification methods for proteins are not only costly, but may also lead to their loss of stability [3]. In addition to the development of cost-effective downstream processes, it is necessary to guarantee that these processes do not lead to changes in the proteins stability and biological activity.

A raw material rich in high-value proteins is egg white, which contains 88% of water and 11% of proteins, including ovalbumin, ovotransferrin, lysozyme and ovomucin [4], for which the development of efficient protein fractionation processes is required [5]. Ovalbumin represents ca. 54% of the total protein content in egg white, being a fosfoglycoprotein with 385 amino acids, with a molecular weight of 45 kDa, and an isoelectric point of 4.5 - 4.6 [6–8]. Ovalbumin is widely used as a nutrient supplement and as an allergen in establishing different animal models of asthma, food and dermal allergy [9,10]. On the other hand, lysozyme constitutes 3.4 - 3.5% of the total protein content in egg white, has a low molecular weight (14.3 kDa) and a high isoelectric point (10.7) [6,11]. Given its multiple functions (antiviral, antitumor and immune modulatory activities), lysozyme is often used as a model protein, ranging from enzymatic reactivity to proteins aggregation and crystallization studies [12–14]. Furthermore, lysozyme is an enzyme with bactericidal and bacteriostatic properties, used as a natural preservative by the food industry [15]. The potential of lysozyme as an anticancer drug and in the treatment of HIV has also been discussed [16]. Both lysozyme and ovalbumin are present in a low-cost raw material, namely egg white, requiring the development of cost-effective separation and fractionation processes in order to obtain highly pure and stable/biologically active proteins at low cost.

Amongst the various separation and purification methods applied to proteins, aqueous biphasic systems (ABS) have been largely investigated. ABS are formed by combining in aqueous solution two polymers, one polymer and one salt, or two salts above given concentrations [17]. These systems are mainly composed of water, and thus represent a favorable environment for the purification of biologically active biomolecules [17]. ABS are also considered as biocompatible and environmentally friendly extraction methods since they do not use volatile organic solvents [17]. Due to these advantages, ABS have been investigated for the recovery of proteins, enzymes and antibodies from their biological-containing media [18]. In addition to the widely investigated polymer-based ABS, Rogers and co-workers [19] reported the possibility of creating ABS by mixing ionic liquids (ILs) and inorganic salts in aqueous solutions, leading to a plethora of ABS with remarkable advantages, such as low viscosity, fast phase separation, and tunable polarities

[20]. Based on these advantages, a large number of ABS composed of ILs + water + organic/inorganic salts, amino acids, polymers or carbohydrates has been investigated in the past decade [21]. ILs are salts composed of large organic cations and organic or inorganic anions. Although they display negligible vapor pressure at ambient conditions, with inherent benefits from an environmental point of view, the main advantage of ILs as phase-forming components of ABS conveys on the possibility of tailoring the polarities of the coexisting phases by the manipulation of their ions chemical structures, therefore allowing the design of improved ABS [20,22].

IL-based ABS have been investigated in the extraction of several proteins, such as bovine serum albumin, lysozyme, trypsin, myoglobin, peroxidase, cytochrome c, hemoglobin, ovalbumin, among others [1,23–25]. In these studies, imidazolium-based ILs and inorganic salts have been the preferred choice as ABS phase-forming components [23]. However, these ILs may raise some biocompatibility and biodegradability concerns [26]. Accordingly, the synthesis and use of ILs featuring enhanced biocompatibility and a low environmental footprint have been proposed in recent years [27–31]. Among these, tetraalkylammonium-based fluids have been described as ILs of lower environmental impact and of lower cost [32]. However, few studies have considered tetraalkylammonium-based ILs as phase-forming constituents of ABS for the extraction of proteins [33–35]. Furthermore, in most IL-based ABS studied hitherto the pH was not adequately controlled, which is a crucial factor regarding the separation of proteins and enzymes, either because of their susceptible nature or differences in partition due to their isoelectric point.

In this work, a series of ABS composed of tetraalkylammonium-based ILs and potassium phosphate buffer solutions at different pH values (pH = 7, 8, 9 and 13, achieved by applying different K_2HPO_4:KH_2PO_4 mole ratios or K_3PO_4) were evaluated for the extraction of ovalbumin and lysozyme, by determining both the extraction efficiencies and recovery yields. The goal of this work is to better understand the IL chemical structure of less investigated ILs and pH effects on the extraction and recovery yield of ovalbumin and lysozyme, foreseeing the design of effective separation processes based on ILs for proteins.

3.2. Experimental Section

3.2.1. Materials

Eight ILs were investigated in what concerns their capacity for ABS formation when combined with buffer aqueous solutions constituted by potassium dihydrogen phosphate, KH_2PO_4 (99.5 wt% of purity), and potassium hydrogen phosphate trihydrate, $K_2HPO_4{\cdot}3H_2O$ (>98 wt% of purity), both acquired from Sigma–Aldrich, and tribasic potassium phosphate, K_3PO_4 (98 wt% of purity), supplied from Acros Organics. All ILs, as well as the proteins studied, namely ovalbumin (>98% of purity) and lysozyme (>90% of purity), were purchased from Sigma–Aldrich. The chemical

structures of the investigated ILs are depicted in Table 3.1, which additionally comprises their full name, acronym, and purities. The water used was double distilled, passed by a reverse osmosis system and further treated with a Milli-Q plus 185 water purification apparatus.

Table 3.1. Identification, purity and chemical structure of the studied ILs.

Name	Acronym	Purity (wt%)	Chemical structure
Benzyltrimethylammonium chloride	$[N_{111(C7H7)}]Cl$	>98%	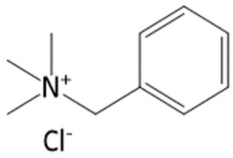
Benzyltriethylammonium chloride	$[N_{222(C7H7)}]Cl$	>99%	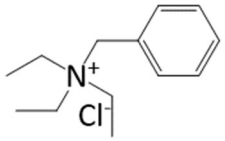
Benzyltributylammonium chloride	$[N_{444(C7H7)}]Cl$	>98%	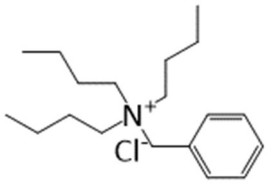
Tetraethylammonium chloride	$[N_{2222}]Cl$	>98%	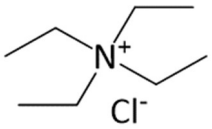
Tetrabutylammonium chloride	$[N_{4444}]Cl$	>96%	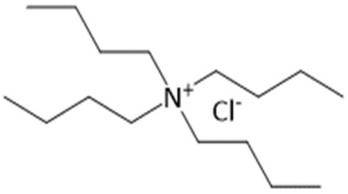
Tetraethylammonium bromide	$[N_{2222}]Br$	>99%	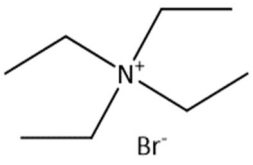
Tetrabutylammonium bromide	$[N_{4444}]Br$	>97%	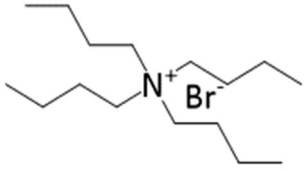
n-Octyltrimethylammonium bromide	$[N_{1118}]Br$	>98%	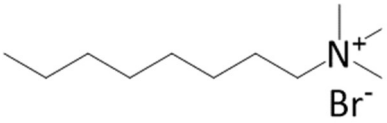

3.2.2. Determination of the ABS phase diagrams

Aqueous solutions containing 40 wt% of the salts K_2HPO_4 and KH_2PO_4 or K_3PO_4 at different mole ratio depending on the target pH, and aqueous solutions of the different ILs, with concentrations ranging from 40 wt% to 80 wt%, were initially prepared and used for the determination of the binodal curves. The pH of the prepared buffer solutions was confirmed using a Mettler Toledo S47 Seven Multi^{TM} dual meter pH equipment with an uncertainty of ± 0.02. The binodal curves of the ABS phase diagrams formed by each IL and K_2HPO_4/KH_2PO_4 or K_3PO_4 were determined through the cloud point titration method at (25 ± 1) °C and atmospheric pressure [36,37].The cloud point titration method consists in the repetitive dropwise addition of the salt solution into the aqueous solution of each IL until the detection of a cloudy (biphasic) solution, followed by the dropwise addition of ultrapure water until the observation of a limpid solution (falling within the monophasic region). All additions were carried out under constant stirring. The ternary system compositions were determined by the weight quantification of all components added (± 10^{-4} g). The experimental solubility curves were correlated using the following equation proposed by Merchuk et al. [38]:

$$[\mathrm{IL}] = A \exp[(B \times [\mathrm{Salt}]^{0.5}) - (C \times [\mathrm{Salt}]^{3})] \quad (1)$$

where [IL] and [Salt] represent the IL and salt weight fraction percentages, respectively, and *A*, *B*, and *C* are constants obtained by the regression of the experimental binodal data.

TLs, which give the composition of each phase for a given initial mixture composition, were determined by a gravimetric method originally proposed by Merchuk et al. [38], which is based on the relationship between the weight of both phases and the total system composition by the lever-arm rule. Ternary mixtures composed of IL + K_2HPO_4/KH_2PO_4 or K_3PO_4 + water were chosen at the biphasic region, gravimetrically prepared (± 10^{-4} g), and vigorously agitated. The ABS were then allowed to equilibrate for at least 12 h at (25 ± 1)°C aiming the complete separation of the coexisting phases. Both phases were carefully separated and individually weigthed. At the conditions used in this work, all systems have a top IL-rich phase and a salt-rich phase as the bottom layer. Further details on the determination of the TLs and respective length, i.e. tie-line lengths (TLLs), are given in the Supporting Information.

3.2.3. Extraction of proteins using ABS

The ternary mixture compositions used in the extraction experiments were chosen based on the phase diagrams determined in this work for each IL-salt-water ABS. Aqueous solution of ovalbumin and lysozyme at concentrations *ca.* 0.5 g·L^{-1} were used as the aqueous solutions added to each ternary mixture. Aqueous solutions of different molar ratio of the salts

K_2HPO_4/KH_2PO_4 were used to prepare aqueous solutions with pH values ranging between 7 and 9, while aqueous solutions of K_3PO_4 were used for pH 13. Each mixture was vigorously stirred, centrifuged for 10 min, and left to equilibrate and phase separate for 10 min at 25°C. After, each phase was recovered and diluted at a 1:10 (v:v) ratio in a phosphate buffer aqueous solution before the injection in a size exclusion high performance liquid chromatography (SE-HPLC) for quantification. At least three independent ABS at each condition were prepared and analyzed. The equipment used was a Chromaster HPLC system (VWR Hitachi) equipped with a binary pump, column oven, temperature controlled auto-sampler, DAD detector and a Shodex Protein KW- 802.5 (8 mm × 300 mm) column. For the detection of the two proteins in each phase, different HPLC conditions need however to be applied. The description of the HPLC conditions used for the identification and quantification of each protein is given in the Supporting Information. The temperature of the column and auto-sampler was kept constant at 25°C. The injection volume was of 25 µL. The wavelength was set at 280 nm, whereas the retention times of ovalbumin and lysozyme were found to be 15 min and 9 min, respectively. The quantification of proteins in each phase was carried out using the respective calibration curves.

The percentage extraction efficiency of the studied ABS for each protein to the IL-rich phase, EE_{Prot}%, was determined according to Eq. (2):

$$EE\% = \frac{w_{IL_{\mathrm{Prot}}}}{w_{IL_{\mathrm{Prot}}} + w_{salt_{\mathrm{Prot}}}} \times 100 \quad (2)$$

where w_{ILProt} and $w_{SaltProt}$ are the total weight of each protein in the IL-rich and in the salt-rich aqueous phases, respectively.

The recovery yield of each protein into to IL-rich phase, RY_{Prot}%, is the percentage ratio between the amount of protein in the IL-rich aqueous phase (w_{ILProt}) to that present in the initial mixture ($w_{InitialProt}$), defined according to Eq. (3),

$$RY\% = \frac{w_{IL_{Prot}}}{w_{InitialProt}} \times 100 \quad (3)$$

Finally, attempts on the recovery of the proteins from the IL-rich phase were carried out. To this end, ice cold ethanol was added to the IL-rich phase containing the target protein, and the solution was kept at -80 °C for 1 h. The precipitated fraction was carefully separated using centrifugation (3 min at 500 rpm) and dried under inert atmosphere. Proteins were redissolved in PBS buffer (100mM and pH 7.4) and quantified by SE-HPLC as described before.

3.2.4. Molecular docking

The interaction sites of Ova and Lys with the ILs ions were identified using the Auto-dock vina 1.1.2 program [39]. The following crystal structures were used: Lysozyme (PDB 4ym8) and Ova (PDB: 1ovalbumin adapted removing B, C and D chains). The Auto DockTools (ADT) [40] program was used to prepare the protein input files by merging non-polar hydrogen atoms, adding partial charges and atom types. Ligand (ILs ions) 3D atomic coordinates were computed by the Discovery Studio Visualizer [41] and ligand rigid root was generated using AutoDockTools (ADT), setting all possible rotatable bonds defined as active by torsions. The grid center at the center of mass (x-, y-, and z-axes, respectively) to cover the whole interaction surface of ovalbumin was 104 Å× 98 Å × 88 Å and of lysozyme was 100 Å× 112 Å × 126 Å. The binding model was searched out from 10 different conformers for each ligand (IL cation or anion).

3.3. Results and Discussion

3.3.1. ABS phase diagrams

The experimental ABS phase diagrams determined at 25 °C and at atmospheric pressure for each IL + water + K_2HPO_4/KH_2PO_4 system at pH 7 are illustrated in Figure 3.1.

The binodal curves are plotted both in weight fraction and in molality units. The first representation is useful to directly identify the mixture compositions required to form and prepare ABS for separation purposes, whereas the second representation is valuable to remove the effects related with differences in the ILs and salts molecular weight aiming the interpretation of the molecular-level mechanisms responsible for phase separation. The experimental weight fraction data of binodal curves, tie-lines and tie-line length data are provided in the Appendix B. All the calculations considering the weight fraction of the phase-forming components were carried out discounting the complexed water in the commercial phosphate-based salts. The experimental binodal data were fitted using the empirical relationship described by Eq. (1), also shown in Figure 3.1 The regression parameters estimated by the least-squares regression method, respective standard deviations, and correlation coefficients are provided in the Appendix B.

Figure 3.1 depicts the phase diagrams obtained at a constant pH, namely pH 7, allowing to address both the effect of the IL cation and anion to form two-phase systems. For a given salt composition, for instance, using K_2HPO_4/KH_2PO_4 at ≈ 0.25 mol·kg^{-1}, the capacity of ammonium-based ILs to form ABS follows the order: $[N_{4444}]Br \approx [N_{4444}]Cl \approx [N_{444(C7H7)}]Cl > [N_{222(C7H7)}]Cl > [N_{2222}]Br > [N_{1118}]Br > [N_{2222}]Cl \approx [N_{111(C7H7)}]Cl$. Diagrams with a larger area above the binodal curve have a higher ability to form two phases, i.e. the IL is more easily salted out by the phosphate-based salt due to a decrease in the IL affinity for water. In general, ILs with longer alkyl side chains are more prone to be salted-out and to form ABS, in agreement with previously published

data [42,43]. Furthermore, bromide-based ILs are more able to form ABS than the chloride IL equivalents due to the bromide lower affinity for water, in agreement with their hydrogen-bond basicity values [44].

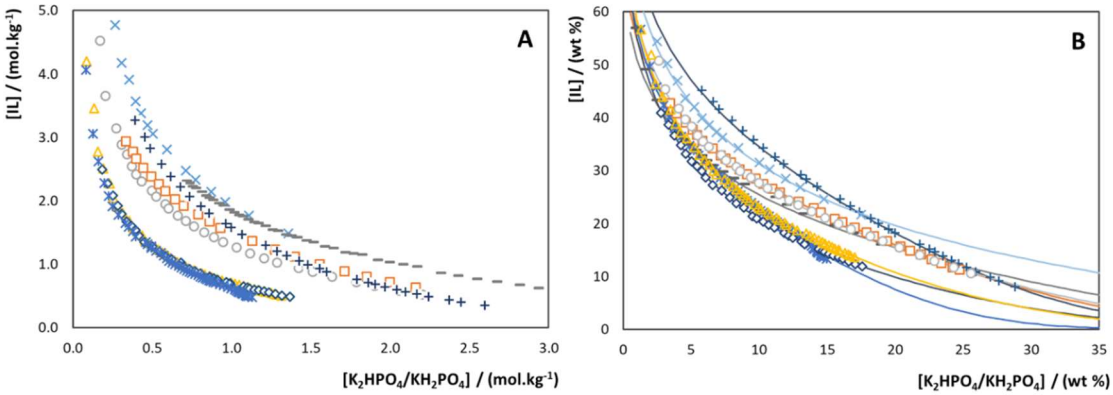

Figure 3.1. Phases diagrams of the ABS formed by IL + K_2HPO_4/KH_2PO_4 + water at pH 7, 25°C and atmospheric pressure in molality units (A) and weigth fraction percentage (B). ILs: $[N_{111(C7H7)}]Cl$ (×); $[N_{2222}]Cl$ (–); $[N_{2222}]Br$ (□); $[N_{222(C7H7)}]Cl$ (○); $[N_{444(C7H7)}]Cl$ (△); $[N_{4444}]Cl$ (◊); $[N_{4444}]Br$ (✳); $[N_{1118}]Br$ (+). Lines correspond to the fitting by Eq. (1).

The pH effect (pH 7, 8, 9 and 13) on ABS formation was evaluated using three tetraalkylammonium-based ILs, namely $[N_{2222}]Cl$, $[N_{2222}]Br$ and $[N_{222(C7H7)}]Cl$. The results depicted in Figure 3.2 show that for all ILs investigated the capacity to form ABS decreases with the decrease of the pH (13 > 9 > 8 > 7). Overall, the decreasing of the pH value leads to a decreasing in the phase-separation ability, as a result of the salts speciation and respective salting-out aptitude. These results are in agreement with previous published results with ABS formed by other ILs and salts [23,45,46].

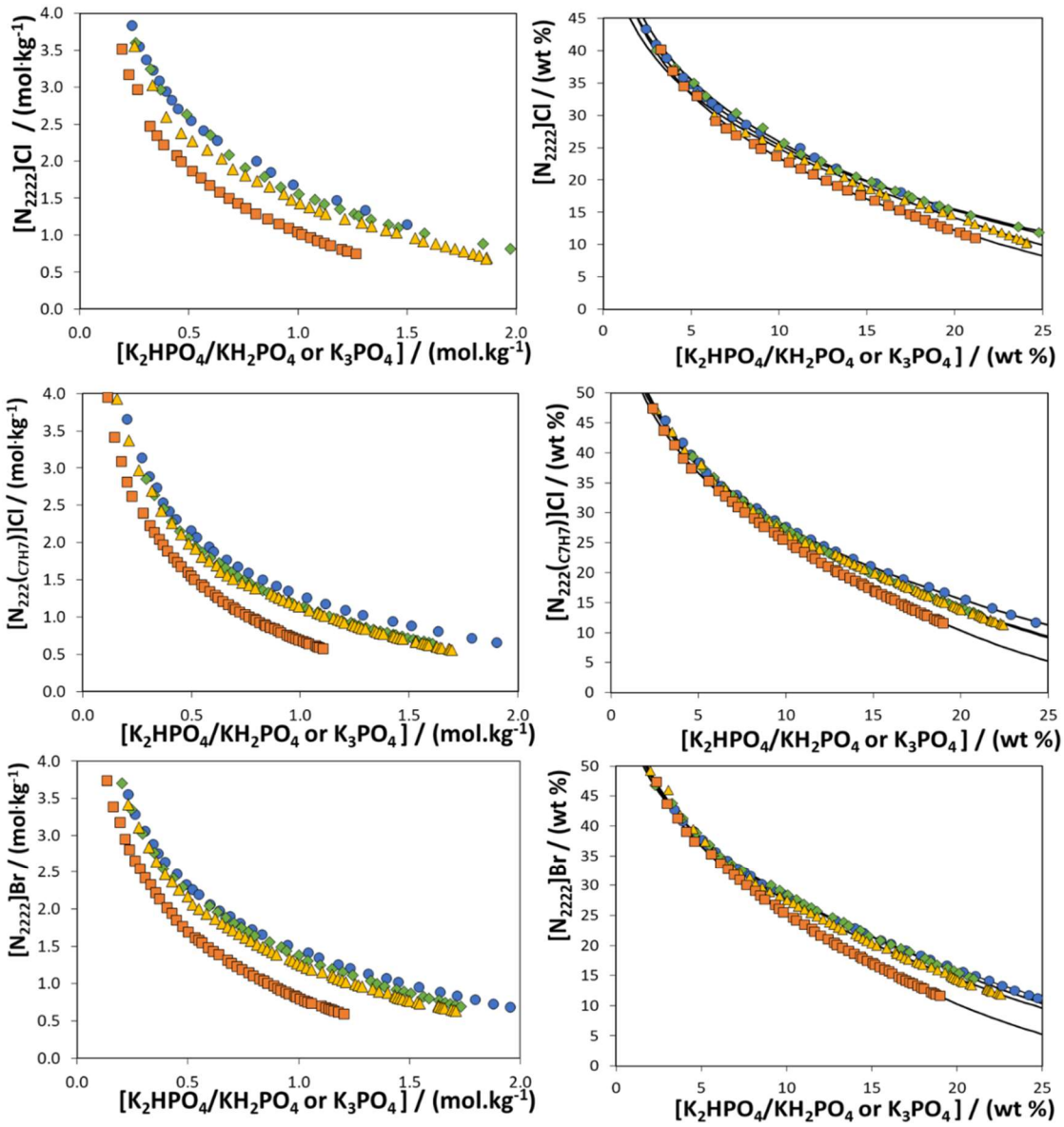

Figure 3.2. Phase diagrams in molality units and weight fraction units for ABS formed by IL ([N_{2222}]Cl, [$N_{222(C7H7)}$] and [N_{2222}]Br) + K_2HPO_4/KH_2PO_4 or K_3PO_4 + H_2O at 25°C and atmospheric pressure: pH 7 (●), pH 8 (◆), pH 9 (▲) and pH 13 (■). Lines correspond to the fitting by Eq. (1).

3.3.2. Extraction of ovalbumin and lysozyme using ABS, molecular docking studies and recovery strategies

Ternary mixtures at pH 7 were initially selected to evaluate the ABS performance to extract lysozyme and ovalbumin. Based on the phase diagrams, mixture compositions with a similar tie-line length (50 ± 2) were chosen to minize the differences in the proteins partition behavior arising from differences between the two phases compositions. These ABS are composed of 16-24 wt% of K_2HPO_4/KH_2PO_4 and 21-35 wt% of IL. The detailed mixture compositions, compositions of each phase, tie-line length values, extraction efficiencies and recovery yields of the ABS at pH 7 for ovalbumin and lysozyme are given in the Appendix B.

Figure 3.3 depicts the extraction efficiencies and recovery yields of the studied ABS for ovalbumin at pH 7. In all investigated systems, ovalbumin preferentially partitions to the top

phase (IL-rich phase), with extraction efficiencies of 100% obtained in a single-step. In general, the partitioning of proteins between the two phases of ABS is a complex phenomenon, guided either by differences in the hydrophobicity of the phases or by preferential interactions established between the protein being partitioned and the phase-forming components, being the latter possibility particularly relevant when dealing with ILs. Proteins can interact with ILs through hydrogen-bonding, electrostatic interactions and dispersive forces. Given that the isoelectric point of ovalbumin is 4.5 - 4.6 [6–8], in all systems and results shown in Figure 3.3 at pH 7, ovalbumin is negatively charged and prefers the phase of lower ionic strength (IL-rich). This trend reinforces the salting-out effect exerted by the salt used and possible preferential interactions, such as hydrogen-bonding and dispersive interactions, occurring between the protein and the IL. Although no differences are observed in terms of extraction efficiency with the IL chemical structure and thus on the IL-protein interactions, there is a different scenario when evaluating the recovery yield, which reflects the amount of the non-disturbed protein at the IL-rich phase in respect to that initially added to the system. By using SE-HPLC as quantification technique, with examples of chromatograms shown in Figure 3.3, it is possible to identify ovalbumin aggregates that appear at lower retention times in some ABS. It should be however remarked that the presence of aggregates, even though in a lower extent, is also seen in the protein aqueous solution prepared as standard.

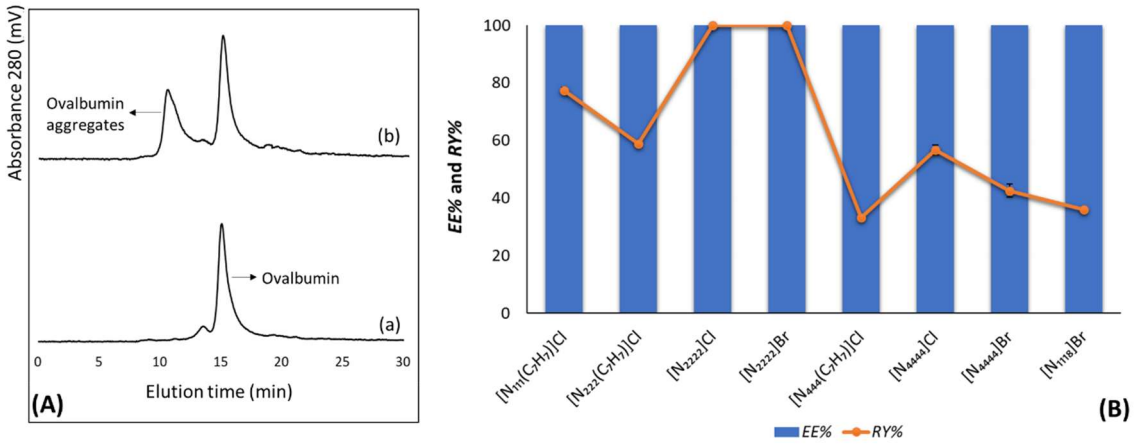

Figure 3.3. (A) Size exclusion chromatograms of (a) ovalbumin solution in PBS (b) IL–rich phase of the ABS composed of $[N_{222(C7H7)}]Cl$ + K_2HPO_4/KH_2PO_4 + ovalbumin aqueous solution at pH 7. (B) Average extraction efficiencies (*EE*%, bars) and percentage recovery yield (*RY*%, symbols and line) of the ABS composed of ILs + K_2HPO_4/KH_2PO_4 + H_2O at pH 7 for ovalbumin.

Although all the studied ABS at pH 7 allow the complete extraction of ovalbumin to the IL-rich phase, some ILs lead to a decrease on the protein recovery yield. Recovery yields ranging between 33 and 100% were obtained, and decrease according to the following ILs trend: $[N_{2222}]Cl \approx [N_{2222}]Br > [N_{111(C7H7)}]Cl > [N_{222(C7H7)}]Cl > [N_{4444}]Cl > [N_{4444}]Br > [N_{1118}]Br > [N_{444(C7H7)}]Cl$. The higher the decrease in the recovery yield, the higher is the amount of ovalbumin aggregates identified by SE-HPLC. In general, ABS formed by ILs with shorter alkyl side chains lead to higher

recovery yields. Moreover, the presence of an aromatic ring at the IL cation leads to a decrease of the recovery yield of ovalbumin, addressed by comparing the pairs of ILs: $[N_{2222}]Cl$ vs. $[N_{222(C7H7)}]Cl$ and $[N_{4444}]Cl$ vs. $[N_{444(C7H7)}]Cl$. This trend reflects that π···π stacking between the IL aromatic groups and the aromatic amino acids residues of ovalbumin are not relevant and do not positively contribute to the protein recovery in the IL-rich phase.

Figure 3.4 depicts the *EE*% of the same ABS and at the same mixture compositions at pH 7 for lysozyme; in all systems there is the preferential partition of the protein to the IL-rich aqueous phase, with complete extraction efficiencies achieved in one-step (as observed before with ovalbumin). Lysozyme has a low molecular weight (14.3 kDa) and a high isoelectric point (10.7) [6,11], being positively charged at pH 7. As verified with ovalbumin, lysozyme prefers the phase of lower ionic strength (IL-rich), reinforcing the possible salting-out effect exerted by K_2HPO_4/KH_2PO_4 and preferential interactions established with ILs. However, at pH 7 ovalbumin is negatively charged whereas lysozyme is positively charged. Although with ovalbumin some losses on the protein yield were observed due the protein aggregation, with lysozyme the percentage recovery yield with the investigated ABS is of 100%, meaning that there are no losses of lysozyme or the formation of protein aggregates during the extraction step with none of the systems investigated (Figure 4A). This set of results suggest that the investigated IL-based ABS lead to higher recovery yields when dealing with positively charged and smaller proteins, such as lysozyme [47].

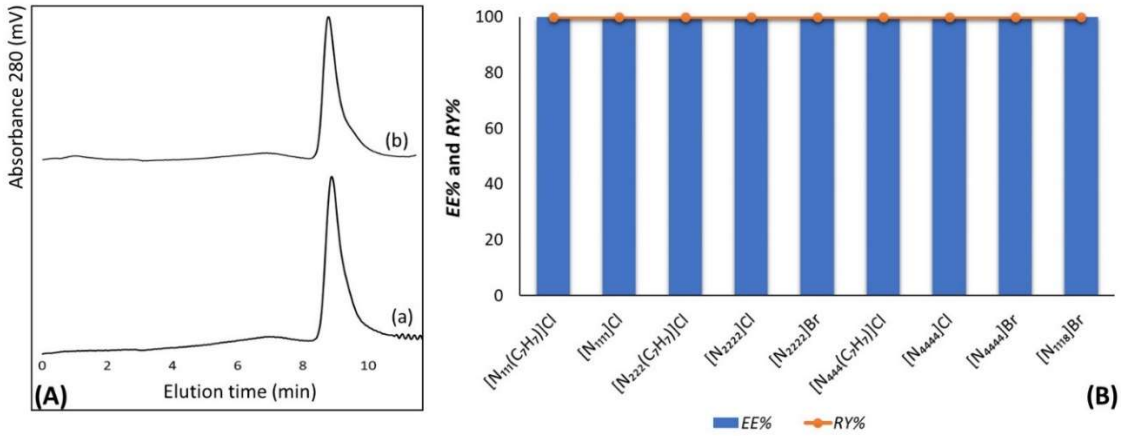

Figure 3.4. A) Size exclusion chromatograms of (a) lysozyme solution in PBS, (b) IL–rich phase of the ABS composed of $[N_{222(C7H7)}]Cl$ + K_2HPO_4/KH_2PO_4 + lysozyme aqueous solution at pH 7. ((B) Average extraction efficiencies (*EE*%, bars) and percentage recovery yield (*RY*%, symbols and line) of the ABS composed of ILs + K_2HPO_4/KH_2PO_4 + H_2O at pH 7 for lysozyme.

Ovalbumin and lysozyme are usually studied as model proteins to investigate the driving forces of protein partition in IL-based ABS. Chen et al. [33] evaluated the effect of several parameters to identify the optimal conditions in the extraction of ovalbumin, bovine serum albumin (BSA) and bovine hemoglobin (BHb) in ABS formed by hydroxyl ammonium-based ILs. The authors showed that under the optimum conditions, the extraction efficiency of ovalbumin could reach

68%. Comparing these results with ours, particularly when addressing the recovery yield values obtained with ovalbumin, it is clear that the chemical structure of the IL also plays a major role in the ovalbumin partition and recovery. Desai et al. [48] revealed that the size and complexity of the protein influences protein aggregation and its stability in ILs. In some works, it has been reported that larger proteins are less prone to migrate to the IL-rich phase compared to smaller ones [49,50], in agreement with the results obtained in this work since there are no losses of the smaller (lysozyme) protein using IL-based ABS. The use of ABS in the extraction of ovalbumin, cytochrome C, myoglobin, and hemoglobin was investigated and further compared with traditional PEG-based ABS by Ruiz-Angel et al. [51]. Larger partition coefficients in IL-based ABS were reported [51], reinforcing the usefulness of these systems comprising ILs for proteins extraction and recovery, and as demonstrated in this work with extraction efficiencies of 100% achieved in one-step.

When dealing with proteins or enzymes, the pH is one of the most important parameters to take into account. Some studies showed that the closer the pH of the system is to the pI of each protein, the more significant the hydrophobic interactions are and the easier it is to manipulate the migration of proteins between the phases [48]. Aiming at better understanding the pH effect in the ABS extraction and recovery of proteins, additional ABS were prepared at pH values of 8, 9 and 13. The minimum pH that can be investigated is 7.0 since it is not possible to create ABS with the studied ILs at lower pH values, as experimentally verified by us (no cloud point or two-phase separation observed). Lysozyme was the protein studied since it has an isoelectric point of (10.7) [6,11] (higher than 7) and as such it is possible to address changes in pH below and above its isoelectric point.

Figure 3.5 shows the extraction efficiency and recovery yield of the studied ABS at the pH values 7, 8, 9 and 13 for lysozyme. The mixture compositions, compositions of each phase and tie-line length values of each mixture point are given in the Supporting Information. Up to a pH of 9, all ABS investigated, composed of 16-24 wt% of K_2HPO_4/KH_2PO_4 and 21-35 wt% of IL to obtain a TLL ca. (50 ± 2), provide 100% of extraction efficiency and 100% of recovery yield for lysozyme. However, at pH 13, and although extraction efficiencies are still kept at 100%, there is the loss of the protein, with recovery yields ranging from 31 to 78% (depending on the IL chemical structure). This trend is in agreement with the trend observed before with ovalbumin that was negatively charged in all conditions studied. Lysozyme is negatively charged at pH 13, and as observed before with ovalbumin, there is a decrease in the recovery yield when using IL-based ABS. Accordingly, the IL chemical structure plays a more significant role when evaluating their application to extract negatively charged proteins. As observed with ovalbumin, ILs with shorter alkyl side chains at the cation and comprising chloride anions are more favorable to recover lysozyme in the IL-rich phase. Besides these assumptions, it should not be discarded that an extreme pH value is being used in this case (pH=13) to extract lysozyme.

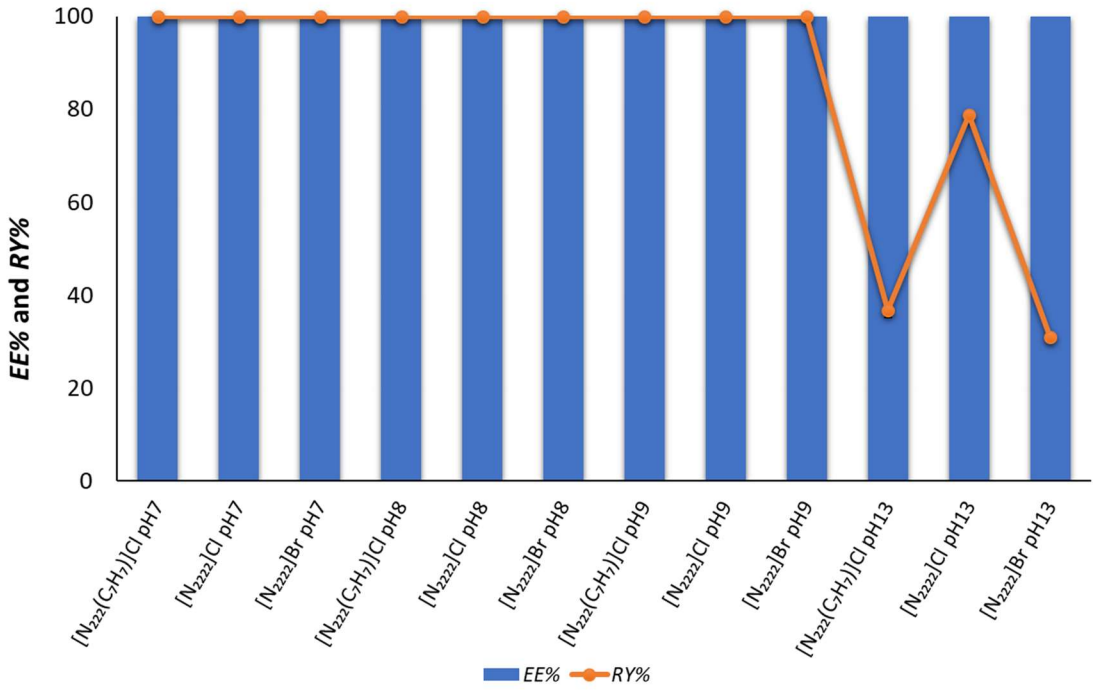

Figure 3.5. Extraction efficiencies (*EE*%, bars) and percentage recovery yields (*RY*%, symbols and line) of the ABS composed of ILs + K_2HPO_4/KH_2PO_4 (pH 7,8,9) or K_3PO_4 (pH 13) + H_2O for lysozyme.

Molecular docking was used to better understand the obtained extraction efficiencies and recovery yields for both proteins with the different ILs. In particular, docking interactions of all ILs ions (anions and cations) with the two proteins were determined. The results obtained show that IL cations display distinct interactions according to the respective chemical structure and the protein surface. The docking bind pose for the IL cations with both proteins are displayed in Figures 3.6 and 3.7. The docking bind pose for the IL anions with both proteins are displayed in the Appendix B. The best binding poses and docking affinities, interacting amino acids residues, type of interaction and geometry distance (Å) of each IL ion are provided in the Appendix B.

For both proteins, IL anions preferentially interact by hydrogen-bonding; e.g. the docking values of affinity for ovalbumin and Cl^- and Br^- anions are similar, namely -1.3 kcal/mol and -1.2 kcal/mol, justifying the less significant differences observed in the recovery yields of ovalbumin by changing the anion when compared to the IL cation effect. Furthermore, and for both proteins, Cl^- and Br^- display a smaller distance to the protein when compared to the distance shown by the IL cations, meaning that they have a high probability to be present in both proteins first solvation layer. On the other hand, IL cations with higher absolute values of docking affinity energies with the interacting amino acids residues of ovalbumin are those that lead to lower recovery yields. The tetraalkylammonium-based cations with shorter alkyl side chains ($[N_{2222}]^+$ and $[N_{4444}]^+$) display mainly hydrogen-bonding and electrostatic interactions with both proteins. However, an increase in the size of the aliphatic moieties ($[N_{1118}]^+$) or the presence of aromatic rings ($[N_{111(C7H7)}]^+$, $[N_{222(C7H7)}]^+$ and $[N_{444(C7H7)}]^+$) lead to the establishment of hydrophobic

interactions with both proteins. Therefore, it seems that ILs comprising cations that preferentially interact by hydrophobic interactions are those that lead to the formation of protein aggregates and lower recovery yields, which is particularly seen with ovalbumin.

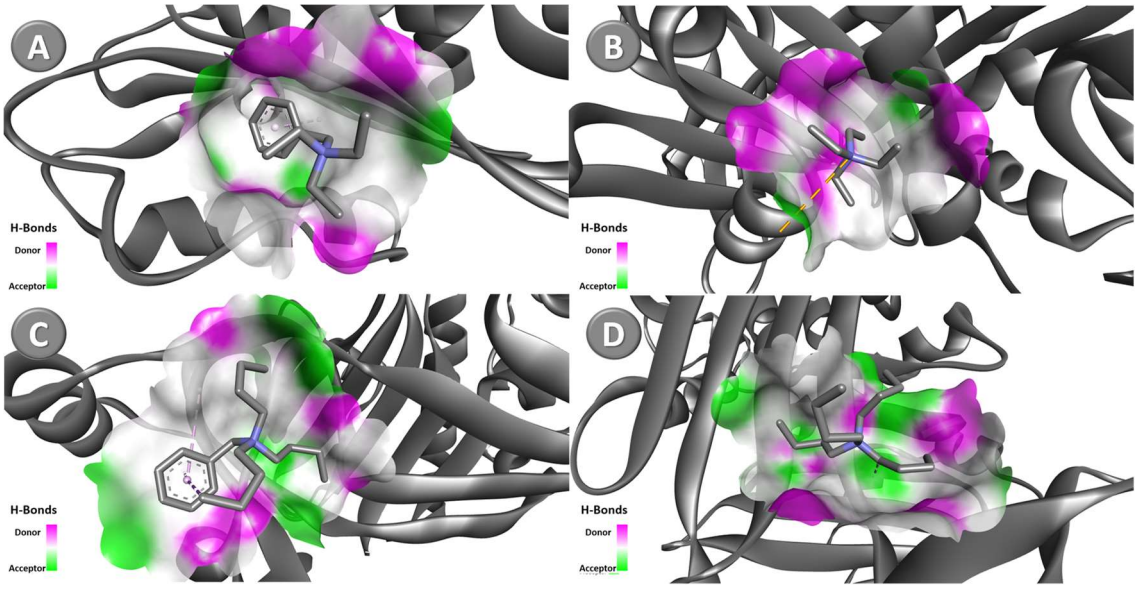

Figure 3.6. Docking pose with the lowest absolute value of affinity for ovalbumin with: (A) $[N_{222(C7H7)}]^+$, (B) $[N_{2222}]^+$, (C) $[N_{444(C7H7)}]^+$ and (D) $[N_{4444}]^+$.

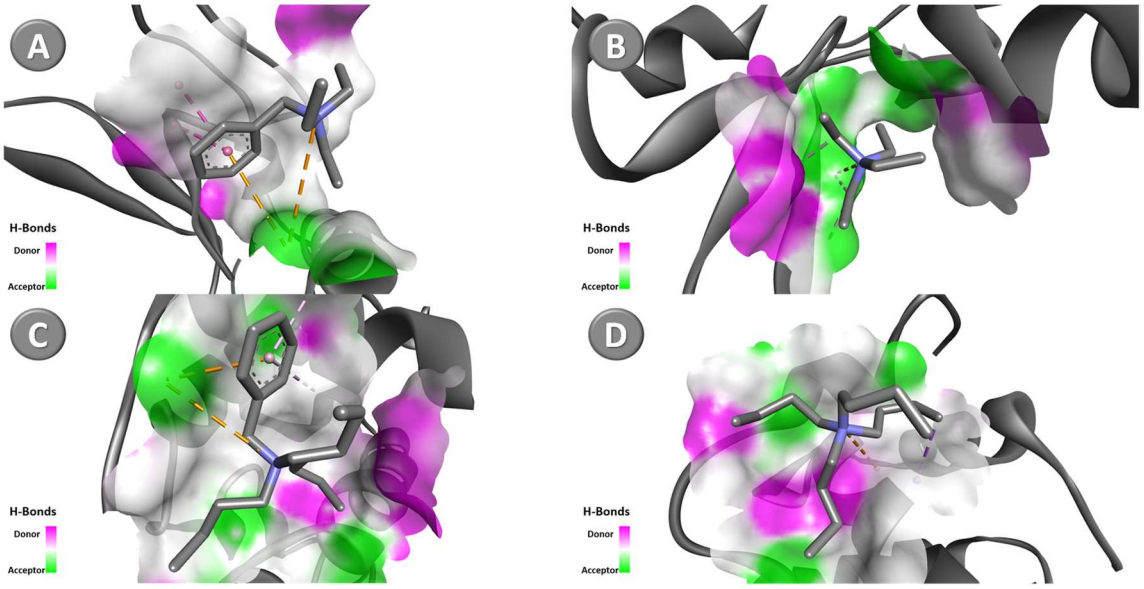

Figure 3.7. Docking pose with the lowest absolute value of affinity for lysozyme with: (A) $[N_{222(C7H7)}]^+$, (B) $[N_{2222}]^+$, (C) $[N_{444(C7H7)}]^+$ and (D) $[N_{4444}]^+$.

In addition to the complete extraction and recovery yield of proteins using IL-based ABS it is highly relevant to develop methodologies to further recover the target proteins from the IL-rich phase. In this work, lysozyme was precipitated from the IL-rich phase of the ABS composed of $[N_{2222}]Cl$, $[N_{2222}]Br$ and $[N_{222(C7H7)}]Cl$ + K_2HPO_4/KH_2PO_4 (pH 7 and 8) or K_3PO_4 (pH 13) using ice cold ethanol. Lysozyme was resuspended in phosphate buffer (100 mM) aqueous solutions at pH 7.4 and analyzed and quantified by SE-HPLC. From the SE-HPLC results (cf. the Appendix B), in all systems at pH 7 and 8 it is shown that lysozyme is stable after the induced precipitation and

resuspension steps. Upon increasing the pH up to 13, significative changes in the chromatograms are observed, in agreement with previous studies demonstrating conformational changes of lysozyme at extreme alkaline pH values [52]. At pH 7 and 8, with ABS formed by $[N_{222(C7H7)}]Cl$ ca. 81% of lysozyme can be recovered, whereas with the ABS formed by $[N_{2222}]Br$ and $[N_{2222}]Cl$ the recovery of lysozyme increases up to 95 and 99%, respectively. In summary, the obtained results indicate no structural changes in the protein by the formation of aggregates after the recovery step at pH 7 and 8, and confirm the viability of using the proposed ABS for the extraction of lysozyme and of the proposed recovery strategy of proteins from the IL-rich phase.

3.4. Conclusions

In this work, novel ABS composed of tetraalkylammonium-based ILs and potassium phosphate solutions at different pH values (pH = 7, 8, 9 and 13 using K_2HPO_4:KH_2PO_4 at different mole ratios or K_3PO_4) were investigated in the extraction of ovalbumin and lysozyme. The respective ABS ternary phase diagrams, as well as the tie-lines and tie-line lengths, were also determined at 25°C, where an increase in the pH and in the IL hydrophobicity by the increase of the IL cation alkyl side chain length or by using anions with lower hydrogen-bond basicity is favorable for two-phase separation.

At pH 7 the complete extraction and recovery of lysozyme was achieved in a single-step with all IL-based ABS. However, low recovery yields and the formation of aggregates of ovalbumin occur with ABS formed by ILs with longer alkyl side chains. Furthermore, pH plays a crucial role in two proteins recovery yield. pH values higher than the proteins isoelectric point lead to lower recovery yields, being the respective magnitude dependent on the IL chemical structure. Overall, the increase in the pH above the two proteins isoelectric point is not beneficial for their extraction using the investigated IL-based ABS. Finally, it was proposed one strategy for the proteins recovery from the IL-rich phase, namely by ice cold ethanol induced precipitation, where up to 99% of lysozyme can be recovered with no changes in their structure. These results support the viability of adequate IL-based ABS to extract proteins and the possibility of recovering stable proteins from the IL-rich phase into an adequate buffered aqueous solution. The selected ABS allowed to better identify the molecular-level mechanisms and conditions that maximize ovalbumin and lysozyme extraction efficiencies and recovery yields, while contributing to the design of effective separation processes for proteins from complex matrices.

3.5. References

1. Pei Y, Wang J, Wu K, Xuan X, Lu X (2009) Ionic liquid-based aqueous two-phase extraction of selected proteins. Sep Purif Technol 64:288–295.
2. Patel R, Kumari M, Khan AB (2014) Recent advances in the applications of ionic liquids in protein stability and activity: A review. Appl Biochem Biotechnol 172:3701–3720.

3. Lin X, Wang Y, Zeng Q, Ding X, Chen J (2013) Extraction and separation of proteins by ionic liquid aqueous two-phase system. Analyst 138:6445–6453.
4. Omana DA, Wang J, Wu J (2010) Co-extraction of egg white proteins using ion-exchange chromatography from ovomucin-removed egg whites. J Chromatogr B 878:1771–1776.
5. Abeyrathne EDNS, Lee HY, Ahn DU (2013) Egg white proteins and their potential use in food processing or as nutraceutical and pharmaceutical agents – a review. Poult Sci 92:3292–3299.
6. Hatta H, Kapoor MP, Juneja LR (2008) Bioactive Components in Egg Yolk. In: Mine Y (ed) Egg Bioscience and Biotechnology. pp 185–237
7. Savadkoohi S, Bannikova A, Mantri N, Kasapis S (2014) Structural properties of condensed ovalbumin systems following application of high pressure. Food Hydrocoll 53:104–114.
8. Wang Y, Zhou Y, Sokolov J, Rigas B, Levon K, Rafailovich M (2008) A potentiometric protein sensor built with surface molecular imprinting method. Biosens Bioelectron 24:162–166.
9. Sun LZ, Elsayed S, Aasen TB, Van Do T, Aardal NP, Florvaag E, Vaali K (2010) Comparison between ovalbumin and ovalbumin peptide 323-339 responses in allergic mice: Humoral and cellular aspects. Scand J Immunol 71:329–335.
10. Yang WH, Tu ZC, Wang H, Li X, Tian M (2017) High-intensity ultrasound enhances the immunoglobulin (Ig)G and IgE binding of ovalbumin. J Sci Food Agric 97:2714–2720. https://doi.org/10.1002/jsfa.8095
11. Iwashita K, Handa A, Shiraki K (2017) Co-aggregation of ovalbumin and lysozyme. Food Hydrocoll 67:206–215.
12. Mine S, Tate S, Ueda T, et al (1999) Analysis of the Relationship Between Enzyme Activity and its Internal Motion using Nuclear Magnetic Resonance : 15 N Relaxation Studies of Wild-type and Mutant Lysozyme. J Mol Biol 286:1547–1565.
13. Singh S, Singh J (2003) Effect of polyols on the conformational stability and biological activity of a model protein lysozyme. AAPS PharmSciTech 4:101–109.
14. Maosoongnern S, Flood C, Flood AE, Ulrich J (2017) Crystallization of lysozyme from lysozyme – ovalbumin mixtures: Separation potential and crystal growth kinetics. J Cryst Growth 469:2–7.
15. Mecitoğlu Ç, Yemenicioğlu A, Arslanoğlu A, et al (2006) Incorporation of partially purified hen egg white lysozyme into zein films for antimicrobial food packaging. Food Res Int 39:12–21.
16. Arica MY, Bayramŏlu G (2005) Purification of lysozyme from egg white by Reactive Blue 4 and Reactive Red 120 dye-ligands immobilised composite membranes. Process Biochem 40:1433–1442.
17. Albertsson P (1986) Partition of Cell Particles and Macromolecules: Separation and Purification of Biomolecules, Cell Organelles, Membranes, and Cells in Aqueous Polymer Two-phase Systems and Their Use in Biochemical Analysis and Biotechnology. 3rd ed.; John Wiley and Sons: Chichester, New York.
18. Rito-Palomares M (2004) Practical application of aqueous two-phase partition to process development for the recovery of biological products. J Chromatogr B 807:3–11.
19. Gutowski KE, Broker G a., Willauer HD, Huddleston JG, Swatloski RP, Holbrey JD, Rogers RD (2003) Controlling the aqueous miscibility of ionic liquids: Aqueous biphasic systems of water-miscible ionic liquids and water-structuring salts for recycle, metathesis, and separations. J Am Chem Soc 125:6632–6633.
20. Pereira JFB, Rebelo LPN, Rogers RD, Coutinho JAP, Freire MG (2013) Combining ionic liquids and polyethylene glycols to boost the hydrophobic-hydrophilic range of aqueous biphasic systems. PhysChemChemPhys 15:19580–19583.
21. Freire MG, Pereira JFB, Francisco M, Rodríguez H, Rebelo LPN, Rogers RD, Coutinho JAP (2012) Insight into the interactions that control the phase behaviour of new aqueous biphasic systems composed of polyethylene glycol polymers and ionic liquids. Chemi Eur J 18:1831–1839.
22. Cláudio AFM, Freire MG, Freire CSR, Silvestre AJD, Coutinho JAP (2010) Extraction of vanillin using ionic-liquid-based aqueous two-phase systems. Sep Purif Technol 75:39–47.
23. Freire MG, Cláudio AFM, Araújo JMM, Coutinho JAP, Marrucho IM, Lopes JNC, Rebelo L.PN (2012) Aqueous biphasic systems: a boost brought about by using ionic liquids. Chem Soc Rev 41:4966–4995.
24. Selvakumar P, Ling TC, Walker S, Lyddiatt A (2012) Partitioning of haemoglobin and bovine serum albumin from whole bovine blood using aqueous two-phase systems. Sep Purif Technol 90:182–188.
25. Yan JK, Ma H Le, Pei JJ, Wang Z Bin, Wu JY (2014) Facile and effective separation of polysaccharides and proteins from Cordyceps sinensis mycelia by ionic liquid aqueous two-phase system. Sep Purif Technol 135:278–284.
26. Thuy Pham TP, Cho CW, Yun YS (2010) Environmental fate and toxicity of ionic liquids: A review. Water Res 44:352–372.
27. Quental M V, Caban M, Pereira MM, Stepnowski P, Coutinho JAP, Freire MG (2015) Enhanced extraction of proteins using cholinium-based ionic liquids as phase-forming components of aqueous biphasic systems. Biotechnol J 10:1457–1466.
28. Taha M, Quental M V, Correia I, Freire MG, Coutinho JAP (2015) Extraction and stability of bovine serum albumin (BSA) using cholinium-based Good's buffers ionic liquids. Process Biochem 50:1158–1166.

29. Shahriari S, Tomé LC, Araújo JMM, Rebelo LPN, Coutinho JAP, Marrucho IM, Freire MG (2013) Aqueous biphasic systems: a benign route using cholinium-based ionic liquids. RSC Adv 3:1835–1843.
30. Souza RL, Lima RA, Coutinho JAP, Soares CMF, Lima AS (2014) Aqueous two-phase systems based on cholinium salts and tetrahydrofuran and their use for lipase purification. Sep Purif Technol 155:118–126.
31. Zafarani-Moattar MT, Shekaari H, Jafari P (2017) Aqueous two-phase system based on cholinium chloride and polyethylene glycol di-methyl ether 250 and it use for acetaminophen separation. J Chem Thermodyn 107:85–94.
32. Ventura SPM, Marques CS, Rosatella AA, Afonso CAM, Gonçalves F, Coutinho JAP (2012) Toxicity assessment of various ionic liquid families towards Vibrio fischeri marine bacteria. Ecotoxicol Environ Saf 76:162–168.
33. Chen J, Wang Y, Zeng Q, Ding X, Huang Y (2014) Partition of proteins with extraction in aqueous two-phase system by hydroxyl ammonium-based ionic liquid. Anal Methods 6:4067–4076.
34. Pereira MM, Pedro SN, Quental M V, Lima ÁS, Coutinho JAP, Freire MG (2015) Enhanced extraction of bovine serum albumin with aqueous biphasic systems of phosphonium- and ammonium-based ionic liquids. J Biotechnol 206:17–25.
35. Zeng CX, Xin RP, Qi SJ, Yang B, Wang YH (2016) Aqueous two-phase system based on natural quaternary ammonium compounds for the extraction of proteins. J Sep Sci 39:648–654.
36. Ventura SPM, Sousa SG, Serafim LS, Lima ÁS, Freire MG, Coutinho JAP (2011) Ionic liquid based aqueous biphasic systems with controlled pH: The ionic liquid cation effect. J Chem Eng Data 56:4253–4260.
37. Neves CMSS, Ventura PM, Freire MG, Marrucho IM (2009) Evaluation of Cation Influence on the Formation and Extraction Capability of Ionic-Liquid-Based Aqueous Biphasic Systems. J Phys Chem B 113:5194–5199
38. Merchuk JC, Andrews BA, Asenjo JA (1998) Aqueous Two-Phase Systems for Protein Separation. Studies on phase inversion. J Chromatogr B Biomed Sci Appl 711: 285-293.
39. Trott O, Olson A (2010) AutoDock Vina: improving the speed and accuracy of docking with a new scoring function, efficient optimization and multithreading. J Comput Chem 31:455–461.
40. Morris G, Huey R, William Lindstrom, Michel F. Sanner RKB, David S. Goodsell AJO (2009) AutoDock4 and AutoDockTools4: Automated docking with selective receptor flexibility. J Comput Chem 30:2785–2791.
41. Discovery Studio Visualizer v17. 2. 0. 1634. DSB (2017) Discovery Studio Visualizer, v17.2.0.16349, Dassault Systèmes BIOVIA. San Diego: Dassault Systèmes
42. Sintra TE, Cruz R, Ventura SPM, Coutinho JAP (2014) Phase diagrams of ionic liquids-based aqueous biphasic systems as a platform for extraction processes. J Chem Thermodyn 77:206–213.
43. Silva F, Sintra T, Ventura SPM, Coutinho JAP (2014) Recovery of paracetamol from pharmaceutical wastes. Sep Purif Technol 122:315–322.
44. Cláudio AFM, Swift L, Hallett JP, Welton T, Coutinho JAP, Freire MG (2014) Extended scale for the hydrogen-bond basicity of ionic liquids. Phys Chem Chem Phys 16:6593–6601.
45. Mourão T, Claudio AFM, Boal-Palheiros I, Freire MG, Coutinho JAP (2012) Evaluation of the impact of phosphate salts on the formation of ionic-liquid-based aqueous biphasic systems. J Chem Thermodyn 54:398–405.
46. Zafarani-Moattar MT, Hamzehzadeh S (2011) Effect of pH on the phase separation in the ternary aqueous system containing the hydrophilic ionic liquid 1-butyl-3-methylimidazolium bromide and the kosmotropic salt potassium citrate at T=298.15K. Fluid Phase Equilib 304:110–120.
47. Dallora NLP, Klemz JGD, Pessôa Filho P de A (2007) Partitioning of model proteins in aqueous two-phase systems containing polyethylene glycol and ammonium carbamate. Biochem Eng J 34:92–97.
48. Desai RK, Streefland M, Wijffels RH, H. M. Eppink M (2014) Extraction and stability of selected proteins in ionic liquid based aqueous two phase systems. Green Chem 16:2670–2679.
49. Li Z, Liu X, Pei Y, Wang J, He M (2012) Design of environmentally friendly ionic liquid aqueous two-phase systems for the efficient and high activity extraction of proteins. Green Chem 14:2941.
50. Ding X, Wang Y, Zeng Q, Chen J, Huang Y, Xu K (2014) Design of functional guanidinium ionic liquid aqueous two-phase systems for the efficient purification of protein. Anal Chim Acta 815:22–32.
51. Ruiz-Angel MJ, Pino V, Carda-Broch S, Berthod A (2007) Solvent systems for countercurrent chromatography: An aqueous two phase liquid system based on a room temperature ionic liquid. J Chromatogr A 1151:65–73.
52. Hameed M, Ahmad B, Fazili KM, Andrabi K, Khan RH (2007) Different Molten Globule-like Folding Intermediates of Hen Egg White Lysozyme Induced by High pH and Tertiary Butanol. J Biochem 141:573–583.

4. Separation of Ovalbumin and Lysozyme Using Aqueous Biphasic Systems and the Effect of Using Ionic Liquids as Adjuvants

Separation of Ovalbumin and Lysozyme Using Aqueous Biphasic Systems and the Effect of Using Ionic Liquids as Adjuvants

Based on the manuscript under preparation: [4]

D. C. V. Belchior, Iola F. Duarte and M. G. Freire

Abstract

Egg white is rich in a diversity of functionally important proteins, such as ovalbumin and lysozyme. However, in most of their applications both proteins should be at a high purity level and should keep their biological function. In this work, aqueous biphasic systems (ABS) composed of polymers and salts employing ionic liquids (ILs) as adjuvants were investigated as alternative processes to separate ovalbumin and lysozyme. Studies with both commercial proteins and egg white were carried out. Furthermore, the respective phase diagrams were determined to infer the mixture compositions required to form two-phase systems and each phase composition. With the systems in which no IL was added it was observed a preferential partition of ovalbumin to the PEG-rich phase, whereas lysozyme tends to precipitate at the interphase. A similar behavior was observed when applying the same systems to separate the two proteins from egg white. Nevertheless, when ILs are added as adjuvants at 5 wt%, an inversion on the partitioning trend is observed in most systems. When applying these ABS to extract commercial proteins, ovalbumin is preferentially enriched in the salt-rich whereas lysozyme tends to majorly partition to the PEG-rich phase. Furthermore, the addition of ILs avoids the precipitation of lysozyme at the interphase. However, when the same systems are applied to egg white, a more complex phenomenon takes place. With the exception of two ABS comprising ILs as adjuvants, both proteins tend to migrate to the same phase, whereas the phase to which they migrate depends on the egg white dilution. Two systems that allow the separation of both proteins have been identified, providing extraction efficiencies ranging between 81% and 88% for ovalbumin to the PEG-rich phase and between 92% and 94% for lysozyme. However, low recovery yields were obtained, ranging between 27% and 28% for ovalbumin and between 21% and 23% for lysozyme. Accordingly, future investigations are still needed to improve the separation performance of the studied ABS, namely by studying other egg white dilutions and by analyzing the proteins profile in each phase and fraction to infer their purity level.

Keywords: Egg white • Proteins • Aqueous biphasic systems • Ionic Liquids • Adjuvants.

[4]Contributions: M.G.F. and I.F.D. conceived and directed this work. D.C.V.B. acquired the experimental data. D.C.V.B., M.G.F. and I.F.D. interpreted the obtained experimental data. The manuscript was mainly written by D.C.V.B. and M.G.F. with contributions from I.F.D.

4.1 Introduction

Egg white is a low-cost source of proteins with high interest. Egg white contains 88% of water and 11% of proteins, including ovalbumin, ovotransferrin, lysozyme and ovomucin [1]. Among these, lysozyme represents 3.4 - 3.5% of the total protein content in egg white, has a low molecular weight (14.3 kDa) and a high isoelectric point (10.7)[2, 3], while ovalbumin represents ca. 54% of the total protein content, being a fosfoglycoprotein with a molecular weight of 45 kDa [4] and an isoelectric point of 4.5 - 4.6 [2, 5, 6]. Ovalbumin is widely used as a nutrient supplement and as an allergen in establishing different animal models of asthma, food and dermal allergy [4, 7], and used in foaming and gelling applications [8]. Lysozyme is commonly used as antimicrobial agent and food preservative [9]. Given its multiple functions (antiviral, antitumor and immune modulatory activities), lysozyme is also frequently used as a model protein in enzymatic reactivity, proteins aggregation and crystallization studies [10–12]. In most of these applications both proteins need to be applied with high purity levels, thus requiring the development of cost-effective methods for their isolation from egg white.

Different methods have been described and applied for the separation and recovery of proteins from egg white, such as induced precipitation, filtration-related techniques, reverse micelle-based approaches, electrophoresis, affinity chromatography, among others [13, 14]. However, when dealing with complex matrices such as egg white, the downstream processing of proteins is a difficult task due to the crucial requirement of achieving high protein yields with the desired purity level, while retaining their biological activity [15]. In order to fulfill such requirements, a large interest has been devoted to aqueous biphasic systems (ABS) as an alternative separation technique for proteins [16]. ABS are composed of two water-soluble compounds dissolved in aqueous media, which above given concentrations form two immiscible aqueous-rich phases, therefore able to provide milder and biocompatible conditions for the separation of biologically active products such as proteins [17].

ABS formed by poly(ethyleneglycol) (PEG) and salts or PEG and dextran have been investigated by several authors for the extraction of ovalbumin and lysozyme [18–23]. Saravan et al. [18] studied the partitioning behavior of ovalbumin in ABS formed by PEG and poly(acrylic acid) (PAA), at pH 8.0, 20 °C and with 1 M NaCl, achieving an extraction yield of 87.4% Nerli et al. [19] investigated the thermodynamic forces involved in the partitioning of ovalbumin in various aqueous two-phase polymer systems, i.e. constituted by PEGs of different molecular weights and dextran, while demonstrating that the ovalbumin transfer to the top phase is exothermic. Pereira et al. [20] extracted ovalbumin from egg white using ABS constituted by PEGs of different molecular weights (400, 600 and 1000 $g \cdot mol^{-1}$) and buffered aqueous solutions of potassium citrate/citric acid. Under the optimal conditions, ovalbumin majorly migrates to the PEG-rich phase with extraction efficiencies of up to 98.9% achieved in a single-step[20]. Su and Chiang [21]

investigated the extraction of lysozyme from egg white using PEG 6000/sodium sulfate ABS. At room temperature (ca. 25°C) and pH 10, approximately 70% of lysozyme could be extracted from the diluted chicken egg white [21]. On the other hand, Yang and co-workers [22]used PEG 4000/potassium citrate ABS for purification of lysozyme from crude hen egg white; under the optimized conditions, namely at pH 5.5 and 30°C, lysozyme was recovered in the PEG-rich top phase with an activity yield of 103% and a purification factor of 21.11. Diederich et al. [23] revealed significant differences in the partitioning of lysozyme and ovalbumin from chicken egg white solutions in PEG/salt ABS by varying the polymer molecular weight. Ovalbumin preferentially partitions to the salt-rich bottom phase, while lysozyme is enriched in the top phase when using low molecular weight polymers. By increasing the PEG molecular weight, the distribution of lysozyme decreases and its partitioning changes from the top to the bottom phase [23].

Besides the widely studied polymer-based ABS, ABS constituted by ionic liquids (ILs) were proposed in the last decade [24], being now considered alternative systems with a broader range of phases' polarities [25, 26]. ILs have a large number of possible variations in the cation and anion chemical structures, allowing the fine-tuning of their physicochemical properties, which is transferred to IL-based ABS. In addition to the use of ILs as main phase-forming components of ABS, it has been shown that their use as adjuvants [27–30]or electrolytes [28, 31], i.e. at low amounts in ABS formation (usually in the range from 0.1 to 10 wt%), also permits the fine tuning of the characteristics of the coexisting phases, leading to improved partition coefficients, extraction efficiencies, purification factors and yields. These systems have been studied in the extraction of a wide range of biomolecules [32], ranging from amino acids to proteins, although few studies have focused on their application to separate proteins from real matrices [29, 33].

In this work, ABS formed by polyethylene glycol of different molecular weights (PEG 400, PEG 1000, PEG 1500 and PEG 2000) and a phosphate-buffered salt at pH 7, employing ILs as adjuvants (at 5 wt%) to tailor the phases' selectivity for each protein, were investigated to separate ovalbumin and lysozyme from egg white, being the major goal the partition of each protein to a different ABS phase. Tetraalkylammonium-based ILs were chosen due to their more attractive environmental and biocompatible characteristics [34]. The phase diagrams of each ternary system were determined at 25°C to appraise the mixture compositions required to form ABS. ABS were optimized regarding their extraction performance for commercial lysozyme and ovalbumin, and finally employed to separate both proteins from egg white.

4.2. Experimental Section

4.2.1. Materials

The ABS studied in this work were established using PEGs of different molecular weights, namely 400 g.mol^{-1} (PEG 400), 1000 g.mol^{-1} (PEG 1000), 1500 g.mol^{-1} (PEG 1500), and 2000 g.mol^{-1} (PEG 2000). The prepared buffered salt aqueous solution is constituted by potassium dihydrogen phosphate, KH_2PO_4, ≥ 99 wt% pure from Sigma–Aldrich, and potassium hydrogen phosphate trihydrate, $K_2HPO_4{\cdot}3H_2O$, 100 wt% pure from Fisher Scientific. Ionic liquids used as adjuvants are as follows: cholinium chloride ([Ch]Cl, > 98 wt% pure), cholinium acetate ([Ch][Ac], > 99 wt% pure), tetraethylammonium bromide ([N_{2222}]Br, > 98 wt% pure), tetraethylammonium chloride ([N_{2222}]Cl, > 98 wt% pure), and benzyltriethylammonium chloride ([$N_{222}(C_7H_7)$]Cl, > 98 wt% pure). [N_{2222}]Br and [N_{2222}]Cl were purchased from Alfa Aesar, [Ch][Ac] was supplied from Iolitec, and [$N_{222}(C_7H_7)$]Cl and [Ch]Cl were acquired from Acros Organics. The chemical structures of PEG and of the investigated ILs are depicted in Figure 4.1.

Pure ovalbumin and lysozyme from hen egg white were acquired from Sigma–Aldrich. Fresh eggs were bought in a local supermarket.

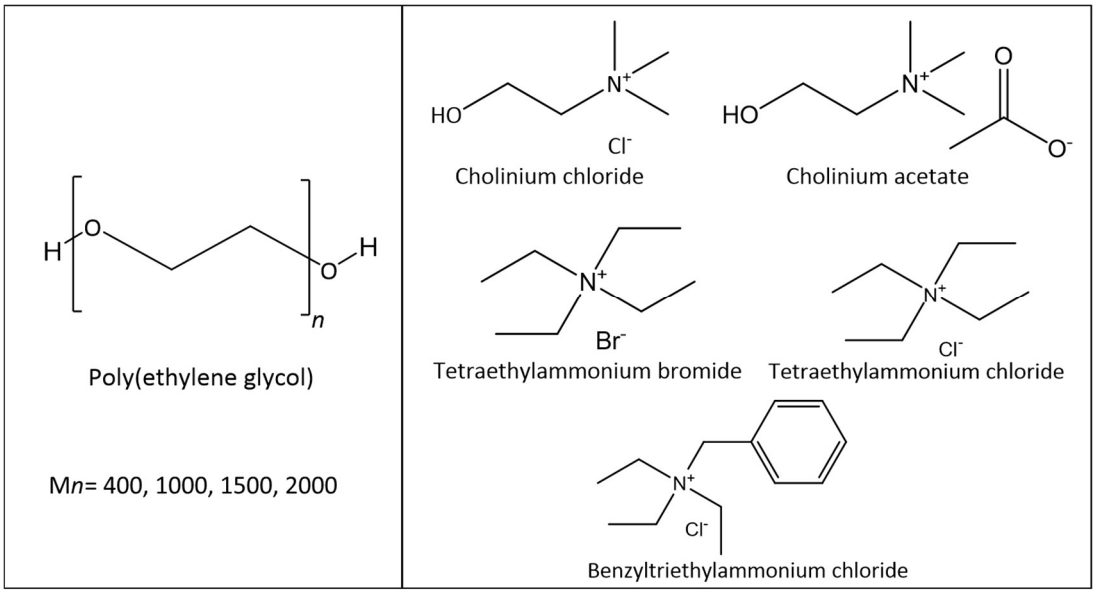

Figure 4.1. Chemical structures of the PEG and ILs investigated.

4.2.2. Phase diagrams

The binodal curve of each ABS phase diagram was determined using the cloud point titration method at (25 ± 1)°C and at atmospheric pressure, as described elsewhere [35]. Aqueous solutions of different PEGs (ca. 90 wt%) and potassium phosphate buffer (≈ 40 wt% of K_2HPO_4/KH_2PO_4 at pH 7) were prepared gravimetrically. The phase diagrams were determined through the consecutive identification of a cloudy solution (corresponding to the biphasic

region), and a clear solution (corresponding to the monophasic region) by the drop-wise addition of the potassium phosphate buffer aqueous solution and water, respectively, to each PEG aqueous solution. The same procedure was followed for the determination of the phase diagrams with ILs as adjuvants; however, water and the aqueous solutions of salt and PEG contained 5 wt% of the respective ILs, allowing to keep the IL concentration constant along all the phase diagram regions. This procedure was carried out under constant stirring. Each total mixture composition was determined by the weight quantification of all components added within $\pm 10^{-4}$ g (using an analytical balance, Mettler Toledo Excellence XS205 Dual Range). The tie-lines (TLs), which give the composition of each phase for a given mixture composition, were gravimetrically determined at 25°C, according to the original method reported by Merchuk et al [36]. Further details are given in the Appendix C.

4.2.3. Extraction of ovalbumin and lysozyme using PEG-salt ABS

After the determination of the ABS phase diagrams to infer the mixture compositions required to form two-phase systems, mixture compositions in the several ABS were selected and used to evaluate their performance to extract commercial ovalbumin and lysozyme. Aqueous solutions of commercial proteins diluted in PBS (phosphate buffered saline aqueous solutions at 0.05 M, pH ≈ 7.4) at a concentration around 1 $g \cdot L^{-1}$ were used in the formation of each ABS. Each ABS was mixed in a vortex, centrifuged (10 min at 1000 rpm), and left at (25 ± 1)°C for 120 min. The upper and lower phases were carefully separated and the ovalbumin and lysozyme concentrations in each phase were determined. The proteins content in both the top and bottom phases were determined by size exclusion high performance liquid chromatography (SE-HPLC). Before injection in the SE-HPLC, each phase was diluted at a 1:10 (v:v) ratio in PBS buffer (50 mM, pH ≈ 7.4).

The percentage extraction efficiency of the studied ABS to the PEG-rich for each protein, EE_{Prot}%, was determined according to Eq. (1):

$$EE_{\mathrm{Prot}}\% = \frac{\mathrm{wPEG_{Prot}}}{\mathrm{wPEG_{Prot}} + \mathrm{wSalt_{Prot}}} \times 100 \qquad (1)$$

where w_{PEG} and w_{Salt} are the total weight of each protein in the PEG-rich and in the salt-rich aqueous phases, respectively.

The recovery yield of each protein into to PEG-rich phase, RY_{Prot}%, is the percentage ratio between the amount of protein in the PEG-rich aqueous phase (w_{PEG}) to that present in the initial/original mixture ($w_{Initial}$), defined according to Eq. (2),

$$RY_{\mathrm{Prot}}\% = \frac{w_{\frac{\mathrm{PEG}}{\mathrm{Prot}}}}{w_{\frac{\mathrm{Initial}}{\mathrm{Prot}}}} \times 100 \quad (2)$$

After identifying the favorable systems for the lysozyme and ovalbumin separation, where the goal is to identify systems where each protein should partition to opposite phases of each ABS, they were then applied in the extraction of the same proteins from egg white samples. ABS were prepared using egg white diluted in water at 1:10 (v:v). Each mixture was mixed, centrifuged (10 min at 1000 rpm), and left for 120 min at (25 ± 1)°C in order to attain the complete partitioning of proteins between the two phases. After the separation of the coexisting phases, each protein was quantified by SE-HPLC. The percentage extraction efficiency and recovery yield of lysozyme and ovalbumin to the PEG-rich phase were determined according to Eqs. (1) and (2), respectively.

After identifying the most promising polymer-salt systems to extract lysozyme and ovalbumin from egg white, the addition of ILs as adjuvants was investigated with the goal of improving the ABS selectivity and simultaneous separation performance. Fixed compositions of these pseudo-ternary systems (composed of 30 wt% of PEG 1000 and 2000 + 8 wt% of K_2HPO_4/KH_2PO_4 at pH 7 + 5 wt% of each IL) were chosen based on the phase diagrams obtained. The ILs investigated were [Ch]Cl, [Ch][Ac], [N_{2222}]Br, [N_{2222}]Cl and [$N_{222(C7H7)}$]Cl. The stock solutions of commercial proteins were prepared with a concentration ca. 1 g·L^{-1} in PBS, and for studies comprising egg white different dilutions in water (1:5, 1:a0 and 1:50, v:v) were studied. As described before, each mixture was stirred, centrifuged for 10 min at 1000 rpm, and left to equilibrate for more 120 min. After the phases' separation, the proteins content in each phase was determined by SE-HPLC, as previously described. EE_{prot}% and RY_{prot}% were determined using Eqs. (1) and (2). However, with the systems comprising ILs as adjuvants, inversions on the preferential partitioning of the proteins was observed. In these cases, where the proteins are majorly enriched in the salt-rich phase, both parameters were determined in respect to the salt-rich phase. At least three individual ABS at each set of conditions were prepared and analyzed.

4.2.4. Size exclusion high performance liquid chromatography (SE-HPLC)

A Chromaster HPLC system (VWR Hitachi) equipped with a binary pump, column oven, temperature controlled auto-sampler and DAD detector was used as the quantification technique for proteins. SE-HPLC was performed using an analytical column Shodex Protein KW-802.5 (8 mm × 300 mm). For the detection of each protein, different HPLC conditions were chosen. For lysozyme, solvent A (100 wt% -water/0.1% trifluoroacetic acid (v:v): 38.4 wt% -acetonitrile/0.1% trifluoroacetic acid (v:v) and solvent B (acetonitrile/0.1% trifluoroacetic acid (v:v)) were run in gradient (expressed as proportion of solvent A: 0-20 min, 100%; 20-21 min,

100-50%; 21-22 min, 50%; 22-23 min, 50-100%; 23-35 min, 100%) with a flow rate of 1 mL·min^{-1}. For ovalbumin, a 100 mM phosphate buffer pH 7.0 with NaCl 0.3 M was run isocratically with a flow rate of 0.5 mL·min^{-1}. The temperature of the column and auto-sampler was kept constant at 25°C. The injection volume was of 25 µL. The wavelength was set at 280 nm, whereas the retention time of lysozyme and ovalbumin were found to be 9 and 15 min, respectively. The quantification of each protein in each phase was carried out using the established calibration curves at each condition.

4.3. Results and Discussion

4.3.1. ABS phase diagrams

The phase diagrams of ternary ABS formed by PEGs of different molecular weight and K_2HPO_4/KH_2PO_4 at pH 7.0, as well as pseudo-ternary ABS composed of PEG (1000 or 2000), K_2HPO_4/KH_2PO_4 at pH 7.0 and 5 wt% of each IL, were determined at 25°C and atmospheric pressure. It should be remarked that the IL concentration was always kept at 5 wt% and was considered as part of the solvent in the phase diagrams representation. The determined phase diagrams are depicted in Figures 4.2 and 4.3, respectively, in both weight fraction and molality units (mol·kg^{-1}). The phase diagrams in molality are shown since they allow a more accurate analysis of the effect of individual solutes on promoting the liquid–liquid demixing since the effect of the phase-forming components molecular weight is not taken into account. The detailed experimental weight fraction data are given in Tables C1-C14 in the Appendix C. The binodal data were fitted according to the regression proposed by Merchuk et al. [36], shown in Figures 4.2 and 4.3, whereas the respective regression parameters are given in the Appendix C (Table C15). Experimental tie-lines, which give the composition of each phase for a given mixture composition, and respective length (TLLs), are provided in Tables C16 in the Appendix C. In all studied ABS the top phase is majorly composed of PEG and water, while the bottom phase is enriched in salt and water.

The closer each binodal curve is to the axes, the lower the amount of each compound required to form two-phase systems. Therefore, the results depicted in Figure 4.2 show that the phase separation ability increases with the increase of the size of the polymer chain, according to the rank: PEG 2000 > PEG 1500 > PEG 1000 > PEG 400. This effect is well-known, being observed in polymer/ionic liquid, polymer/salt and polymer/polymer combinations [20, 26, 37, 39], and is directly connected to the higher hydrophobicity or lower affinity for water of polymers with higher molecular weight.

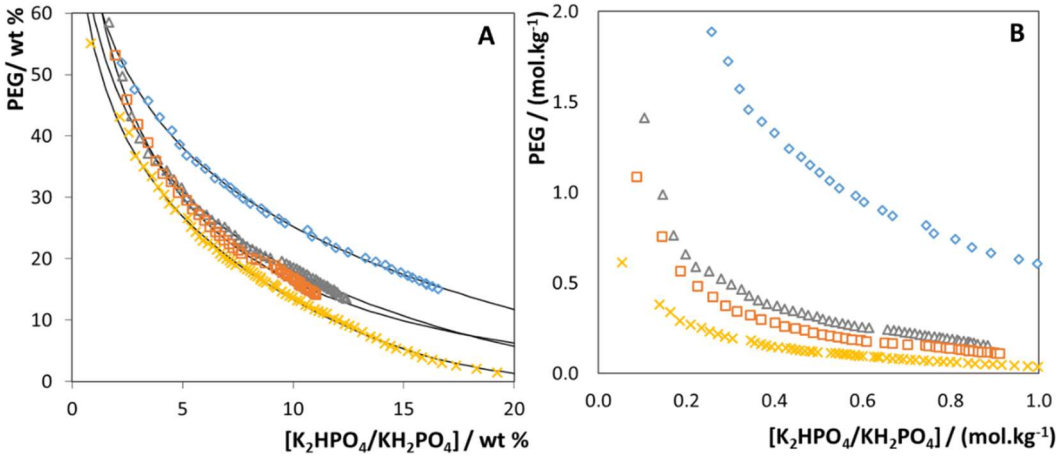

Figure 4.2. Phase diagrams at 25°C and atmospheric pressure in weight fraction (A) and molality units (B) for ABS composed of PEG + K_2HPO_4/KH_2PO_4 (pH 7) + water: PEG 400 (◊); PEG 1000 (△); PEG 1500 (□); PEG 2000 (×).

Figure 4.3 shows the phase diagrams for the ABS composed or PEG 2000 or PEG 1000, K_2HPO_4/KH_2PO_4 and several ILs at 5 wt% as adjuvants. The addition of ILs as adjuvants leads to a slight increase or decrease in the biphasic region, depending on the IL chemical structure, and as observed in previous works [38, 39]. In general, the ability of ILs when used as adjuvants to induce the two-phase formation in the ABS containing PEG 1000 or PEG 2000, for instance at 0.3 mol·kg^{-1} of K_2HPO_4/KH_2PO_4, follows the trend: [Ch]Cl > [Ch][Ac] > $[N_{2222}]$Cl ≈ $[N_{2222}]$Br > $[N_{222(C7H7)}]$Cl Although the IL effect seems to be more pronounced in ABS formed by polymers of lower molecular weight, this trend shows that the ILs rank on changing the phase behavior does not depend on the PEG molecular weight, at least if varied from 1000 to 2000 g·mol^{-1}. Overall, the ILs [Ch]Cl and [Ch][Ac] favor phase separation if compared with the system in which no IL was added, whereas $[N_{2222}]$Cl, $[N_{2222}]$Br and $[N_{222(C7H7)}]$Cl lead to a lower ability of the system to undergo liquid-liquid demixing. Overall, more hydrophilic ILs, such as cholinium-based combined with anions with high hydrogen-bond basicity [40], favor the creation of ABS. Nevertheless, in this type of systems, PEG-IL interactions over the water-IL and water-PEG interactions cannot be discarded, as previously demonstrated [41, 42].

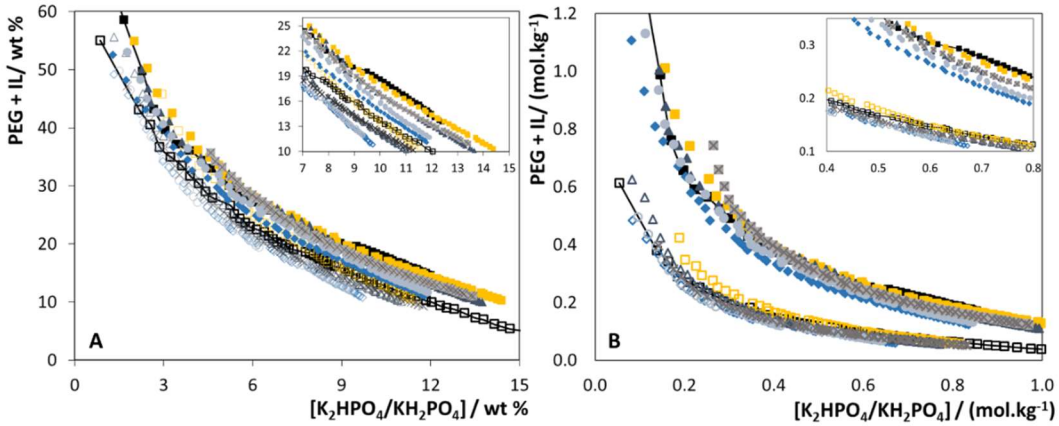

Figure 4.3. Phase diagrams at 25°C and atmospheric pressure in weight fraction (A) and molality units (B) for ABS composed of PEG (1000 or 2000) + K_2HPO_4/KH_2PO_4 + water + 5 wt% IL. Full symbols correspond to ABS comprising PEG 1000 and open symbols correspond to ABS constituted by PEG 2000. The symbols with lines correspond to the corresponding ABS in which no IL was added. ILs: [Ch]Cl (◆); [Ch][Ac] (●); $[N_{2222}]$Cl (■); $[N_{2222}]$Br (▲); $[N_{222(C7H7)}]$Cl (☒).

4.3.2. Extraction of commercial proteins using polymer-based ABS

It is well-known that the polymer molecular weight and its concentration have a strong influence on the partitioning behavior of proteins in PEG-salt ABS [21, 43–45]. Accordingly, the effect of PEG 400, 1000, 1500 and 2000 at different concentrations (25, 30 and 35 wt%) in the ABS formulation to extract lysozyme and ovalbumin was investigated. In this set of studies, a fixed amount of 12 wt% of phosphate buffer (K_2HPO_4/KH_2PO_4, pH 7) was used. This set of results was carried out with individual proteins in each ABS to infer the independent proteins partitioning between the coexisting phases. The results obtained in terms of the extraction efficiencies and recovery yields of lysozyme and ovalbumin to the polymer-rich phase are shown in Fig. 4.4. Detailed data are provided in Table C17 in the Appendix C.

With the exception of ovalbumin in the ABS composed of 25 wt% of PEG 2000, both proteins preferentially partition towards the PEG-rich (top) phase, independently of the polymer molecular weight and mixture composition. However, the ovalbumin partitioning to the PEG-rich phase is more favorable in ABS composed of higher amounts of polymer, whereas the opposite trend is seen with the increase of the polymer molecular weight (with the increased hydrophobicity of the PEG-rich phase). This behavior is in accordance to the results reported by Pereira et al. [20] using other PEG-salt ABS. Although an increase in the polymer molecular weight leads to a decrease in the ovalbumin extraction efficiencies, in all ABS composed of 35 wt% of PEG there is the complete extraction of the protein added to the PEG-rich phase. At pH 7, ovalbumin is negatively charged (isoelectric point = 4.5-4.6[2, 5, 6]) and preferentially partitions to the phase of lower ionic strength (polymer-rich), reinforcing the salting-out effect exerted by the phosphate buffered salt and/or favorable interactions established between

ovalbumin and the PEG-rich phase components. As observed with ovalbumin, lysozyme also has a preferential partitioning to the PEG-rich phase. However, the increasing size of the PEG chain length results in slightly higher extraction efficiencies to the PEG-rich phase when using mixture compositions with higher amounts of polymer, while the opposite occurs when using ABS with lower amounts of PEG. At pH 7 lysozyme is positively charged (isoelectric point = 10.7) [2, 3], and as ovalbumin that is negatively charged at this pH, the protein preferentially enriches in the phase with lower ionic strength (PEG-rich).

Although the extraction efficiencies of all studied systems are significantly high for both proteins (> 83%, with the exception of ovalbumin in the ABS composed of 25 wt% of PEG 2000), their recovery yield is more affected by the polymer molecular weight and composition of the ABS. Recovery yields ranging from 20 to 100% were obtained. For both proteins, ABS formed by PEGs of lower molecular weight and lower amounts of polymer in the mixture compositions lead to 100% of protein recovery yield (no losses of protein). The increase of the polymer molecular weight leads to lower recovery yields of both lysozyme and ovalbumin. The effect of the ABS composition is however different for both proteins. Higher concentrations of polymer lead to higher losses of lysozyme (lower recovery yields), while the opposite effect is observed with ovalbumin. The losses of lysozyme mainly correspond to protein precipitation occurring during the ABS extraction step (as shown in some pictures given in Figure C3 in the Appendix C). Overall, it is known that the partitioning and solubilization of biomolecules in ABS is affected by several factors, including the biomolecule characteristics, molecular weight and concentration of the polymers, ionic strength, pH, among others. Results previously reported in the literature [46] show that the solubility of lysozyme in aqueous solutions decreases with the addition of polyethylene glycol, and that the protein solubility is lower for PEGs with a higher degree of polymerization, which is in close agreement with the current results, i.e. proteins tend to precipitate at the ABS interface when their saturation values decrease.

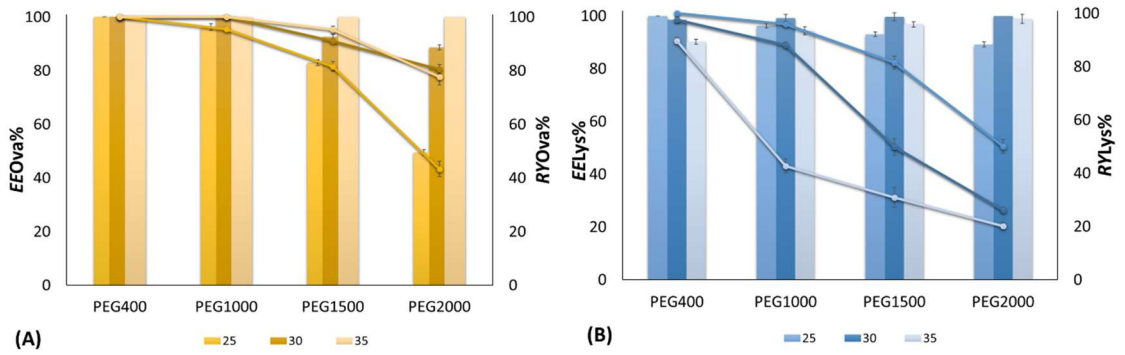

Figure 4.4. Extraction efficiency (*EE*%, bars) and recovery yield (*RY*%, symbols and line) of (A) Ovalbumin and (B) Lysozyme in ABS composed of 12 wt% of (K_2HPO_4/KH_2PO_4) and different concentrations of PEG (25, 30 and 35 wt%) at 25°C and pH 7.

Several studies demonstrated that an increase in the salt concentration results in an increase in the partition coefficients of biomolecules toward the upper phase or creation of a precipitate enriched in proteins at the ABS interphase promoted by salting-out effects [47–49]. Accordingly, and aiming at identifying promising conditions to separate and recover ovalbumin and lysozyme, the effect of different concentrations of potassium phosphate buffer salt-K_2HPO_4/KH_2PO_4 (at 11, 12, and 13 wt%, pH 7) in the ABS composed of PEG 400, 1000, 1500 and 2000 was investigated. Based on the previous results regarding the polymer concentration, a fixed concentration of 30 wt% of PEG 400, 1000, 1500 and 2000 was used. The detailed extraction efficiency and recovery yield results are given in Tables C17 in the Appendix C, being depicted in Figure 4.5.

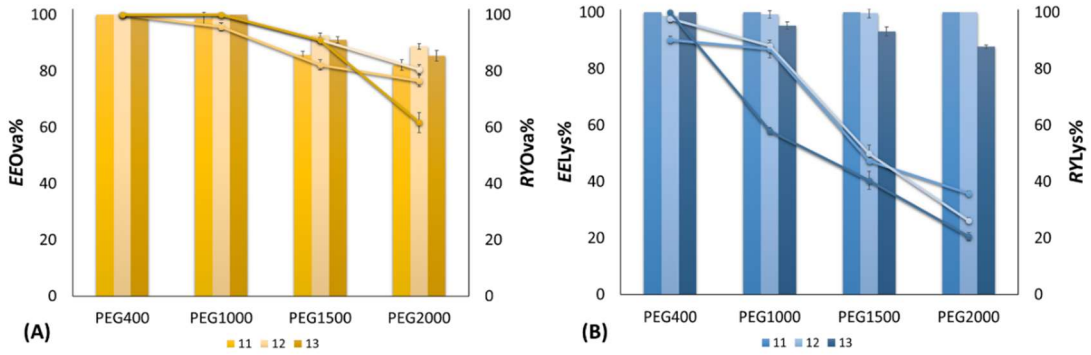

Figure 4.5. Extraction efficiency (*EE*%, bars) and recovery yield (*RY*%, symbols and line) of (A) Ovalbumin and (B) Lysozyme in ABS composed of 30 wt% of PEG and different concentrations of (K_2HPO_4/KH_2PO_4) wt%: 11, 12 and 13 at 25 °C and pH 7.

Similarly to the observed effect in the study of the concentration of polymers, both proteins have a preferential partition to the PEG-rich phase, independently of the polymer and mixture composition. With ovalbumin no significant differences occur with the salt concentration, being the effect of the PEG molecular weight more significant when addressing the protein extraction efficiencies. On the other hand, with lysozyme, the effect of the salt concentration is more pronounced, with a decrease in the protein extraction efficiency occurring at higher salt concentrations. Furthermore, for both proteins there is a decrease on the extraction yield both with the salt concentration and PEG molecular weight increase.

4.3.3. Extraction and separation of ovalbumin and lysozyme from egg white using ABS

After the evaluation of the extraction/separation process with commercial ovalbumin and lysozyme, the ABS performance to separate both proteins from real samples was evaluated. With this goal, three mixture compositions (30 wt% of PEG 1000 or 2000 + (11, 12, 13) wt% of K_2HPO_4/KH_2PO_4 at pH 7 + aqueous solution containing egg white diluted at 1:10 (v:v)) were investigated. The total amount of proteins in egg white and extraction efficiency values are provided in the Appendix C, Table C18. Fig. 4.6 depicts that the extraction efficiency and recovery yield values obtained for the two proteins extracted from egg white. As observed with

the pure proteins, both proteins tend to partition to the PEG-rich phase, with extraction efficiencies ranging between 87 and 100%. Furthermore, an increase in the polymer molecular weight leads to a decrease on the extraction efficiency and recovery yields of both proteins, particularly visible in systems with higher contents of salt. With the ABS formed by the PEGs 1000 and 2000, recovery yields ranging between 22 and 100% were obtained with both proteins, and where up to (77 ± 1.2)% of lysozyme precipitates at the interface. Overall, the results and trends obtained are similar to those found with the commercial lysozyme and ovalbumin, although a larger amount of precipitated proteins at the interface was observed when working with the overall fraction of proteins from egg white, meaning that other proteins present in egg white are being precipitated, and thus requiring SDS-PAGE analysis to confirm the proteins profile in each phase and precipitated fraction.

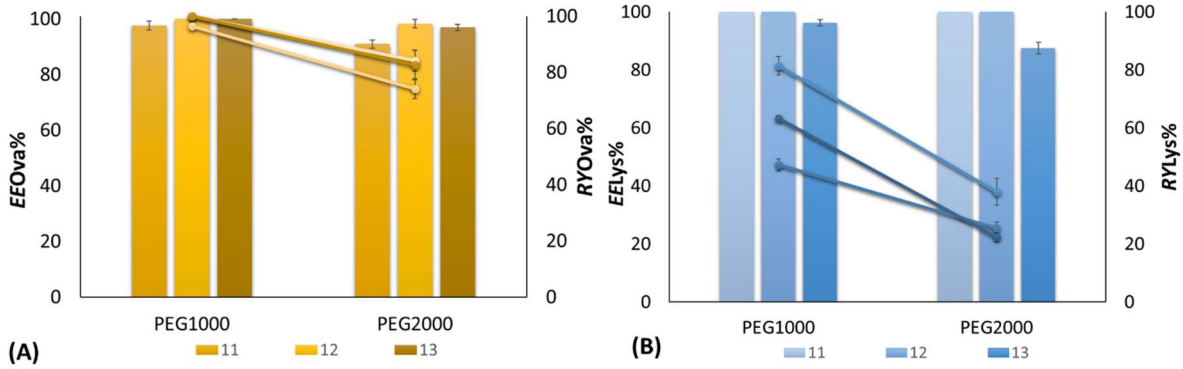

Figure 4.6. Extraction efficiency (*EE*%, bars) and recovery yield (*RY*%, symbols and line) of (A) Ovalbumin and (B) Lysozyme from egg white dissolved in water (1:10, v:v) in ABS composed of 30 wt% of PEG and different concentrations of K_2HPO_4/KH_2PO_4 (11, 12 and 13 wt%) at 25°C and pH 7.

Separation of more than one protein from egg white has been done by few research groups, but none of these studied attempted to do it a single-step. Tankrathok et al. [50] separated ovalbumin, lysozyme, ovotransferrin, and ovomucoid using Q-Sepharose fast-flow anion exchange and CM-Toyopearl 650M cation exchange chromatography, with yields of 54, 55 and 21%, respectively. Lysozyme, ovomucin, ovotransferrin and ovalbumin were separated in sequential steps by Abeyrathne et al. [51] The authors separated first lysozyme, using a FPC3500 cation exchange resin and then ovomucin by isoelectric precipitation; ovalbumin and ovotransferrin were separated from the lysozyme- and ovomucin-free egg white by precipitating ovotransferrin, first using 5.0% of $(NH_4)_2SO_4$ and 2.5% of citric acid. The supernatant (S1) obtained was used for the ovalbumin separation and the precipitant was dissolved in water, and reprecipitated using 2.0% of ammonium sulfate and 1.5% of citric acid. Finally, the precipitant was used as ovotransferrin fraction, and this supernatant was pooled with the first supernatant obtained, followed by ultrafiltration and heat-treatment to remove impurities [51]. Although

large yields of lysozyme and ovalbumin (>82% and >98%, respectively) have been reported, these methods require multiple steps.

4.3.4. Extraction of commercial proteins using ABS composed of ILs as adjuvants

The limited polarity between both aqueous phases is one of the major drawbacks in the application of conventional polymer–salt-based ABS. In this sense, the number of studies describing new ABS and strategies to improve their selectivity is vast [28]. In this work, the effect of ILs at 5 wt% (as adjuvants) in polymer-based ABS was investigated. The major goal of using ILs is to tailor the selectivity of the ABS for each protein, ideally avoiding the precipitation of lysozyme at the interphase while promoting the migration of both proteins to opposite phases. Accordingly, two ABS were chosen, namely those based on PEG 1000 and PEG 2000 + potassium phosphate buffer (pH 7), represented by the mixture point composed of 30 wt% of PEG 1000/2000 + 8 wt% of K_2HPO_4/KH_2PO_4 + 5 wt% of each IL. The extraction efficiencies and recovery yields of the two proteins by each ABS comprising the different ILs are shown in Fig. 4.7 (the respective detailed data are reported in the Appendix C, Table C19).

The extraction efficiencies and recovery yields of ovalbumin in the systems composed of PEG 2000 + 11 wt% of K_2HPO_4/KH_2PO_4 (no IL added) was found to be 82% and 76% (Fig. 4.5(A)), respectively, at the PEG-rich phase; however, for systems where ILs were added, extraction efficiencies of ovalbumin ranging between 58 and 100% and recovery yields ranging from 11 to 100% were obtained (Fig. 4.7), meaning that ILs exert a significant effect on both parameters. On the other hand, the addition of ILs as adjuvants in polymer-based ABS leads to an increase on the recovery yield of lysozyme from 35% (with no IL added) to 100% and complete extraction in a single-step with the systems composed of 5 wt% of $[N_{2222}]Br$ and $[N_{2222}]Cl$ (Fig. 4.7). The results sketched in Fig. 4.7 show that the IL addition on the ABS formation when compared to the system with no IL have a significant impact upon the separation of proteins studied, which can be explained by their interactions with each phase-forming component of the phases.

According to the results shown in Fig.4.7, when ILs are present, the extraction efficiencies and yields of lysozyme are higher toward the PEG-rich phase, thus reducing the amount of precipitated lysozyme. Although the recovery yields of lysozyme are not always 100%, no protein precipitation was macroscopically observed with ABS comprising ILs as adjuvants. Accordingly, the lower recovery yields correspond to the formation of lysozyme aggregates, as confirmed by SE-HPLC. As previously demonstrated [30, 52], ILs tend to partition to the PEG-rich top phase, suggesting the favorable interactions between ILs and lysozyme may exist. Lysozyme is more hydrophobic than ovalbumin [53], meaning that the addition of ILs may enhance the hydrophobicity of the PEG-rich phase, being favorable for the enrichment of lysozyme at this phase. On the contrary, the IL presence in the PEG-rich phase has a direct impact in the ovalbumin migration, which presents a different behavior in most systems comprising ILs. In ABS

in which no IL was added, ovalbumin preferentially partitions to the PEG-rich phase. However, in most ABS employing ILs, being the exception the ABS formed by PEG 1000 and [Ch][Ac], $[N_{2222}]Cl$ and $[N_{2222}]Br$, ovalbumin majorly migrates to the salt-rich phase. As previously highlighted, ovalbumin is more hydrophilic than lysozyme [53], and as such the addition of ILs that may turn the PEG-rich phase more hydrophobic is not beneficial for its partition. Overall, the best results to achieve the separation of both proteins to opposite phases, with lower losses and higher recovery yields in each phase, were obtained with the ABS formed by PEG 2000 and [Ch][Ac]. With this system, an extraction efficiency and recovery yield of ovalbumin of 100% to the salt-rich phase and an extraction efficiency and recovery yield of lysozyme of 80% and 78% to the PEG-rich phase were obtained.

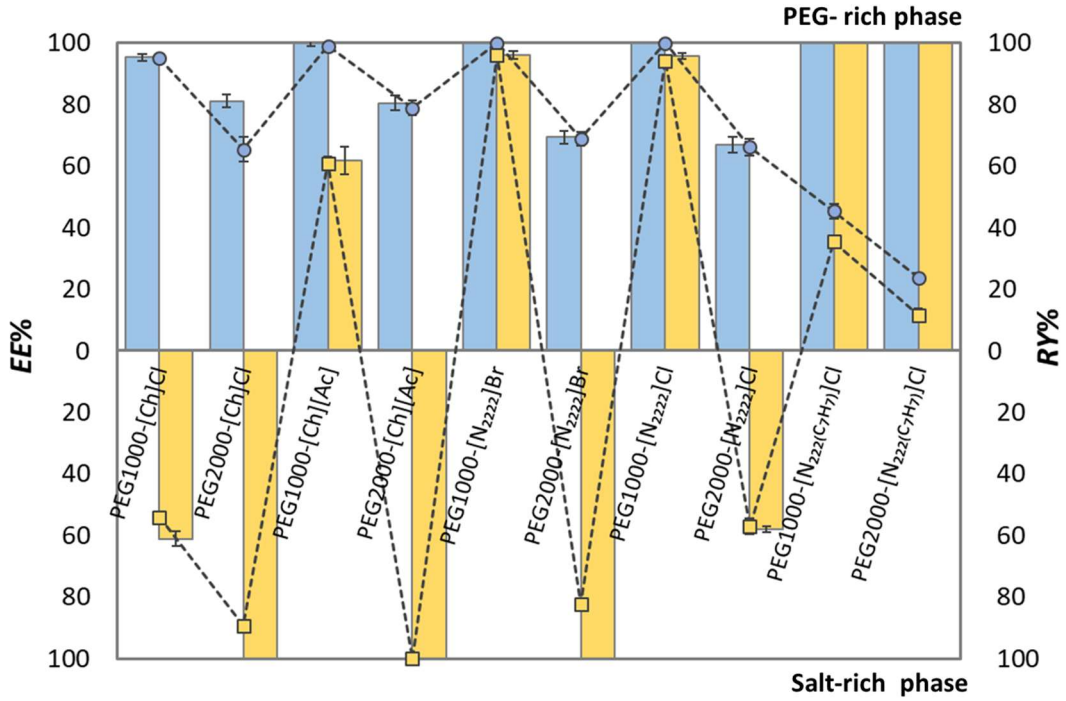

Figure 4.7. Extraction efficiency (EE_{prot}%, columns) and recovery yield (RY_{prot}%, symbols) of Lysozyme (blue) and Ovalbumin (yellow) in ABS composed of 30 wt% of PEG, 8 wt% of (K_2HPO_4/KH_2PO_4) + H_2O + 5 wt% of ILs at 25°C and pH 7.

4.3.5. Extraction of ovalbumin and lysozyme using ABS composed of ILs as adjuvants

Although it was demonstrated that small amounts of appropriate ILs in conventional ABS enhance the partition and recovery yield of ovalbumin and commercial lysozyme, by mainly avoiding the precipitation of lysozyme, further studies were carried out to evaluate the effect of ILs on these systems performance to extract both proteins from egg white. At this stage, egg white dissolved in water at three different ratio were considered (1:5, 1:10 and 1:50, v:v). The respective results are shown in Figure 4.8 (A-C) - detailed results are given in the Appendix C.

No major differences are observed in the extraction efficiencies and recovery yields of both proteins at the egg white dilutions 1:5 and 1:10 (v:v). However, according to the results shown

in Fig. 4.8, the partition of both proteins when a more complex matrix is used is different to that obtained with the commercial/standard proteins. In most systems investigated, both ovalbumin and lysozyme partition to the same phase, and in most of the cases to the less hydrophobic phase (salt-rich phase). These results suggest that the presence of other proteins may be responsible for the phenomena observed, assuming that the remaining proteins from egg white may be saturating the PEG-rich phase. However, to confirm this behavior, SDS-PAGE analysis of each phase to infer the protein profile must be carried out.

In what concerns the two target proteins separation to opposite phases, the best systems identified are those composed of PEG 1000 and $[N_{2222}]Cl$ or $[N_{2222}]Br$. These systems allow to obtain extraction efficiencies and recovery yields of ovalbumin to the PEG-rich phase ranging between 81% and 88% and between 27% and 28% respectively, and extraction efficiencies and recovery yields of lysozyme to the salt-rich phase ranging between 92% and 94% and between 21% and 23%, respectively. Although high extraction efficiencies have been obtained, this set of results demonstrates that the yields of each protein are low and further investigations are needed. Given the large differences obtained when changing the egg white dilution from 1:10 to 1:50 (v:v), the next step to consider should be the investigation of an intermediate dilution.

With the systems formed by ILs $[N_{222(C7H7)}]Cl$, the complete precipitation of lysozyme at the interphase was observed. For systems composed of PEG 1000 and $[N_{222(C7H7)}]Cl$, the decrease the egg white concentration lead the lysozyme precipitation from egg white dilution of 1:50 (v:v), while that the increase the alkyl chain length of PEG, using PEG 2000, the presence of the IL in the PEG-rich phase it seems to impact to the partition of this protein toward both phases, given precipitation complete this protein in all egg white dilutions studied. Although it was not the goal of this work, this possibility could be considered as an alternative purification strategy, i.e. to recover ovalbumin at the PEG-rich phase and lysozyme as a precipitate. However, further studies are still required, particularly to guarantee that lysozyme keeps its native confirmation after dissolution in an aqueous buffer solution. Furthermore, SDS-PAGE analysis to each ABS phase and precipitated fraction of proteins should be conducted to infer the proteins purity and selectivity of the investigated systems.

Some works on the use of ABS comprising ILs as adjuvants to separate proteins can be found in the literature. For instance, Souza et al. [33] reported high purification factors of lipase produced by submerged fermentation by Bacillus sp. ITP-001 using ABS containing 1-hexyl-3-methylimidazolium chloride ($[C_6mim]Cl$) as an adjuvant. Although the authors obtained higher purification factors for the enzyme with this IL, the opposite behavior was observed in presence of other ILs of the same family with shorter and longer alkyl side chains. These results suggest that the effect of ILs is intricate, particularly when dealing with complex matrices rich in proteins, and that a multitude of interactions may take place. Previous studies reporting to the use of

polymer-based ABS using ILs as adjuvants show that, although it is possible to enhance the systems separation performance, the effect of ILs does not follow an universal trend and that the outcome is influenced by a diversity of effects and interactions [30].

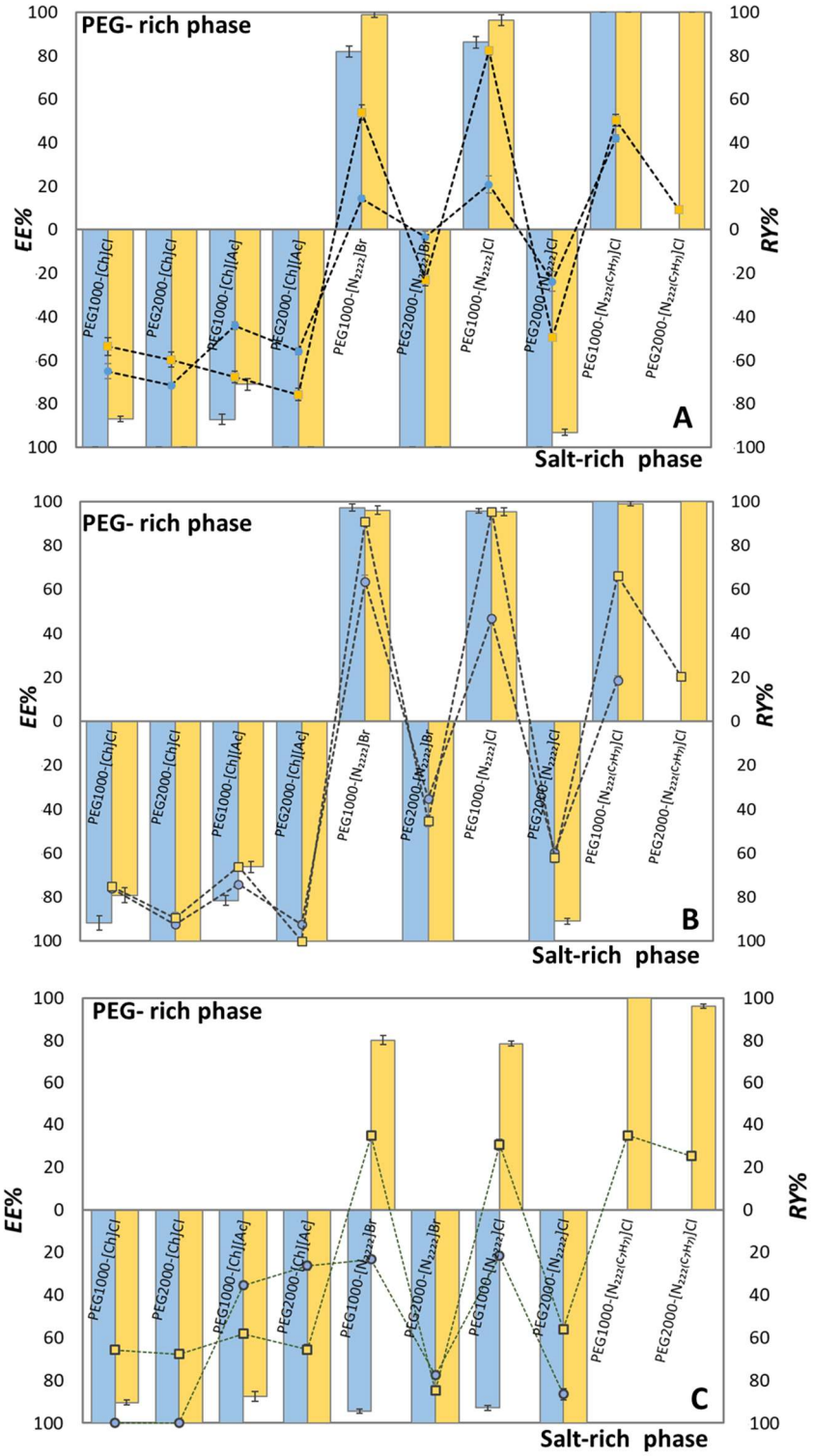

Figure 4.8. Extraction efficiency (EE_{prot}%, columns) and recovery yield (RY_{prot}%, symbols) of Lysozyme (blue) and Ovalbumin (yellow) from egg white dissolved in water (A): (1:5, v:v); (B): (1:10, v:v); (C): (1:50, v:v) in ABS composed of 30 wt% of PEG, 8 wt% of (K_2HPO_4/KH_2PO_4) + H_2O + 5 wt% of ILs at 25°C and pH 7.

4.4. Conclusions

ABS have been investigated as a suitable technique for the separation and purification of a multitude of bioproducts. However, conventional polymer-based ABS exhibit a small range of polarities in their coexisting phases, narrowing their application in the development of effective separation processes. To overcome this drawback, alternative ABS constituted by ILs as adjuvants in polymer-salt ABS have been investigated. In the current work, the partition behavior of two proteins, namely ovalbumin and lysozyme, was investigated in conventional PEG-salt ABS and in ABS comprising ILs as adjuvants. Two set of studied have been carried out, namely with commercial proteins and with egg white.

Overall, with the systems in which no IL was added it was observed a preferential partition of ovalbumin to the PEG-rich phase, whereas lysozyme tends to precipitate at the interphase. A similar trend was observed when applying the same systems to separate both proteins from egg white. However, when ILs are added at 5 wt%, mots systems lead to an inversion on the partitioning trend. With the commercial proteins, ovalbumin preferentially enriched in the salt-rich whereas lysozyme tends to majorly partition to the PEG-rich phase, while avoiding the precipitation of the last protein. However, when the same systems are applied to egg white, a more complex phenomenon takes place. With the exception of two systems, both proteins tend to migrate to the same phase, and the phase to which they migrate depends on the egg white dilution. Two systems that allow the separation of both proteins have been identified, although with low recovery yields. Accordingly, future investigations are suggested to improve the separation performance of the studied ABS, namely by studying other egg white dilutions and by analyzing the proteins profile in each phase and fraction to infer their purity level.

4.5. References

1. Omana DA, Wang J, Wu J (2010) Co-extraction of egg white proteins using ion-exchange chromatography from ovomucin-removed egg whites. J Chromatogr B A 878:1771–1776.
2. Hatta H, Kapoor MP, Juneja LR (2008) Bioactive Components in Egg Yolk. In: Mine Y (ed) Egg Bioscience and Biotechnology. pp 185–237
3. Iwashita K, Handa A, Shiraki K (2017) Co-aggregation of ovalbumin and lysozyme. Food Hydrocoll 67:206–215.
4. Sun LZ, Elsayed S, Aasen TB, Van Do T, Aardal NP, Florvaag E, Vaali K (2010) Comparison between ovalbumin and ovalbumin peptide 323-339 responses in allergic mice: Humoral and cellular aspects. Scand J Immunol 71:329–335.
5. Savadkoohi S, Bannikova A, Mantri N, Kasapis S (2014) Structural properties of condensed ovalbumin systems following application of high pressure. Food Hydrocoll 53:104–114.
6. Wang Y, Zhou Y, Sokolov J, Rigas B, Levon K, Rafailovich M (2008) A potentiometric protein sensor built with surface molecular imprinting method. Biosens Bioelectron 24:162–166.
7. Yang WH, Tu ZC, Wang H, Li X, Tian M (2017) High-intensity ultrasound enhances the immunoglobulin (Ig)G and IgE binding of ovalbumin. J Sci Food Agric 97:2714–2720.
8. Abeyrathne EDNS, Lee HY, Ahn DU (2013) Egg white proteins and their potential use in food processing or as nutraceutical and pharmaceutical agents – a review. Poult Sci 92:3292–3299.
9. Mecitoğlu Ç, Yemenicioğlu A, Arslanoğlu A, Elmaci ZS, Korel F, Çetin AE (2006) Incorporation of partially purified hen egg white lysozyme into zein films for antimicrobial food packaging. Food Res Int 39:12–21.
10. Mine S, Tate S, Ueda T, Kainosho M, Imoto T (1999) Analysis of the Relationship Between Enzyme

Activity and its Internal Motion using Nuclear Magnetic Resonance : 15 N Relaxation Studies of Wild-type and Mutant Lysozyme. J Mol Biol 286:1547–1565.
11. Singh S, Singh J (2003) Effect of polyols on the conformational stability and biological activity of a model protein lysozyme. AAPS PharmSciTech 4:101–109.
12. Maosoongnern S, Flood C, Flood AE, Ulrich J (2017) Crystallization of lysozyme from lysozyme – ovalbumin mixtures: Separation potential and crystal growth kinetics. J Cryst Growth 469:2–7.
13. Johnson RD, Arnold FH (1995) Review: Multipoint binding and heterogeneity in immobilized metal affinity chromatography. Biotechnol Bioeng 48:437–443.
14. R.K S (1994) Protein Purification:Principles and Practice. Springer
15. Carta G, Jungbauer A (2010) Protein Chromatography: Process Development and Scale-Up
16. Albertsson P. A (1958) Partition of proteins in liquid polymer-polymer two-phase systems. Nature 182:709–711.
17. Martínez-Aragón M, Burghoff S, Goetheer ELV, de Haan AB (2009) Guidelines for solvent selection for carrier mediated extraction of proteins. Sep Purif Technol 65:65–72.
18. Saravanan S, Rao JR, Nair BU, Ramasami T (2008) Aqueous two-phase poly(ethylene glycol)-poly(acrylic acid) system for protein partitioning: Influence of molecular weight, pH and temperature. Process Biochem 43:905–911.
19. Nerli BB, Espariz M, Pico GA (2001) Thermodynamic study of forces involved in bovine serum albumin and ovalbumin partitioning in aqueous two-phase systems. Biotechnol Bioeng 72:468–474.
20. Pereira MM, Cruz RAP, Almeida MR, Lima ÁS, Coutinho JAP, Freire MG (2016) Single-Step Purification of Ovalbumin from Egg White Using Aqueous Biphasic Systems. Process Biochem 51:781–791.
21. Su CK, Chiang BH (2006) Partitioning and purification of lysozyme from chicken egg white using aqueous two-phase system. Process Biochem 41:257–263.
22. Lu Y, Lu W, Wang W, Guo Q, Yang Y (2013) The optimization of aqueous two-phase extraction of lysozyme from crude hen egg white using response surface methodology. J Chem Technol Biotechnol 88:415–421.
23. Diederich P, Amrhein S, Hämmerling F, Hubbuch J (2013) Evaluation of PEG/phosphate aqueous two-phase systems for the purification of the chicken egg white protein avidin by using high-throughput techniques. Chem Eng Sci 104:945–956.
24. Gutowski KE, Broker GA, Willauer HD, Huddleston JG, Swatloski RP, Holbrey JD, Rogers RD (2003) Controlling the Aqueous Miscibility of Ionic Liquids: Aqueous Biphasic Systems of Water-Miscible Ionic Liquids and Water-Structuring Salts for Recycle, Metathesis, and Separations. J Am Chem Soc 125:6632–6633.
25. He C, Li S, Liu H, Li K, Liu F (2005) Extraction of testosterone and epitestosterone in human urine using aqueous two-phase systems of ionic liquid and salt. J Chromatogr A 1082:143–149.
26. Freire MG, Pereira JFB, Francisco M, Rodríguez H, Rebelo LPN, Rogers RD, Coutinho JAP (2012) Insight into the interactions that control the phase behaviour of new aqueous biphasic systems composed of polyethylene glycol polymers and ionic liquids. Chemi Eur J 18:1831–1839.
27. Pereira JF., Lima AS, Freire MG, Coutinho JAP (2010) Ionic liquids as adjuvants for the tailored extraction of biomolecules in aqueous biphasic systems. Green Chem, 12:1661–1669.
28. Souza RL, Campos VC, Ventura SPM, Soares CMF, Coutinho JAP, Lima ÁS (2014) Effect of ionic liquids as adjuvants on PEG-based ABS formation and the extraction of two probe dyes. Fluid Phase Equilib 375:30–36.
29. Ferreira AM, Faustino VFM, Mondal D, Coutinho JAP, Freire MG (2016) Improving the extraction and purification of immunoglobulin G by the use of ionic liquids as adjuvants in aqueous biphasic systems. J Biotechnol 236:166–175.
30. CatarinaM.S.S N, Sousa RCS, Matheus M P, Freire MG, Coutinho JAP (2018) Understanding the effect of ionic liquids as adjuvants in the partition of biomolecules in aqueous two-phase systems formed by polymers and weak salting-out agents. Biochem Eng J 141:239–246.
31. Santos JHP., A.eSilva F, Coutinho JA., Ventura S, Pessoa AJ (2015) Ionic liquids as a novel class of electrolytes in polymeric aqueous biphasic systems. Process Biochem 50:661–668.
32. Ventura SPM, e Silva FA, Quental M V, Mondal D, Freire MG, Coutinho JAP (2017) Ionic-Liquid-Mediated Extraction and Separation Processes for Bioactive Compounds: Past, Present, and Future Trends. Chem Rev 117:6984–7052.
33. Souza RL, Ventura SPM, Soares CMF, Coutinho JAP, Lima ÁS (2015) Lipase purification using ionic liquids as adjuvants in aqueous two-phase systems. Green Chem 17:3026–3034.
34. Ventura SPM, Marques CS, Rosatella AA, Afonso CAM, Gonçalves F, Coutinho JAP (2012) Toxicity assessment of various ionic liquid families towards Vibrio fischeri marine bacteria. Ecotoxicol Environ Saf 76:162–168.
35. Neves CMSS, Ventura PM, Freire MG, Marrucho IM (2009) Evaluation of Cation Influence on the

Formation and Extraction Capability of Ionic-Liquid-Based Aqueous Biphasic Systems. J Phys Chem B 113:5194–5199
36. Merchuk JC, Andrews BA, Asenjo JA (1998) Aqueous Two-Phase Systems for Protein Separation. Studies on phase inversion. J Chromatogr B Biomed Sci Appl 711: 285-293
37. Piculell L, Bjorn L (1992) Physical Chemistry I, University of Lund, Chemical Center, Box 124,. Adv Colloid Interface Sci 41:149–178
38. Sousa R de CS, Neves CMSS, Pereira MM, Freire MG, Coutinho JAP (2018) Potential of aqueous two-phase systems for the separation of levodopa from similar biomolecules. J Chem Technol Biotechnol 93:1940–1947
39. Almeida MR, Passos H, Pereira MM, et al (2014) Ionic liquids as additives to enhance the extraction of antioxidants in aqueous two-phase systems. Sep Purif Technol 128:1–10.
40. Ventura SPM, Neves CMSS, Freire MG, Lima ÁS, Coutinho JAP, Freire MG (2009) Evaluation of Anion Influence on the Formation and Extraction Capacity of Ionic-Liquid-Based Aqueous Biphasic Systems. J Phys Chem B 113:9304–9310
41. Pereira JFB, Kurnia KA, Cojocaru OA, Gurau G, Rebelo LPN, Rogers RD, Freire MG, Coutinho JAP (2014) Molecular interactions in aqueous biphasic systems composed of polyethylene glycol and crystalline vs. liquid cholinium-based salts. Phys Chem Chem Phys 16:5723–5731.
42. Tomé LIN, Pereira JFB, Rogers RD, Freire MG, Gomes JRB, Coutinho JAP (2014) "Washing-Out" Ionic Liquids From Polyethylene Glycol To Form Aqueous Biphasic Systems. Phys Chem Chem Phys 16:2271–2274.
43. Ilke, Yücekan S il Ö (2011) Partitioning of invertase from tomato in poly (ethylene glycol)/ sodium sulfate aqueous two-phase systems. Process Biochem 46:226–232.
44. Ashipala OK, He Q (2008) Optimization of fibrinolytic enzyme production by Bacillus subtilis DC-2 in aqueous two-phase system (poly-ethylene glycol 4000 and sodium sulfate). Bioresour Technol 99:4112–4119.
45. Rao JR, Nair BU (2011) Bioresource Technology Novel approach towards recovery of glycosaminoglycans from tannery wastewater. Bioresour Technol 102:872–878.
46. Boncina M, Rescic J, Vlachy V (2008) Solubility of Lysozyme in Polyethylene Glycol-Electrolyte Mixtures : The Depletion Interaction and Ion-Specific Effects. Biophys J 95:1285–1294.
47. Johansson H-O, Karlstrom G, Tjerneld F, Haynes CA (1998) Driving forces for phase separation and partitioning in aqueous two-phase systems. J Chromatogr B 711:3–17
48. Teixeira Franco T H-KR (2000) Single-Step Partitioning in Aqueous Two-Phase Systems: Methods and Protocols, Hatti-Kaul
49. Yavari M, Pazuki GR, Vossoughi M, Mirkhani SA, Seifkordi AA (2013) Fluid Phase Equilibria Partitioning of alkaline protease from Bacillus licheniformis (ATCC 21424) using PEG – K 2 HPO 4 aqueous two-phase system. Fluid Phase Equilib 337:1–5.
50. Tankrathok A, Daduang S, Patramanon R, Araki T, Sompong Thammasirirak (2009) Preparative Biochemistry and Biotechnology Purification Process for the Preparation and Characterizations of Hen Egg White Ovalbumin, Lysozyme, ovotransferrin, and ovomucoid. Prep Biochem Biotechnol 39:380–399
51. Abeyrathne EDNS, Lee HY, Ahn DU (2014) Sequential separation of lysozyme, ovomucin, ovotransferrin, and ovalbumin from egg white. Poult Sci 93:1001–1009
52. Cássia R De, Sousa S, Pereira MM, Freire MG, Coutinho JAP (2018) Evaluation of the effect of ionic liquids as adjuvants in polymer-based aqueous biphasic systems using biomolecules as molecular probes. Sep Purif Technol 196:244–253.
53. Glyk A, Solle D, Scheper T, Beutel S (2017) Evaluation of Driving Forces for Protein Partition in PEG-Salt Aqueous Two- Phase Systems and Optimization by Design of Experiments. J Chromatogr Sep Tech 8:1–16.

5. Conclusions & Future work

To design IL-based sustainable separation processes other types of ILs instead of the well-studied imidazolium-based should be chosen. In this context, this thesis is focused on the use of tetraalkylammonium-based ILs to form ABS aiming the separation of amino acids and proteins. In this thesis, most works were carried out with the goal of understanding the partitioning behavior of amino acids and proteins in IL-based ABS to design effective separation platforms. In addition to the literature review on the use of hydrophobic ILs and IL-based ABS to separate amino acids and proteins, in this thesis results on the use of ABS composed of cholinium-based ILs and K_2HPO_4 to separate amino acids are provided. These systems were evaluated regarding their ability to separate amino acids, allowing to comprehensively address the IL anion alkyl chain length effect and to identify odd-even effects in both these systems salting-out aptitude and extraction performance. ABS composed of ammonium-based ILs and phosphate-based salts were then investigated to separate ovalbumin and lysozyme (proteins present in egg white). The ABS phase diagrams were determined and these systems performance to extract and recover the two proteins was evaluated in respect to the IL chemical structure and pH. Finally, ILs have been investigated as adjuvants in polymer-based ABS to tailor the coexisting phase's polarities aiming at improving the ABS selectivity. All the respective phase diagrams were determined and these systems extraction efficiencies and recoveries were evaluated with model proteins and egg white samples.

Based on the results achieved and discussed in this thesis, as future work the following steps should be addressed:

- To investigate IL-based ABS for the simultaneous separation of different amino acids or to fractionate amino acids from complex samples;

- To carry out studies on the extraction of ovalbumin and lysozyme with other IL-based ABS to better understand the IL effect on the proteins separation;

- To appraise the use of ABS comprising ILs as adjuvants (and other types of ILs) in the extraction of ovalbumin and lysozyme from egg white at other dilutions;

- To analyze the proteins profile in each phase and fraction when using real samples to infer their purity level, e.g. by SDS-PAGE.

List of Publications

Publications in the current thesis

Belchior, D. C. V., Duarte, I. F., & Freire, M. G. Ionic Liquids in Bioseparation Processes. Chapter 1 in Advances in Biochemical Engineering/Biotechnology, Springer, Berlin, Heidelberg, 2018. pp 1-29. doi:10.1007/10_2018_66

Belchior, D. C. V., Almeida M.R., Sintra, T.E., Ventura, S. P. M., Duarte, I. F., & Freire, M. G. Odd–Even Effect in the Formation and Extraction Performance of Ionic-Liquid-Based Aqueous Biphasic Systems. Industrial & Engineering Chemistry Research, 2019, 58(19), 8323-8331. doi: 10.1021/acs.iecr.9b00663

Belchior, D. C. V., Quental, M. V., Pereira, M. M., Mendonça, C. M. N., Duarte, I. F. and Freire, M. G. Performance of tetraalkylammonium-based ionic liquids as constituents of aqueous biphasic systems in the extraction of ovalbumin and lysozyme, Separation and Purification Technology, 2019. Submitted.

Other publications

Belchior, D. C. V., Sintra, T. E., Carvalho, P. J., Soromenho, M. R. C., Esperança, J. M. S. S., Ventura, S. P. M., Rogers, R. D., Coutinho, J. A.P., Freire, M. G. Odd-even effect on the formation of aqueous biphasic systems formed by 1-alkyl-3-methylimidazolium chloride ionic liquids and salts. The Journal of Chemical Physics, 2018, 148(19), 193842. doi:10.1063/1.5012020

Almeida, M. R., Belchior, D. C. V., Carvalho, P. J. and Freire, M. G. Liquid-liquid equilibrium and extraction performance of aqueous biphasic systems composed of water, cholinium carboxylate ionic liquids and K_2CO_3. Journal of Chemical & Engineering Data, 2019, submitted.

Appendix A

Odd-even effect in the formation and extraction performance of ionic-liquid-based aqueous biphasic systems - CHAPTER 2

NMR spectra and data of cholinium-based ILs

Cholinium propanoate, [Ch][C_2CO_2]

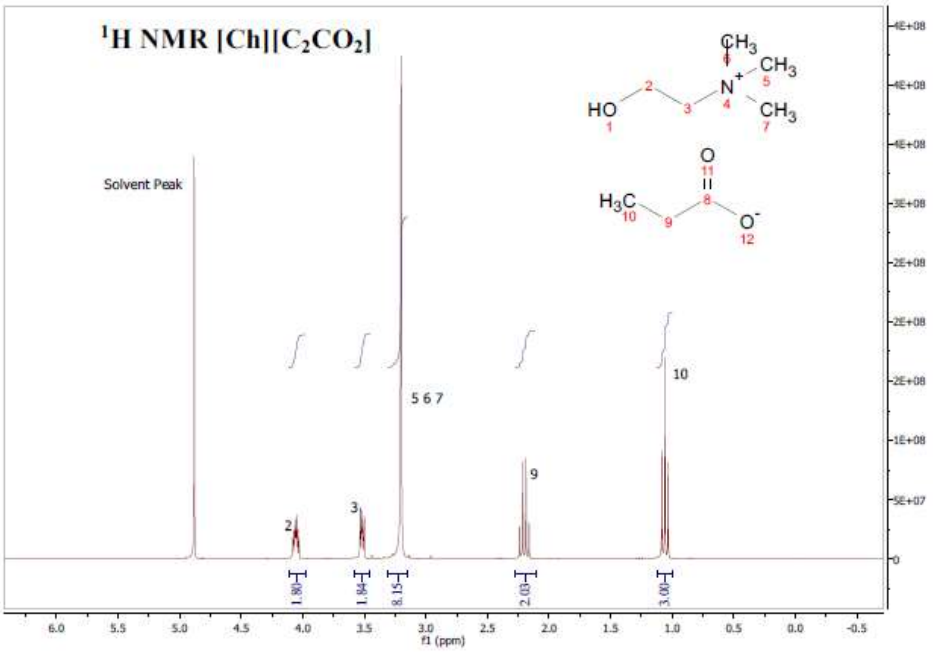

^{1}H NMR (D_2O, 300 MHz, [ppm]): 4.06 (m,); 3.52 (m, 2H); 3.20 (s, 9H); 2.20 (q, 2H, J_{HH}=7.7 Hz); 1.06 (t, 3H, J_{HH}=7.7 Hz).

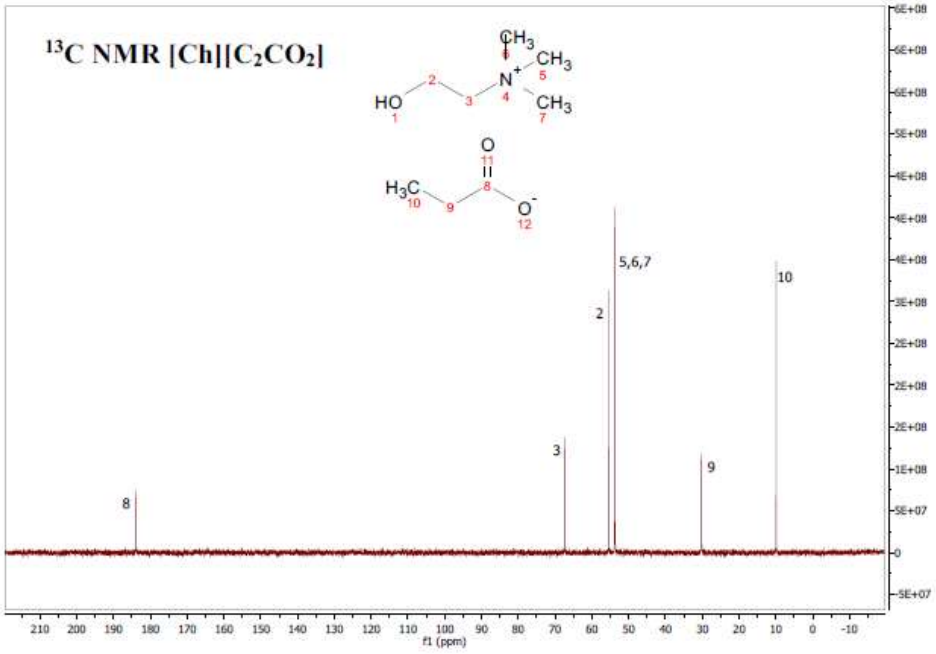

^{13}C NMR (D_2O, 75.47 MHz, [ppm]): 184.04; 67.40; 55.69; 53.75; 30.25; 9.60.

Cholinium Butanoate, [Ch][C_3CO_2]

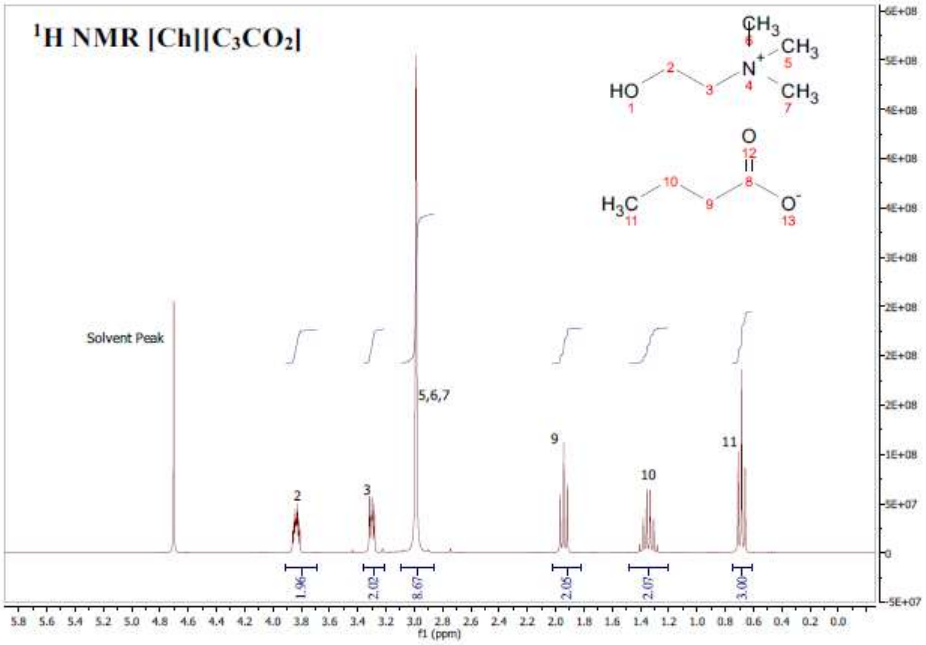

^{1}H NMR (D_2O, 300 MHz, [ppm]): 3.66 (m, 2H); 3.32 (m, 2H); 3.01 (s, 9H); 1.98 (t, 2H, J_{HH}=7.7 Hz); 1.37 (m, 2H,); 0.71 (t, 3H, J_{HH}=7.7 Hz).

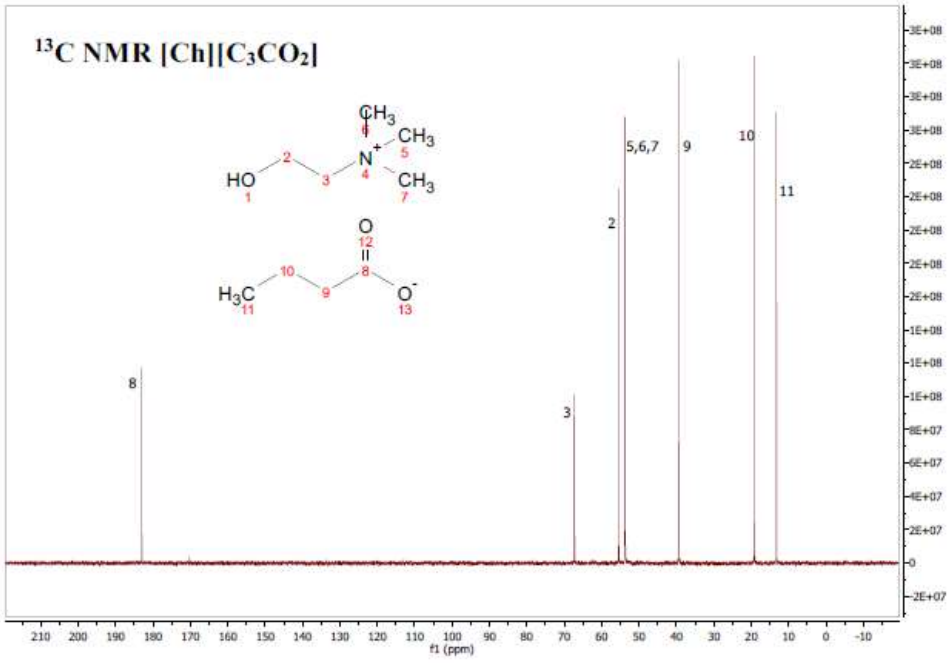

^{13}C NMR (D_2O, 75.47 MHz, [ppm]): 183.07; 67.28; 55.43; 53.68.15; 39.30; 19.12; 13.27.

Cholinium Pentanoate, [Ch][C_4CO_2]

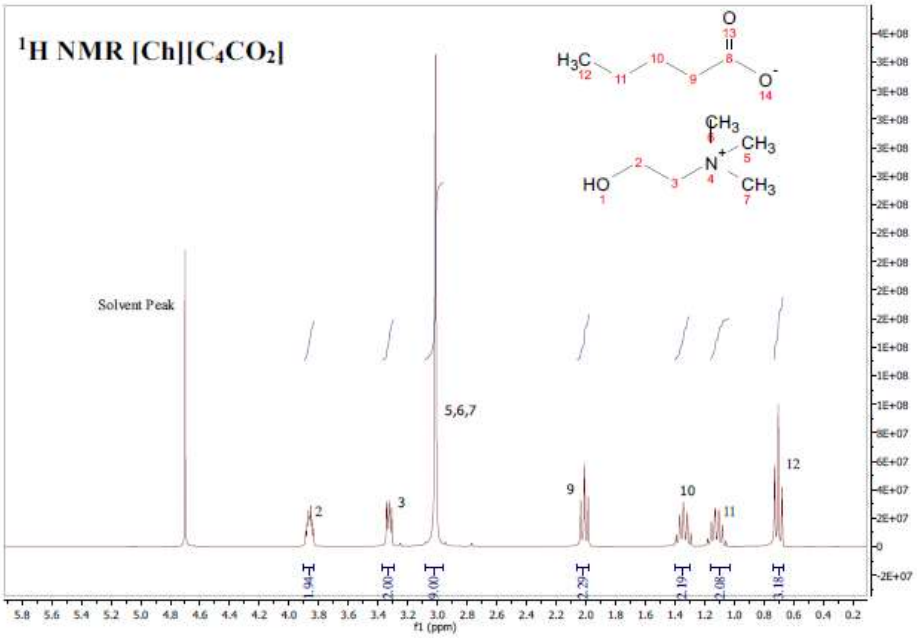

^{1}H NMR (D_2O, 300 MHz, [ppm]): 3.83 (m, 2H); 3.30 (m, 2H); 2.99 (s, 9H); 1.98 (t, 2H, J_{HH}=7.7 Hz); 1.31 (m, 2H,); 1.09 (m, 2H,); 0.68 (t, 3H, J_{HH}=7.7 Hz).

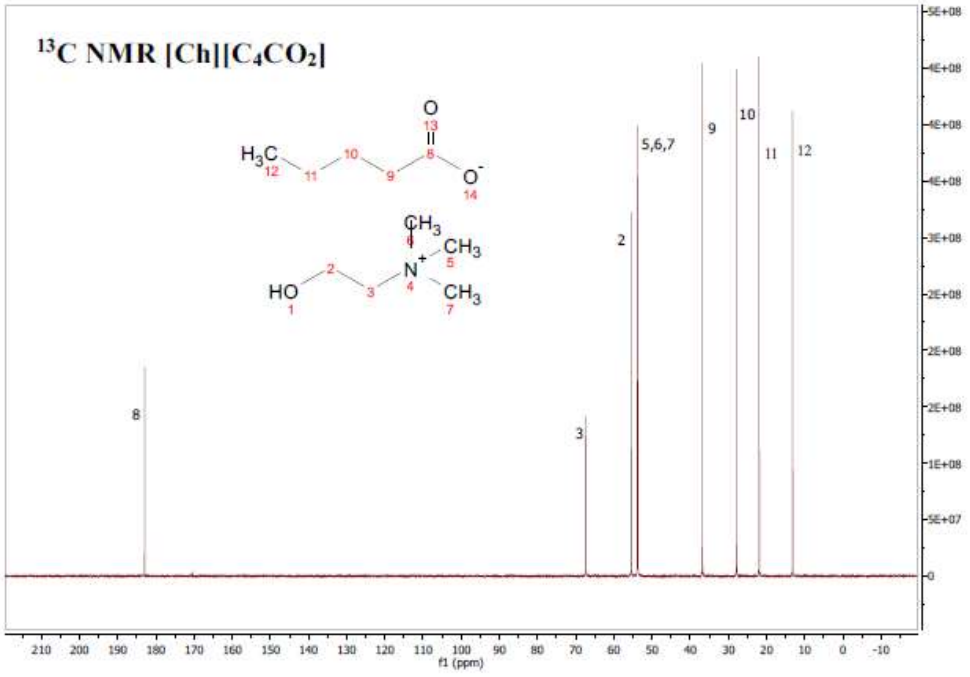

^{13}C NMR (D_2O, 75.47 MHz, [ppm]): 183.04; 67.35; 55.46; 53.71; 37.03; 27.96; 21.93; 13.57.

Cholinium Hexanoate, [Ch][C_5CO_2]

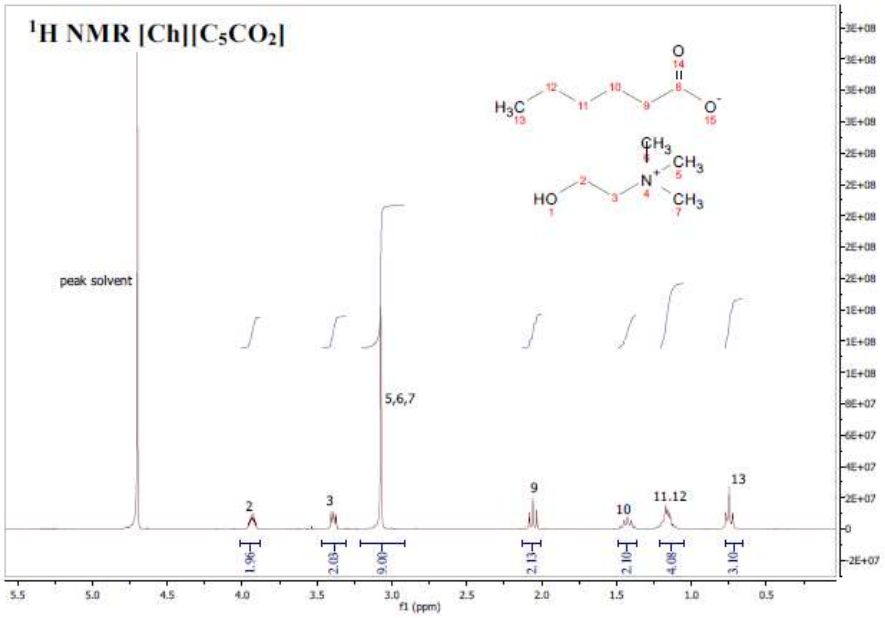

^{1}H NMR (D_2O, 300 MHz, [ppm]): 3.93 (m, 2H); 3.39 (m, 2H); 3.07 (s, 9H); 2.06 (t, 2H, J_{HH}=7.7 Hz); 1.41 (m, 2H,); 1.16 (m, 2H,); 0.75 (t, 3H, J_{HH}=7.7 Hz).

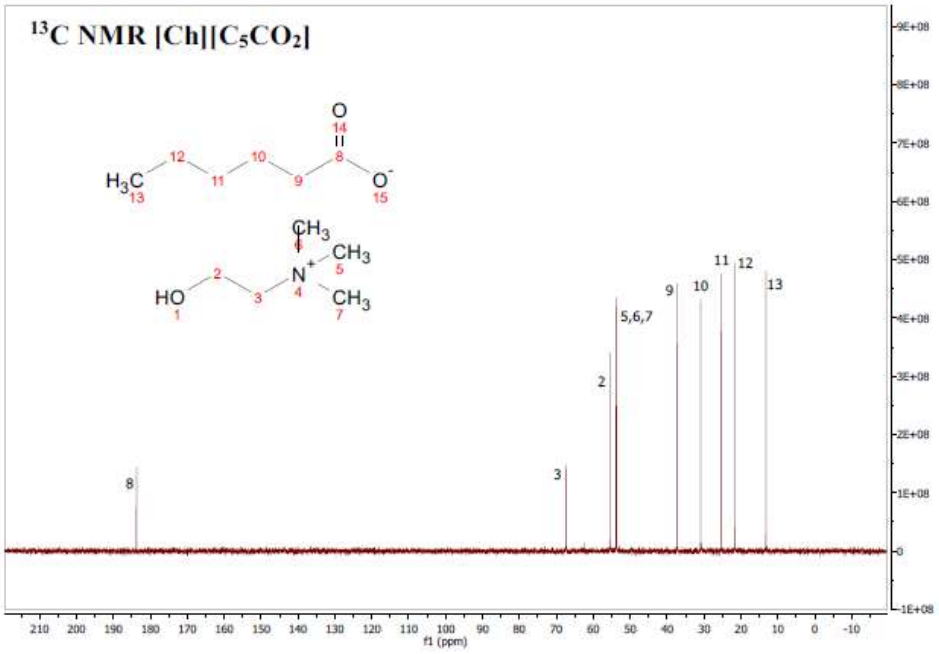

^{13}C NMR (D_2O, 75.47 MHz, [ppm]): 184.04; 67.38; 55.38; 53.74; 37.25; 30.92; 25.64; 21.55; 13.23.

Cholinium Heptanoate, [Ch][C_6CO_2]

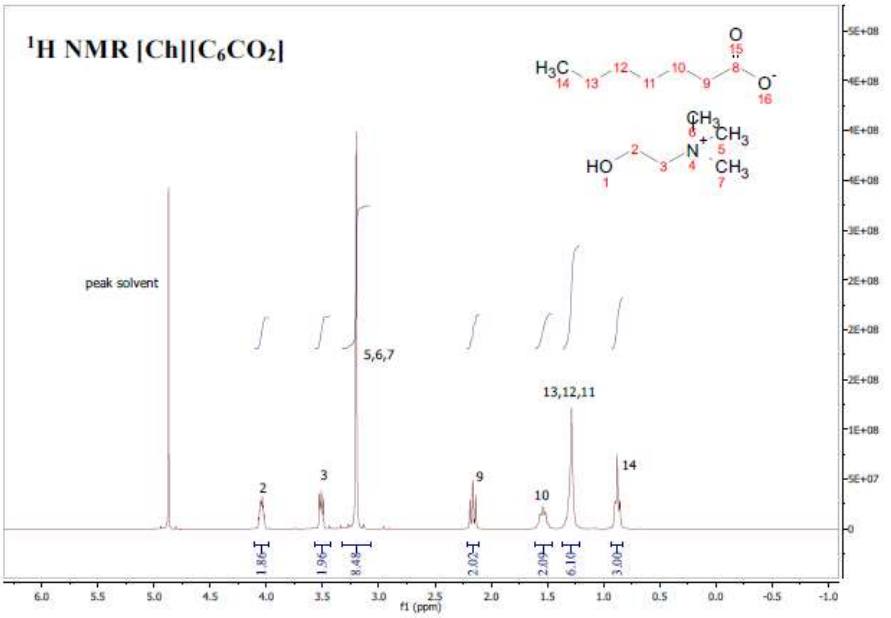

^{1}H NMR (D_2O, 300 MHz, [ppm]): 4.04 (m, 2H); 3.52 (m, 2H); 3.20 (s, 9H); 2.16 (t, 2H, J_{HH}=7.7 Hz); 1.54 (m, 2H,); 1.29 (s, 6H,); 0.88 (t, 3H, J_{HH}=7.7 Hz).

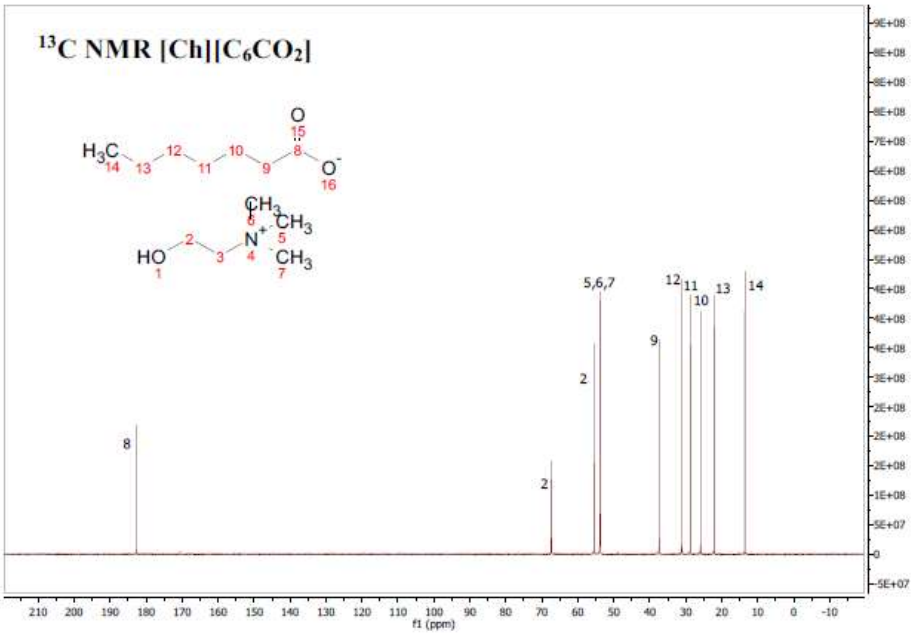

^{13}C NMR (D_2O, 75.47 MHz, [ppm]): 182.59; 68.38; 56.06; 52.32; 37.61; 30.60; 28.28; 25.63; 21.89; 13.90.

Cholinium Octanoate, [Ch][C_7CO_2]

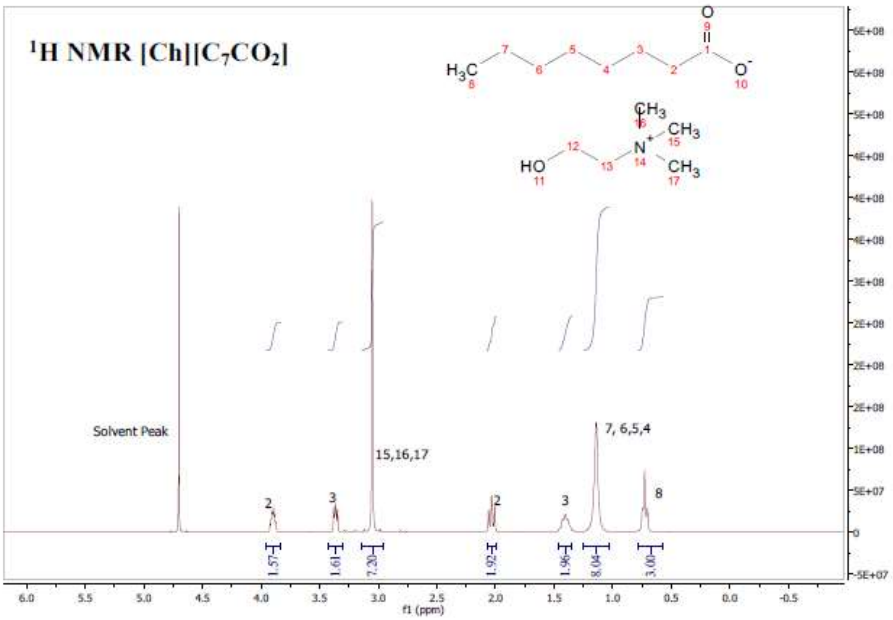

^{1}H NMR (D_2O, 300 MHz, [ppm]): 3.90 (m, 2H); 3.34 (m, 2H); 3.05 (s, 9H); 2.03 (t, 2H, J_{HH}=7.7 Hz); 1.40 (m, 2H,); 1.14 (s, 6H,); 0.74 (t, 3H, J_{HH}=7.7 Hz).

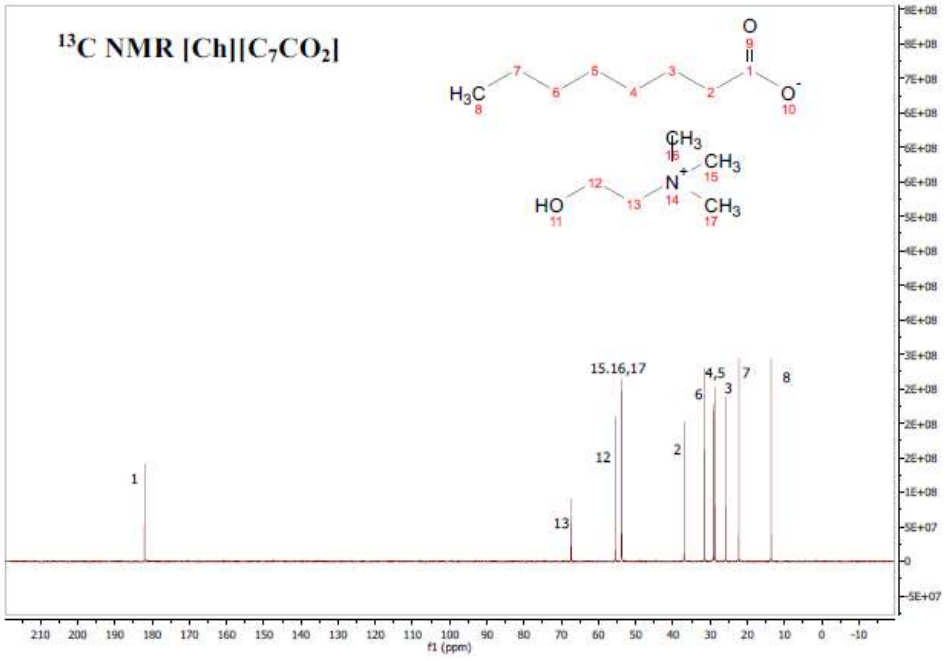

^{13}C NMR (D_2O, 75.47 MHz, [ppm]): 182.39; 67.41; 55.36; 54.02; 36.99; 31.96; 28.94; 25.63; 22.30; 13.60.

Tables A1 to A7 present the weight fraction data for the binodal curves of the ABS formed by each ionic liquid, K_2HPO_4 and water.

Table A1. Experimental data for the binodal weight fraction percentage of the ABS formed by [Ch][C_1CO_2] (1) + K_2HPO_4 (2) + water (3) at (298 ± 1) K and atmospheric pressure.

[Ch][C_1CO_2] (1) + K_2HPO_4 (2) + water (3)					
$100w_1$	$100w_2$	$100w_1$	$100w_2$	$100w_1$	$100w_2$
56.62	7.79	22.68	27.09	12.58	36.50
53.55	7.37	22.53	26.91	12.53	36.36
51.66	9.23	22.15	27.48	12.31	36.78
48.90	8.74	21.91	27.18	12.26	36.64
47.35	10.36	21.02	28.50	12.05	37.06
45.67	9.99	20.90	28.33	11.97	36.83
44.23	11.57	20.25	29.31	11.69	37.37
43.21	11.31	20.14	29.15	11.65	37.24
41.95	12.73	19.57	30.02	11.37	37.79
41.02	12.45	19.47	29.86	11.33	37.66
39.86	13.80	18.94	30.67	11.09	38.14
39.41	13.64	18.85	30.53	11.05	38.01
38.40	14.83	18.59	30.93	10.88	38.36
37.64	14.54	18.41	30.62	10.84	38.24
36.74	15.63	17.75	31.66	10.68	38.57
36.36	15.47	17.65	31.48	10.64	38.45
35.52	16.51	17.18	32.24	10.49	38.77
34.85	16.20	17.10	32.08	10.46	38.66
34.10	17.14	16.71	32.71	10.30	38.98
33.78	16.98	16.64	32.57	10.27	38.88
33.04	17.91	16.24	33.22	10.06	39.30
32.71	17.74	16.16	33.06	10.01	39.10
32.02	18.63	15.75	33.75	9.78	39.58
31.77	18.48	15.62	33.47	9.75	39.48
31.10	19.36	15.28	34.04	9.62	39.77
30.85	19.20	15.21	33.89	9.59	39.67
30.24	20.00	15.05	34.17	9.36	40.16
29.98	19.83	14.91	33.87	9.31	39.94
29.43	20.57	14.61	34.40	9.06	40.47
29.20	20.41	14.55	34.27	9.01	40.26
27.89	22.18	14.40	34.53	8.83	40.66
27.69	22.01	14.29	34.26	8.81	40.56
26.71	23.34	13.72	35.28	8.64	40.94
26.53	23.18	13.67	35.15	8.62	40.85
25.64	24.42	13.43	35.60	8.46	41.19
25.31	24.10	13.37	35.46	8.42	41.00
24.48	25.27	13.17	35.83	8.17	41.56
24.32	25.11	13.12	35.71	8.13	41.36
23.61	26.13	12.87	36.16	7.95	41.79
23.45	25.96	12.83	36.03	7.91	41.58

Table A2. Experimental data for the binodal weight fraction percentage of the ABS formed by [Ch][C_2CO_2] (1) + K_2HPO_4 (2) + water (3) at (298 ± 1) K and atmospheric pressure.

[Ch][C_2CO_2] (1) + K_2HPO_4 (2) + water (3)					
$100w_1$	$100w_2$	$100w_1$	$100w_2$	$100w_1$	$100w_2$
59.03	4.52	17.81	27.70	9.06	37.06
54.64	4.18	17.63	27.43	8.97	36.71
52.51	6.35	17.14	28.34	8.78	37.21
48.66	5.89	16.97	28.05	8.73	37.03
46.49	8.31	16.48	28.97	8.50	37.65
44.31	7.92	16.34	28.72	8.46	37.47
42.88	9.60	15.98	29.41	8.29	37.90
40.95	9.17	15.82	29.12	8.22	37.57
39.73	10.68	15.20	30.33	8.01	38.15
38.83	10.44	15.09	30.10	7.98	37.98
37.75	11.81	14.74	30.79	7.74	38.64
36.98	11.57	14.62	30.52	7.67	38.30
36.01	12.84	14.31	31.16	7.40	39.07
35.31	12.59	14.19	30.89	7.36	38.87
34.50	13.69	13.72	31.85	7.19	39.34
33.90	13.45	13.62	31.62	7.15	39.11
33.07	14.60	13.34	32.22	6.99	39.59
32.39	14.30	13.24	31.99	6.93	39.26
31.62	15.37	12.95	32.61	6.65	40.08
31.11	15.13	12.85	32.37	6.61	39.80
30.40	16.15	12.59	32.94	6.42	40.35
29.90	15.89	12.50	32.71	6.38	40.08
28.69	17.68	12.14	33.50	6.18	40.69
28.21	17.38	12.05	33.27	6.14	40.42
27.08	19.09	11.81	33.80	5.99	40.91
26.71	18.83	11.75	33.61	5.97	40.77
26.19	19.62	11.43	34.32	5.85	41.13
25.81	19.33	11.35	34.09	5.83	40.99
24.86	20.83	11.15	34.56	5.72	41.35
24.48	20.51	11.08	34.36	5.68	41.08
23.63	21.89	10.88	34.83	5.34	42.23
23.38	21.65	10.83	34.67	5.28	41.81
22.55	23.01	10.57	35.29	5.09	42.48
22.24	22.70	10.50	35.08	5.06	42.23
21.54	23.89	10.32	35.52	4.93	42.66
21.28	23.59	10.26	35.30	4.91	42.43
20.37	25.15	10.00	35.92	4.44	44.12
20.11	24.83	9.90	35.57	4.36	43.32
19.49	25.92	9.65	36.19	4.17	44.01
19.29	25.65	9.60	36.00	4.15	43.70
18.53	26.99	9.37	36.57		
18.35	26.72	9.32	36.38		

Table A3. Experimental data for the binodal weight fraction percentage of the ABS formed by [Ch][C_3CO_2] (1) + K_2HPO_4 (2) + water (3) at (298 ± 1) K and atmospheric pressure.

[Ch][C_3CO_2] (1) + K_2HPO_4 (2) + water (3)					
$100w_1$	$100w_2$	$100w_1$	$100w_2$	$100w_1$	$100w_2$
54.51	5.07	19.36	23.25	10.51	31.97
50.70	4.72	19.13	22.98	10.45	31.76
48.57	7.05	18.85	23.52	10.24	32.32
43.70	6.34	18.64	23.26	10.18	32.14
42.33	8.01	18.07	24.38	10.00	32.63
40.41	7.65	17.85	24.09	9.94	32.42
39.12	9.32	17.30	25.20	9.78	32.87
37.43	8.92	17.10	24.90	9.67	32.50
36.34	10.40	16.64	25.84	9.45	33.13
34.86	9.98	16.42	25.50	9.40	32.94
34.02	11.18	16.00	26.37	9.15	33.64
33.35	10.96	15.83	26.09	9.04	33.25
32.48	12.24	15.41	27.00	8.69	34.30
31.88	12.01	15.31	26.81	8.63	34.08
31.06	13.24	14.90	27.68	8.58	34.24
30.56	13.03	14.76	27.42	8.50	33.93
29.85	14.13	14.40	28.22	8.32	34.47
29.34	13.89	14.29	28.01	8.24	34.13
28.74	14.83	14.13	28.35	7.93	35.11
28.29	14.60	14.02	28.12	7.86	34.79
27.73	15.50	13.70	28.84	7.70	35.29
27.26	15.24	13.58	28.59	7.62	34.93
26.69	16.18	13.26	29.33	7.42	35.60
26.33	15.96	13.15	29.09	7.34	35.24
25.75	16.92	12.86	29.79	7.12	35.97
25.39	16.68	12.75	29.54	7.09	35.80
24.31	18.51	12.48	30.19	6.93	36.34
23.97	18.25	12.39	29.99	6.87	35.99
23.52	19.04	12.21	30.42	6.74	36.44
23.25	18.82	12.06	30.03	6.69	36.18
22.82	19.58	11.82	30.62	6.41	37.18
22.52	19.32	11.72	30.37	6.33	36.74
21.71	20.80	11.47	31.00	6.36	36.64
21.52	20.62	11.39	30.78	6.33	36.49
21.17	21.26	11.16	31.37	5.97	37.83
20.93	21.01	11.03	31.00	5.86	37.13
20.22	22.32	10.80	31.60	5.57	38.25
19.98	22.06	10.73	31.40	5.50	37.73

Table A4. Experimental data for the binodal weight fraction percentage of the ABS formed by [Ch][C_4CO_2] (1) + K_2HPO_4 (2) + water (3) at (298 ± 1) K and atmospheric pressure.

[Ch][C_4CO_2] (1) + K_2HPO_4 (2) + water (3)					
$100w_1$	$100w_2$	$100w_1$	$100w_2$	$100w_1$	$100w_2$
47.20	13.63	15.93	25.26	8.85	33.03
36.66	10.59	15.48	26.23	8.76	32.70
35.58	12.04	15.33	25.98	8.63	33.09
34.45	11.66	15.14	26.41	8.59	32.91
33.55	12.92	15.01	26.19	8.45	33.32
32.51	12.52	14.69	26.91	8.41	33.15
31.63	13.80	14.57	26.69	8.22	33.76
30.59	13.35	14.40	27.09	8.17	33.57
29.83	14.50	14.28	26.87	8.06	33.93
29.33	14.25	13.95	27.64	8.02	33.78
28.63	15.34	13.83	27.40	7.90	34.16
28.12	15.07	13.54	28.08	7.87	34.02
27.52	16.02	13.44	27.88	7.75	34.42
27.12	15.78	13.17	28.51	7.72	34.25
26.52	16.75	12.99	28.10	7.62	34.58
26.10	16.48	12.71	28.79	7.55	34.28
25.55	17.41	12.62	28.59	7.46	34.60
25.20	17.17	12.36	29.22	7.42	34.45
24.68	18.06	12.27	29.00	7.33	34.76
24.30	17.79	12.03	29.60	7.30	34.64
23.81	18.65	11.94	29.39	7.18	35.09
23.48	18.40	11.71	29.96	7.13	34.87
23.02	19.21	11.63	29.75	7.00	35.32
22.69	18.93	11.43	30.27	6.95	35.10
21.87	20.39	11.30	29.91	6.87	35.38
21.64	20.18	11.07	30.51	6.84	35.22
21.25	20.89	11.00	30.30	6.60	36.11
21.00	20.64	10.80	30.82	6.54	35.82
20.66	21.28	10.75	30.67	6.40	36.36
20.43	21.05	10.56	31.18	6.36	36.14
20.08	21.71	10.45	30.85	6.22	36.66
19.88	21.49	10.27	31.35	6.18	36.46
19.52	22.18	10.21	31.16	5.96	37.31
19.31	21.93	10.03	31.65	5.88	36.82
18.73	23.06	9.97	31.46	5.68	37.61
18.53	22.81	9.88	31.70	5.60	37.12
18.24	23.39	9.83	31.52	5.38	38.01
18.06	23.17	9.67	31.98	5.32	37.56
17.53	24.25	9.61	31.79	5.19	38.11
17.34	23.99	9.45	32.24	5.11	37.56
17.08	24.52	9.40	32.05	4.83	38.79
16.92	24.30	9.24	32.51	4.77	38.30
16.46	25.26	9.19	32.33	4.51	39.45
16.30	25.02	9.04	32.78	4.42	38.60
16.08	25.50	8.99	32.59		

Table A5. Experimental data for the binodal weight fraction percentage of the ABS formed by [Ch][C_5CO_2] (1) + K_2HPO_4 (2) + water (3) at (298 ± 1) K and atmospheric pressure.

[Ch][C_5CO_2] (1) + K_2HPO_4 (2) + water (3)					
$100w_1$	$100w_2$	$100w_1$	$100w_2$	$100w_1$	$100w_2$
56.58	5.57	20.22	22.86	11.82	30.59
53.28	5.24	19.87	23.50	11.74	30.38
50.91	7.68	19.66	23.26	11.64	30.61
48.26	7.27	19.39	23.76	11.56	30.39
46.32	9.38	19.21	23.54	11.34	30.95
43.01	8.71	18.91	24.11	11.27	30.75
41.53	10.47	18.71	23.85	10.95	31.58
40.60	10.24	18.19	24.85	10.82	31.20
39.28	11.86	17.99	24.58	10.63	31.70
37.60	11.35	17.70	25.16	10.56	31.50
36.37	12.94	17.52	24.90	10.35	32.08
35.64	12.68	16.99	25.95	10.31	31.94
34.75	13.87	16.82	25.70	10.20	32.24
33.74	13.47	16.58	26.20	10.14	32.07
32.92	14.60	16.43	25.97	9.95	32.60
32.31	14.34	16.20	26.46	9.83	32.20
31.59	15.36	16.03	26.18	9.49	33.16
30.99	15.07	15.60	27.08	9.38	32.81
30.29	16.09	15.46	26.84	9.15	33.48
29.78	15.82	15.25	27.30	9.05	33.13
29.17	16.73	15.10	27.03	8.82	33.82
28.66	16.43	14.72	27.85	8.73	33.47
28.05	17.36	14.64	27.70	8.54	34.05
27.60	17.08	14.46	28.11	8.45	33.70
27.08	17.89	14.32	27.84	8.12	34.73
26.59	17.57	14.12	28.27	8.04	34.39
25.99	18.52	14.02	28.07	7.47	36.20
25.61	18.24	13.66	28.90	7.25	35.13
24.61	19.87	13.55	28.67	6.70	37.04
24.28	19.61	13.38	29.07	6.55	36.24
23.81	20.39	13.28	28.84	6.14	37.72
23.47	20.10	13.13	29.20	5.99	36.77
23.03	20.84	13.03	28.97	5.59	38.31
22.73	20.57	12.73	29.67	5.49	37.61
22.04	21.76	12.63	29.43	5.10	39.18
21.73	21.45	12.49	29.78	5.00	38.39
21.34	22.13	12.40	29.56	4.52	40.45
21.08	21.85	12.14	30.21	4.41	39.45
20.41	23.07	12.05	30.01		

Table A6. Experimental data for the binodal weight fraction percentage of the ABS formed by [Ch][C_6CO_2] (1) + K_2HPO_4 (2) + water (3) at (298 ± 1) K and atmospheric pressure.

[Ch][C_6CO_2] (1) + K_2HPO_4 (2) + water (3)					
$100w_1$	$100w_2$	$100w_1$	$100w_2$	$100w_1$	$100w_2$
56.21	7.79	19.47	25.87	10.33	33.43
52.88	7.33	18.92	26.82	10.28	33.27
50.81	9.38	18.72	26.54	10.13	33.66
49.37	9.11	18.52	26.89	10.08	33.48
47.67	10.85	18.35	26.64	9.86	34.04
45.43	10.34	17.91	27.42	9.77	33.72
43.99	11.90	17.75	27.17	9.58	34.20
42.93	11.61	17.28	28.02	9.49	33.85
41.55	13.15	16.99	27.54	9.32	34.31
40.56	12.84	16.54	28.37	9.27	34.15
39.49	14.07	16.42	28.17	9.06	34.73
38.81	13.82	16.21	28.57	8.98	34.40
37.78	15.04	16.07	28.33	8.80	34.89
37.04	14.75	15.68	29.09	8.75	34.70
36.08	15.89	15.55	28.84	8.61	35.12
35.27	15.54	15.16	29.59	8.55	34.90
34.41	16.62	15.03	29.32	8.39	35.35
33.76	16.30	14.71	29.95	8.34	35.10
32.93	17.36	14.59	29.72	8.13	35.70
32.38	17.06	14.44	30.04	8.06	35.37
31.69	17.97	14.33	29.81	7.86	35.97
31.17	17.67	14.17	30.15	7.79	35.69
29.91	19.37	14.05	29.90	7.56	36.41
29.43	19.07	13.76	30.51	7.45	35.92
28.79	19.94	13.66	30.28	7.29	36.43
28.34	19.63	13.27	31.11	7.24	36.16
27.77	20.43	13.18	30.90	7.04	36.80
27.31	20.09	13.05	31.17	6.98	36.50
26.26	21.60	12.95	30.94	6.79	37.12
25.85	21.26	12.70	31.51	6.74	36.83
24.96	22.57	12.61	31.28	6.57	37.40
24.72	22.35	12.36	31.84	6.52	37.09
24.32	22.95	12.27	31.62	6.37	37.62
24.00	22.65	12.04	32.14	6.32	37.36
23.60	23.26	11.95	31.90	6.17	37.89
23.31	22.99	11.83	32.17	6.11	37.56
22.57	24.16	11.75	31.96	5.94	38.16
22.31	23.89	11.54	32.46	5.88	37.78
21.98	24.42	11.48	32.29	5.73	38.34
21.71	24.12	11.29	32.74	5.68	37.99
21.05	25.19	11.17	32.38	5.48	38.73
20.75	24.83	10.91	33.02	5.42	38.31
20.11	25.91	10.84	32.80	5.24	39.00
19.92	25.66	10.59	33.40	5.20	38.66
19.65	26.10	10.48	33.05		

Table A7. Experimental data for the binodal weight fraction percentage of the ABS formed by [Ch][C_7CO_2] (1) + K_2HPO_4 (2) + water (3) at (298 ± 1) K and atmospheric pressure.

[Ch][C_7CO_2] (1) + K_2HPO_4 (2) + water (3)					
$100w_1$	$100w_2$	$100w_1$	$100w_2$	$100w_1$	$100w_2$
53.94	9.55	17.76	28.78	9.56	35.02
52.62	9.32	17.57	28.47	9.51	34.83
50.68	11.16	17.34	28.88	9.37	35.19
48.18	10.61	17.18	28.60	9.29	34.87
46.54	12.28	16.72	29.42	9.06	35.46
45.34	11.96	16.59	29.20	8.96	35.08
43.95	13.42	16.21	29.90	8.74	35.68
43.05	13.14	16.07	29.63	8.69	35.49
41.76	14.54	15.86	30.02	8.59	35.78
40.82	14.21	15.70	29.71	8.53	35.54
39.64	15.53	15.36	30.36	8.34	36.08
38.74	15.18	15.21	30.08	8.30	35.90
37.69	16.37	14.88	30.72	8.17	36.27
36.90	16.03	14.76	30.48	8.12	36.06
35.92	17.18	14.43	31.13	8.04	36.30
35.24	16.85	14.30	30.85	7.97	36.00
34.33	17.96	14.00	31.46	7.78	36.55
33.81	17.69	13.89	31.20	7.75	36.39
32.27	19.59	13.66	31.66	7.62	36.77
31.71	19.25	13.55	31.42	7.55	36.45
30.97	20.19	13.42	31.69	7.39	36.95
30.42	19.83	13.33	31.46	7.32	36.61
29.80	20.64	12.95	32.24	7.09	37.35
29.31	20.31	12.87	32.02	7.01	36.95
28.07	21.96	12.64	32.51	6.84	37.51
27.68	21.65	12.55	32.28	6.78	37.23
27.08	22.47	12.33	32.76	6.61	37.79
26.71	22.17	12.23	32.51	6.57	37.52
26.21	22.87	12.03	32.96	6.40	38.07
25.79	22.50	11.95	32.73	6.35	37.72
24.86	23.85	11.74	33.19	6.20	38.24
24.53	23.54	11.66	32.96	6.15	37.97
23.67	24.80	11.46	33.41	6.04	38.36
23.38	24.49	11.39	33.20	5.98	38.01
23.00	25.06	11.21	33.62	5.81	38.64
22.67	24.71	11.14	33.42	5.75	38.28
21.97	25.79	11.06	33.62	5.63	38.72
21.73	25.50	10.98	33.40	5.57	38.24
21.37	26.06	10.71	34.05	5.36	39.01
21.14	25.77	10.60	33.71	5.32	38.72
20.50	26.79	10.44	34.11	5.16	39.36
20.29	26.52	10.37	33.87	5.11	38.96
19.69	27.49	10.21	34.25	4.92	39.71
19.46	27.17	10.15	34.05	4.85	39.18
19.19	27.63	10.00	34.44	4.70	39.82
18.96	27.31	9.95	34.26	4.65	39.40
18.42	28.24	9.69	34.92		
18.24	27.96	9.65	34.79		

Table A8. Adjusted parameters and respective standard deviations (σ) obtained by the fitting of the experimental data by equation (1).

IL	$A \pm \sigma$	$B \pm \sigma$	$10^5 (C \pm \sigma)$
[Ch][C_1CO_2]	113.95 ± 4.78	-0.274 ± 0.011	1.12 ± 0.07
[Ch][C_2CO_2]	100.58 ± 3.16	-0.280 ± 0.009	1.41 ± 0.07
[Ch][C_3CO_2]	102.27 ± 5.05	-0.316 ± 0.015	1.52 ± 0,15
[Ch][C_4CO_2]	117.05 ± 2.31	-0.338 ± 0.527	1.80 ± 0.34
[Ch][C_5CO_2]	117.16 ± 4.44	-0.319 ± 0.011	1.90 ± 0.11
[Ch][C_6CO_2]	111.05 ± 4.46	-0.273 ± 0,010	2.25 ± 0.87
[Ch][C_7CO_2]	115.77 ± 5.50	-0.252 ± 0,012	2.23 ± 0.08

Table A9. Weight Fraction Compositions (wt %) of the Top (T) Phase, Initial Mixture (M) and Bottom (B) Phase of the ABS composed of IL + K_2HPO_4 + water, and respective TLL and Tie-Line Slope (TLS).

	weight fraction composition/wt %							
IL	$[IL]_T$	$[K_2HPO_4]_T$	$[IL]_M$	$[K_2HPO_4]_M$	$[IL]_B$	$[K_2HPO_4]_B$	**TLS**	**TLL**
[Ch][C_1CO_2]	36.28	16.01	30.24	21.11	14.12	34.70	-1.53	28.99
	37.72	15.10	30.22	21.90	8.87	41.24	-1.33	38.93
	41.47	12.92	30.13	23.04	7.58	43.17	-1.26	45.42
	41.57	12.86	30.10	23.82	4.96	47.86	-1.20	50.65
[Ch][C_2CO_2]	37.91	11.60	29.59	19.84	4.25	44.95	-1.35	47.38
	41.35	9.77	30.17	20.97	2.94	48.23	-1.31	54.36
	43.17	8.91	30.15	22.05	2.32	50.17	-1.31	58.07
	43.38	8.81	29.87	22.98	1.70	52.51	-1.36	60.39
	47.06	7.25	30.90	23.56	1.56	53.17	-1.34	64.65
[Ch][C_3CO_2]	37.73	9.68	30.16	17.01	4.15	42.25	-1.39	46.78
	37.96	9.57	30.07	18.17	1.88	48.91	-1.40	53.38
	39.97	8.64	30.14	20.02	0.93	53.81	-1.39	59.70
	41.75	7.90	30.06	21.18	0.85	54.39	-1.34	61.92
[Ch][C_4CO_2]	32.00	13.64	25.10	20.04	4.98	38.73	-1.51	36.88
	34.39	12.35	25.09	21.00	4.05	40.58	-1.51	41.44
	35.04	12.02	25.14	21.95	2.43	44.69	-1.49	46.17
	36.70	11.21	25.30	23.09	1.56	47.83	-1.54	50.75
	38.00	10.61	25.23	24.96	0.74	52.46	-1.42	56.03
[Ch][C_5CO_2]	34.41	13.57	25.26	21.99	3.65	41.89	-1.60	41.81
	36.09	12.68	25.03	23.06	2.81	43.90	-1.58	45.63
	38.05	11.71	25.15	23.90	2.23	45.58	-1.60	49.31
	40.41	10.61	25.25	24.97	1.75	47.23	-1.53	53.26
	43.16	9.44	25.19	26.09	1.56	47.98	-1.62	56.70
[Ch][C_6CO_2]	42.44	12.37	29.19	22.14	4.73	40.18	-1.53	46.85
	46.92	10.34	30.05	23.07	2.99	43.47	-1.54	55.02
	48.63	9.63	30.05	23.83	2.36	45.02	-1.55	58.25
	50.64	8.83	30.34	24.91	1.50	47.75	-1.47	62.69
[Ch][C_7CO_2]	43.99	13.13	30.20	22.88	4.37	41.14	-1.71	48.52
	46.97	11.73	30.06	23.79	3.43	42.80	-1.71	53.48
	49.36	10.66	30.08	24.91	2.24	45.48	-1.67	58.58
	53.43	8.98	30.21	25.86	1.91	46.42	-1.65	63.69

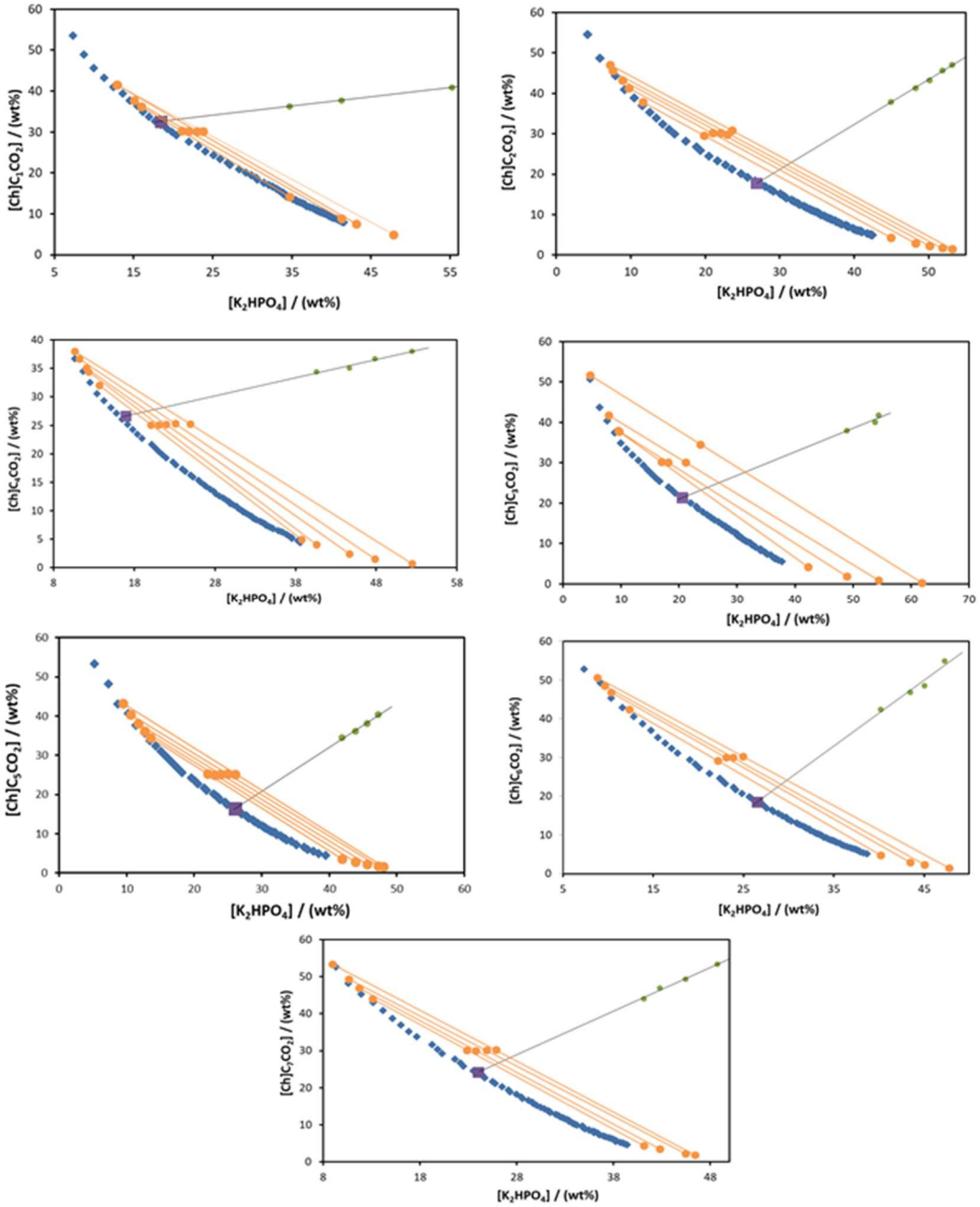

Figure A1. Phase diagrams comprising the respective TLs data required for the determination of the critical point of each ABS.

Table A10. Critical Point of each ABS composed of IL + K_2HPO_4 + H_2O determined by Equation $[IL] = f[salt] + g$ and respective correlation coefficient (R^2).

		critical point/wt %		
IL	R^2	**[IL]**	**[K_2HPO_4]**	**[H_2O]**
[Ch][C_1CO_2]	0.9999	32.60	18.49	48.91
[Ch][C_2CO_2]	0.9957	17.86	26.9	55.24
[Ch][C_3CO_2]	0.9995	21.33	20.56	58.02
[Ch][C_4CO_2]	0.9637	26.62	16.92	56.46
[Ch][C_5CO_2]	0.9851	16.37	26.04	57.59
[Ch][C_6CO_2]	0.9525	18.58	26.53	54.89
[Ch][C_7CO_2]	0.9879	24.18	24.01	51.81

Table A11. Salting-out coefficients (k_s) of each ABS formed by IL + K_2HPO_4 + H_2O at 298 K and correlation coefficient (R^2) of the fitting by the following Eq.:

$$ln\frac{[\mathrm{IL}]_\mathrm{T}}{[\mathrm{IL}]_\mathrm{B}} = k_{IL}([\mathrm{IL}]_\mathrm{B} - ([\mathrm{IL}]_\mathrm{T}) + k_s([\mathrm{Salt}]_\mathrm{B} - [\mathrm{Salt}]_\mathrm{T}) \quad \text{(A1)}$$

IL	k_s **/(kg.mol^{-1})**	k_{IL} **([IL]$_B$ - [IL]$_T$)**	R^2
[Ch][C_1CO_2]	0.5085	0.2695	0.9994
[Ch][C_2CO_2]	0.6002	0.3193	0.9983
[Ch][C_3CO_2]	0.6431	0.3224	0.9999
[Ch][C_4CO_2]	0.7691	0.1120	0.9997
[Ch][C_5CO_2]	0.8292	-0.0313	1.0000
[Ch][C_6CO_2]	0.9205	-0.1016	0.9999
[Ch][C_7CO_2]	0.952	-0.1477	0.9995

The CMC of [Ch][C_6CO_2] was determined by electrical conductivity using a SevenMulti® conductivimeter (Mettler Toledo Instruments) at (298 ± 1) K, with an uncertainty of ± 0.01 mS cm^{-1}. The conductivity meter was calibrated with standard solutions of KCl with known conductivity values (84 µS cm^{-1}, 1413 cm^{-1} and 12.88 mS cm^{-1}). The conductivity measurements were carried out by continuous dilution of a concentrated solution of IL. After each addition of the IL solution, the solution was stirred and equilibrated for 10 min, and then three successive measurements of conductivity were performed. Figure S2 shows the conductivity values as a function of the IL concentration used in the CMC determination.

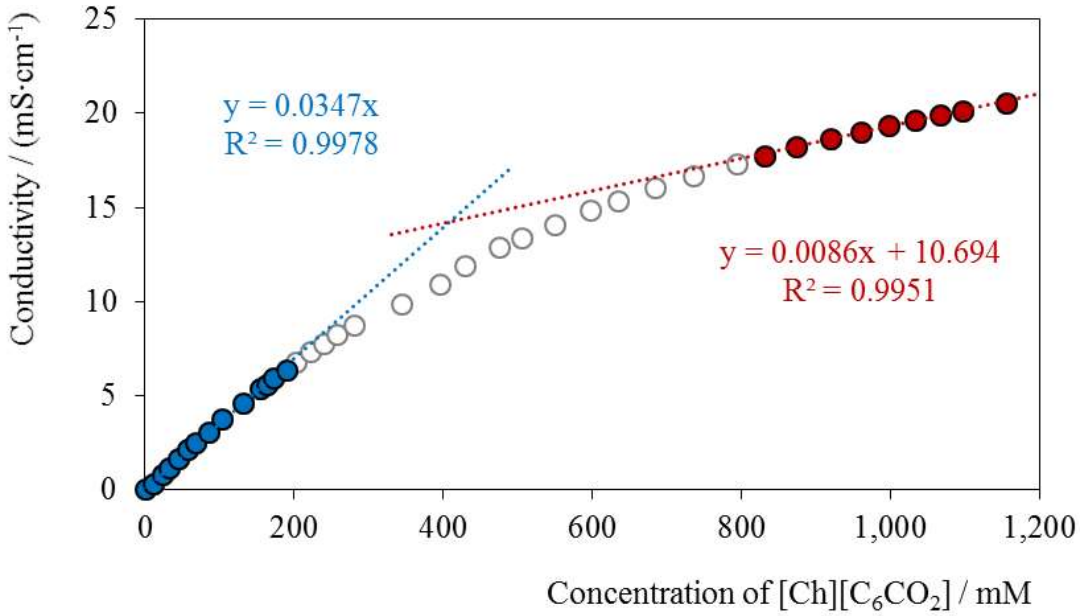

Figure A2. Conductivity as a function of the IL concentration to determine the CMC of [Ch][C_6CO_2] at 298 K.

The extraction efficiency (*EE*%), which corresponds to the percentage ratio between the weight of each amino acid in the IL-rich phase to that in the total mixture, was determined according to the following Eq.:

$$EE\% = \frac{w_{AA}^{IL}}{w_{AA}^{IL}+w_{AA}^{Salt}} \times 100 \qquad \text{(A2)}$$

where w_{AA}^{IL} and w_{AA}^{Salt} are the total weight of each amino acid in the IL-rich and in the salt-rich aqueous phases.

Table A12. Extraction efficiencies (*EE*%) of the studied ABS for L-tryptophan, L-phenylalanine, L-tyrosine, and L-dopa, and respective standard deviation (σ), at 298 K, and pH pf the coexisting phases.

IL	$EE\%_{TRP} \pm \sigma$	$EE\%_{L\text{-}PHE} \pm \sigma$	$EE\%_{TYR} \pm \sigma$	$EE\%_{L\text{-}DOPA} \pm \sigma$	pH	
					IL-rich phase	K_2HPO_4-rich
[Ch][C_1CO_2]	99.93 ± 0.10	99.04 ± 0.05	96.93 ± 0.25	95.82 ± 1.07	10.52 ± 0.03	9.08 ± 0.57
[Ch][C_2CO_2]	99.16 ± 0.02	98.49 ± 0.05	93.92 ± 0.23	83.19 ± 0.91	8.93 ± 0.01	8.27 ± 0.28
[Ch][C_3CO_2]	99.14 ± 0.02	98.56 ± 0.03	96.95 ± 0.44	95.00 ± 0.92	10.34 ± 0.04	9.22 ± 0.38
[Ch][C_4CO_2]	98.34 ± 0.06	96.81 ± 0.07	87.54 ± 0.19	71.32 ± 0.79	9.42 ± 0.02	9.11 ± 0.14
[Ch][C_5CO_2]	98.32 ± 0.05	96.64 ± 0.18	86.00 ± 0.98	66.79 ± 2.00	9.59 ± 0.09	9.41 ± 0.12
[Ch][C_6CO_2]	98.47 ± 0.45	97.34 ± 0.11	89.86 ± 0.01	72.87 ± 0.58	9.04 ± 0.04	8.41 ± 0.24
[Ch][C_7CO_2]	98.20 ± 0.32	96.98 ± 0.05	83.13 ± 0.49	69.14 ± 1.87	9.59 ± 0.16	8.97 ± 0.29

Table A13. Partition coefficients (K_{AA}) of the studied ABS for L-tryptophan (TRP), L-phenylalanine (L-PHE), L-tyrosine (TYR), and L-dopa, and respective standard deviation (σ), at 298 K.

IL	$K_{TRP} \pm \sigma$	$K_{L\text{-}PHE} \pm \sigma$	$K_{TYR} \pm \sigma$	$K_{L\text{-}DOPA} \pm \sigma$
[Ch][C_1CO_2]	Complete extraction	78.25 ± 2.47	19.86 ± 0.86	12.76 ± 0.53
[Ch][C_2CO_2]	56.81 ± 3.29	30.38 ± 0.71	7.82 ± 0.06	2.37 ± 0.12
[Ch][C_3CO_2]	54.04 ± 0.22	32.64 ± 1.09	14.17 ± 2.79	7.12 ± 1.04
[Ch][C_4CO_2]	51.35 ± 1.32	26.25 ± 0.87	5.74 ± 0.27	2.08 ± 0.07
[Ch][C_5CO_2]	55.12 ± 3.79	28.00 ± 1.05	10.28 ± 0.85	1.97 ± 0.03
[Ch][C_6CO_2]	46.05 ± 2.18	27.05 ± 1.35	6.46 ± 0.10	1.88 ± 0.09
[Ch][C_7CO_2]	49.49 ± 3.24	27.62 ± 0.70	4.29 ± 0.88	2.14 ± 0.08

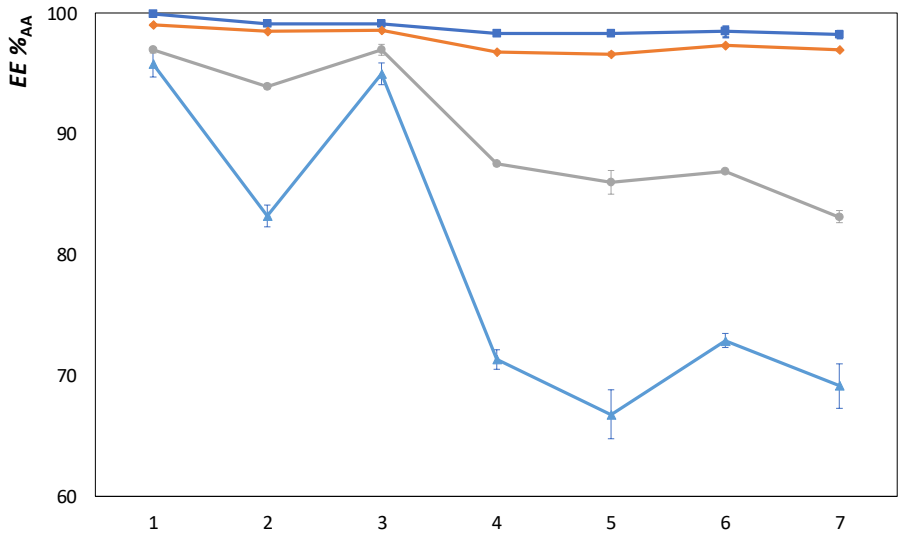

Figure A3. Extraction efficiencies (*EE*%) of the studied ABS at 25°C for L-tryptophan (■), L-phenylalanine (◆), L-tyrosine (●), and L-dopa (▲).

Appendix B

Performance of tetraalkylammonium-based ionic liquids as constituents of aqueous biphasic systems in the extraction of ovalbumin and lysozyme – CHAPTER 3

Table B1. Experimental weight fraction data for the binodal curves of the ABS formed by $[N_{4444}]Br$ (1) + K_2HPO_4/KH_2PO_4 (2) at (25±1) ˚C and pH 7.

w_1	w_2	w_1	w_2	w_1	w_2
57.61	0.66	26.02	8.44	18.65	12.04
56.69	1.27	25.58	8.29	18.48	12.28
50.73	1.14	25.29	8.63	18.33	12.18
49.63	1.96	25.15	8.59	18.01	12.64
46.55	1.84	24.88	8.92	17.84	12.52
45.76	2.46	24.59	8.82	17.57	12.92
43.10	2.32	24.35	9.12	17.38	12.78
42.32	2.98	24.22	9.07	17.10	13.20
40.66	2.86	23.94	9.42	16.85	13.01
40.08	3.38	23.67	9.31	16.55	13.48
38.64	3.25	23.39	9.66	16.41	13.37
38.10	3.75	23.16	9.57	16.18	13.73
37.10	3.65	22.92	9.87	15.94	13.53
36.45	4.27	22.65	9.76	15.73	13.86
35.42	4.15	22.41	10.08	15.53	13.68
34.67	4.88	22.31	10.04	15.35	13.99
34.18	4.81	22.10	10.31	15.28	13.93
33.80	5.19	21.87	10.19	15.22	14.04
33.33	5.12	21.67	10.46	15.10	13.93
32.90	5.55	21.56	10.40	14.92	14.23
32.06	5.41	21.33	10.71	14.78	14.10
31.66	5.82	21.21	10.65	14.70	14.24
31.18	5.74	20.98	10.97	14.60	14.14
30.28	6.70	20.75	10.85	14.50	14.32
29.94	6.62	20.53	11.14	14.39	14.22
29.75	6.83	20.43	11.08	14.21	14.53
29.57	6.79	20.26	11.32	14.06	14.39
29.24	7.16	20.10	11.24	13.98	14.54
28.82	7.05	19.92	11.49	13.89	14.45
28.73	7.16	19.74	11.39	13.79	14.61
28.52	7.11	19.58	11.63	13.75	14.56
28.13	7.54	19.52	11.59	13.65	14.73
27.88	7.47	19.37	11.81	13.56	14.63
27.46	7.95	19.22	11.72	13.37	14.97
27.03	7.82	19.06	11.94	13.20	14.78
26.70	8.20	18.94	11.87		
26.32	8.08	18.77	12.12		

Table B2. Experimental weight fraction data for the binodal curves of the ABS formed by $[N_{4444}]Cl$ (1) + K_2HPO_4/KH_2PO_4 (2), at (25±1) ˚C and pH 7.

w_1	w_2	w_1	w_2
41.64	2.16	19.73	10.70
40.93	2.79	19.56	10.61
39.36	2.68	19.19	11.13
38.68	3.31	18.85	10.93
37.26	3.19	18.23	11.85
36.65	3.77	18.03	11.71
35.43	3.65	17.72	12.17
34.83	4.25	17.57	12.06
33.67	4.11	17.30	12.46
33.21	4.58	17.11	12.32
32.30	4.46	16.61	13.10
31.78	5.01	16.48	13.00
31.28	4.93	16.23	13.39
30.82	5.43	16.11	13.29
30.31	5.34	16.07	13.35
29.89	5.79	15.91	13.22
29.05	5.63	15.21	14.36
28.67	6.07	15.11	14.26
27.83	5.89	14.89	14.62
27.26	6.57	14.80	14.53
26.88	6.48	14.63	14.81
26.25	7.25	14.53	14.70
25.58	7.07	14.27	15.12
24.97	7.82	14.22	15.06
24.35	7.63	13.99	15.44
23.81	8.32	13.91	15.36
23.51	8.21	13.64	15.81
23.00	8.87	13.55	15.71
22.77	8.78	13.30	16.14
22.17	9.58	13.21	16.03
21.53	9.31	12.88	16.60
21.41	9.48	12.71	16.39
21.25	9.41	12.34	17.04
20.97	9.81	12.26	16.94
20.75	9.71	11.90	17.59
20.33	10.29	11.83	17.48
20.10	10.17		

Table B3. Experimental weight fraction data for the binodal curves of the ABS formed by $[N_{444(C7H7)}]Cl$ (1) + K_2HPO_4/KH_2PO_4 (2), at (25±1) ˚C and pH 7.

w_1	w_2	w_1	w_2	w_1	w_2
57.64	0.69	27.04	8.07	18.64	12.70
56.69	1.32	26.77	7.99	18.10	13.47
53.05	1.24	26.45	8.36	17.97	13.37
51.90	2.05	26.16	8.27	17.72	13.74
47.07	1.86	25.88	8.60	17.59	13.64
46.40	2.39	25.58	8.50	17.30	14.06
44.65	2.30	25.30	8.83	17.19	13.97
43.91	2.91	25.05	8.75	16.91	14.38
42.30	2.80	24.78	9.07	16.79	14.28
41.49	3.49	24.52	8.98	16.53	14.66
39.48	3.32	24.28	9.27	16.42	14.56
38.89	3.86	24.03	9.18	16.22	14.84
37.75	3.74	23.62	9.69	16.12	14.75
37.27	4.19	23.39	9.60	15.86	15.13
36.67	4.13	23.12	9.94	15.77	15.03
36.09	4.68	22.91	9.85	15.54	15.37
35.11	4.55	22.68	10.15	15.46	15.29
34.43	5.22	22.49	10.07	15.30	15.54
33.43	5.07	22.05	10.63	15.25	15.49
32.92	5.60	21.86	10.54	15.03	15.83
32.44	5.52	21.66	10.81	14.95	15.75
31.99	5.98	21.46	10.71	14.85	15.91
31.52	5.89	21.04	11.27	14.76	15.81
31.09	6.35	20.87	11.18	14.45	16.29
30.33	6.20	20.66	11.45	14.39	16.22
29.96	6.60	20.48	11.35	14.19	16.54
29.61	6.52	20.10	11.86	14.10	16.43
29.31	6.85	19.95	11.76	13.93	16.69
28.95	6.77	19.77	12.00	13.86	16.60
28.33	7.46	19.61	11.90	13.60	17.01
28.03	7.38	19.23	12.42	13.52	16.91
27.70	7.76	19.09	12.32		
27.39	7.67	18.76	12.78		

Table B4. Experimental weight fraction data for the binodal curves of the ABS formed by $[N_{1118}]Br$ (1) + K_2HPO_4/KH_2PO_4 (2), at (25±1) ˚C and pH 7.

w_1	w_2	w_1	w_2
45.17	5.76	20.94	18.19
44.34	5.66	20.75	18.03
43.09	6.60	20.02	18.76
42.33	6.49	19.85	18.60
41.60	7.04	18.95	19.52
40.81	6.91	18.79	19.35
39.43	7.99	18.19	19.97
38.72	7.85	18.04	19.80
37.56	8.78	16.13	21.82
36.99	8.64	16.00	21.64
35.85	9.57	15.20	22.51
35.32	9.43	15.13	22.41
34.27	10.31	14.67	22.91
33.75	10.15	14.57	22.74
32.54	11.18	13.89	23.49
32.12	11.03	13.79	23.32
31.24	11.79	13.06	24.16
30.82	11.63	12.97	24.00
29.19	13.06	12.40	24.65
28.96	12.96	12.33	24.50
28.43	13.44	11.68	25.26
28.05	13.27	11.61	25.10
26.98	14.24	10.93	25.91
26.62	14.06	10.87	25.76
24.60	15.94	9.84	26.99
24.31	15.75	9.79	26.87
23.31	16.70	9.18	27.62
23.05	16.51	9.14	27.50
22.18	17.36	8.08	28.82
21.96	17.18	8.05	28.70

Table B5. Experimental weight fraction data for the binodal curves of the ABS formed by $[N_{111(C7H7)}]Cl$ (1) + K_2HPO_4/KH_2PO_4 (2), at (25±1) ˚C and pH 7.

w_1	w_2	w_1	w_2
55.90	1.47	36.20	7.28
54.39	2.48	35.69	7.17
51.52	2.35	34.25	8.45
50.23	3.26	33.41	8.24
48.17	3.13	31.50	10.00
47.00	3.99	31.13	9.88
44.64	3.79	30.20	10.75
43.67	4.56	29.85	10.62
43.00	4.49	28.45	11.95
42.05	5.24	28.12	11.81
40.71	5.08	26.87	13.02
39.85	5.79	26.59	12.88
39.24	5.70	24.67	14.76
38.55	6.29	24.49	14.65
37.99	6.20	21.63	17.49
37.24	6.84	21.42	17.32
36.79	6.76		

Table B6. Experimental weight fraction data for the binodal curves of the ABS formed by $[N_{222(C7H7)}]Cl$ (1) + K_2HPO_4/KH_2PO_4 (2), at (25±1) ˚C and pH 7.

w_1	w_2	w_1	w_2
53.15	0.89	26.37	10.51
50.76	2.59	25.51	11.44
46.34	2.37	25.24	11.32
45.41	3.10	24.45	12.18
43.06	2.94	24.21	12.06
41.69	4.09	23.50	12.85
40.34	3.95	23.27	12.73
39.65	4.55	22.28	13.84
39.03	4.48	22.06	13.70
38.39	5.04	21.07	14.83
37.26	4.89	20.90	14.70
36.64	5.45	19.92	15.84
36.05	5.36	19.78	15.73
35.52	5.86	18.93	16.73
35.00	5.77	18.87	16.68
34.45	6.30	17.60	18.17
33.98	6.21	17.54	18.10
32.94	7.21	16.73	19.07
32.46	7.10	16.61	18.94
31.99	7.55	15.49	20.29
31.56	7.45	15.39	20.16
30.69	8.32	14.04	21.80
30.30	8.21	13.96	21.67
29.93	8.58	12.97	22.89
29.58	8.48	12.90	22.76
28.72	9.36	11.66	24.31
28.38	9.25	11.61	24.21
27.67	9.99	10.54	25.56
27.35	9.87	10.51	25.47
26.65	10.62		

Table B7. Experimental weight fraction data for the binodal curves of the ABS formed by $[N_{222(C7H7)}]Cl$ (1) + K_2HPO_4/KH_2PO_4 (2), at (25±1) ˚C and pH 8.

w_1	w_2	w_1	w_2
67.52	4.67	20.48	14.53
39.36	4.66	20.10	14.75
37.49	5.23	19.50	15.31
35.81	5.87	19.20	15.41
34.19	6.43	18.67	15.92
32.87	6.97	18.23	16.29
31.98	7.55	17.80	16.65
30.69	7.97	17.37	17.10
29.84	8.44	17.08	17.27
28.98	8.95	16.75	17.52
28.20	9.48	16.36	17.89
27.44	9.88	15.96	18.25
26.68	10.27	15.58	18.62
26.03	10.66	15.23	18.97
25.38	11.01	14.89	19.28
24.81	11.40	14.70	19.40
24.22	11.80	14.39	19.71
23.67	12.16	14.08	19.99
23.16	12.50	13.79	20.25
22.67	12.79	13.52	20.48
22.24	13.08	13.25	20.79
21.60	13.66	13.00	21.01
21.19	13.88	12.78	21.18

Table B8. Experimental weight fraction data for the binodal curves of the ABS formed by $[N_{222(C7H7)}]Cl$ (1) + K_2HPO_4/KH_2PO_4 (2), at (25±1) ˚C and pH 9.

w_1	w_2	w_1	w_2
47.23	2.62	18.03	16.68
43.46	3.48	17.73	16.84
40.34	4.21	17.45	17.00
38.03	5.15	17.06	17.43
35.57	5.82	16.80	17.58
33.99	6.55	16.52	17.78
32.48	7.15	16.27	17.94
31.15	7.65	16.03	18.14
30.39	8.11	15.67	18.63
29.21	8.54	15.40	18.71
28.50	9.04	15.17	18.89
27.78	9.48	14.95	19.08
26.80	9.75	14.62	19.54
26.21	10.19	14.37	19.61
25.63	10.52	14.20	19.77
24.98	11.11	14.00	19.92
24.48	11.51	13.81	20.04
23.92	11.92	13.43	20.69
23.10	12.83	13.15	20.68
22.67	13.07	12.90	21.01
22.23	13.34	12.73	21.13
21.84	13.58	12.56	21.24
21.43	13.91	12.40	21.34
21.03	14.23	12.17	21.69
20.62	14.49	12.00	21.73
19.90	15.09	11.88	21.87
19.45	15.54	11.74	21.97
19.13	15.70	11.54	22.28
18.80	15.91	11.41	22.35
18.35	16.44	11.29	22.45

Table B9. Experimental weight fraction data for the binodal curves of the ABS formed by $[N_{222(C7H7)}]Cl$ (1) + K_2HPO_4/KH_2PO_4 (2), at (25±1) ˚C and pH 13.

w_1	w_2	w_1	w_2
68.94	1.08	20.41	12.83
61.89	1.68	20.06	12.96
47.36	2.39	19.57	13.30
43.72	3.02	19.05	13.67
41.27	3.62	18.57	13.98
39.03	4.13	18.14	14.34
37.37	4.60	17.87	14.45
35.25	5.60	17.44	14.74
33.69	6.16	17.02	15.08
32.70	6.57	16.78	15.17
31.79	6.94	16.39	15.47
30.91	7.27	16.01	15.77
30.04	7.66	15.65	16.00
29.03	8.18	15.33	16.21
28.30	8.47	14.73	16.61
27.63	8.74	14.45	16.80
26.69	9.34	14.14	17.01
26.07	9.59	13.88	17.22
25.49	9.83	13.64	17.40
24.64	10.39	13.28	17.70
24.13	10.60	12.98	17.92
23.40	11.05	12.74	18.07
22.72	11.49	12.23	18.51
22.27	11.66	12.03	18.64
21.62	12.02	11.85	18.77
21.00	12.43	11.60	19.00

Table B10. Experimental weight fraction data for the binodal curves of the ABS formed by $[N_{2222}]Br$ (1) + K_2HPO_4/KH_2PO_4 (2), at (25±1) ˚C and pH 7.

w_1	w_2	w_1	w_2
43.55	2.77	24.16	12.90
42.73	3.46	24.00	12.82
41.47	3.35	22.90	14.01
40.81	3.92	22.66	13.86
39.93	3.84	22.05	14.53
39.09	4.58	21.85	14.40
38.39	4.50	20.82	15.55
37.71	5.10	20.76	15.51
37.11	5.02	20.22	16.12
36.68	5.41	20.08	16.01
36.17	5.33	19.19	17.02
35.63	5.84	19.12	16.96
35.03	5.74	18.32	17.87
34.17	6.55	18.22	17.78
33.61	6.44	17.65	18.44
32.87	7.16	17.58	18.37
32.63	7.11	16.70	19.40
32.22	7.51	16.58	19.26
31.97	7.46	15.65	20.37
31.53	7.90	15.58	20.28
30.98	7.76	14.89	21.10
30.19	8.55	14.84	21.03
29.96	8.48	14.12	21.90
29.33	9.12	14.02	21.74
29.18	9.07	13.26	22.67
28.53	9.74	13.18	22.54
28.16	9.61	12.51	23.38
27.50	10.30	12.47	23.32
27.29	10.22	11.75	24.22
26.59	10.96	11.72	24.16
26.43	10.89	11.25	24.75
25.84	11.52	11.19	24.60
25.56	11.39		

Table B11. Experimental weight fraction data for the binodal curves of the ABS formed by $[N_{2222}]Br$ (1) + K_2HPO_4/KH_2PO_4 (2), at (25±1) ˚C and pH 8.

w_1	w_2	w_1	w_2
67.11	1.56	22.45	14.35
46.77	2.31	21.54	14.82
43.78	3.29	20.80	15.51
41.29	3.92	20.10	16.14
38.82	4.72	19.45	16.71
36.76	5.50	18.90	17.22
34.83	6.09	17.84	18.15
33.65	6.76	17.22	18.45
32.50	7.37	16.77	18.83
30.02	9.10	16.23	19.43
29.13	9.60	15.81	19.80
28.37	10.09	15.44	20.13
27.56	10.58	14.76	20.72
26.87	11.02	14.42	20.98
26.20	11.45	13.98	21.46
25.63	11.80	13.54	21.74
24.61	12.70	13.26	21.97
23.78	13.35	12.98	22.21
23.22	13.65	12.72	22.46

Table B12. Experimental weight fraction data for the binodal curves of the ABS formed by $[N_{2222}]Br$ (1) + K_2HPO_4/KH_2PO_4 (2), at (25±1) ˚C and pH 9.

w_1	w_2	w_1	w_2
74.69	1.15	19.96	15.29
49.15	2.03	19.48	15.87
46.04	3.07	19.00	16.41
41.80	3.79	18.60	16.48
39.48	4.55	18.29	16.71
37.35	5.25	17.97	16.94
35.72	5.73	17.67	17.14
34.15	6.33	17.26	17.61
33.23	6.81	17.01	17.79
32.16	7.26	16.75	17.99
31.32	7.85	16.35	18.52
30.22	8.18	15.86	18.85
29.59	8.58	15.51	19.30
28.89	9.03	15.08	19.63
28.15	9.60	14.79	19.65
27.53	10.03	14.60	19.78
27.01	10.40	14.41	19.92
26.45	10.71	14.22	20.05
25.92	11.05	14.02	20.25
25.38	11.44	13.84	20.38
24.79	11.80	13.60	20.74
24.28	12.15	13.41	20.87
23.79	12.51	12.97	21.76
23.40	12.76	12.74	21.75
22.98	13.03	12.59	21.87
22.54	13.28	12.44	21.95
21.86	14.04	12.29	22.05
21.49	14.24	12.07	22.35
21.08	14.48	11.94	22.48
20.71	14.72	11.80	22.58
20.33	15.01		

Table B13. Experimental weight fraction data for the binodal curves of the ABS formed by $[N_{2222}]Br$ (1) + K_2HPO_4/KH_2PO_4 (2), at (25±1) ˚C and pH 13.

w_1	w_2	w_1	w_2
69.86	2.21	20.54	13.27
64.21	2.20	19.97	13.64
43.99	2.77	19.36	14.12
41.55	3.35	18.86	14.43
39.98	3.96	18.24	14.90
38.24	4.41	17.82	15.16
37.10	4.77	17.40	15.43
35.79	5.28	16.87	15.85
34.83	5.71	16.44	16.11
33.73	6.13	16.09	16.34
32.83	6.60	15.67	16.67
31.83	6.99	15.36	16.87
30.95	7.30	14.95	17.22
29.74	7.94	14.64	17.38
29.02	8.36	14.29	17.61
28.00	8.70	13.92	17.91
27.04	9.17	13.66	18.09
26.22	9.63	13.36	18.32
25.34	10.17	12.80	18.96
24.94	10.44	12.49	19.23
24.56	10.70	12.21	19.46
23.77	11.19	11.99	19.58
23.11	11.55	11.74	19.76
22.54	11.94	11.43	20.02
21.67	12.59	11.08	20.37
21.12	12.90		

Table B14. Experimental weight fraction data for the binodal curves of the ABS formed by $[N_{2222}]Cl$ (1) + K_2HPO_4/KH_2PO_4 (2), at (25±1) ˚C and pH 7.

w_1	w_2	w_1	w_2
56.85	0.92	31.42	6.10
50.07	0.81	30.98	6.55
49.01	1.61	30.55	6.46
44.44	1.46	29.70	7.37
43.27	2.44	29.32	7.27
41.72	2.36	28.52	8.13
40.97	3.02	28.22	8.05
39.61	2.92	27.41	8.93
38.86	3.60	27.07	8.82
37.63	3.48	24.93	11.20
37.00	4.08	24.39	10.96
36.40	4.01	23.47	12.01
35.83	4.56	23.01	11.78
35.31	4.49	21.76	13.25
34.82	4.97	21.56	13.12
34.28	4.89	19.55	15.52
33.81	5.36	19.38	15.38
33.31	5.28	18.09	16.95
32.78	5.81	17.79	16.67
32.30	5.72	15.96	18.96
31.86	6.18	15.73	18.69

Table B15. Experimental weight fraction data for the binodal curves of the ABS formed by $[N_{2222}]Cl$ (1) + K_2HPO_4/KH_2PO_4 (2), at (25±1) ˚C and pH 8.

w_1	w_2	w_1	w_2
56.35	2.14	19.66	15.26
40.10	3.05	19.02	15.80
37.36	4.10	18.29	16.63
34.94	5.15	17.57	17.36
32.98	5.82	17.24	17.59
30.36	7.58	16.73	18.24
28.08	9.08	15.97	19.13
25.65	10.27	15.46	19.62
24.02	11.26	14.55	20.90
22.87	12.40	12.72	23.61
21.47	13.36	11.86	24.80
20.50	14.38	11.24	25.72

Table B16. Experimental weight fraction data for the binodal curves of the ABS formed by $[N_{2222}]Cl$ (1) + K_2HPO_4/KH_2PO_4 (2), at (25±1) ˚C and pH 9.

w_1	w_2	w_1	w_2
55.06	1.93	18.00	15.75
42.11	3.47	17.57	16.09
37.04	4.10	16.84	17.15
33.39	5.37	16.22	18.03
30.08	6.34	15.67	18.55
28.29	7.33	15.07	19.30
27.32	8.08	14.63	19.82
26.24	9.05	13.68	20.75
25.20	9.97	13.17	21.14
23.88	10.70	12.79	21.74
23.03	11.44	12.34	22.22
22.28	12.16	11.88	22.67
21.51	12.92	11.44	23.08
20.50	13.74	11.04	23.51
19.66	14.18	10.70	23.79
19.10	14.67	10.40	24.13
18.55	15.20	10.19	24.10

Table B17. Experimental weight fraction data for the binodal curves of the ABS formed by $[N_{2222}]Cl$ (1) + K_2HPO_4/KH_2PO_4 (2), at (25±1) ˚C and pH 13.

w_1	w_2	w_1	w_2
56.93	1.38	19.12	13.33
50.30	2.26	18.41	13.91
40.18	3.30	17.60	14.62
36.81	3.94	16.77	15.46
34.42	4.58	15.99	16.23
32.95	5.35	15.33	16.89
29.08	6.39	14.72	17.48
27.97	6.99	14.32	17.78
26.91	7.57	13.76	18.32
25.57	8.60	13.26	18.79
24.79	8.99	12.83	19.20
23.64	9.88	12.40	19.61
22.71	10.56	11.84	20.29
21.70	11.24	11.47	20.64
20.79	11.97	11.00	21.19
19.90	12.69		

For the determination of each TL, the following system of four equations (equations (B1)– (B4)) and four unknown parameters ($[IL]_T$, $[IL]_B$, $[Salt]_T$, $[Salt]_B$) was applied:

$$[\mathrm{IL}]_\mathrm{T} = A\exp[(B \times [\mathrm{Salt}]_\mathrm{T}^{0.5}) - (C \times [\mathrm{Salt}]_\mathrm{T}^{3})] \quad \text{(B1)}$$

$$[\mathrm{IL}]_\mathrm{B} = A\exp[(B \times [\mathrm{Salt}]_\mathrm{B}^{0.5}) - (C \times [\mathrm{Salt}]_\mathrm{B}^{3})] \quad \text{(B2)}$$

$$[\mathrm{IL}]_\mathrm{T} = \frac{[\mathrm{IL}]_\mathrm{M}}{\alpha} - \frac{1-\alpha}{\alpha} \times [\mathrm{IL}]_\mathrm{B} \quad \text{(B3)}$$

$$[\mathrm{Salt}]_\mathrm{T} = \frac{[\mathrm{Salt}]_\mathrm{M}}{\alpha} - \frac{1-\alpha}{\alpha} \times [\mathrm{Salt}]_\mathrm{B} \quad \text{(B4)}$$

where the subscripts M, T and B designate, respectively, the initial mixture, the top and bottom phases. The value α is the ratio between the mass of the top phase and the total mass of the mixture experimentally determined. Each tie-line length (TLL) was determined through the application of the following equation:

$$\mathrm{TLL} = \sqrt{([\mathrm{Salt}]_\mathrm{T} - [\mathrm{Salt}]_\mathrm{B})^2 + ([\mathrm{IL}]_\mathrm{T} - [\mathrm{IL}]_\mathrm{B})^2} \quad \text{(B5)}$$

Table B18. HPLC conditions used for the identification and quantification of ovalbumin and lysozyme.

	Ovalbumin	**Lysozyme**
Eluent	50 mM sodium phosphate buffer (NaH_2PO_4/Na_2HPO_4), 0.3 M NaCl at pH 7.0	Solvent A = 100 : 38.4 (Stock solution I:Stock solution II), Solvent B = Stock solution II; Stock solution I = aq. 0.01% TFAA solution, Stock solution I = 0.01% TFAA in ACN solution
Eluting conditions	Isocratically	Gradient†
Run time	45 min	40 min
Flow rate	0.5 $mL.min^{-1}$	1.0 $mL.min^{-1}$

†expressed as proportion of solvent A: 0 − 20 min, 100%; 20 − 21 min, 100 − 50%; 21 − 22 min, 50%; 22− 23 min, 50 − 100%; 23 − 45 min, 100%

Table B19. Weight fraction compositions for the TLs and respective Tie-Line Lengths (TLLs), at the Top (T) and Bottom (B) phases, and at the initial biphasic composition of the mixture (M), composed of ILs and salts at T = (25 ± 1) °C and atmospheric pressure.

IL +	weight fraction composition/wt %							
$[KH_2PO_4/K_2HPO_4$ at pH 7]	$[IL]_T$	$[Salt]_T$	$[IL]_M$	$[Salt]_M$	$[IL]_B$	$[Salt]_B$	TLS	TLL
$[N_{111(C7H7)}]Cl$	35.16	7.90	27.99	16.13	9.86	36.97	-0.87	38.54
	39.48	6.08	31.08	16.09	6.96	44.84	-0.84	50.60
$[N_{222(C7H7)}]Cl$	35.00	6.04	29.14	11.96	2.94	38.60	-0.98	45.83
	38.80	4.82	27.81	15.42	3.04	39.29	-1.04	49.67
$[N_{2222}]Cl$	33.13	5.74	27.90	14.92	5.27	37.39	-0.88	42.09
	40.18	3.80	31.35	14.72	1.14	43.22	-0.99	52.65
$[N_{2222}]Br$	34.13	6.74	26.90	13.92	4.27	36.39	-1.01	42.09
	39.18	4.80	30.35	13.72	2.14	42.22	-0.99	52.65
$[N_{444(C7H7)}]Cl$	40.41	3.57	21.82	18.97	1.81	35.54	-1.21	50.12
	44.50	2.76	21.33	20.99	1.54	36.56	-1.27	54.67
$[N_{4444}]Cl$	28.88	5.87	23.15	11.99	1.80	34.74	-0.94	39.58
	38.27	3.36	29.13	11.62	1.89	36.25	-1.11	49.04
$[N_{4444}]Br$	38.63	3.71	30.04	9.03	2.37	26.54	-1.59	43.36
	45.93	2.17	29.67	11.74	1.49	28.33	-1.70	51.56
$[N_{1118}]Br$	51.48	3.81	33.04	15.99	3.16	35.72	-1.51	57.91
	45.21	5.60	30.15	15.96	4.19	33.85	-1.45	49.81

Table B20. Adjusted parameters and respective standard deviations obtained from the regression of equation (1) at (25 ± 1) °C and different pH values.

IL	pH	$A \pm \sigma$	$B \pm \sigma$	$10^5 (C \pm \sigma)$
$[N_{111(C7H7)}]Cl$	pH7	90.02 ± 5.39	-0.334 ± 0.02	0.35 ± 0.62
$[N_{222(C7H7)}]Cl$		80.53 ± 1.74	-0.337 ± 0.008	1.97 ± 0.22
$[N_{2222}]Cl$		70.11 ± 2.94	-0.317 ± 0.021	1.17 ± 1.64
$[N_{2222}]Br$		73.88 ± 0.91	-0.298 ± 0.004	2.49 ± 0.14
$[N_{444(C7H7)}]Cl$		88.70 ± 1.33	-0.415 ± 0.001	3.15 ± 0.42
$[N_{4444}]Cl$		79.40 ± 2.41	-0.414 ± 0.013	3.20 ± 0.88
$[N_{4444}]Br$		77.76 ± 1.83	-0.360 ± 0.012	10.2 ± 1.23
$[N_{1118}]Br$		93.37 ± 2.63	-0.304 ± 0.009	3.44 ± 1.79
$[N_{222(C7H7)}]Cl$	pH8	81.97 ± 1.20	-0.340 ± 0.005	2.99 ± 0.13
$[N_{2222}]Cl$		73.43 ± 3.16	-0.324 ± 0.015	1.43 ± 0.34
$[N_{2222}]Br$		71.27 ± 1.39	-0.280 ± 0.007	3.38 ± 0.20
$[N_{222(C7H7)}]Cl$	pH9	79.26 ± 2.05	-0.329 ± 0.009	3.27 ± 0.24
$[N_{2222}]Cl$		64.35 ± 3.30	-0.292 ± 0.017	2.59 ± 0.36
$[N_{2222}]Br$		76.51 ± 1.23	-0.313 ± 0.005	3.26 ± 0.16
$[N_{222(C7H7)}]Cl$	pH13	78.60 ± 0.87	-0.337 ± 0.004	6.50 ± 0.20
$[N_{2222}]Cl$		73.67 ± 3.03	-0.354 ± 0.016	2.62 ± 0.54
$[N_{2222}]Br$		75.88 ± 0.87	-0.323 ± 0.004	5.54 ± 0.18

Table B21. Extraction efficiencies (*EE*%) and recovery yields (*RY*%) of ovalbumin and lysozyme at pH 7 and respective mixture compositions.

Ionic liquid	weight fraction percentage / wt %		EE_{Ova}%	RY_{Ova}%	EE_{Lys}%	RY_{Lys}%
	$[IL]_M$	$[Salt]_M$				
$[N_{111(C7H7)}]Cl$	31.08	16.09	100.0 ± 0.2	77.3 ± 1.1	100.0 ± 0.2	100.0 ± 0.2
$[N_{222(C7H7)}]Cl$	27.81	15.42	100.0 ± 0.2	58.8 ± 0.9	100.0 ± 0.2	100.0 ± 0.2
$[N_{2222}]Cl$	31.35	14.72	100.0 ± 0.2	100.0 ± 0.2	100.0 ± 0.2	100.0 ± 0.2
$[N_{2222}]Br$	30.35	13.72	100.0 ± 0.2	100.0 ± 0.2	100.0 ± 0.2	100.0 ± 0.2
$[N_{444(C7H7)}]Cl$	21.33	20.99	100.0 ± 0.2	33.3 ± 1.8	100.0 ± 0.2	100.0 ± 0.2
$[N_{4444}]Cl$	29.13	11.62	100.0 ± 0.2	56.7 ± 1.7	100.0 ± 0.2	100.0 ± 0.2
$[N_{4444}]Br$	29.67	11.74	100.0 ± 0.2	42.6 ± 2.3	100.0 ± 0.2	100.0 ± 0.2
$[N_{1118}]Br$	30.15	15.96	100.0 ± 0.2	36.0 ± 1.6	100.0 ± 0.2	100.0 ± 0.2

Table B22. Extraction efficiencies (*EE*%) and recovery yields (*RY*%) of lysozyme at different pH values and respective mixture compositions.

Ionic liquid	pH	weight fraction percentage / wt %		EE_{Lys}%	RY_{Lys}%
		$[IL]_M$	$[Salt]_M$		
$[N_{222(C7H7)}]Cl$	pH7	27.81	15.42	100.0 ± 0.2	100.0 ± 0.2
$[N_{2222}]Cl$		31.35	14.72	100.0 ± 0.2	100.0 ± 0.2
$[N_{2222}]Br$		30.35	13.72	100.0 ± 0.2	100.0 ± 0.2
$[N_{222(C7H7)}]Cl$	pH8	27.81	15.42	100.0 ± 0.2	100.0 ± 0.2
$[N_{2222}]Cl$		31.35	14.72	100.0 ± 0.2	100.0 ± 0.2
$[N_{2222}]Br$		30.35	13.72	100.0 ± 0.2	100.0 ± 0.2
$[N_{222(C7H7)}]Cl$	pH9	27.81	15.42	100.0 ± 0.2	100.0 ± 0.2
$[N_{2222}]Cl$		31.35	14.72	100.0 ± 0.2	100.0 ± 0.2
$[N_{2222}]Br$		30.35	13.72	100.0 ± 0.2	100.0 ± 0.2
$[N_{222(C7H7)}]Cl$	pH13	27.81	15.42	100.0 ± 0.2	36.7 ± 1.5
$[N_{2222}]Cl$		31.35	14.72	100.0 ± 0.2	78.8 ± 0.4
$[N_{2222}]Br$		30.35	13.72	100.0 ± 0.2	30.9 ± 1.9

Table B23. Percentage recovery yield (*RY*%) of Lysozyme after the purification and precipitation steps the ABS composed of ILs + K_2HPO_4/KH_2PO_4 + H_2O at pH 7 and 8.

IL-rich phase	RY_{Lys}%
$[N_{222(C7H7)}]Cl$ pH7	80.76 ± 2.25
$[N_{2222}]Cl$ pH7	99.04 ± 2.98
$[N_{2222}]Br$ pH7	93.45 ± 3.45
$[N_{222(C7H7)}]Cl$ pH8	81.02 ± 1.67
$[N_{2222}]Cl$ pH8	99.32 ± 2.72
$[N_{2222}]Br$ pH8	96.68 ± 2.05

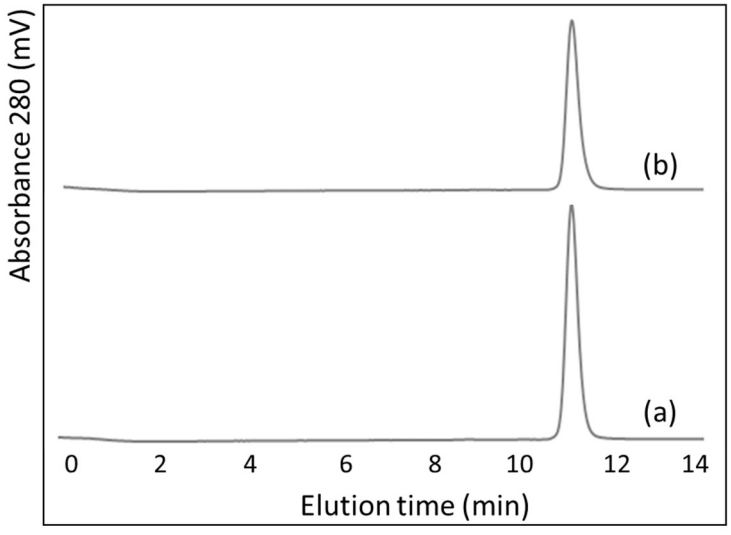

Figure B1. Size exclusion chromatograms of (a) lysozyme solution in PBS and (b) recovered lysozyme from the IL-rich phase of the ABS composed of $[N_{2222}]Cl$ + K_2HPO_4/KH_2PO_4 + H_2O at pH 8.

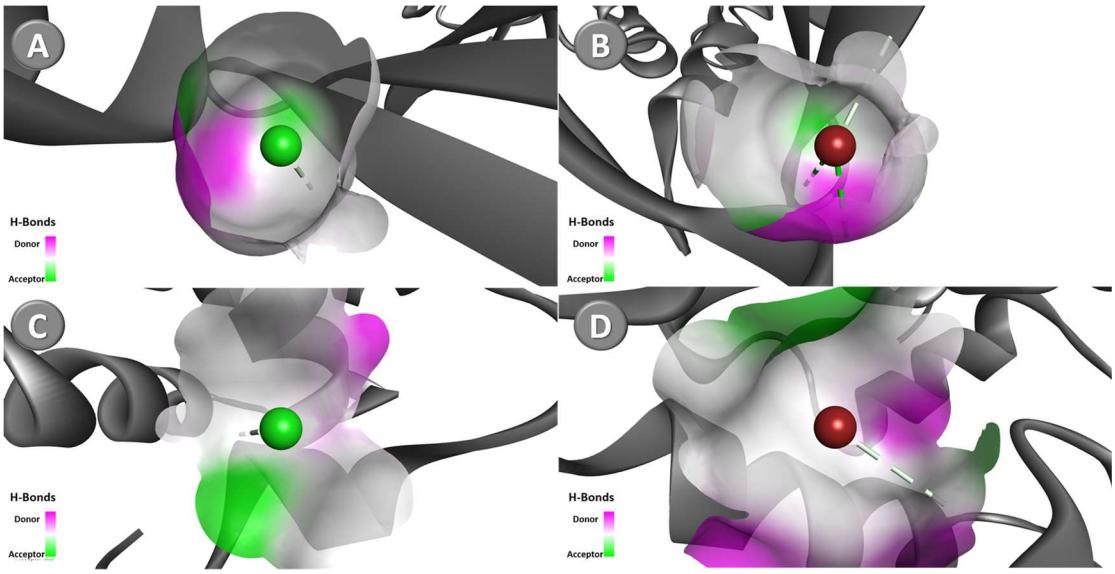

Figure B2. Docking pose with the lowest absolute value of affinity for ovalbumin: (A) Cl^- and (B) Br^-; and lysozyme with: (C) Cl^- and (D) Br^-.

Table B24. Docking affinity energy and interacting amino acids residues predicted by AutoDock vinna for Ovalbumin-IL ions.

IL ion	Affinity (kcal/mol)	Interacting nucleic acids	Type of interaction	From	To	Distance (Å)
$[N_{111(C7H7)}]^+$	-3.8	ARG290	Hydrophobic	$[N_{111(C7H7)}]^+$	ARG290	4.49
$[N_{2222}]^+$	-2.9	GLU27	Electrostatic	$[N_{2222}]^+$	GLU27	4.94
$[N_{222(C7H7)}]^+$	-4.4	VAL333	Hydrophobic	$[N_{222(C7H7)}]^+$	VAL333	3.95
$[N_{4444}]^+$	-3.6	ARG29	Hydrogen Bond	$[N_{4444}]^+$	ARG29	3.53
$[N_{444(C7H7)}]^+$	-3.6	LYS199	Hydrophobic	$[N_{444(C7H7)}]^+$	LYS199	3.61
		VAL347			VAL347	5.31
$[N_{1118}]^+$	-3.2	GLU122	Electrostatic	$[N_{1118}]^+$	GLU122	5.50
		ALA149	Hydrophobic	ALA149	$[N_{1118}]^+$	4.00
Cl^-	-1.2	PRO243	Hydrogen Bond	PRO243	Cl^-	2.72
Br^-	-1.3	GLU195	Hydrogen Bond	GLU195	Br^-	3.81
		LYS196		LYS196		3.00
		LEU242		LEU242		3.75

Table B25. Docking affinity energy and interacting amino acids residues predicted by AutoDock vinna for Lysozyme-IL ions.

IL ion	Affinity (kcal/mol)	Interacting nucleic acids	Type of interaction	From	To	Distance (Å)
$[N_{111(C7H7)}]^+$	-4.3	ALA107	Hydrogen Bond	$[N_{111(C7H7)}]^+$	ALA107	3.57
		TRP108	Hydrophobic	TRP108	$[N_{111(C7H7)}]^+$	4.93
		ILE98		$[N_{111(C7H7)}]^+$	ILE98	5.16
		ALA107			ALA107	4.36
$[N_{2222}]^+$	-2.7	ASP52	Electrostatic	$[N_{2222}]^+$	ASP52	3.88
		ASP46	Hydrogen Bond		ASP46	3.66
		ASP52			ASP52	3.31
						3.75
$[N_{222(C7H7)}]^+$	-3.8	ASP101	Electrostatic	$[N_{222(C7H7)}]^+$	ASP101	5.33
				ASP101	$[N_{222(C7H7)}]^+$	4.51
		TRP62	Hydrophobic	TRP62		4.02
						3.72
$[N_{4444}]^+$	-3.1	TRP123	Electrostatic	$[N_{4444}]^+$	TRP123	4.92
			Hydrophobic			3.79
$[N_{444(C7H7)}]^+$	-3.6	GLU7	Electrostatic	$[N_{444(C7H7)}]^+$	GLU7	5.12
				GLU7	$[N_{444(C7H7)}]^+$	4.00
		ALA10	Hydrophobic	$[N_{444(C7H7)}]^+$	ALA10	5.43
		ALA11			ALA11	4.84
$[N_{1118}]^+$	-2.8	CYS76	Hydrogen Bond	$[N_{1118}]^+$	CYS76	3.55
						3.47
		LYS96	Hydrophobic		LYS96	4.67
Cl^-	-0.8	TRP123	Hydrogen Bond	TRP123	Cl^-	3.17
Br^-	-1.0	ILE58	Hydrogen Bond	GLU195	Br^-	3.89

Appendix C

Separation of ovalbumin and lysozyme using aqueous biphasic systems and the effect of using ionic liquids as adjuvants – CHAPTER 4

Table C1. Experimental weight fraction data for the ternary systems composed of PEG 400 (w_1) + KH_2PO_4/K_2HPO_4 (w_2) at pH 7 at (25 ± 1) °C.

PEG 400			
100 w_1	**100 w_2**	**100 w_1**	**100 w_2**
85.87	1.01	26.50	9.35
63.93	1.77	25.85	9.65
51.93	2.25	24.66	10.64
47.55	2.82	23.66	10.86
45.68	3.43	22.85	11.48
43.02	3.95	21.76	11.95
40.83	4.50	21.04	12.48
38.61	4.87	20.15	13.26
36.83	5.17	19.50	13.75
35.77	5.61	18.96	14.16
34.69	6.02	18.30	14.47
33.17	6.47	17.78	14.86
32.35	6.86	17.29	15.20
31.56	7.15	16.91	15.39
30.74	7.43	16.46	15.70
29.85	7.75	16.04	16.01
29.05	8.05	15.84	16.03
28.17	8.55	15.47	16.31
27.46	8.80	15.12	16.56

Table C2. Experimental weight fraction data for the ternary systems composed of PEG 1000 (w_1) + KH_2PO_4/K_2HPO_4 (w_2) at pH 7 at (25 ± 1) °C.

PEG 1000			
100 w_1	**100 w_2**	**100 w_1**	**100 w_2**
70.77	0.89	20.10	8.96
58.56	1.64	19.59	9.50
49.74	2.27	19.24	9.69
43.24	2.66	18.94	9.84
39.66	3.06	18.63	10.01
37.13	3.42	18.35	10.16
36.10	3.87	18.06	10.30
34.38	4.27	17.75	10.45
32.97	4.60	17.46	10.61
31.63	4.94	17.16	10.72
30.03	5.18	16.88	10.88
28.87	5.48	16.64	11.02
27.84	5.76	16.35	11.11
27.19	6.10	16.10	11.25
26.32	6.33	15.85	11.39
25.75	6.60	15.64	11.53
25.19	6.89	15.34	11.59
24.43	7.08	15.13	11.71
23.90	7.35	14.93	11.84
23.18	7.54	14.71	11.89
22.48	7.72	14.52	11.99
22.00	7.93	14.42	11.91
21.58	8.14	14.05	12.10
21.21	8.32	13.71	12.28
20.83	8.50	13.53	12.40
20.46	8.74		

Table C3. Experimental weight fraction data for the ternary systems composed of PEG 1500 (w_1) + KH_2PO_4/K_2HPO_4 (w_2) at pH 7 at (25 ± 1) °C.

PEG 1500			
100 w_1	100 w_2	100 w_1	100 w_2
61.99	1.17	19.78	8.33
53.15	1.94	19.33	8.72
45.88	2.47	18.88	9.17
41.87	2.97	18.41	9.26
38.88	3.42	18.15	9.44
35.91	3.78	17.76	9.52
33.88	4.10	17.48	9.69
32.48	4.48	17.10	9.79
30.77	4.79	16.83	10.01
29.57	5.18	16.51	10.07
28.13	5.43	16.29	10.19
27.13	5.74	16.08	10.32
26.22	6.00	15.79	10.26
25.18	6.22	15.59	10.37
24.40	6.48	15.39	10.50
23.71	6.68	15.09	10.59
23.02	6.88	14.93	10.71
22.40	7.10	14.75	10.79
21.77	7.26	14.56	10.91
21.39	7.50	14.29	10.96
20.82	7.65	14.13	11.04
20.08	8.13		

Table C4. Experimental weight fraction data for the ternary systems composed of PEG 2000 (w_1) + KH_2PO_4/K_2HPO_4 (w_2) at pH 7 at (25 ± 1) °C.

PEG 2000			
100 w_1	100 w_2	100 w_1	100 w_2
55.07	0.85	20.87	6.68
43.15	2.17	20.33	6.81
40.53	2.55	20.06	6.98
36.71	2.87	19.77	7.13
35.01	3.23	19.31	7.22
33.49	3.61	19.03	7.39
31.74	3.89	18.59	7.79
30.47	4.17	18.32	7.93
29.00	4.40	18.03	8.05
27.97	4.65	17.78	8.19
26.67	5.24	17.40	8.26
25.22	5.38	17.15	8.38
24.42	5.58	16.93	8.52
23.68	5.75	16.59	8.54
22.96	5.91	16.36	8.64
22.53	6.14	16.15	8.76
22.09	6.38	15.84	9.10
21.45	6.54	15.63	9.21

Table C5. Experimental weight fraction data for the ternary systems composed of PEG 1000 (w_1) + KH_2PO_4/K_2HPO_4 (w_2) + 5 wt% of IL at pH 7 at (25 ± 1) °C.

PEG 1000 - [Ch]Cl			
100 w_1	100 w_2	100 w_1	100 w_2
52.54	1.29	17.82	8.71
48.21	1.73	17.50	8.85
44.75	2.10	17.13	9.08
43.08	2.39	16.91	9.12
40.14	2.89	16.68	9.17
38.83	3.14	16.34	9.36
36.72	3.32	16.01	9.54
35.53	3.58	15.79	9.56
34.48	3.80	15.50	9.71
32.58	3.96	15.24	9.87
31.30	4.49	15.04	9.89
29.71	4.79	14.78	10.02
28.95	4.94	14.52	10.17
28.25	5.08	14.26	10.31
27.59	5.17	14.10	10.34
26.75	5.53	13.86	10.48
26.18	5.67	13.64	10.60
25.63	5.79	13.42	10.71
24.91	6.11	13.22	10.82
24.36	6.20	13.01	10.93
23.53	6.47	12.85	10.95
22.95	6.76	12.64	11.10
22.49	6.86	12.50	11.12
21.92	7.12	12.31	11.25
21.41	7.19	12.13	11.36
20.93	7.41	12.00	11.37
20.44	7.65	11.81	11.52
20.09	7.69	11.70	11.53
19.62	7.91	11.53	11.65
19.18	8.15	11.36	11.75
18.85	8.21	11.24	11.72
18.47	8.44	11.09	11.80
18.09	8.65		

Table C6. Experimental weight fraction data for the ternary systems composed of PEG 2000 (w_1) + KH_2PO_4/K_2HPO_4 (w_2) + 5 wt% of IL at pH 7 at (25 ± 1) °C.

PEG 2000 - [Ch]Cl			
100 w_1	100 w_2	100 w_1	100 w_2
49.21	1.33	17.45	7.06
45.61	1.81	17.09	7.25
42.41	2.20	16.81	7.32
39.79	2.41	16.48	7.52
38.30	2.66	16.23	7.84
36.11	2.87	15.97	7.88
34.25	2.98	15.67	8.07
33.22	3.16	15.45	8.07
32.32	3.30	15.24	8.07
30.45	3.68	14.99	8.19
29.07	3.78	14.77	8.22
27.69	4.32	14.51	8.36
26.34	4.47	14.31	8.37
25.64	4.60	14.06	8.53
25.01	4.72	13.85	8.57
24.48	4.84	13.59	8.73
23.92	4.99	13.39	8.71
23.37	5.19	13.08	8.78
22.97	5.19	12.86	8.95
22.62	5.25	12.72	9.01
22.21	5.34	12.57	9.04
21.68	5.66	12.38	9.17
21.31	5.79	12.22	9.21
20.98	5.87	12.09	9.24
20.65	5.86	11.90	9.39
20.21	6.13	11.76	9.43
19.86	6.17	11.64	9.43
19.36	6.59	11.52	9.43
19.02	6.66	11.35	9.52
18.71	6.72	11.24	9.55
18.29	6.92	11.09	9.63
18.00	6.97	10.96	9.61
17.70	7.04	10.82	9.71

Table C7. Experimental weight fraction data for the ternary systems composed of PEG 1000 (w_1) + KH_2PO_4/K_2HPO_4 (w_2) + 5 wt% of IL at pH 7 at (25 ± 1) °C.

PEG 1000 - [Ch][Ac]			
100 w_1	**100 w_2**	**100 w_1**	**100 w_2**
53.06	1.76	19.09	8.67
48.32	2.23	18.77	8.76
44.99	2.44	18.50	8.83
42.75	2.74	17.81	9.18
40.68	2.97	17.57	9.20
38.57	3.27	17.22	9.38
36.47	3.80	16.91	9.54
34.04	4.25	16.48	9.67
32.98	4.41	15.90	10.02
31.90	4.85	15.72	10.00
30.65	4.93	15.43	10.20
29.88	5.21	15.25	10.21
28.69	5.29	14.97	10.39
28.07	5.46	14.81	10.40
27.46	5.68	14.55	10.51
26.98	5.92	14.33	10.64
26.32	6.24	14.16	10.67
25.53	6.32	13.94	10.81
25.25	6.26	13.78	10.84
24.60	6.72	13.59	10.97
24.17	6.85	13.44	11.00
23.75	7.00	13.26	11.12
23.34	7.12	13.07	11.26
22.95	7.22	12.90	11.35
22.38	7.51	12.76	11.36
22.02	7.61	12.57	11.49
21.67	7.68	12.45	11.52
21.40	7.72	12.28	11.62
20.94	7.97	12.15	11.65
20.62	8.03	11.98	11.79
19.82	8.37	11.86	11.81
19.54	8.42	11.70	11.90

Table C8. Experimental weight fraction data for the ternary systems composed of PEG 2000 (w_1) + KH_2PO_4/K_2HPO_4 (w_2) + 5 wt% of IL at pH 7 at (25 ± 1) °C.

PEG 2000 - [Ch][Ac]			
100 w_1	**100 w_2**	**100 w_1**	**100 w_2**
49.74	1.50	17.80	7.13
46.51	1.86	17.51	7.23
44.06	2.14	17.24	7.33
40.97	2.33	16.96	7.44
38.45	2.58	16.73	7.50
36.65	2.84	16.40	7.70
34.62	2.99	16.27	7.85
33.35	3.20	15.94	7.88
32.10	3.37	15.71	7.98
30.92	3.51	15.49	8.08
29.82	3.66	15.29	8.14
29.21	3.87	15.07	8.24
28.13	4.00	14.88	8.30
27.21	4.15	14.68	8.34
26.27	4.49	14.52	8.41
25.74	4.67	14.34	8.47
25.16	4.86	14.15	8.53
24.37	4.98	13.94	8.55
23.91	5.13	13.79	8.62
23.25	5.19	13.62	8.70
22.79	5.34	13.46	8.75
22.37	5.51	13.31	8.82
21.97	5.67	13.16	8.86
21.37	5.77	13.02	8.90
21.02	5.91	12.82	9.07
20.48	5.95	12.60	9.07
20.18	6.06	12.45	9.13
19.74	6.12	12.32	9.18
19.45	6.22	12.17	9.24
18.85	6.84	12.05	9.29
18.56	6.96	11.92	9.33
18.09	7.01		

Table C9. Experimental weight fraction data for the ternary systems composed of PEG 1000 (w_1) + KH_2PO_4/K_2HPO_4 (w_2) + 5 wt% of IL at pH 7 at (25 ± 1) °C.

PEG 1000 - $[N_{2222}]Br$			
100 w_1	100 w_2	100 w_1	100 w_2
50.11	2.25	18.27	9.24
46.78	2.47	17.78	9.50
44.28	2.57	17.40	9.67
42.66	2.90	16.99	9.87
41.15	3.18	16.60	10.10
38.95	3.31	16.17	10.37
37.61	3.61	15.79	10.56
36.34	3.80	15.44	10.75
34.91	4.25	15.08	10.95
34.02	4.37	13.89	11.51
32.16	5.21	13.63	11.67
30.47	5.36	13.38	11.78
29.61	5.56	13.15	11.88
28.78	5.75	12.84	12.10
27.73	6.17	12.62	12.24
27.03	6.34	12.41	12.35
26.15	6.82	12.25	12.38
25.52	7.00	12.03	12.51
24.72	7.32	11.78	12.71
23.92	7.64	11.57	12.84
23.20	7.91	11.37	12.94
22.53	7.91	11.18	13.02
21.96	8.15	11.00	13.12
21.38	8.36	10.81	13.20
20.87	8.55	10.65	13.29
20.28	8.70	10.43	13.47
19.65	8.65	10.27	13.56
19.18	8.83	10.12	13.65
18.66	9.15	9.96	13.74

Table C10. Experimental weight fraction data for the ternary systems composed of PEG 2000 (w_1) + KH_2PO_4/K_2HPO_4 (w_2) + 5 wt% of IL at pH 7 at (25 ± 1) °C.

PEG 2000 - $[N_{2222}]Br$			
100 w_1	**100 w_2**	***100 w_1***	***100 w_2***
55.60	1.31	18.03	7.43
52.97	1.74	17.68	7.55
49.34	2.02	16.59	7.98
45.91	2.29	16.22	8.20
42.62	2.55	15.95	8.26
40.01	2.71	15.73	8.30
38.56	2.98	15.40	8.49
37.23	3.21	15.15	8.57
35.05	3.39	14.83	8.77
33.83	3.64	14.60	8.81
32.73	3.85	14.28	9.02
31.77	4.02	14.05	9.06
30.83	4.18	13.85	9.13
29.93	4.36	13.57	9.33
29.03	4.53	13.38	9.37
28.25	4.71	13.12	9.57
27.47	4.86	12.93	9.61
26.76	5.02	12.74	9.67
26.04	5.15	12.48	9.88
25.35	5.29	12.31	9.91
24.57	5.38	12.08	10.07
24.00	5.54	11.94	10.10
23.48	5.63	11.78	10.14
23.02	5.71	11.56	10.31
22.54	5.87	11.42	10.34
21.89	6.16	11.20	10.50
21.47	6.24	11.07	10.51
20.91	6.46	10.90	10.63
20.51	6.54	10.77	10.65
20.12	6.64	10.60	10.80
19.58	6.96	10.38	10.87
19.21	7.05	10.27	10.89
18.86	7.11	10.12	11.01
18.39	7.39		

Table C11. Experimental weight fraction data for the ternary systems composed of PEG 1000 (w_1) + KH_2PO_4/K_2HPO_4 (w_2) + 5 wt% of IL at pH 7 at (25 ± 1) °C.

PEG 1000 - $[N_{2222}]Cl$			
100 w_1	100 w_2	100 w_1	100 w_2
60.21	1.47	17.9	10.1
54.89	2.00	17.5	10.2
50.27	2.45	17.0	10.5
46.00	2.78	16.7	10.7
42.57	3.28	16.3	10.9
38.58	3.91	16.0	11.1
36.18	4.16	15.7	11.2
34.86	4.54	15.3	11.5
33.61	4.86	14.9	11.7
31.87	5.08	14.7	11.8
30.77	5.30	14.4	12.0
29.80	5.55	14.1	12.2
28.93	5.82	13.9	12.3
28.08	6.06	13.6	12.5
27.31	6.30	13.3	12.7
26.54	6.56	13.0	12.8
25.88	6.80	12.8	12.9
24.97	7.27	12.6	13.0
24.37	7.47	12.3	13.2
23.79	7.65	12.10	13.4
23.19	7.79	11.92	13.4
22.43	8.19	11.64	13.7
21.92	8.35	11.37	13.8
21.20	8.73	11.14	13.9
20.81	8.76	11.00	14.0
20.30	8.84	10.81	14.1
19.75	9.18	10.61	14.2
19.32	9.31	10.49	14.3
18.80	9.64	10.32	14.4
18.42	9.76		

Table C12. Experimental weight fraction data for the ternary systems composed of PEG 2000 (w_1) + KH_2PO_4/K_2HPO_4 (w_2) + 5 wt% of IL at pH 7 at (25 ± 1) °C.

PEG 2000 - $[N_{2222}]Cl$			
100 w_1	100 w_2	100 w_1	100 w_2
45.82	2.93	16.41	8.84
41.08	3.13	16.14	8.91
39.47	3.50	15.86	9.03
37.00	3.70	15.58	9.11
35.56	4.05	15.29	9.19
33.53	4.20	14.85	9.44
32.37	4.46	14.62	9.51
31.27	4.74	14.40	9.59
29.74	4.91	14.07	9.83
28.15	5.35	13.86	9.91
27.31	5.57	13.64	9.96
26.52	5.80	13.42	10.02
25.40	5.87	13.15	10.25
24.79	6.07	12.96	10.39
24.17	6.24	12.78	10.45
23.54	6.40	12.60	10.49
22.95	6.55	12.35	10.68
22.38	6.71	12.18	10.75
21.67	7.11	12.02	10.71
21.17	7.25	11.85	10.75
20.69	7.39	11.62	10.94
20.25	7.55	11.46	10.99
19.81	7.68	11.30	11.05
19.39	7.80	11.14	11.11
19.06	7.94	10.99	11.17
18.64	8.08	10.85	11.24
18.24	8.19	10.72	11.30
17.85	8.29	10.58	11.37
17.31	8.44	10.41	11.53
16.85	8.54		

Table C13. Experimental weight fraction data for the ternary systems composed of PEG 1000 (w_1) + KH_2PO_4/K_2HPO_4 (w_2) + 5 wt% of IL at pH 7 at (25 ± 1) °C.

PEG 1000 - $[N_{222(C7H7)}]Cl$			
100 w_1	**100 w_2**	***100 w_1***	***100 w_2***
52.28	3.31	18.98	9.08
49.14	3.60	18.59	9.27
45.29	3.81	18.26	9.33
42.61	4.07	17.87	9.53
39.73	4.23	17.49	9.72
37.53	4.43	17.10	9.92
35.71	4.57	16.86	9.97
34.23	4.73	16.50	10.15
33.21	4.97	16.18	10.35
31.57	5.28	15.97	10.41
30.75	5.48	15.64	10.58
29.76	5.58	15.36	10.75
29.03	5.81	15.03	10.95
28.42	5.98	14.74	11.14
27.86	6.13	14.49	11.26
27.25	6.34	14.21	11.42
26.69	6.53	13.82	11.62
25.87	6.61	13.58	11.79
25.33	6.78	13.34	11.92
24.80	6.91	13.11	12.06
24.25	7.09	12.87	12.20
23.71	7.26	12.57	12.44
23.09	7.54	12.35	12.59
22.64	7.65	12.14	12.70
22.18	7.78	11.92	12.83
21.55	8.09	11.73	12.93
21.15	8.20	11.55	13.05
20.77	8.27	11.38	13.13
20.28	8.52	11.14	13.34
19.92	8.61	10.95	13.42
19.46	8.85		

Table C14. Experimental weight fraction data for the ternary systems composed of PEG 2000 (w_1) + KH_2PO_4/K_2HPO_4 (w_2) + 5 wt% of IL at pH 7 at (25 ± 1) °C.

PEG 2000 -[$N_{222(C7H7)}$][Cl]			
100 w_1	100 w_2	100 w_1	100 w_2
47.18	1.78	15.64	8.36
44.14	2.22	15.45	8.46
41.02	2.49	15.27	8.52
38.64	2.74	15.08	8.60
36.71	2.99	14.91	8.66
34.74	3.20	14.61	8.92
33.40	3.38	14.36	8.91
31.88	3.53	14.14	9.06
30.54	3.85	13.99	9.10
28.94	4.22	13.77	9.27
28.06	4.38	13.62	9.30
27.38	4.50	13.41	9.45
26.79	4.65	13.12	9.59
26.26	4.84	12.97	9.64
25.47	5.02	12.75	9.81
24.86	5.16	12.62	9.87
24.42	5.24	12.49	9.91
23.76	5.32	12.30	10.06
23.33	5.49	12.17	10.11
22.73	5.66	12.05	10.15
22.29	5.82	11.87	10.30
21.88	5.96	11.73	10.34
21.23	6.21	11.55	10.50
20.64	6.22	11.31	10.62
20.28	6.37	11.18	10.64
19.81	6.67	11.07	10.71
19.36	6.73	10.90	10.87
19.06	6.83	10.68	10.96
18.77	6.95	10.57	10.99
18.48	7.05	10.41	11.12
18.10	7.32	10.31	11.14
17.81	7.41	10.16	11.27
17.57	7.49	9.98	11.36
17.32	7.57	9.86	11.46
17.06	7.67	9.78	11.49
16.83	7.75	9.66	11.58
16.50	8.00	9.57	11.61
16.05	8.19	9.45	11.72
15.83	8.26	9.30	11.76

The experimental binodal curves were fitted by equation (C1):

$$[\mathrm{PEG}] = A \exp[(B[\mathrm{Salt}]^{0.5}) - (C[\mathrm{Salt}]^3)] \quad \text{(C1)}$$

where [PEG] and [Salt] are the PEG and salt weight fraction percentages, respectively, and the coefficients *A*, *B*, and *C* are the fitting parameters.

The tie-lines (TLs), which give the composition of each phase for a given mixture composition, were determined by a gravimetric method described by Merchuk et al[36]. The mixtures were vigorously stirred and allowed to equilibrate at (25 ± 1)°C and atmospheric pressure for at least 12 h. After separation of the two phases, the top and bottom phases were weighted. Finally, each TL was determined by the application of the lever-arm rule (Eqs. C2 to C5) to the relationship between the weight of the top and bottom phases and the overall system composition.

$$[\mathrm{PEG}]_{\mathrm{T}} = A\exp[(B \times [\mathrm{Salt}]_{\mathrm{T}}^{0.5}) - (C \times [\mathrm{Salt}]_{\mathrm{T}}^{3})] \quad \text{(C2)}$$

$$[\mathrm{PEG}]_{\mathrm{B}} = A\exp[(B \times [\mathrm{Salt}]_{\mathrm{B}}^{0.5}) - (C \times [\mathrm{Salt}]_{\mathrm{B}}^{3})] \quad \text{(C3)}$$

$$[\mathrm{PEG}]_{\mathrm{T}} = \frac{[\mathrm{PEG}]_{\mathrm{M}}}{\alpha} - \frac{1-\alpha}{\alpha} \times [\mathrm{PEG}]_{\mathrm{B}} \quad \text{(C4)}$$

$$[\mathrm{Salt}]_{\mathrm{T}} = \frac{[\mathrm{Salt}]_{\mathrm{M}}}{\alpha} - \frac{1-\alpha}{\alpha} \times [\mathrm{Salt}]_{\mathrm{B}} \quad \text{(C5)}$$

where the subscripts T, B and M designate, respectively, the top phase, bottom phase, and the mixture. The value α is the ratio between the mass of the top phase and the total mass of the mixture experimentally determined. The calculation of the each tie-line length (TLL) was determined through the application of the following equation:

$$\mathrm{TLL} = \sqrt{([\mathrm{Salt}]_{\mathrm{T}} - [\mathrm{Salt}]_{\mathrm{B}})^2 + ([\mathrm{PEG}]_{\mathrm{T}} - [\mathrm{PEG}]_{\mathrm{B}})^2} \quad \text{(C6)}$$

Table C15. Parameters *A*, *B* and *C* of equation (1) and respective standard deviations (σ) for ternary and quaternary ABS.

Ternary systems: PEG + (K_2HPO_4/KH_2PO_4) + H_2O

PEG	*A* ± σ	*B* ± σ	10^5 (*C* ± σ)
PEG400	97.19 ± 3.07	-0.416 ± 0.013	3.15 ± 0.83
PEG1000	98.52 ± 4.46	-0.513 ± 0.021	6.90 ± 2.34
PEG1500	125.8 ± 8.05	-0.640 ± 0.031	1.72 ± 0.50
PEG2000	92.98 ± 3.69	-0.542 ± 0.024	22.5 ± 7.28

Quaternary systems: PEG + (K_2HPO_4/KH_2PO_4) + H_2O + IL at 5 wt%

PEG-IL	*A* ± σ	*B* ± σ	10^5 (*C* ± σ)
PEG1000-[Ch]Cl	97.70 ± 1.61	-0.534 ± 0.009	19.6 ± 1.49
PEG2000-[Ch]Cl	108.2 ± 3.95	-0.654 ± 0.021	23.7 ± 5.06
PEG1000-[Ch][Ac]	71.18 ± 1.16	-0.287 ± 0.006	2.70 ± 0.19
PEG2000-[Ch][Ac]	121.0 ± 4.44	-0.713 ± 0.021	10.4 ± 5.35
PEG1000-[N_{2222}]Br	105.5 ± 4.29	-0.525 ± 0.020	15.8 ± 2.30
PEG2000-[N_{2222}]Br	128.8 ± 3.52	-0.695 ± 0.015	16.9 ± 3.21
PEG1000-[N_{2222}]Cl	124.6 ± 2.38	-0.592 ± 0.009	6.79 ± 1.09
PEG2000-[N_{2222}]Cl	132.1 ± 6.27	-0.656 ± 0.022	20.1 ± 2.44
PEG1000-[$N_{222(C7H7)}$]Cl	143.9 ± 5.89	-0.658 ± 0.016	6.39 ± 1.04
PEG2000-[$N_{222(C7H7)}$]Cl	120.1 ± 2.32	-0.688 ± 0.010	10.2 ± 1.59

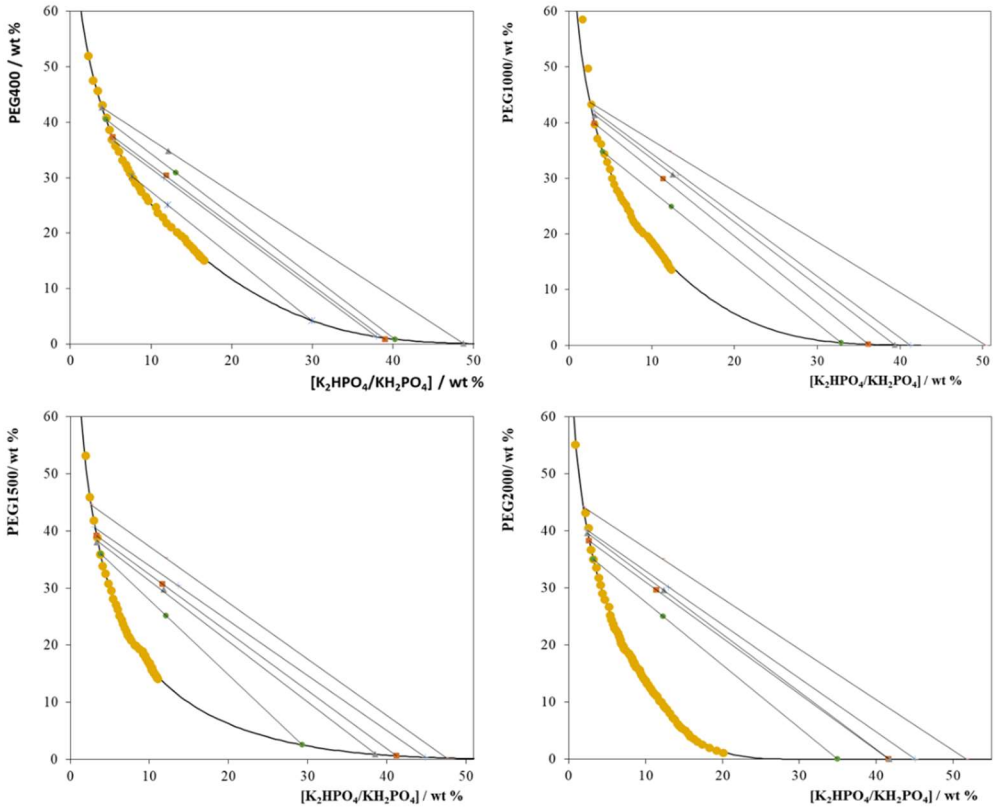

Figure C1. Phase diagrams for the ternary systems PEG + K_2HPO_4/KH_2PO_4 at pH 7 + H_2O at (25 ± 1) °C and atmospheric pressure.

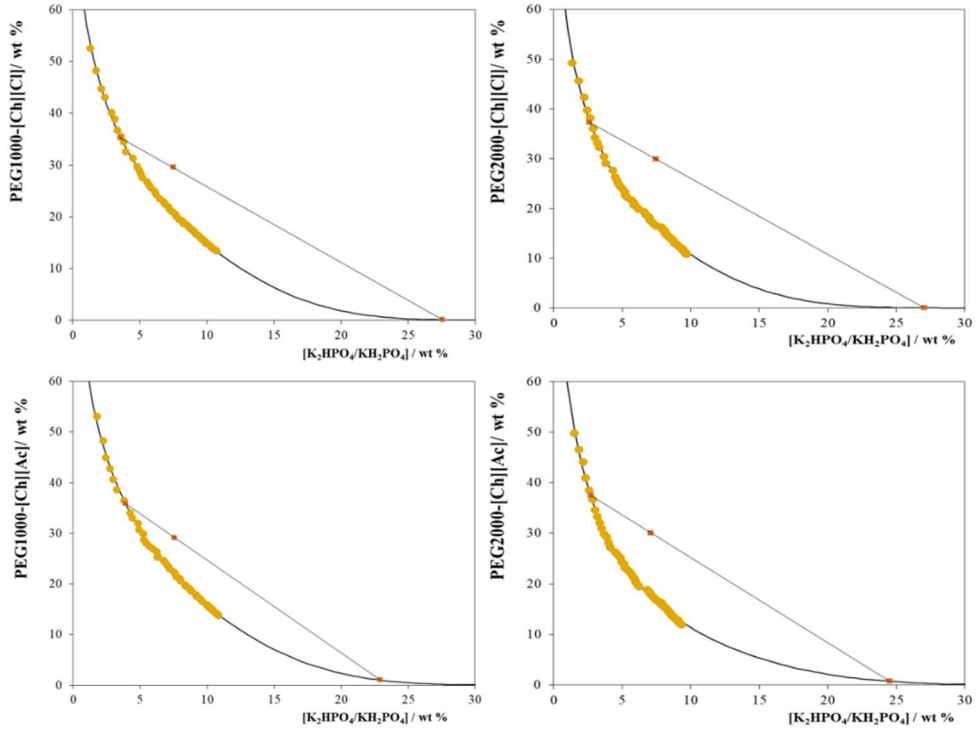

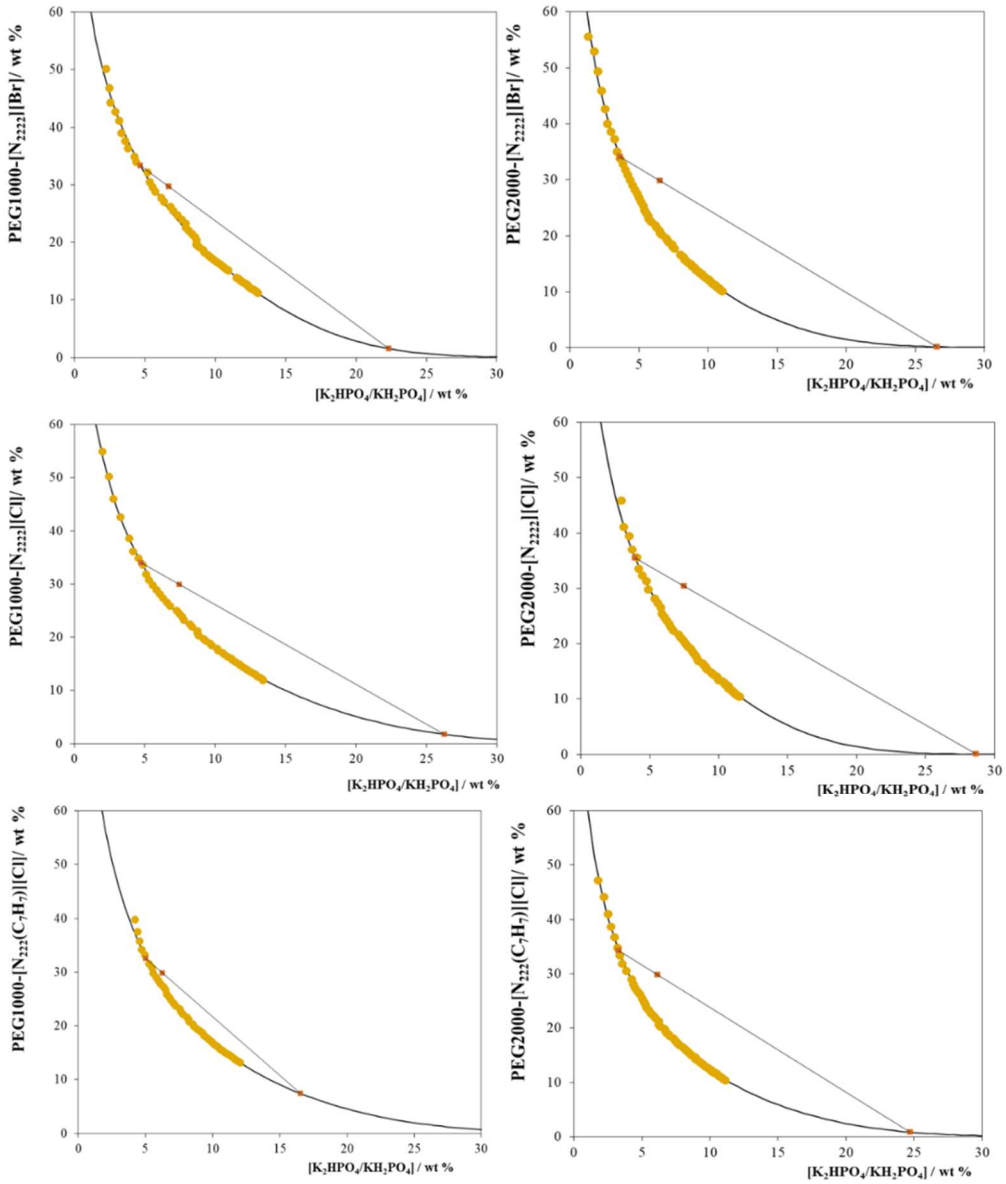

Figure C2. Phase diagrams for the quaternary systems PEG + K_2HPO_4/KH_2PO_4 at pH 7 + H_2O + IL at 5wt% at (25 ± 1) °C and atmospheric pressure.

Table C16. Mass fraction compositions for the TLs and respective Tie-Line Lengths (TLLs), at the Top (T) and Bottom (B) phases, and at the initial mixture composition (M), composed of PEG (Y) and salt (X), at (25 ± 1) °C and atmospheric pressure.

Ternary systems: PEG + (K_2HPO_4/KH_2PO_4) + H_2O

PEG	weight fraction composition/wt %							
	$[PEG]_T$	$[K_2HPO_4/KH_2PO_4]_T$	$[PEG]_M$	$[K_2HPO_4/KH_2PO_4]_M$	$[PEG]_B$	$[K_2HPO_4/KH_2PO_4]_B$	TLS	TLL
PEG400	36.52	5.47	29.94	11.56	1.33	37.99	-1.08	47.91
	37.24	5.26	30.33	11.95	0.85	39.07	-1.08	50.64
	30.29	7.66	25.12	12.08	4.26	29.97	-1.17	34.28
	40.53	4.39	30.89	13.13	0.88	40.31	-1.10	53.51
	42.67	3.89	34.85	12.14	0.14	48.77	-0.95	61.83
PEG1000	39.89	3.09	29.92	11.40	0.17	36.23	-1.20	51.73
	41.33	3.08	30.71	12.53	0.04	39.37	-1.14	54.10
	34.80	4.07	24.89	12.39	0.44	32.92	-1.19	44.86
	42.39	2.95	30.61	13.17	0.03	41.29	-1.10	55.55
	43.62	2.51	34.87	12.12	3.7E-04	50.30	-0.91	64.76
PEG1500	39.19	3.32	30.70	11.66	0.62	41.27	-1.02	54.11
	38.04	3.36	29.73	11.80	0.89	38.52	-1.06	52.34
	35.96	3.83	25.12	12.11	2.55	29.37	-1.31	42.05
	40.66	3.04	30.42	13.63	0.37	44.87	-0.96	56.76
	44.54	2.63	35.25	12.03	0.24	47.50	-0.99	63.05
PEG2000	38.22	2.66	29.65	11.39	2.5E-07	41.61	-0.98	54.57
	39.24	2.45	29.97	12.33	2.2E-07	42.80	-0.97	55.78
	35.04	3.19	25.06	12.25	2.3E-04	35.01	-1.10	47.33
	40.06	2.39	30.12	12.98	1.9E-09	45.04	-0.94	58.51
	44.20	1.87	35.07	12.18	6.8E-10	51.75	-0.89	66.65

Quaternary systems: PEG + (K_2HPO_4/KH_2PO_4) + H_2O + IL at 5 wt%

PEG-IL	weight fraction composition/wt %							
	$[PEG]_T$	$[K_2HPO_4/KH_2PO_4]_T$	$[PEG]_M$	$[K_2HPO_4/KH_2PO_4]_M$	$[PEG]_B$	$[K_2HPO_4/KH_2PO_4]_B$	TLS	TLL
PEG1000-[Ch][Cl]	35.29	3.57	29.53	7.50	0.10	27.56	-1.47	42.59
PEG2000-[Ch][Cl]	37.31	2.63	29.91	7.48	0.03	27.08	-1.52	44.58
PEG1000-[Ch][Ac]	35.86	3.90	29.15	7.56	0.99	22.91	-1.83	39.71
PEG2000-[Ch][Ac]	37.46	2.69	30.05	7.10	0.75	24.52	-1.68	42.71
PEG1000-$[N_{2222}]$Br	33.32	4.67	29.66	6.71	1.50	22.35	-1.80	36.39
PEG2000-$[N_{2222}]$Br	34.13	3.61	29.81	6.52	0.15	26.56	-1.48	41.01
PEG1000-$[N_{2222}]$Cl	33.99	4.75	29.93	7.46	1.74	26.28	-1.50	38.78
PEG2000-$[N_{2222}]$Cl	35.44	3.95	30.35	7.51	0.03	28.69	-1.43	43.19
PEG1000-$[N_{222}(C_7H_7)]$Cl	32.55	5.05	29.83	6.30	7.41	16.55	-2.19	27.65
PEG2000-$[N_{222}(C_7H_7)]$Cl	34.24	3.30	29.84	6.12	0.83	24.74	-1.56	39.70

Table C17. Extraction efficiencies (EE%) and Recovery yields (RY%) of commercial Ovalbumin and Lysozyme in the ternary and quaternary ABS and respective mixture compositions.

Ternary systems: PEG + (K_2HPO_4/KH_2PO_4) + H_2O

PEG	weight fraction percentage / wt %		EE_{Ova}%	EE_{Lys}%	RY_{Ova}%	RY_{Lys}%
	$[PEG]_M$	$[K_2HPO_4/KH_2PO_4]_M$				
PEG 400	30.33	11.95	100.00	100.00	100.00	90.2 ± 1.32
	29.94	11.56	100.00	98.6 ± 0.98	100.00	97.4 ± 1.65
	25.12	12.08	100.00	100.00	100.00	100.00
	30.89	13.13	100.00	100.00	100.00	100.00
	34.85	12.14	100.00	90.2 ± 0.96	100.00	89.6 ± 1.34
PEG 1000	29.92	11.40	98.5 ± 2.4	100.00	98.03 ± 1.5	86.9 ± 3.1
	30.71	12.53	100.00	99.2 ± 1.32	100.00	88.1 ± 0.28
	24.89	12.39	96 ± 0.96	96.2 ± 0.86	95.8 ± 1.5	95.8 ± 0.97
	30.61	13.17	100.00	95.2 ± 1.3	100.00	57.9 ± 1.21
	34.87	12.12	100.00	94.4 ± 1.56	100.00	42.7 ± 2.65
PEG 1500	30.70	11.66	85.7 ± 1.30	100.00	82.1 ± 1.30	47.2 ± 0.94
	29.73	11.80	92.6 ± 0.83	99.6 ± 1.54	92.0 ± 0.70	49.8.± 3.14
	25.12	12.11	82.9 ± 1.1	93.02 ± 0.87	82.9 ± 1.85	81.5 ± 2.4
	30.42	13.63	91.0 ± 1.2	93.1 ± 1.5	90.9 ± 1.2	40.4 ± 3.2
	35.25	12.03	100.00	96.8 ± 0.97	95.3 ± 1.34	30.8 ± 3.7
PEG 2000	29.65	11.39	82.1 ± 1.87	100.00	76.4 ± 1.8	35.7 ± 0.87
	29.67	12.33	88.6 ± 0.98	100.00	80.5 ± 1.74	26.1 ± 1.09
	25.06	12.25	49.4 ± 1.07	89.2 ± 1.09	43.3 ± 2.87	50.08 ± 1.05
	30.12	12.98	85.4 ± 1.90	87.7 ± 0.67	61.6 ± 3.5	20.4 ± 1.45
	35.07	12.18	100.00	98.9 ± 1.65	77.7 ± 3.03	20.1 ± 1.40

Table C18. Extraction efficiencies (EE%) and Recovery yields (RY%) of Ovalbumin and Lysozyme from Egg White (1:10, v:v) in the ternary ABS and respective mixture compositions.

Ternary systems: PEG + (K_2HPO_4/KH_2PO_4) + egg white (1:10, v:v)

PEG-IL	weight fraction percentage / wt %		EE_{Ova}%	EE_{Lys}%	RY_{Ova}%	RY_{Lys}%
	$[PEG]_M$	$[K_2HPO_4/KH_2PO_4]_M$				
PEG1000	29.92	11.40	97.6 ± 1.5	100.00	95.5 ± 1.6	81.4 ± 3.2
	30.71	12.53	100.00	100.00	100.00	47.3 ± 2.1
	30.61	13.17	100.00	96.2 ± 1.1	100.00	63.3 ± 1.
PEG2000	29.65	11.39	90.9 ± 3.6	100.00	74.1 ± 1.5	37.9 ± 4.6
	29.67	12.33	98.3 ± 3.2	100.00	84.2 ± 1.4	25.3 ± 2.2
	30.12	12.98	96.9 ± 5.7	87.5 ± 1.9	82.5 ± 1.09	22.2 ± 1.3

Table C19. Extraction efficiencies (EE%) and Recovery yields (RY%) of commercial Ovalbumin and Lysozyme in the quaternary ABS and respective mixture compositions.

Quaternary systems: PEG + (K_2HPO_4/KH_2PO_4) + H_2O + IL at 5 wt%

PEG-IL	weight fraction percentage / wt %		EE_{Ova}%	EE_{Lys}%	RY_{Ova}%	RY_{Lys}%
	$[PEG]_M$	$[K_2HPO_4/KH_2PO_4]_M$				
PEG1000-[Ch][Cl]	29.53	7.50	61.16 ± 2.4	95.4 ± 1.2	54.1 ± 1.3	95.1 ± 1.6
PEG2000-[Ch][Cl]	29.91	7.48	100.00	81.1 ± 2.1	89.4 ± 1.7	65.4 ± 3.9
PEG1000-[Ch][Ac]	29.15	7.56	61.8 ± 4.5	99.9 ± 1.01	60.9 ± 2.1	99.0 ± 1.4
PEG2000-[Ch][Ac]	30.05	7.10	100.00	80.4 ± 2.4	100.00	78.9 ± 2.5
PEG1000-[N_{2222}]Br	29.66	6.71	96.1 ± 1.2	100.00	95.9 ± 1.8	100.00
PEG2000-[N_{2222}]Br	29.81	6.52	100.00	69.4 ± 2.3	82.2 ± 1.8	68.9 ± 2.1
PEG1000-[N_{2222}]Cl	29.93	7.46	95.9 ± 1.0	100	94.2 ± 1.3	100.00
PEG2000-[N_{2222}]Cl	30.35	7.51	58.1 ± 0.9	66.8 ± 2.5	57.1 ± 2.4	66.2 ± 2.7
PEG1000-[$N_{222(C7H7)}$]Cl	29.83	6.30	100.00	100.00	35. 5 ± 1.4	45.4 ± 2.4
PEG2000-[$N_{222(C7H7)}$]Cl	29.84	6.12	100.00	100.00	11.6 ± 1.9	23.8 ± 1.5

Table C20. Extraction efficiencies (EE%) and Recovery yields (RY%) of Ovalbumin and Lysozyme from Egg White (different dilutions) in the quaternary ABS and respective mixture compositions.

Quaternary systems: PEG + (K_2HPO_4/KH_2PO_4) + Egg White (1:5, v:v) + IL at 5 wt%

PEG-IL	weight fraction percentage / wt %		EE_{Ova}%	EE_{Lys}%	RY_{Ova}%	RY_{Lys}%
	$[PEG]_M$	$[K_2HPO_4/KH_2PO_4]_M$				
PEG1000-[Ch][Cl]	29.53	7.80	86.9 ± 1.2	100.00	53.7 ± 4.1	65.1 ± 3.4
PEG2000-[Ch][Cl]	29.96	7.68	100.00	100.00	59.8 ± 3.4	71.6 ± 1.3
PEG1000-[Ch][Ac]	29.25	7.60	71.1 ± 2.6	87.2 ± 2.3	67.7 ± 2.7	44.1 ± 1.7
PEG2000-[Ch][Ac]	30.15	7.30	100.00	100.00	75.8 ± 2.9	55.8 ± 1.5
PEG1000-[N_{2222}]Br	29.76	6.61	98.9 ± 1.2	81.9 ± 2.4	53.8 ± 3.5	14.2 ± 1.2
PEG2000-[N_{2222}]Br	29.72	6.53	100.00	100.00	23.1 ± 2.6	3.4 ± 2.6
PEG1000-[N_{2222}]Cl	29.93	7.46	96.2 ± 2.4	86.2 ± 2.6	82.2 ± 1.8	20.7 ± 3.9
PEG2000-[N_{2222}]Cl	30.38	7.56	93.1 ± 1.3	100.00	49.3 ± 1.2	23.8 ± 4.5
PEG1000-[$N_{222}(C_7H_7)$]Cl	29.89	6.40	100.00	100.00	50.3 ± 2.7	42.1 ± 1.4
PEG2000-[$N_{222}(C_7H_7)$]Cl	29.86	6.32	100.00	-	9.3 ± 1.6	-

Quaternary systems: PEG + (K_2HPO_4/KH_2PO_4) + Egg White (1:10, v:v) + IL at 5 wt%

PEG-IL	weight fraction percentage / wt %		EE_{Ova}% ± 0.2	EE_{Lys}% ± 0.2	RY_{Ova}% ± 0.2	RY_{Lys}% ± 0.2
	$[PEG]_M$	$[K_2HPO_4/KH_2PO_4]_M$				
PEG1000-[Ch][Cl]	29.88	7.90	79.2 ± 3.4	91.8 ± 3.2	75.2 ± 1.4	76.1 ± 3.2
PEG2000-[Ch][Cl]	30.15	7.48	100.00	100.00	89.4 ± 2.4	92.5 ± 2.1
PEG1000-[Ch][Ac]	29.75	7.86	66.4 ± 2.4	81.5 ± 2.3	66.2 ± 1.3	74.5 ± 1.2
PEG2000-[Ch][Ac]	30.05	7.30	100.00	100.00	100.00	92.5 ± 1.6
PEG1000-[N_{2222}]Br	29.66	6.71	96.1 ± 1.8	97.2 ± 1.6	90.9 ± 1.7	63.6 ± 2.8
PEG2000-[N_{2222}]Br	29.81	6.52	100.00	100.00	45.4 ± 2.7	35.2 ± 1.2
PEG1000-[N_{2222}]Cl	29.93	7.56	95.6 ± 1.7	95.7 ± 1.05	95.4 ± 1.3	46.7 ± 1.4
PEG2000-[N_{2222}]Cl	30.35	7.51	90.9 ± 1.3	100.00	62.1 ± 2.4	59.5 ± 2.5
PEG1000-[$N_{222}(C_7H_7)$]Cl	29.83	6.30	98.9 ± 1.02	100.00	66.2 ± 1.09	18.6 ± 1.8
PEG2000-[$N_{222}(C_7H_7)$]Cl	29.84	6.25	100.00	-	-	-

Quaternary systems: PEG + (K_2HPO_4/KH_2PO_4) + Egg White (1:50, v:v) + IL at 5 wt%

PEG-IL	weight fraction percentage / wt %		EE_{Ova}%	EE_{Lys}%	RY_{Ova}%	RY_{Lys}%
	$[PEG]_M$	$[K_2HPO_4/KH_2PO_4]_M$				
PEG1000-[Ch][Cl]	30.26	7.70	77.2 ± 1.2	100.00	67.6 ± 1.3	100
PEG2000-[Ch][Cl]	29.99	7.58	100.00	100.00	73.9 ± 1.9	100
PEG1000-[Ch][Ac]	29.47	7.86	74.6 ± 2.3	100.00	24.3 ± 1.2	35.3 ± 1.6
PEG2000-[Ch][Ac]	30.05	7.20	100.00	100.00	34.7 ± 2.3	26.2 ± 2.8
PEG1000-[N_{2222}]Br	29.96	6.71	88.3 ± 2.2	94.3 ± 1.09	28.6 ± 1.6	23.2 ± 1.3
PEG2000-[N_{2222}]Br	29.81	6.52	100.00	100.00	30.9 ± 1.3	77.5 ± 1.8
PEG1000-[N_{2222}]Cl	30.13	7.56	81.9 ± 1.1	92.87 ± 1.1	27.5 ± 2.4	21.6 ± 1.9
PEG2000-[N_{2222}]Cl	30.35	7.51	100.00	100.00	30.1 ± 1.8	86.4 ± 2.6
PEG1000-[$N_{222}(C_7H_7)$]Cl	29.83	6.40	100.00	-	34.8 ± 1.9	-
PEG2000-[$N_{222}(C_7H_7)$]Cl	29.84	6.15	96.1 ± 1.02	-	25.07 ± 1.5	-

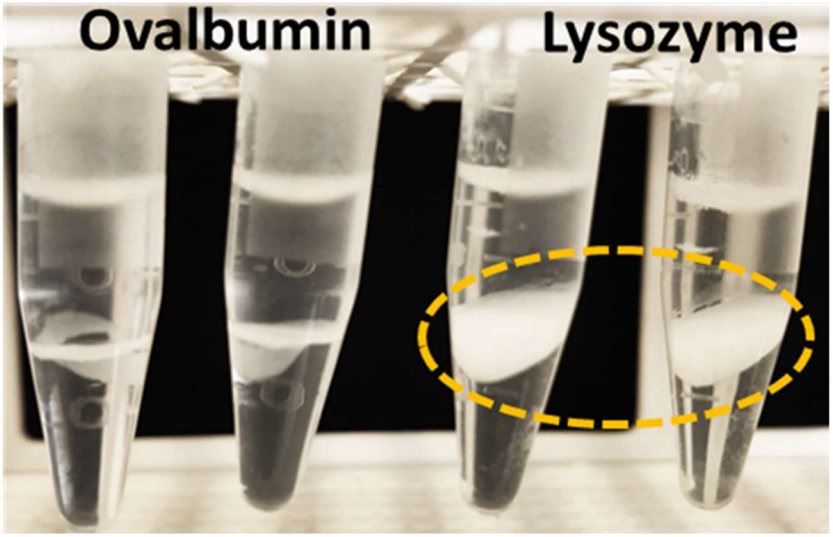

Figure C3. Precipitated protein in ABS composed of 30 wt% of PEG 2000 + 12 wt% of K_2HPO_4/KH_2PO_4.